NANYANG TECHNOLOGICAL UNIVERSITY

DIVISION OF CHEMISTRY AND BIOLOGICAL CHEMISTRY
SCHOOL OF PHYSICAL & MATHEMATICAL SCIENCES

ELECTROCHEMISTRY OF FLAVINS

TAN LI JUN, SERENA

School of Physical & Mathematical Sciences

A thesis submitted to the Nanyang Technological University in fulfillment of the requirements for the degree of Doctor of Philosophy of Chemistry

2014

Acknowledgements

First and foremost, I would like to thank Nanyang Technological University (NTU) for awarding me the Nanyang President's Graduate Scholarship, and giving me opportunities to attending 2 conferences which has broadened my horizons both scientifically and personally.

I would also like to thank my PhD supervisor, Assoc. Prof. Richard David Webster, for accepting me into his group without prior experience, for providing guidance over these 4 years, for giving me space and freedom to explore the field, for understanding, for never having any harsh words and being really great to talk to even for non-electrochemistry topics.

Much love to my lunch buddies, Gwen, Shu Jun, Novi, for being the best part of these 4 years, making me look forward to school every day. Also, I am really thankful to my student Jiamin, for being so reliable, meticulous and determined. I could not have done it without you, and could not have asked for a better student! To all Gwen's ex-students and my ex-lunch buddies (Marcus, Shu Jun, Li Zhen, Li Lin and Wen Hui), it has been great knowing all of you! Special thanks to Shu Jun and Novi for the last few months, starving yourselves till 2 pm to lunch with me, to Novi for stepping up without complaints to help me with data collection, to Yanni for always being so kind and sweet, and to Diane for understanding! Also, thanks to Shu Hui for our dinners, for working late together and for the trips home. To Colin, thanks for your friendship and "thanks" for scaring me while making sure I am not holding any glassware. To Weejian, thanks for your kind notes of encouragement during my FYP days, and being the kind of friend that sticks around. To Boon Hong, thanks for being mature and understanding, for helping me with ithenticate

and so much more, you are truly a much better person than you are given credit for! You are friends I wish I knew earlier and hope to keep for many years to come!

To my other labmates, Xiuhui, Bahareh, Yayun, Malcolm, KK, Sherman, Jazreen, Yingshan, Shan Shan, Yan Lan, Wei Wei, thanks for the good times and chats and making sure there's never a boring moment.

Thanks to Prof. Loh Teck Peng, Assoc. Prof. Edwin Yeow, Assoc. Prof. Tan Howe Siang for your guidance and inspiration during my undergraduate days, and to Dr. Zhao Yujun and Dr. Li Bin for being the best mentors (and best friends) during my FYP days, for your guidance and for all the interesting discussions we used to have.

Thanks to all other CBC friends and professors who always have a ready smile and a friendly word: Nisha, Adeline, Jasmine, Joel, Siva, Mianrong, Aihua, Nicole, Jefri, CK, guanjia, Profs. Li Tianhu, Chen Hongyu, Philip Chan, Roderick Bates, Tan Choon Hong, Motoki Yamane, Lee Soo Ying, Park Cheol Min, Xing Bengang and Zhang Dawei.

Last but not least, I would like to thank my family members for being my pillars of support. To my mum, thanks for always waking up early to prepare breakfast, and for caring for me all these years. To my dad, thanks for being concerned about my work, and for sending me to school and back at unearthly hours. To my newly-wedded husband, Eric, thanks for your love and support, for accompanying me in school when I stay late and every time you have a free day, for being the sweetest and the best.

Table of Contents

List of Figures

List of Tables

List of Schemes

Abstract

The electrochemical behavior of riboflavin, FMN, FAD and 2 synthesized flavins were examined in aqueous (buffered and non-buffered) and non-aqueous media (with varying amounts of water and free protons), using voltammetry, electrolysis, UV-vis and EPR spectroscopy, and were found to display a range of electron-transfer mechanisms from the most hydrophobic environments to environments with the most number of free protons.

In aprotic organic solvents, the N3-protonated riboflavin (and flavin **1**) are reduced by one-electron to form the anionic radical, which undergo a homogeneous proton transfer reaction with another oxidized flavin (starting material) to produce the neutral radical and deprotonated flavin, which are both able to undergo further reduction at the electrode surface, forming FlH^{-} and $Fl^{2\bullet-}$ respectively. At faster scan rates the proton transfer reaction is outrun, and the anionic radical is further reduced to the dianion. Digital simulation techniques enabled the determination of four formal electrode potentials as well as the equilibrium and rate constants associated with four homogeneous reactions.

For the N3-methylated flavin **2**, the radical anion does not undergo a proton transfer reaction in aprotic organic solvents due to the lack of a suitable proton source, and is reduced to the dianion, resembling N3-protonated flavins at high scan rates. The dianion, however, is able to deprotonate the trace water present in the solvent, forming FlH^{-}. Addition of excess water to these solutions showed that the anionic radical also undergoes proton transfer reactions with water at very high water concentrations.

For unbuffered aqueous solutions of FMN and FAD at intermediate to high pH, the hydrogen-bonded dianion is formed in one voltammetric wave, which can then deprotonate water to form FlH^{-}, while at sufficiently low pH ($[H^{+}] \geq [Fl]$), a $2e^{-}/2H^{+}$ reduction occurs in one voltammetric wave. In buffered aqueous solutions at pH 3 – 5, a

direct a $2e^-/2H^+$ reduction to FlH_2 was observed, while at pH 7 – 11, a $2e^-/H^+$ reduction to FlH^- was observed. At sufficiently high scan rates, another oxidative wave was observed corresponding to the oxidation of the hydrogen-bonded dianion, indicating that an equilibrium process is occurring after reduction.

List of Abbreviations

C Step	Chemical step
CYPOR	NADPH-Cytochrome P450 oxidoreductase
CV	Cyclic voltammetry/ cyclic voltammogram
DMSO	Dimethyl sulfoxide
DNA	Deoxyribonucleic acid
ECE	Electron transfer – Chemical – Electron transfer (mechanism)
EE	Electron transfer – Electron transfer (mechanism)
EEC	Electron transfer – Electron transfer – Chemical (mechanism)
EPR	Electron paramagnetic resonance
E step	Electron transfer step
Fc/Fc^+	Ferrocene/ferricenium redox couple
Fl	Flavin
FMN	Flavin mononucleotide
FAD	Flavin adenine dinucleotide
FNR	Ferredoxin $NADP^+$ reductases
GC	Glassy carbon (electrode)
HDME	Hanging drop mercury electrode
Hq	Hydroquinone
NAD	Nicotinamide adenine dinucleotide
NADP	Nicotinamide adenine dinucleotide phosphate
NMR	Nuclear Magnetic Resonance
OLED	Organic light-emitting diodes
OSTLE	Optically semi-transparent thin layer electrochemical (cell)
PCET	proton-coupled electron transfer
PDH	pyranose dehydrogenase
PDR	phthalate dioxygenase reductase
Rb	Riboflavin

RDE	Rotating disk electrode
SCE	Saturated calomel electrode
Sq	Semiquinone
UV-vis	Ultraviolet-visible
UV-vis-NIR	Ultraviolet-visible-near Infrared
VK_1	Vitamin K_1

List of Symbols

D	diffusion coefficient
E^0	formal potential
ΔE_{pp}	peak-to-peak separation
E_p^{ox}	oxidative (anodic) peak potential
E_p^{red}	reductive (cathodic) peak potential
i_p^{ox}	oxidative (anodic) peak current
i_p^{red}	reductive (cathodic) peak current
K_a	acid dissociation constant
k_b	backward rate constant
K_{eq}	equilibrium constant
k_f	forward rate constant
k_s	heterogeneous electron transfer rate

Chapter 1

Introduction

1.1. Flavins as coenzymes – the importance of flavin coenzymes in biological systems

Riboflavin (vitamin B_2), like all vitamins, is an essential dietary requirement for humans because our bodies are unable to synthesize it. Once ingested, riboflavin is first modified to flavin mononucleotide (FMN) by riboflavin kinase and further converted to and flavin adenine dinucleotide (FAD) by FAD synthetase.[1] FMN and FAD are cofactors of many flavoproteins which catalyze a large number of redox reactions in biological systems, because flavins have the ability to accept and donate electrons from a large number of functional groups.[2–11] This makes riboflavin essential in ensuring that our body functions normally as well as maintaining good health.

Scheme 1.1. The structure of biologically available flavins, including riboflavin (vitamin B_2), flavin mononucleotide (FMN), and flavin adenine dinucleotide (FAD).

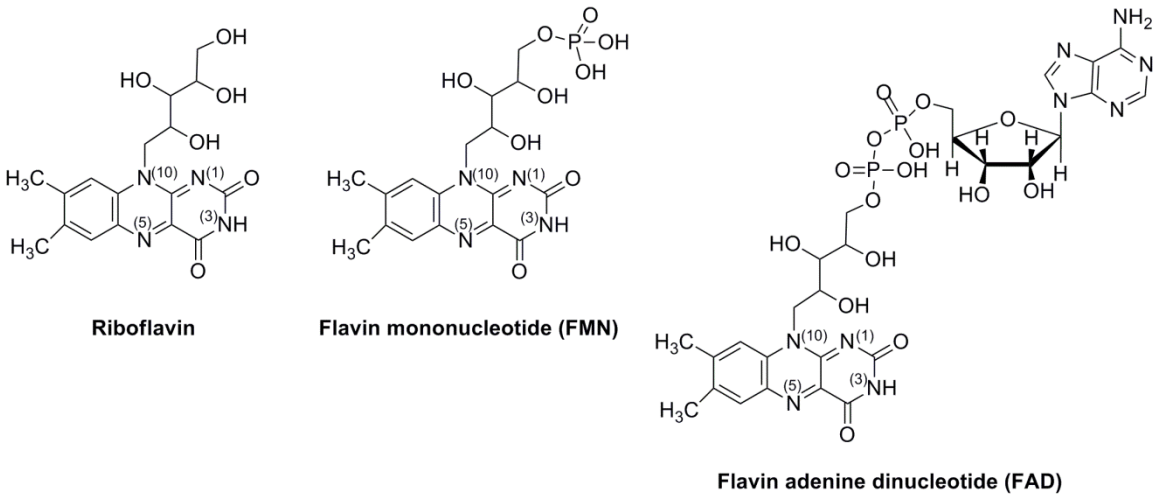

When bound to a flavoprotein, flavins are capable of catalysing the dehydrogenation of many organic compounds, including alcohols, amines, α-amino acids, reduced nicotinamide nucleotides, dithiols, and even saturated C-C bonds.[12] The flavin becomes reduced to the dihydroflavin in order to dehydrogenate the organic substrate, and needs to be oxidized back to the fully-oxidized flavin in order for the flavoprotein to function catalytically. The fully-oxidized flavin would then be regenerated by reducing a suitable electron acceptor. The acceptor may in some cases be the oxidized form of the same type of compound that serves as the reducing substrate, e.g. an oxidized nicotinamide nucleotide, a disulphide or an unsaturated compound such as crotonyl-CoA. In such cases, the flavoprotein would be classified as a transhydrogenase.[12] In other cases, the electron acceptor will be molecular O_2 (such a flavoprotein would be classified as an oxidase or a oxygenase depending on the types of reactions that occur when oxygen is reduced). Often, another redox protein could also be the electron acceptor, such as an iron-sulphur protein or even a different flavoprotein.

Although flavins are cofactors of flavoproteins which catalyse many reactions, the particular importance of flavins as cofactors is because flavins have unique properties that other cofactors such as nicotinamide do not possess: that is the reactivity with oxygen and the ability to undergo both two-electron and one-electron processes.[11–12]

There exist a number of flavoproteins which do not function as enzymes, and instead take part in different biological processes. For example, phototropins are blue-light photosensor proteins that regular phototropism, chloroplast movement and stomata opening.[13–14] Photolyase uses blue light for ultraviolet-damaged DNA repair.[15–20] LOV domains and cryptochrome photoreceptors participate in the entrainment of circadian rhythms (i.e. the biological clock), where the photoexcitation of the flavin cofactor leads to changes in redox and protonation states that ultimately couple to protein conformation

change and target engagement.[21–23] It has also been proposed that cryptochromes could act as magnetoreceptors that allow migratory birds to navigate via the direction of the Earth's magnetic field, where photochemically formed flavin-tryptophan radical pairs are responsible.[24–27]

There also exist a number of complex flavoproteins that incorporate more than one flavin cofactor (e.g. hepatic NADPH-cytochrome P-450 reductase and Na^+-pumping NADH-ubiquinone oxidoreductase[28–29]). For some of the more complex flavoproteins, the exact mechanisms are still under debate and highly controversial.

1.1.1. Reactivity with oxygen

A large number of flavoproteins can use molecular oxygen as an electron acceptor, and this enables flavoproteins to be involved in aerobic processes.[12] The reported reduction potentials of the Fl/FlH_2 couple in protein environments[32], are lower than the reduction potential of the O_2/H_2O_2 couple. As a result, flavin-mediated oxidations that involve dioxygen as an electron acceptor are thermodynamically favourable.[30–32] However, the reaction is spin forbidden because the electrons in the dioxygen are in a triplet state, but the flavin oxidases overcome this restriction by a stepwise electron transfer,[31] first forming the anionic radical that is thermodynamically stabilized. Thus, the ability of flavins to use molecular oxygen as an electron acceptor is due to the ability of the fully-reduced flavin to undergo a one-electron oxidation.

Different flavoproteins can also react differently with molecular O_2, in some cases one electron transfer is carried out, with superoxide (O_2^-) and flavin semiquinone as the intermediate products of the reaction. For flavoproteins where the two-electron reduction of O_2 to H_2O_2 occurs, such a protein is classified as an oxidase. In another class of flavoproteins, classified as the oxygenases, one atom of the O_2 molecule is incorporated

into H_2O, and the other is incorporated into another substrate within the enzyme to form an oxygenated product.[12]

It is important to note that the reduced form of free flavins (flavins not bound to a flavoprotein) are reactive with oxygen, however it is the flavoprotein structure and interactions that occur at the flavin binding site that dictate the reactivity of the reduced flavoprotein with molecular oxygen. For example, if a flavoprotein is not known to include molecular oxygen as an electron acceptor, it is likely that oxygen is not able to access the flavin binding site.[32] Different intermolecular interactions between the flavin and the protein structure could stabilize a particular flavin species, and direct the oxygen to react with the flavin at a particular location of the flavin isoalloxazine ring.

1.1.2. Versatility of undergoing one- or two-electron processes

Flavin cofactors (FMN and FAD) have a higher versatility than nicotinamide cofactors (NADP and NAD) as flavin cofactors can undergo both one- and two-electrons processes, while nicotinamide cofactors strictly undergo two-electron processes. Some flavoproteins mediate two-electron processes (e.g. lipoyl dehydrogenase and gluthathione reductase), some flavoproteins mediate one-electron processes (e.g. flavodoxin[33–34]), while others have a unique versatility to act as mediators between two-electron donors such as NADH and succinate, and one-electron acceptors such as heme Fe (e.g. ferrodoxin-$NADP^+$ reductase and NADH-cytochrome b_5 reductase[35]).[12]

This versatility is due to the ability of flavins to form a stable radical species (the flavosemiquinone). Some flavoproteins are able to stabilize the anionic radical species while others are able to stabilize the neutral radical species, and a large part of the reason why the radical species can be stabilized is due to the intermolecular interactions between the flavin cofactor and the protein or water molecules that are bound within the protein.

The effects of different types of intermolecular interactions will be further discussed in the following sections (**1.1.2** and **1.2**).

1.1.3. Deficiency of flavoproteins

As most flavoproteins are located in the mitochondria, a deficiency of riboflavin, due to insufficient dietary intake or due to gene mutation of the riboflavin transporter or other flavoproteins, would result in diseases connected to deficiencies in mitochondrial processes.[36] Other compartments (e.g. endoplasmic reticulum and peroxisomes) could also be affected by flavoprotein dysfunctions and deficiencies. The large quantities of flavoproteins indicate that a large number of regular biological functions could be affected when riboflavin intake is insufficient. However, the mutation of a single gene affecting a flavoprotein could also cause adverse effects and diseases. Similar clinical manifestations could be observed when any one of the flavoproteins involved in the same metabolic pathway is affected. For example, Leigh syndrome may be caused by a defect or deficiency in any of the respiratory electron transfer complexes in the inner mitochondria membrane including complex I (which contains the FMN-dependent NDUFV1), complex II (which contains the FAD-dependent subunit A) and FOXRED1 (a molecular chaperone of complex I which contains FAD).[36] Also, glutaric acidemia can be caused by a deficiency of electron transferring flavoprotein, glutaryl-CoA dehydrogenase or electron transferring flavoprotein-ubiquinone oxidoreductase.[36]

Since mutations are irreversible, effects on the biological function of a protein caused by such mutations are generally untreatable. However, in some flavoproteins, it was found that the mutation involving an amino acid exchange led to a decreased binding affinity of the flavin cofactor. In these cases, a much higher riboflavin intake may increase the concentration of FMN and FAD in the body and thus increase the amount of active holo-enzyme, and have a positive effect on the symptoms.[36–37] Ames and

coworkers have compiled a list of flavoproteins where this method could be implemented.[37] It was recently discovered that the neurological disorders, Brown-Vialetto-Van Laere and Fazio-Londe syndrome, were caused by mutations in the gene encoding an intestinal riboflavin transporter[38–39] and initial results indicate some positive results of increasing the riboflavin intake of patients.[38,40–41] However, as the structure of the intestinal riboflavin transporter and the mutated form have not been extensively studied, it is not clear if riboflavin supplementation would have a lasting effect.[36]

Several other flavoproteins, many of which are located in cellular membranes, have structures that have not been solved as they are more difficult to obtain in sufficient quantity. The lipophilic character of the integral membrane or associated proteins also creates additional challenges for structural elucidation by X-ray crystallography.[36]

It is important to know the structures of flavoproteins and understand the reaction mechanisms, thus, when a mutation is present, the structure of the mutated flavoprotein would allow for the understanding of what causes the flavoprotein to be unable to perform its regular function. Mutations that cause small structural changes could retain most of its function, but less efficiently. However, mutations that affect important structural features, and those that affect the binding of the flavin cofactor or substrate, as well as those that affect the direct environment of the flavin cofactor are expected to result in large changes in flavoprotein function. The effects of intermolecular interactions on flavoprotein function are discussed in the following section.

1.1.4. The relation between intermolecular interactions and flavoprotein function

The ability of flavins to undergo different processes in different flavoproteins indicates the importance of the immediate environment of the flavin (e.g. the isoalloxazine ring of the flavin accessible by solvent[35–42] and/ or oxygen[5], or buried in a hydrophobic region[33–

[34]), and intermolecular interactions between flavin and the flavoprotein (e.g. π–stacking[43] and H–bonding[44–47]).

In the next section, some examples of such interactions will be briefly discussed, based on known flavoprotein structures and mechanisms. Particular attention will be placed on the effect on these interactions on the thermodynamic stabilization or destabilization of the different flavin species (i.e. shifting the reduction potentials of certain flavin redox couples towards more positive or negative values).

The understanding that the mutation of a flavoprotein could lead to large changes in its function is also indicative of the importance of the environment where the flavin is located.

1.2. The different classes of flavoproteins

Flavin researchers have compared the structure of wild-type flavoproteins and mutated flavoproteins to study the environment of the flavin cofactors as well as the interactions between the flavin cofactor and the protein, to discover the mechanism of each flavoprotein. Using synthetically modified flavins in place of FMN and FAD have also allowed for the better understanding of individual flavoprotein mechanisms.[12]

In order to develop a deeper understanding of the electron transfer mechanism of flavins in biological systems, it is important to first understand the interactions between flavins and its immediate environment in each flavoprotein. However, due to the large number of flavoproteins that are currently known, a more systematic approach would be to group flavoproteins that have similar functions.

In 1980, Hemmerich and Massey developed a method of classification of simple flavoproteins (excluding metal and haem-containing flavoproteins) into five major

divisions, based on the function of the flavoprotein, and discussed the similar reactivities of the flavoproteins in each division and their ability to thermodynamically stabilize the flavin radical.[12] Thermodynamic stabilization results in greater equilibrium concentrations of the radical and a shift in redox potentials, such that the oxidized-flavin/semiquinone couple is more positive than the semiquinone/hydroquinone couple.[12] The ability of the flavoprotein to thermodynamically stabilize the flavin radical is especially important as it would allow a fully-reduced flavin to donate one electron to a one-electron acceptor, a reaction unique to flavins.

Due to the difference in function of the different classes of flavoproteins, it is important to understand the structure of the flavin binding sites of each class of flavoproteins, especially the intermolecular interactions of the protein or substrate with the flavin cofactor. However, exceptions still exist within each class; the examples below would only be able to provide a general understanding, and is not representative of all the flavoproteins under that classification.

Flavoproteins that do not fall within this classification will also be briefly discussed, showing that much is yet to be understood regarding the possible flavin mechanisms, and much care must be taken when proposing mechanisms of less-understood flavoproteins.

1.2.1. Class 1: Transhydrogenases/ dehydrogenases

These enzymes catalyze 2-electron transfer between obligate 2 e^- donors and obligate 2 e^- acceptors. Transhydrogenases do not thermodynamically stabilize either flavin radical and do not show activity with oxygen.[12] Most flavin dehydrogenases fall under this classification, although some dehydrogenases have been named so because of their sluggish reaction with oxygen. It should not be assumed that all flavoproteins with a sluggish reaction with oxygen are transhydrogenases/ dehydrogenases. Some are actually

more structurally similar to oxidases or oxygenases, but whose structure prevents oxygen from accessing the flavin cofactor.

An example of a transhydrogenase is glutathione reductase, which catalyzes the reduction of glutathione disulfide at the expense of NADPH. Glutathione reductase forms a homo-dimer and glutathione disulfide is processed by side chains from both subunits and is bound between the subunits.[48–49] The dimer interface is an important part of the enzyme and no enzymatic activity would be observed with only one subunit. [48–49] At the interface area, a cavity with channel extensions to the solvent was observed. Large clusters of integral water molecules are found around the binding sites of NADPH, glutathione disulfide and FAD.[50] At the active site, hydride transfer from nicotinamide to flavin N5 occurs while the 2 rings are stacked together.[51]

1.2.2. Class 2: oxidases

These enzymes combine the dehydrogenation of a substrate with the reduction of molecular O_2 to generate H_2O_2.[12]

In the reductive half reaction, the organic substrate is oxidized by a hydride (H^-) transfer to the initially fully-oxidized flavin, forming the (net) $2e^-$ reduced flavin (FlH^-) and the oxidized product or product intermediate. The protonated base of the protein close to the N1 position exerts an inductive effect and facilitating nucleophilic addition to the flavin at the N5 position,[12] such as the direct hydride transfer from a substrate, as shown in Scheme 1.2. The crystal structure of glycolate oxidase has shown that a lysine residue of the protein backbone is orientated to the flavin N1–C2=O locus and is within hydrogen bonding distance to both atoms.[52] Ghisla *et al.*[8] and Mattevi *et al.*[53] have proposed that the protein substrate is oxidized by direct hydride transfer to the flavin N5, and the proper positioning of the substrate and the reactive flavin N5 atom is essential.[54]

Another example of a nucleophilic addition to the flavin N5 position is in fungal nitroalkane oxidase. The α-proton of the nitroalkane is abstracted, and the resultant carbanion attacks the flavin N5 position to form a covalent adduct with the flavin, generating a cation flavin imine. Attack by water forms the reduced flavin and the final product, the aldehyde or ketone.[55]

Scheme 1.2. Hydride transfer mechanism to the flavin cofactor. [Adapted from Ref. 12]

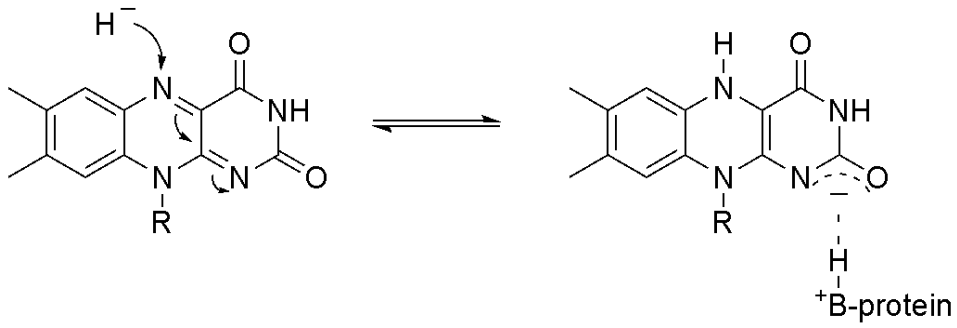

In the oxidative half reaction, O_2 is reduced to H_2O_2 via a stepwise electron transfer.[31] During the stepwise electron transfer to molecular oxygen in the reductive half reaction, the red anionic radical ($Fl^{-\bullet}$) is stabilized by hydrogen-bonding from the protein to the radical anion with its negative charge localized in the N1–C2=O position.

Scheme 1.3. Stabilization of the red anionic radical [Adapted from Ref. 12]

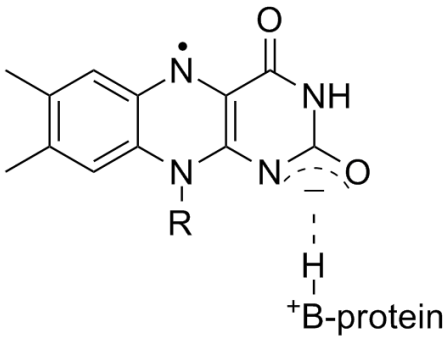

For GMC (glucose-methanol-choline)-type oxidases (e.g. glucose oxidase, pyranose oxidase and cholesterol oxidase), a conserved histidine residue at the active site[56] is able to assist in substrate oxidation as well as flavin reoxidation by O_2.[32] Mutagenesis studies on glucose oxidase has shown that protonation of this histidine is essential for catalysing O_2 reduction.[57] In other oxidases, a positively charged residue is present around the flavin N5,[58] and is postulated to stabilize the superoxide anion (formed during the first stepwise electron transfer to dioxygen) via electrostatic interactions.[58–63]

In vanillyl alcohol oxidase-type flavoproteins, it was observed that a covalent linkage between the flavin cofactor and the protein increases the redox potential of the flavin significantly, limiting the number of feasible electron acceptors.[32,64] It was also observed that bicovalently linked flavin cofactors have a very open active site, while retaining the cofactor in position for catalysis, allowing them to accept bulky substrates.[65–66]

The accessibility of the active site is a factor for the ability of oxidases to use O_2 as an electron acceptor.[32] Cholesterol oxidase and alditol oxidase contain oxygen channels that lead oxygen to the flavin binding site.[67–68] In yeast Ery, a hydrophobic channel leads to the oxygen-reactive N5-C4a of FAD, but rat Erv1 without this channel has poor reactivity with O_2.[69] In this case, it has been proposed that flavin transfers an electron to cytochrome c oxidase, leading to water as a by-product instead of hydrogen peroxide.[69]

1.2.3. Class 3: oxygenases

Oxygenases catalyze the dehydrogenation of a substrate and the reduction of molecular O_2, with one oxygen atom forming H_2O and the other incorporated into a different substrate (AH → AOH). These enzymes display no stabilization of either radical form.[12]

Of the Class 3 enzymes, para-hydroxybenzoate hydroxylase is one of the most extensively studied and it belongs to the biggest subgroup of the flavoprotein monooxygenases.[70]

The flavin isoalloxazine ring is observed to move during catalysis, pivoting 7–8 angstroms from the hydrophobic environment within the protein to the protein edge exposed to solvent.[71–74] In the resting enzyme the isoalloxazine ring resides within the flavoprotein[75–76], and in this position, the substrate is directed by surface residues through a channel into a binding pocket, and held by hydrogen-bonding interactions and/or charge pairing interactions.[72,77] For the Class A flavoprotein monooxygenases, substrate binding stimulates the reaction with the electron donor (NADPH).[78] Binding of this electron donor by positively-charged residues at the solvent interface causes conformation changes in the protein that induces the isoalloxazine ring to pivot to the solvent exposed conformation where 2 e^- reduction of the flavin cofactor occurs via a hydride transfer from NADPH[77,79–81]. Hydride transfer occurs due to the proximity of 4-R hydrogen of NADPH and the flavin N5 position.[49] The oxidized NADP+ dissociates and the reduced flavin (FlH^-), now negatively-charged, is drawn back to the solvent-free positive electrostatic field of the active site.[82–84]

After flavin reduction, the target substrate and reduced flavin reside in a hydrophobic environment where the reaction with O_2 can occur in the absence of the destabilizing influence of water.[85] A single e^- transfer from the reduced flavin to O_2 occurs.[86–87] As a result of the 1 e^- transfer, a radical pair of the flavin semiquinone radical ($FlH^{\bullet}$) and the superoxide anion ($O_2^{\bullet-}$) is formed.[88] The second e^- transfer from the flavin semiquinone radical to the superoxide anion leads to the formation of the C4a-peroxyflavin key intermediate. Electrophilic attack of the substrate by C4a-peroxyflavin, and the transfer of an oxygen atom of the peroxo group, leads to the formation the hydroxylated intermediate

and a C4a-hydroxyflavin[89], which then decays to form the oxidized flavin and water.[90] It is believed that these steps are required to occur when the flavin is residing within the protein and not in contact with solvent molecules, otherwise radical recombination and solvent-induced elimination would lead to the production of hydrogen peroxide (H_2O_2), without the incorporation of an oxygen atom into the substrate.[71]

1.2.4. Class 4: Dehydrogenase/ Electron-transferases

These enzymes transform a two-electron process into a one-electron process. The reverse reaction is carried out during photosynthesis. All biological redox chains contain at least one such flavoprotein, in order to allow transfer of electrons between obligate 2 e^- donors (nicotinamide nucleotides) and obligate 1 e^- acceptors (haem proteins and iron-sulphur proteins). The semiquinone form is essential for this transformation, and the thermodynamic stabilization of the blue neutral radical is almost always observed in the class of flavoproteins.[12] As shown in Scheme 1.4, the blue neutral radical reflects a strong hydrogen bridge between the protein and the flavin N5.

Scheme 1.4. Stabilization of the blue neutral radical. [Adapted from Ref. 12]

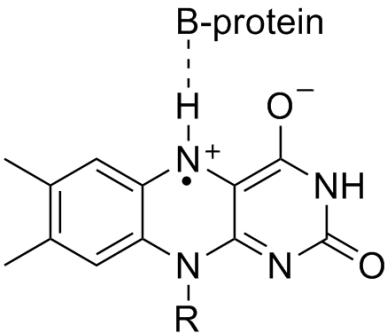

Ferredoxin $NADP^+$ reductases (FNRs) catalyze electron transfer between NADP(H) (2 e^- donor) and their cognate ferredoxin or flavodoxin partners (1 e^- acceptor).[91] In a large number of flavoproteins, the flavin cofactor is reduced by 2 e^- by a direct hydride transfer. However, X-ray crystallography and NMR spectroscopy of ferrodoxin NADP reductase

from *Pseudomonas aeruginosa* in complex with $NADP^+$ has shown that this mechanism is unlikely for this family of flavoproteins. This is due to the side chain of the C'-terminal Tyr blocking the parallel and adjacent stacking of the nicotinamide ring (of $NADP^+$) and the isoalloxazine ring (of FAD), and the large conformational changes required in order for direct hydride transfer to occur. Instead, stepwise hydride transfer in the form of sequential electron-proton-electron transfer was proposed, where a tunneling pathway facilitates electron transfer and a network of structural water molecules facilitates the translocation of a proton from NADPH to FAD.[91]

Another flavoprotein within this class is phthalate dioxygenase reductase, which catalyzes electron transfer between NADH and [2Fe-2S]. FMN, NAD and [2Fe-2S] are bound in different domains, and domain-domain packing places the isoalloxazine ring of FMN in the central cleft in the molecule, where it is optimally positioned for the electron transfer from NADH to [2Fe-2S]. The flavoprotein structure is similar to FNR above, such that direct hydride transfer might not occur. Analysis of the crystal structure of NADH:PDR^{2-} and the fully reduced species PDR^{3-} shows structural changes that accompany reduction. Two rearrangements that stabilize the reduced species (both the semiquinone and hydroquinone forms) are observed, with the O_γ of Ser58 moving closer to N5 of the flavin to form a hydrogen bond and a solvent moves to interact with N1 of the flavin.[45] This provides physical evidence that hydrogen bonding of the protein with N5 of the flavin would stabilize the neutral radical, as is observed for this class of flavoproteins.

The binding site of the flavin cofactor in NADH-cytochrome b_5 reductase is situated in a large crevice between the two domains of the flavoprotein,[42] and there is sufficient open space at the *re* side of the flavin N5 position, which would allow easy access to NADH for the direct or stepwise hydride transfer to the fully reduced flavin. NAD^+ binds

preferentially to the reduced enzyme, and when NAD^+ is bound, the flavoprotein is able to stabilize the flavosemiquinone form,[35] enabling it to donate one electron to one-electron acceptors. It is important to note that, unlike the other class 4 flavoproteins, NADH-cytochrome b_5 reductase stabilizes the anionic radical instead of the neutral radical.

1.2.5. Class 5: Pure Electron-Transferases

These enzymes (e.g. flavodoxin) catalyze one-electron transfers, where the flavoproteins function catalytically between the fully-reduced species and the semiquinone species. Class 5 enzymes are involved in obligatory one electron transfer reactions, and stabilize the blue neutral radical (Scheme 1.4).[12]

In flavodoxin, the flavin cofactor exists in a hydrophobic environment, with one or two bound water molecules in its vicinity. While the dimethylbenzene moiety of the flavin cofactor is solvent accessible and appears to be utilized for electron transfer, the reactive isoalloxazine ring is buried in the interior of the protein. After the flavin is reduced to its anionic radical form, the flavin N5 position is protonated to form the neutral radical species by a proximal amide proton of the protein structure.[34,44,92] It has been proposed that the reduction potential of the neutral radical bound in flavodoxin is more negative (harder to reduce) than in free flavin by 0.3 – 0.4 V, due to thermodynamic stabilization of the species by H-bonding interactions of the flavin N5-H with a carbonyl oxygen of the protein structure.[34] Therefore, after the anionic radical is protonated to form the neutral radical, it is not further reduced, as it does for free flavin. Thus, flavodoxins are able to catalyze a 1 e^- process.

Interestingly, the stabilization of the neutral radical differs for different flavodoxins, as the reduction potentials for the fully-oxidized flavin/ flavin semiquinone couple fall into

two groups with significantly different reduction potentials.[93–94] In *D. vulgaris* and *Clostridium MP* flavodoxins in the less negative reduction potential group, a new hydrogen bond to the flavin N5 of the neutral radical is observed. In the more negative reduction potential group, which includes C. crispus and Anabaena 7120 flavodoxins, the hydrogen bond with the flavin N5 was already observed in the oxidized state. In the former case, the semiquinone form is stabilized by the newly formed hydrogen bond, but this effect is not observed for the other group of flavodoxins with an existing hydrogen bond.[93] For the latter group, destabilization of the fully-reduced species by aromatic stacking interactions would ensure flavodoxins catalyze only 1 e^- processes.

X-ray crystallographic studies show significant aromatic stacking interactions between the flavin cofactor and the aromatic side chain residues at the flavin binding site of flavoproteins. For example, the flavin cofactor of flavodoxin isolated from *Desulfovibrio vulgaris* is sandwiched between a tyrosine and a tryptophan.[93] Aromatic stacking interactions play a dual role in flavoprotein function, providing efficient recognition of the flavin cofactor and serving to modulate its reactivity and redox properties.[43]

The structural data of wild type and mutated flavodoxins support the hypothesis that the very negative reduction potential of the semiquinone/hydroquinone couple in the wild-type protein is modulated to a large extent by the energetically unfavorable formation of the flavin hydroquinone anion in the apolar (aromatic) environment of the flavin binding site.[95–97]

A combination of the effects of hydrogen-bonding stabilizing the flavin neutral radical, and aromatic stacking interactions destabilizing the fully-reduced (hydroquinone) form, leads to different flavin reduction reactions from other flavoproteins, which undergo direct 2 e^- reduction.

1.2.6. Exceptions from this classification

Many flavoproteins are excluded from this classification, such as more complex flavoproteins (e.g. diflavin reductases), but recent studies has led to the discovery of exceptions that exist within this classification, which could possibly impact the direction of future flavin research.

1.2.6.1. Diflavin reductases

Cytochrome P450 reductase and Methionine synthase reductase belongs to a family of diflavin reductases, which include one molecule of FAD and one molecule of FMN.

NADPH-Cytochrome P450 oxidoreductase (CYPOR) shuttles electrons from the obligate 2 e^- donor NADPH → FAD → FMN to members of the ubiquitous cytochrome P450 superfamily. FAD is reduced by NADPH via a hydride transfer, and passes the electrons to FMN one at a time. FMN then donates electrons to cytochrome P450 one electron at a time.[98–99] While crystal structures show that the isoalloxazine rings of the two flavins are in van der waals contact[100], but the observed interflavin electron transfer rate[101–102] (30–55 s^{-1}) is approximately 9 orders of magnitude lower than the predicted value[103] (~10^{10} s^{-1}) suggesting that the electron transfer is conformationally gated, with large structural changes occurring within the flavoproteins when shuttling electrons between NADPH and cytochrome P450. It was shown that in the "closed" conformation, FAD and FMN are in contact, but FMN would pivot away from FAD in the "open" conformation in order to transfer electrons to cytochrome P450.[98]

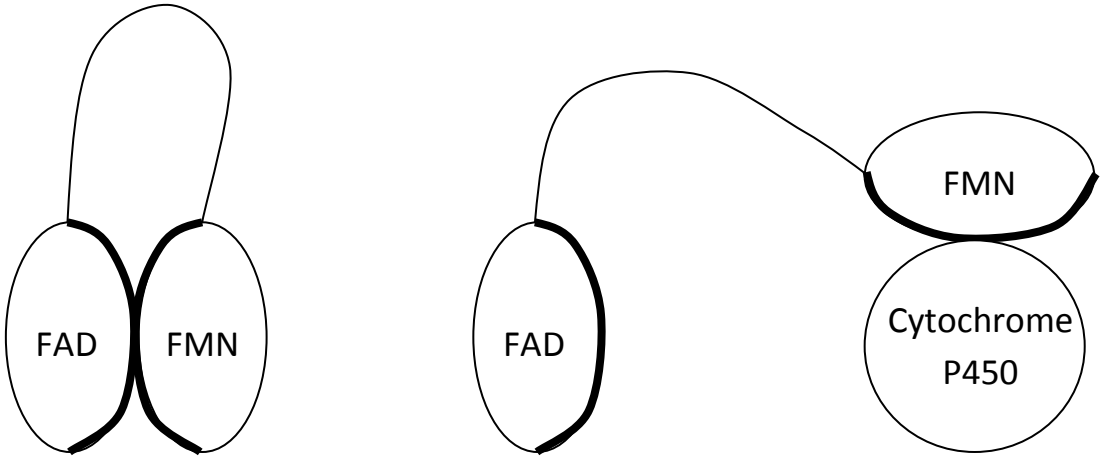

"Closed" Conformation of CYPOR

"Open" Conformation of CYPOR

Figure 1.1. Schematic representation of the "Closed" and "Open" conformations of CYPOR and related diflavin reductases.

It is interesting to note that while obligate 2 e^- donors like NADPH often donate 2 e^- in a direct hydride transfer, electron transfer between two flavins instead occur one at a time. The reported reduction potentials of FMN ($FMN_{ox/sq}$ = –110 mV *vs.* SCE, $FMN_{sq/hq}$ = –270 mV *vs.* SCE) and FAD ($FAD_{ox/sq}$ = –290 mV *vs.* SCE, and $FAD_{sq/hq}$ = –365 mV *vs.* SCE) in CYPOR[104–106] indicate significant stabilization and destabilization of some of the flavin species.

1.2.6.2. An oxidase (class 2) that undergoes proton-coupled electron transfer reactions

Pyranose 2-oxidase is the only one in the family of flavin oxidases that the C4a-hydroperoxyflavin has been observed.[107–109] This species is more commonly observed in the monooxygenases.[12] It has recently been proposed that the fully reduced flavin cofactor would reduce the triplet dioxygen via proton-coupled electron transfer, where the proton transfer from a protonated histidine residue occurs concomitantly with the first electron

transfer. This forms the flavin semiquinone:$^{\bullet}$OOH radical pair (FADH$^{\bullet}$:$^{\bullet}$OOH$_T$) in the triplet state, which then undergoes spin transition (with a small energy requirement) to form the open-shell singlet diradical (FADH$^{\bullet}$:$^{\bullet}$OOH$_S$). The opposite spins on the FADH$^{\bullet}$ and $^{\bullet}$OOH facilitates the formation of C4a-hydroperoxyflavin. A direct proton transfer from the flavin N5−H to the peroxide leaving group leads to H_2O_2 elimination.[107, 110]

The proton-coupled electron transfer process for the reaction of reduced flavin and dioxygen described for pyranose 2-oxidase is different from the current understanding that describes the first step as an electron transfer to generate a radical pair of flavinsemiquinone and superoxide anion before subsequent proton transfer.[9, 88] Instead, similarities with monooxygenases are observed with C4a-hydroperoxyflavin as an observed intermediate, but decay via different pathways.

1.2.6.3. A monooxygenase (class 3) with a new redox state

As has been discussed, monooxygenases are known to oxygenate substrates using the C4a-hydroperoxyflavin as a key intermediate. However, EncM, a bacterial flavoprotein from enterocin biosynthesis, has been discovered to use the flavin-N5-oxide to oxygenate enolate substrates.[111] The N5-oxide is a stable flavin oxidation state, and this is the first instance of the N5 oxide observed to be formed in nature. It is an over-oxidized form that carries an oxygen atom derived from reduction of O_2 and cleavage of the O–O bond. However, the mechanism of N5-oxide formation and the mechanism of oxygen transfer is yet unknown, and requires much further study.[111]

It is interesting to note that this N5 oxide intermediate has been previously proposed as part of the oxidation mechanism of reduced monooxygenases,[112–113] but later rejected when the C4a-hydroperoxyflavin intermediate was observed.

Scheme 1.5. Observed flavin-oxygen intermediates during the reduction of dioxygen

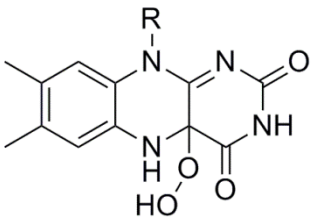

C4a-hydroperoxyflavin

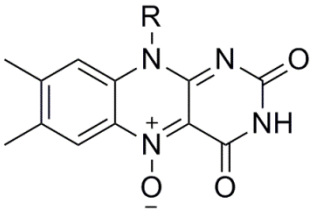

Flavin-N5-Oxide

1.3. Current and potential applications of flavins and flavoproteins

Classical chemical oxidation methods often involve polluting reagents and harsh conditions. Despite of the harsh conditions used, such reactions often result in poor chemoselectivity and enantioselectivity, which are roadblocks for the synthesis of natural products or other compounds required by the flavor, fragrance, pharmaceutical and clinical industries. Meanwhile, in nature, oxidative enzymes such as the oxidases, oxygenases and dehydrogenases perform a wide variety of selective oxidation reactions, and the high selectivity can be exploited and developed for industrial purposes.[32]

In particular, oxidases, which only require molecular oxygen as electron acceptor for catalysis, would be more cost effective in biotechnological applications than the oxygenases or dehydrogenases, as these enzymes require other organic coenzymes (e.g. NAD(P)H and quinones) to function. Current industrial applications include oxidase-based biosensors as well as biocatalysts used in the synthesis of various chemicals.[32]

Flavin oxidases have been known for their ability to oxidize a variety of compounds and functional groups with chemoselectivity, regioselectivity and enantioselectivity, while only requiring molecular oxygen as oxidant.[32]

1.3.1. Flavoproteins as biosensors

Examples of flavin oxidases used as biosensors include glucose oxidase, one of the best known biosensors, which has been successfully and extensively used to monitor the blood glucose levels in diabetics due to its catalytic ability to oxidize glucose.[114] Due to the strict stereoselectivity of D-amino acid oxidases, these enzymes are often used to quantify D-amino acids in biological samples.[115] Fructosyl amino acid oxidase has recently been assessed on its ability to detect glycated proteins, a marker for hyperglycemia in diabetics. This is based on its ability to oxidize the C-N bond of an amino acid-carbohydrate adduct, forming the respective glucosone and amino acid.[116]

1.3.2. Flavoproteins as biocatalysts

Flavin oxidases also have been used extensively as biocatalysts in organic reactions, and well known examples include D-amino acid oxidase (for the synthesis of antibiotics),[117–118] as well as monoamine oxidases (for the synthesis of enantiopure fine chemicals by deracemisation).[119–120] With the large number of flavin oxidases with different substrate scopes that have been more recently discovered, one of which is reticuline oxidase which catalyzes oxidative C–C bond formation[121], there is a huge potential for further development of other flavoproteins as biocatalysts.

1.3.3. Free flavins as photoredox catalysts

While much of the industrial applications of flavins are based on flavins that are bound in a flavoprotein, recent work have shown that free flavins have a large potential as photoredox catalysts in organic synthesis as they absorb blue light (440 nm) in the visible part of the electromagnetic spectrum and are able to accept and donate electrons reversibly. When light is absorbed, the flavin isoalloxazine ring gains energy and can utilize oxygen to oxidize chemical compounds (e.g. benzyl alcohols oxidized into benzyl

aldehydes). Flavins can also be used to catalyze chemical reductions when oxygen is not present.[122–125]

1.3.4. Flavins as photoactive electron transporters

Other than catalysis, flavins also possess properties that are useful in photovoltaic systems, where they could be used as photoactive electron transporters, which is rare in current systems. Many organic semiconductors can be used as hole transport materials, but the electron-deficient property of flavins makes them possible candidates for electron-transporting materials, which are much more uncommon.[43] With the use of fullerenes as the electron acceptor/transport materials, power conversion efficiencies of 7.7% have been achieved.[126] However, fullerenes tend to have low absorption in the visible range, are difficult to synthesize and purify, and also very expensive. Conversely, flavins are known to absorb strongly in the visible range, which should lead to more efficient light harvesting and increased power conversion efficiency.

Organic light-emitting diodes (OLED), organic solar cells and organic field effect transistors are devices that could be developed if flavins can indeed be used as an electron-transporting compound. These devices would then be expected to have the same mechanism as electron transferases which are used as electron carriers in photoinduced electron transfer.[127] Other than their basic electron-deficient nature, flavins could be ideal candidates for electron-transporting materials due to several reasons. This includes the photostability of flavins, their reversible electrochemistry, and the ability for researchers to tune their optical, electronic and redox properties by manipulating the intermolecular interactions (aromatic interactions, H-bonding) and the environment where the flavin is located.[128]

1.3.5. Flavoproteins in biofuel cells

Other potential applications of flavoproteins include the usage of oxidoreductases in enzymatic fuel cells, which allows the direct conversion of chemical to electrical energy via biochemical enzymatic pathways. Like in traditional fuel cells, electrical energy is generated by coupling an oxidation reaction at the anode (e.g. glucose oxidized to gluconic acid) with a reduction reaction at the cathode (e.g. O_2 reduced to H_2O), and electrons generated at the anode flow to the cathode to be used up. As the oxidation and reduction reactions are electronically separated, electrons are forced through an external circuit, while ion movement inside the system maintains charge balance and completes the electrical circuit.[129] In the case of biofuel cells, flavin oxidoreductases show potential at the anodic side of an enzymatic biofuel cell due to their negative redox potential. In particular, fungal pyranose dehydrogenase (PDH) is able to oxidize a variety of sugars,[130] ranging from monosaccharides to polysaccharides and the flavin is bound in a shallow and open pocket. Having the flavin binding site in a shallow pocket means that the distance between the flavin binding site to the electrode is decreased. In the case of PDH, the distance is short enough to allow electron tunnelling (direct electron transfer).[131] While such devices have been shown to work, slow electron transfer rates and stability of the enzymes prevent them from providing a long term energy source. However, there is great potential for such devices when the technology is perfected, with uses such as a self-sustainable power source for implantable medical devices (e.g. pacemakers), requiring only blood sugar and oxygen to provide a constant current.

1.4. Electrochemistry of flavins

Many electrochemical studies have been conducted on flavins in buffered aqueous solutions, as potentiometry is often used to calculate the redox and ionization properties of protein-free flavin, in order to understand the implications of changes in redox and ionization properties of protein-bound flavin. While the exact values of the redox and ionization properties has remained under debate until as recently as 1999[132], it became widely-accepted that in buffered aqueous solution the fully-oxidized flavin (Fl) is reduced to flavohydroquinone (FlH_2) in "one step" in a $2e^-/2H^+$ reduction (by one step it is meant that the individual electron transfer and proton transfer steps occur in one observable voltammetric process).[133–142]

However, electrochemical studies on riboflavin in an aprotic organic media (DMSO) showed significant difference than that in buffered aqueous media. Tatwawadi *et al*.[143] and Sawyer *et al*.[144] investigated the voltammetric behavior of riboflavin in dimethyl sulfoxide and showed independently a reduction wave during the forward (reductive) scan and two oxidation waves after the scan direction was reversed (oxidative scan), which indicated that a chemical reaction had occurred to form a species that could be oxidized during the second oxidation wave. Tatwawadi *et al.* reported that when the scan rate was increased from 0.067 – 0.714 V s^{-1}, the second oxidation wave increased in size. It was postulated that the species that is associated to the second oxidation wave decomposed quickly and could not be observed when the scan rate was too slow.[143]

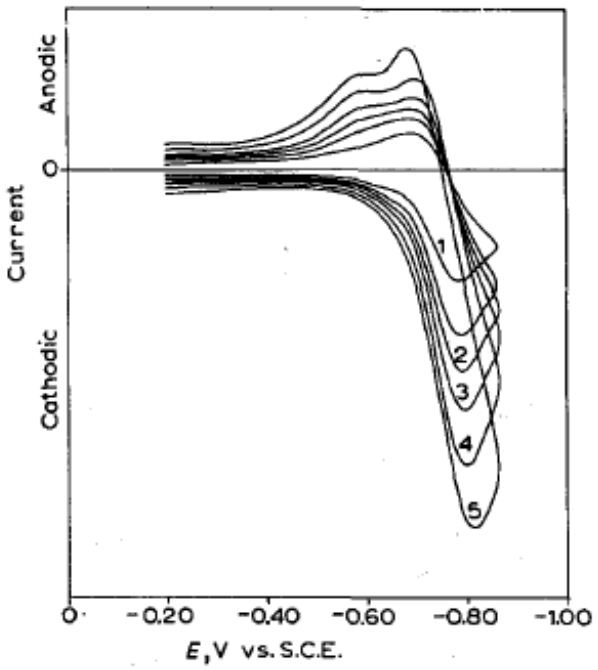

Figure 1.2. Cyclic voltammograms of 1.4 mM riboflavin with 0.1 M $NaClO_4$ in DMSO, where the scan direction was reversed after the first reduction peak, at scan rates of (1) 0.067; (2) 0.222; (3) 0.312; (4) 0.476 and (5) 0.714 V s^{-1} at a hanging drop mercury electrode. [Adapted from Ref. (143)]

Bulk electrolysis at potentials held slightly more negative than the first reduction peak potential, led to the understanding that one electron was transferred per molecule of riboflavin. EPR spectroscopy was used to analyze the reduced species after the first reduction, and the spectrum obtained was similar to that of the flavin anionic radical, but with a poor resolution. It was concluded that the first reduction wave corresponds to a single electron transfer, forming the riboflavin anionic radical species, similar to the reduction mechanism of quinones in aprotic solvents.[145–149] However, it was postulated that the riboflavin anionic radical would then decompose simultaneously into a structurally similar anionic radical and another species A. This species A was assigned to the second oxidation wave, and was expected to further decompose (as a more prominent oxidation wave was observed at higher scan rates). Two closely spaced reduction waves

were also observed at more negative potentials, and were attributed to the reduction of the decomposition products of the flavin anionic radical.[143]

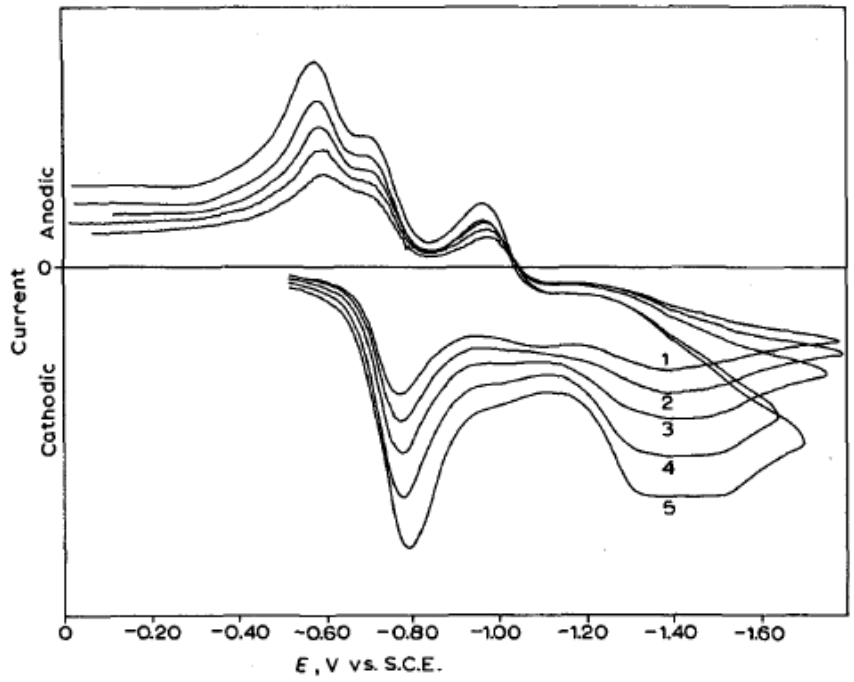

Figure 1.3. Cyclic voltammograms of 1.4 mM riboflavin with 0.1 M $NaClO_4$ in DMSO, where the scan direction was reversed after the second reduction peak, at scan rates of (1) 0.152; (2) 0.222; (3) 0.312; (4) 0.476 and (5) 0.714 V s^{-1} at a hanging drop mercury electrode. [Adapted from Ref. (143)]

It should be noted that at the time of the study conducted by Tatwawadi *et al.*, the working electrode commonly used for cyclic voltammetry was the hanging mercury drop electrode (HMDE) which is not often used in more recent years due to its toxicity. In this thesis, working electrodes used are the planar Pt or glassy carbon (GC) electrodes. It is also important to note that the differences in the electrode used by Tatwawadi *et al.* and in this work, could result in slight changes in the voltammograms obtained.

In a later study, direct current polarography of lumiflavin in methylene chloride solution conducted by Male et al[142] showed that the apparent number of electrons transferred was 1, agreeing with the value obtained by Tatwawadi et al using electrolysis.

Male et al rationalized that this apparent value could have 3 different interpretations, either a reversible one-electron reduction wave, two one-electron reduction waves with similar potentials that have merged, or a quasi-reversible two-electron reduction wave. EPR spectroscopy was conducted to show that the anionic radical was formed by bulk electrolysis, and concluded that in non-aqueous solvents, the anionic radical was formed by comproportionation of the dianion Fl^{2-} and fully-oxidized flavin.[142]

$$Fl + 2e^- \rightleftharpoons Fl^{2-} \qquad (1)$$

$$Fl^{2-} + Fl \rightleftharpoons 2\,Fl^{\bullet-} \qquad (2)$$

Significant progress on the electrochemical behavior of flavins in aprotic solvents was made by Niemz and Rotello and coworkers. In 1997, Niemz *et al*.[11] showed that when the imide proton at N3 was substituted by a methyl group, only one oxidation wave was observed when the scan direction was reversed, indicating that the reduction process was chemically reversible with little or no indication of a chemical reaction taking place. Yet, when a suitable proton donor (DH) was added, two oxidation waves were once again observed during the reverse scan, resembling the cyclic voltammogram of riboflavin. It was postulated that the anionic radical ($Fl^{\bullet-}$) (eq 3) was first formed by a 1 e^- reduction of fully-oxidized flavin, the anionic radical then underwent a homogeneous proton transfer from the proton donor to form the neutral radical $FlH^{\bullet}$ (eq 4). The neutral radical ($FlH^{\bullet}$) was then further reduced to form FlH^- [in either an ECE (eqs 3–5) or DISP1 (eqs 3,4 and 6) mechanism],[150] as the neutral radical was expected to be easier to reduce than the fully-oxidized flavin. Thus, on the reverse scan the first oxidation wave was attributed to the oxidation of $Fl^{\bullet-}$ and the additional (second) oxidation wave was attributed to oxidation of FlH^- (reduction potential less negative than that of $Fl^{\bullet-}$).[11] This indicated that the N3 proton on the flavin isoalloxazine ring was sufficiently acidic and was able to donate a proton to the anionic radical $Fl^{\bullet-}$.

$Fl + e^- \rightleftharpoons Fl^{\bullet -}$ (3)

$Fl^{\bullet -} + DH \rightleftharpoons FlH^{\bullet} + D^-$ (4)

$FlH^{\bullet} + e^- \rightleftharpoons FlH^-$ (5)

$Fl^{\bullet -} + FlH^{\bullet} \rightleftharpoons FlH^- + Fl$ (6)

Bulk electrolysis of N3-methylated flavin showed a stronger EPR signal as compared to N3-protonated flavin, which indicated that less radical species was obtained for N3-protonated flavin. This was reasoned to be due to the radical species being formed by comproportionation of FlH^- and Fl^- (fully-oxidized flavin that is deprotonated at N3) instead of being formed by a direct one-electron reduction of the fully-oxidized flavin.[11] UV-vis spectroscopy were performed in conjunction with electrolysis experiments, and the UV-vis spectra of the reduced compounds showed that the anionic radical was formed, but upon addition of excess proton donor, the anionic radical was protonated and further reduced.

With this basic mechanism in mind, Rotello and coworkers were particularly committed to creating a flavoprotein model and synthesize several receptors to mimic interactions between the flavin cofactor and the flavoprotein. In particular, H-bonding with N3 of the isoalloxazine ring and pi-stacking with the isoalloxazine ring was studied in detail.

It was discovered that as the extent of intermolecular π-orbital overlap increases in the host-guest complexes, where the flavin isoalloxazine ring is stacked between two aromatic residues simulating the interactions in flavodoxins, it was observed that the electrochemical reduction becomes more negative. This indicates that host-guest complexation is more favorable when the flavin is in the oxidized state than when it is reduced to its radical anion state, due to less favorable electrostatic interactions with the reduced flavin.[43] This is consistent with the observations in flavodoxins, where the

reduction potential of the flavin semiquinone/hydroquinone couple is much more negative due to π-stacking interactions.

Diaminopyridine derivatives were synthesized and used as a synthetic receptor which binds selectively to the imide moiety of the isoalloxazine ring through a 3-point hydrogen bonding. Binding to such a receptor generally shifts the reduction potential of the flavin to less negative potentials, regardless of the nature of the substituent groups. However, it appears that the nature of the substituent group plays a role in deciding which species will be formed after reduction.[151] Electron-donating groups attached to the diaminopyridine receptors increase the strength of two hydrogen bonds and weakens the other hydrogen bond, with the net effect of strengthening the binding of the receptor. The anionic radical is also stabilized by such a complex, and the anionic radical does not undergo protonation. Electron withdrawing groups would have the opposite effect, and seemingly promote the proton transfer from N3 of the oxidized flavin to N5 of the anionic radical forming the neutral radical.[43]

Scheme 1.6. Hydrogen-bonding interactions between flavin and diaminopyridine receptors

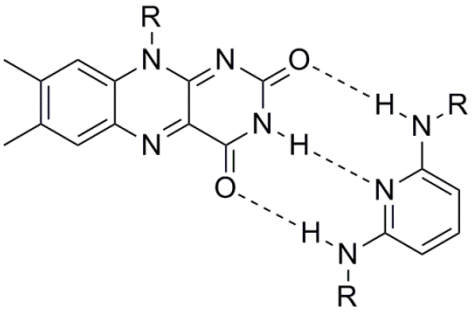

Synthetic flavins with varying substituents on C7 and C8 on the isoalloxazine ring were also investigated. Electron donating substituents would cause the reduction potential

to be more negative, and seems to favour formation of the neutral radical, while electron withdrawing substituents would cause the reduction potential to be less negative and would not form the neutral radical. This is a result of the electron-withdrawing groups lessening the charge at N5 and lowering the pK_a of this position such that it can no longer be protonated by the imide proton.[128]

1.5. Aim of the project

Cyclic voltammetry is a useful technique for studying the redox chemistry of flavins, as the flavins can be first reduced and the reduced forms of the flavins can be subsequently oxidized, much like what would occur in a flavoprotein. These electron transfer reactions are often followed by protonation reactions, also known as proton-coupled electron transfer (PCET) reactions. As flavins have 3 different oxidation states, the fully-oxidized flavin (Fl), the flavin semiquinone radical ($Fl^{\bullet-}$) and the fully-reduced flavin hydroquinone (Fl^{2-}), each with 3 possible ionization states (Scheme 1.7), we might expect to observe any of the 9 possible flavin species.

Scheme 1.7. The possible oxidation and ionization states of flavins.

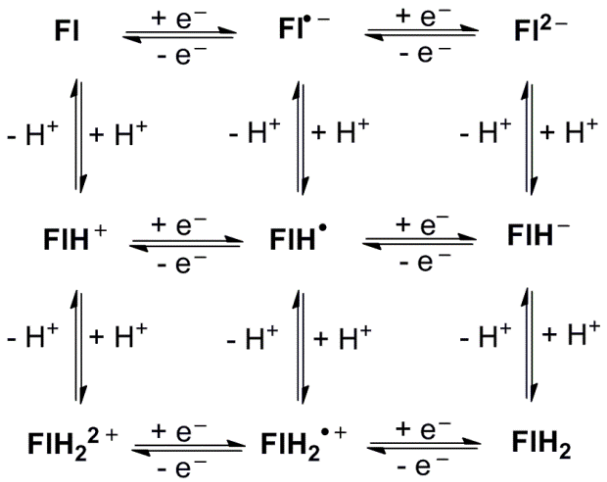

Proton coupled electron transfer (PCET) reactions are fundamentally important to a large number of biological and chemical processes, and plays an important role in

photosynthesis and reactions that occur within enzymes.[152–156] In flavoproteins, a large number of the reductive half reaction occurs via a hydride (H^-) transfer, where the oxidized flavin cofactor is reduced to FlH^- in one direct 2 e^- reduction. However, PCET reactions could occur during the reduction of flavins in class 5 flavoproteins[34,44,92] and the diflavin reductases.[98–99] A stepwise hydride transfer (electron-proton-electron transfer which is essentially a PCET reaction) has also been proposed for class 4 flavoproteins.[91] During the oxidative half reaction, PCET reactions can be expected for all flavoproteins except those that donate electrons to obligate 2 e^- acceptors (class 1 flavoproteins).

At the present moment, slow heterogeneous electron transfer rate between flavin bound to a flavoprotein and the electrode surface have deterred researchers from simply performing cyclic voltammetry on a flavoprotein. Slow heterogeneous electron transfer rates are often due to the significant distance between the flavin binding site and the surface of the protein, and thus the distance between the flavin binding site and the electrode surface. However, by changing the environment of free flavin in a cyclic voltammetry experiment, we are able to gain insights of the possible flavin intermediates and electron transfer pathways in different environments. By analyzing the flavoprotein structure, we aim to take another step towards the understanding of flavoprotein mechanisms.

As new electrode materials and methods are developed and the heterogenous electron transfer rate is increased sufficiently to obtain good voltammetric data of the flavin bound to the flavoprotein, a comparison with current work would yield interesting results. For example, it could be determined if a flavoprotein is able to stabilize a flavin radical, which form of the flavin radical is stabilized, and to what extent this radical is stabilized.

With flavins being regarded as a potential electron-transferring material for organic solar cells and organic light-emitting diodes, it is hoped that this work would also contribute in laying a strong foundation for future studies.[43,127]

Furthermore, the electrochemistry of free flavins in aprotic hydrophobic environments has not been fully understood. Niemz *et al.* had successfully answered some doubts that existed from previous research.[11] While Tatwawadi *et al.* had interpreted the observed one electron transfer per molecule during electrolysis to mean that the reduction wave was a one-electron reduction, and Male *et al.* had correctly interpreted it as a two-electron reduction followed by a comproportionation reaction with another species, but attributed the comproportionation to be between fully-oxidized flavin Fl and the dianion Fl^{2-}.[142–143] Further experimentation allowed Niemz *et al.* to convincingly attribute the comproportionation to be between FlH^- (a two-electron reduced species) and Fl^- (a fully-oxidized species missing a proton).[11] However, accepting the mechanism proposed by either Male *et al.* or Niemz *et al.* would mean some of the reduction waves observed by Tatwawadi *et al.* would remain unidentified, and the difference in ratio of the oxidation waves with varying scan rates would remain unexplained. In this thesis, it was planned to assign the remaining reduction waves and explain the voltammetric data that have been observed.

It is important to note that while the reaction of reduced free flavins with oxygen is interesting to study, it is essential that electrochemical studies of flavins are first carried out in the absence of oxygen, as was carried out in this thesis. When a potential is applied that causes the reduction of the flavin, it is simulating the transfer of electrons from an electron donor, and when the potential causes the oxidation of reduced flavin, it is simulating the transfer of electrons to an electron acceptor (e.g. molecular oxygen). Thus, cyclic voltammetry enables an understanding of the reactions of the different flavin

species (including the radical species) before the addition of substrates further complicate the mechanism with the formation of flavin-oxygen intermediates. Furthermore, it should be noted that problems might arise if the cyclic voltammetry of flavins is conducted in an oxygenated media. Firstly, molecular oxygen dissolved in the solution is expected to undergo reduction, forming a significant reduction peak that could interfere with the interpretation of the voltammetric data. Secondly, in biological systems, molecular oxygen is observed to only react with the fully-reduced hydroquinone form, but in solution, molecular oxygen could react with any of the reduced (semiquinone or hydroquinone) species as it is being formed, which could lead to inaccurate conclusions.

In this thesis, spectroelectrochemical studies were conducted on flavins in different media. Specifically, the voltammetric behaviour of free riboflavin (vitamin B_2) in an aprotic organic solvent (DMSO) was analyzed. Cyclic voltammograms of varying scan rates were obtained for varying concentrations of riboflavin at two potential ranges allowing the identification of the species responsible for each voltammetric wave, and electrolysis conducted in conjunction with spectroscopic techniques such as UV-vis and EPR spectroscopy provided sufficient information to yield an electrochemical reduction mechanism of riboflavin in aprotic organic solvents. Based on this proposed mechanism, digital simulation techniques were used to determine the thermodynamic and kinetic perimeters associated with the heterogenous and homogenous reactions described in the mechanism.[157]

The voltammetric behaviour of the coenzymes FMN and FAD were also studied in buffered and unbuffered aqueous solutions over a range of pHs, due to the ability of some flavoproteins to function at pHs significantly lower or higher than physiological pH. As flavin is bound differently to different flavoproteins, it cannot be certain that it always exists in a well-buffered environment. Using cyclic voltammetry, electrolysis, rotation

disc electrode voltammetry and UV-vis spectroscopy, an electron transfer mechanism was proposed for both systems. Based on the proposed mechanism, the voltammograms could be digitally simulated and produced a good match at each pH.[158]

Lastly, two flavins were synthesized, one with an N3-H on the isoalloxazine ring and the other with an N3-Me on the isoalloxazine ring, to investigate the differences in the electron transfer mechanism when the N3-H of one flavin was not able to act as a proton donor to another flavin radical, as is often the case in most flavoproteins. Detailed variable scan rate cyclic voltammetry was conducted on the fully-oxidized and fully-reduced forms of both flavins in DMSO, and allowed the deduction of their respective electrochemical reduction mechanisms. While significant differences can be observed between the two, addition of a sufficient amount of water appeared to cause the two mechanisms to converge, bridging the gap between the mechanisms of flavins in aqueous and organic solvents.

1.6. References

1. Karthikeyan, S.; Zhou, Q.; Osterman, A. L.; Zhang. H. *Biochemistry*, **2003**, *42*, 12532–12538.

2. Guengerich, F. P.; Munro, A. W. *J. Biol. Chem.* **2013**, *288*, 17065–17073.

3. Mansoorabadi, S. O.; Thibodeaux, C. J.; Liu, H-W. *J. Org. Chem.* **2007**, *72*, 6329–6342.

4. Medina, M. *FEBS J.* **2009**, *276*, 3942–3958.

5. Goswami, P.; Chinnadayyala, S. S. R.; Chakraborty, M.; Kumar, A. K.; Kakoti, A. *Appl. Microbiol. Biotechnol.* **2013**, *97*, 4259–4275.

6. Iyanagi, T.; Watanabe, S.; Anan, K. F. *Biochemistry*, **1984**, *23*, 1418–1425.

7. Walsh, *C. Acc. Chem. Res.* **1980**, *13*, 148–155.

8. Ghisla, S; Massey, V. *Eur. J. Biochem.* **1989**, *181*, 1–17.

9. Bruice, T. C. *Isr. J. Chem.*, **1984**, *24*, 54-61.

10. Mueller, F. In *Topics in Current Chemistry*; Boschke, F. L., Ed.; Springer-Verlag: Berlin, 1983; Vol. 108, pp 71–108.

11. Niemz, A.; Imbriglio, J.; Rotello, V. M. *J. Am. Chem. Soc.* **1997**, *119*, 887–892.

12. Massey, V.; Hemmerich, P. *Biochem. Soc. Trans.* **1980**, *8*, 246–257.

13. Nakasone, Y.; Zikihara, K.; Tokutomi, S.; Terazima, M. *Photochem. Photobiol. Sci.* **2013**, *12*, 1171-1179.

14. Kawaguchi, Y.; Nakasone, Y.; Zikihara, K.; Tokutomi, S.; Terazima, M. *J. Am. Chem. Soc.* **2010**, *132*, 8838–8839.

15. Kao, Y.-T.; Saxena, C.; Wang, L.; Sancar, A.; Zhong, D. *Proc. Natl. Acad. Sci. USA*, **2005**, *102*, 16128–16132.

16. Liu, Z.; Tan, C.; Guo, X.; Kao, Y.-T.; Li, J.; Wang, L.; Sancar, A.; Zhong, D. *Proc. Natl. Acad. Sci. USA*, **2011**, *108*, 14831–14836.

17. Liu, Z.; Zhang, M.; Guo, X.; Tan, C.; Li, J.; Wang, L.; Sancar, A.; Zhong, D. *Proc. Natl. Acad. Sci. USA*, **2013**, *110*, 12972–12977.

18. Liu, Z.; Tan, C.; Guo, X.; Li, J.; Wang, L.; Sancar, A.; Zhong, D. *Proc. Natl. Acad. Sci. USA*, **2013**, *110*, 12966–12971.

19. Liu, Z.; Guo, X.; Tan, C.; Li, J.; Kao, Y.-T.; Wang, L.; Sancar, A.; Zhong, D. *J. Am. Chem. Soc.* **2012**, *134*, 8104–8114.

20. Li, J.; Liu, Z.; Tan, C.; Guo, X.; Wang, L.; Sancar, A.; Zhong, D. *Nature*, **2010**, *466*, 887–890.

21. Burney, S.; Wenzel, R.; Kottke, T.; Roussel, T.; Hoang, N.; Bouly, J.-P.; Bittl, R.; Heberle, J.; Ahmad, M. *Angew. Chem. Int. Ed.* **2012**, *51*, 9356–9360.

22. Zoltowski, B. D.; Vaccaro, B.; Crane, B. R. *Nat. Chem. Biol.* **2009**, *5*, 827–834.

23. Vaidya, A. T.; Chen, C. H.; Dunlap, J. C.; Loros, J. J.; Crane, B. R. *Sci. Signal.* **2011**, *4*, ra50.

24. Engels, S.; Schneider, N.-L.; Lefeldt, N.; Hein, C. M.; Zapka, M.; Michalik, A.; Elbers, D.; Kittel, A.; Hore, P. J.; Mouritsen, H. *Nature*, **2014**, *509*, 353–356.

25. Lee, A. A.; Lau, J. C. S.; Hogben, H. J.; Biskup, T.; Kattnig, D. R.; Hore, P. J. *J. Roy. Soc. Interface.* **2014**, 11, 20131063.

26. Dodson, C. A.; Hore, P. J.; Wallace, M. I. *Trends Biochem. Sci.*, **2013**, *38*, 435–446.

27. Rodgers, C. T.; Hore, P. J. *Proc. Natl. Acad. Sci. USA*, **2009**, *106*, 353–360.

28. Barquera, B.; Morgan, J. E.; Lukoyanov, D.; Scholes, C. P.; Gennis, R. B.; Nilges, M. J. *J. Am. Chem. Soc.* **2003**, *125*, 265–275.

29. Barquera. B.; Ramirez-Silva, L.; Morgan, J. E.; Nilges, M. J. *J. Biol. Chem.* **2006**, *281*, 36482–36491.

30. Chaiyen, P; Fraaije, M. W.; Mattevi, A. *Trends Biochem. Sci.* **2012**, *37*, 373–380.

31. Mattevi, A. *Trends Biochem. Sci.* **2006**, *31*, 276–283.

32. Dijkman, W. P.; de Gonzalo, G.; Mattevi, A.; Fraaije, M. W. *Appl. Microbiol. Biotechnol.* **2013**, *97*, 5177–5188.

33. Heering, H. A.; Hagen, W. R. *J. Electroanal. Chem.* **1996**, *404*, 249–260.

34. Paulsen, K. E.; Stankovich, M. T.; Stockman, B. J.; Markley, J. L. *Arch. Biochem. Biophys.* **1990**, *280*, 68–73.

35. Iyanagi, T. *Biochemistry* **1977**, *16*, 2725–2730.

36. Lienhart, W.-D.; Gudipati, V.; Macheroux, P. *Arch. Biochem. Biophys.* **2013**, 535, 150–162.

37. Ames, B. N.; Elson-Schwab, I.; Silver, E. A.; *Am. J. Clin. Nutr.* **2002**, *75*, 616–658.

38. Bosch, A. M.; Abeling, N. G. G. M.; Ijlst, L.; Knoester, H.; van der Pol, W. L.; Stroomer, A. E. M.; Wanders, R. J.; Visser, G.; Wijburg, F. A.; Duran, M.; Waterham, H. R. *J. Inherit. Metab. Dis.* **2011**, *34*, 159–164.

39. Green, P.; Wiseman, M.; Crow, Y. J.; Houlden, H.; Riphagen, S.; Lin, J. P.; Raymond, F. L.; Childs, A. M.; Sheridan, E.; Edwards, S. *Am. J. Hum. Gen.* **2010**, *86*, 485–489.

40. Anand, G.; Hasan, N.; Jayapal, S.; Huma, Z.; Ali, T.; Hull, J.; Blair, E.; McShane, T.; Jayawant, S. *Dev. Med. Child Neurol.* **2012**, *54*, 187–189.

41. Koy, A.; Pillekamp, F.; Hoehn, T.; Waterham, H.; Klee, D.; Mayatepek, E.; Assmann, B. *Pediatr. Neurol.* **2012**, *46*, 407–409.

42. Nishida, H.; Inaka, K.; Yamanaka, M.; Kaida, S.; Kobayashi, K.; Miki, K. *Biochemistry*, **1995**, *34*, 2763–2767.

43. Nandwana, V.; Samuel, I.; Cooke, G.; Rotello, V. M. *Acc. Chem. Res.* **2013**, *46*, 1000–1009.

44. Burkhart, B. M.; Ramakrishnan, B.; Yan, H.; Reedstorm, R. J.; Markley, J. L.; Straus, N. A.; Sundaralingam, M. *Acta. Cryst. Section D*, **1995**, *51*, 318–330.

45. Correll, C. C.; Batie, C. J.; Ballou, D. P.; Ludwig, M. L. *Science*, **1992**, *258*, 1604–1610.

46. Bruns, C. M.; Karplus, P. A. *J. Mol. Biol.* **1995**, *247*, 125–145.

47. Nascimento, A. S.; Catalano-Dupuy, D. L.; Bernardes, A.; Neto, M. O.; Santos, M. A. M.; Ceccarelli, E. A.; Polikarpov, I. *BMC Struct. Biol.* **2007**, *7*, 69–80.

48. Schulz, G. E.; Schirmer, R. H.; Sashsenheimer, W.; Pai, E. F. *Nature*, **1978**, *273*, 120–124.

49. Pai, E. F.; Schulz, G. E. *J. Biol. Chem.* **1983**, *258*, 1752–1757.

50. Karplus, P. A.; Schulz, G. E. *J. Mol. Biol.* **1987**, *195*, 701–729.

51. Berkholz, D. S.; Faber, H. R.; Savvides, S. N.; Karplus, P. A. *J. Mol. Biol.* **2008**, *382*, 371–384.

52. Lindqvist, Y.; Branden, C.-I. *J. Biol. Chem.* **1989**, *264*, 3624–3628**.**

53. Todone, F.; Vanoni, M. A.; Mozzarelli, A.; Bolognesi, M.; Coda, A.; Curti, B.; Mattevi, A. *Biochemistry*, **1997**, *36*, 5853–5860.

54. Fraaije, M. W.; Mattevi, A. *Trends Biochem. Sci.* **2000**, *25*, 126–132.

55. Tormos, J. R.; Taylor, A. B.; Daubner, S. C.; Hart, P. J.; Fitzpatrick, P. F. *Biochemistry*, **2010**, *24*, 5035-5041.

56. Kiess, M.; Hecht, H. J.; Kalisz, H. M. *Eur. J. Biochem.* **1998**, *252*, 90–99.

57. Roth, J. P.; Klinman, J. P. *Proc. Natl. Acad. Sci. USA*, **2003**, *100*, 62–67.

58. Gadda, G. *Biochemistry*, **2012**, *51*, 2662–2669.

59. Klinman, J. P. *Acc. Chem. Res.* **2007**, *40*, 325−333.

60. Kommoju, P. R.; Chen, Z. W.; Bruckner, R. C.; Mathews, F. S.; Jorns, M. S. *Biochemistry*, **2011**, *50*, 5521−5534.

61. Jorns, M. S.; Chen, Z. W.; Mathews, F. S. *Biochemistry*, **2010**, *49*, 3631−3639.

62. Zhao, G.; Bruckner, R. C.; Jorns, M. S. *Biochemistry*, **2008**, *47*, 9124−9135.

63. Bruckner, R. C.; Winans, J.; Jorns, M. S. *Biochemistry*, **2011**, *50*, 4949−4962.

64. Fraaije, M. W.; van den Heuvel, R. H. H.; van Berkel, W. J. H.; Mattevi, A. *J. Biol. Chem.* **1999**, *274*, 35514–35520.

65. Heuts, D. P. H. M.; Janssen, D. B.; Fraaije, M. W. *FEBS Lett.* **2007**, *581*, 4905–4909.

66. Heuts, D. P. H. M.; Scrutton, N. S.; McIntire, W. S.; Fraaije, M. W. *FEBS J.* **2009**, *276*, 3405–3427.

67. Baron, R.; Riley, C.; Chenprakhon, P.; Thotsaporn, K.; Winter, R. T.; Alfieri, A.; Forneris, F.; Van Berkel, W. J. H.; Chaiyen, P.; Fraaije, M. W.; Mattevi, A.; McCammon, J. A. *Proc. Natl. Acad. Sci. USA*, **2009**, 106, 10603–10608.

68. Coulombe, R.; Yue, K. Q.; Ghisla, S.; Vrielink, A. *J. Biol. Chem.* **2001**, *276*, 30435–30441.

69. Endo, T.; Yamano, K.; Kawano, S.; *Antioxid. Redox Signal.* **2010**, *13*, 1359–1373.

70. Crozier-Reabe, K.; Moran, G. R. *Int. J. Mol. Sci.* **2012**, *13*, 15601–15639.

71. Gatti, D. L.; Palfey, B. A.; Lah, M. S.; Entsch, B.; Massey, V.; Ballou, D. P.; Ludwig, M. L. *Science*, **1994**, *266*, 110–114.

72. Cole, L. J.; Entsch, B.; Ortiz-Maldonado, M.; Ballou, D. P. *Biochemistry*, **2005**, *44*, 14807–14817.

73. Van der Bolt, F. J. T.; Vervoort, J.; van Berkel, W. J. H. *Eur. J. Biochem.* **1996**, *237*, 592–600.

74. Schreuder, H. A.; Mattevi, A.; Obmolova, G.; Kalk, K. H.; Hol, W. G. J.; van der Bolt, F. J. T.; van Berkel, W. J. H. *Biochemistry*, **1994**, *33*, 10161–10170.

75. Brender, J. R.; Dertouzos, J.; Ballou, D. P.; Massey, V.; Palfey, B. A.; Entsch, B.; Steel, D. G.; Gafni, A. *J. Am. Chem. Soc.* **2005**, *127*, 18171–18178.

76. Entsch, B.; Cole, L. J.; Ballou, D. P. *Arch. Biochem. Biophys.* **2005**, *433*, 297–311.

77. Wang, J.; Ortiz-Maldonado, M.; Entsch, B.; Massey, V.; Ballou, D.; Gatti, D. L. *Proc. Natl. Acad. Sci. USA*, **2002**, *99*, 608–613.

78. Husain, M.; Massey, V. *J. Biol. Chem.* **1979**, *254*, 6657–6666.

79. Enroth, C.; Neujahr, H.; Schneider, G.; Lindqvist, Y. *Structure*, **1998**, *6*, 605–617.

80. Moran, G. R.; Entsch, B.; Palfey, B. A.; Ballou, D. P. *Biochemistry*, **1999**, *38*, 6292–6299.

81. Palfey, B. A.; Moran, G. R.; Entsch, B.; Ballou, D. P.; Massey, V. *Biochemistry*, **1999**, *38*, 1153–1158.

82. Schreuder, H. A.; van der Laan, J. M.; Swarte, M. B. A.; Kalk, K. H.; Hol, W. G. J.; Drenth, J. *Proteins*, **1992**, *14*, 178–190.

83. Ryan, K. S.; Chakraborty, S.; Howard-Jones, A. R.; Walsh, C. T.; Ballou, D. P.; Drennan, C. L. *Biochemistry*, **2008**, *47*, 13506–13513.

84. Moran, G. R.; Entsch, B.; Palfey, B. A.; Ballou, D. P. *Biochemistry*, **1997**, *36*, 7548–7556.

85. Ortiz-Maldonado, M.; Cole, L. J.; Dumas, S. M.; Entsch, B.; Ballou, D. P. *Biochemistry*, **2004**, *43*, 1569–1579.

86. Entsch, B.; Ballou, D. P.; Massey, V. *J. Biol. Chem.* **1976**, *251*, 2550–2563.

87. Bruice, T. C. *Acc. Chem. Res.* **1980**, *13*, 256–262.

88. Massey, V. *J. Biol. Chem.* **1994**, *269*, 22459–22462.

89. Wessiak, A.; Schopfer, L. M.; Massey, V. *J. Biol. Chem.* **1984**, *259*, 12547–12556.

90. Crozier-Reabe, K. R.; Phillips, R. S.; Moran, G. R. *Biochemistry*, **2008**, *47*, 12420–12433.

91. Wang, A.; Rodríguez, J. C.; Han, H.; Schönbrunn, E.; Rivera, M. *Biochemistry*, **2008**, *47*, 8080–8093.

92. Stockman, B. J.; Westler, W. M.; Mooberry, E. S.; Markley, J. L. *Biochemistry*, **1988**, *27*, 136–142.

93. Fukuyama, K.; Matsubara, H.; Rogers, L. J. *J. Mol. Biol.* **1992**, *225*, 775–789.

94. Sykes, G. A.; Rogers, L. J. *Biochem. J.* **1984**, *217*, 845–850.

95. Stockman, B. J.; Richardson, T. E.; Swenson, R. P. *Biochemistry*, **1994**, *33*, 15298–15308.

96. Swenson, R. P.; Krey, G. D. *Biochemistry*, **1994**, *33*, 8505–8514.

97. Ludwig, M. L.; Schopfer, L. M.; Metzger, A. L.; Pattridge, K. A.; Massey, V. *Biochemistry*, **1990**, *29*, 10364–10375.

98. Hamdane, D.; Xia, C.; Im, S.-C.; Zhang, H.; Kim, J.-J. P.; Waskell, L. *J. Biol. Chem.* **2009**, *284*, 11374–11384.

99. Masters, B. S.; Okita, R. T. *Pharmacol. Ther.* **1980**, *9*, 227–244.

100. Wang, M.; Roberts, D. L.; Paschke, R.; Shea, T. M.; Siler-Masters, B. S.; Kim, J. J. P. *Proc. Natl. Acad. Sci. USA*, **1997**, *94*, 8411–8416.

101. Bhattacharyya, A. K.; Lipka, J. J.; Waskell, L.; and Tollin, G. *Biochemistry*, **1991**, *30*, 759–765.

102. Gutierrez, A.; Paine, M.; Wolf, C. R.; Scrutton, N. S.; Roberts, G. C. *Biochemistry*, **2002**, *41*, 4626–4637.

103. Page, C. C.; Moser, C. C.; Chen, X.; Dutton, P. L. *Nature*, **1999**, *402*, 47–52.

104. Iyanagi, T.; Makino, N.; and Mason, H. S. *Biochemistry*, **1974**, *13*, 1701–1710.

105. Oprian, D. D.; Coon, M. J. *J. Biol. Chem.* **1982**, *257*, 8935–8944.

106. Vermilion, J. L.; Coon, M. J. *J. Biol. Chem.* **1978**, *253*, 8812–8819.

107. Wongnate, T.; Surawatanawong, P.; Visitsatthawong, S.; Sucharitakul, J.; Scrutton, N. S.; Chaiyen, P. *J. Am. Chem. Soc.* **2014**, *136*, 241–253.

108. Sucharitakul, J.; Prongjit, M.; Haltrich, D.; Chaiyen, P. *Biochemistry*, **2008**, *47*, 8485−8490.

109. Wongnate, T.; Chaiyen, P. *FEBS J.* **2013**, *280*, 3009−3027.

110. Sucharitakul, J.; Wongnate, T.; Chaiyen, P. *J. Biol. Chem.* **2011**, *286*, 16900−16909.

111. Teufel, R.; Miyanaga, A.; Michaudel, Q.; Stull, F.; Louie, G.; Noel, J. P.; Baran, P. S.; Palfey, B.; Moore, B. S. *Nature*, **2013**, *503*, 552–556.

112. Rastetter, W. H.; Gadek, T. R.; Tane, J. P.; Frost, J. W. *J. Am. Chem. Soc.* **1979**, *101*, 2228–2231.

113. Orf, H. W.; Dolphin, D. *Proc. Natl. Acad. Sci. USA*, **1974**, *71*, 2646–2650.

114. Cash, K. J.; Clark, H. A. *Trends Mol. Med.* **2010**, *16*, 584–593.

115. Netto, C. G. C. M.; Toma, H. E.; Andrade, L. H. *J. Mol. Catal. B Enzym.* **2013**, *85*, 71–92.

116. Qian, Y.; Zheng, J.; Lin, Z. *Appl. Microbiol. Biotechnol.* **2013**, *97*, 8599–8607.

117. Pillone, M. S.; Pollegioni, L. *Biocat. Biotrans.* **2002**, *20*, 145–159.

118. Pollegioni, L.; Molla, G.; Sacchi, S.; Rosini, E.; Verga, R.; Pilone, M. S. *Appl. Microbiol. Biotechnol.* **2008**, *78*, 1–16.

119. Patel, R. N. *ACS Catal.* **2011**, *1*, 1056–1074.

120. Turner, N. J. *Chem. Rev.* **2011**, *111*, 4073–4087.

121. Schrittwieser, J. H.; Resch, V.; Wallner, S.; Lienhart, W. D.; Sattler, J. H.; Resch, J.; Macheroux, P.; Kroutil, W. *J. Org. Chem.* **2011**, *76*, 6703–6714.

122. Dadova, J.; Kümmel, S.; Feldmeier, C.; Cibulkova, J.; Pazout, R.; Maixner, J.; Gschwind, R. M.; König, B.; Cibulka, R. *Chem. Eur. J.* **2013**, *19*, 1066–1075.

123. Lechner, R.; Kümmel, S.; König, B. *Photochem. Photobiol. Sci.* **2010**, *9*, 1367–1377.

124. Schmaderer, H.; Hilgers, P.; Lechner, R.; König, B. *Adv. Synth. Catal.* **2009**, *351*, 163–174.

125. Svoboda, J.; Schmaderer, H.; König, B. *Chem. Eur. J.* **2008**, *14*, 1854–1865.

126. Chen, H.-Y.; Hou, J.; Zhang, S.; Liang, Y.; Yang, G.; Yang, Y.; Yu, L.; Wu, Y.; Li, G. *Nat. Photonics*, **2009**, *3*, 649–653.

127. Toogood, H. S.; Leys, D.; Scrutton, N. S. *FEBS J.* **2007**, *274*, 5481–5504.

128. Legrand, Y.-M.; Gray, M.; Cooke, G.; Rotello, V. M. *J. Am. Chem. Soc.* **2003**, *125*, 15789–15795.

129. Coman, V.; Vaz-Domínguez, C.; Ludwig, R.; Harreither, W.; Haltrich, D.; De Lacey, A. L.; Ruzgas, T.; Gorton, L.; Shleev, S. *Phys. Chem. Chem. Phys.*, **2008**, *10*, 6093–6096.

130. Zafar, M. N.; Tasca, F.; Boland, S.; Kujawa, M.; Patel, I.; Peterbauer, C. K.; Leech, D.; Gorton, L. *Bioelectrochemistry*, **2010**, *80*, 38–42.

131. Yakovleva, M. E.; Killyéni, A.; Ortiz, R.; Schulz, C.; MacAodha, D.; Conghaile, P. Ó.; Leech, D.; Popescu, I. C.; Gonaus, C.; Peterbauer, C. K.; Gorton, L. *Electrochem. Comm.* **2012**, *24*, 120–122.

132. Mayhew, S. G. *Eur. J. Biochem*, **1999**, *265*, 698–702.

133. Janik, B.; Elving, P. J. *Chem. Rev.* **1968**, *68*, 295–319.

134. Michaelis, L.; Schwarzenbach, G. *J. Biol. Chem.* **1938**, *123*, 527–542.

135. Draper, R. D.; Ingraham, L. L. *Arch. Biochem. Biophys.* **1968**, *125*, 802–808.

136. Hartley, A. M.; Wilson, G. S. *Anal. Chem.* **1966**, *38*, 681–687.

137. Clark, W. M.; Lowe, H. J. *J. Biol. Chem.* **1956**, *220*, 983–992.

138. Wei, H.; Omanovic, S. *Chem. Biodiv.* **2008**, *5*, 1622–1639.

139. Cable, M.; Smith, E. T. *Anal. Chim. Acta.* **2005**, *537*, 299–306.

140. Ksenzhek, O. S.; Petrova, S. A. *Bioelectrochem. Bioenerg.* **1983**, *11*, 105–127.

141. Diculescu, V. C.; Militaru, A.; Shah, A.; Qureshi, R.; Tugulea, L.; Brett, A. M. O. *J. Electroanal. Chem.* **2010**, *647*, 1–7.

142. Male, R.; Samotowka, M. A.; Allendoerfer, R. D. *Electroanalysis* **1989**, *1*, 333–339.

143. Tatwawadi, S. V.; Santhanam, K. S. V.; Bard, A. J. *J. Electroanal. Chem.* **1968**, *17*, 411–420.

144. Sawyer, D. T.; McCreery, R. L. *Inorg. Chem.* **1972**, *11*, 779–782.

145 (a) Hammerich, O.; Svensmark, B. In *Organic Electrochemistry,* 3rd ed.; Lund, H., Baizer, M. M., Eds.; Marcel Dekker: New York, 1991; Chapter 16.

145 (b) Morrow, G. W. In *Organic Electrochemistry*, 4th ed.; Lund, H., Hammerich, O., Eds.; Marcel Dekker: New York, 2000; Chapter 16.

146. Gupta, N.; Linschitz, H. *J. Am. Chem. Soc.* **1997**, *119*, 6384–6391.

147. Quan, M.; Sanchez, D.; Wasylkiw, M. F.; Smith, D. K. *J. Am. Chem. Soc.* **2007**, *129*, 12847–12856.

148. Hui, Y.; Chng, E. L. K.; Chng, C. Y. L.; Poh, H. L.; Webster, R. D. *J. Am. Chem. Soc.* **2009**, *131*, 1523–1534.

149. Hui, Y.; Chng, E. L. K.; Chua, L. P.-L.; Liu, W. Z.; Webster, R. D. *Anal. Chem.* **2010**, *82*, 1928–1934.

150. Amatore, C.; Savéant, J.-M. *J. Electroanal. Chem.* **1977**, *85*, 27–46.

151. Breinlinger, E.; Niemz, A.; Rotello, V. M. *J. Am. Chem. Soc.* **1995**, *117*, 5379–5380.

152. Huynh, M. H. V.; Meyer, T. J. *Chem. Rev.* **2007**, *107*, 5004–5064.

153. Costentin, C. *Chem. Rev.* **2008**, *108*, 2145–2179.

154 (a) Costentin, C.; Robert, M.; Savéant, J.-M. *Acc. Chem. Res.* **2010**, *43*, 1019–1029.

154 (b) Savéant, J.-M., *Elements of Molecular and Biomolecular Electrochemistry: An Electrochemical Approach to Electron Transfer Chemistry*, John Wiley & Sons: New Jersey, 2006.

155. Warren, J. J.; Tronic, T. A.; Mayer, J. M. *Chem. Rev.* **2010**, *110*, 6961–7001.

156. Bonin, J.; Robert, M. *Photochem. Photobiol.* **2011**, *87*, 1190–1203.

157. Tan, S. L. J.; Webster, R. D. *J. Am. Chem. Soc.* **2012**, *134*, 5954–5964.

158. Tan, S. L. J.; Kan, J. M.; Webster, R. D. *J. Phys. Chem. B* **2013**, *117*, 13755–13766.

Chapter 2

Electrochemically Induced Chemically Reversible Proton-Coupled Electron Transfer Reactions of Riboflavin (Vitamin B_2).

2.1. Introduction

In many biological and chemical processes, such as photosynthesis as well as enzymatic reactions, proton-coupled electron transfer (PCET) reactions are observed to play an important role.[1-5] In recent years, PCET reactions have been examined in detail, with a significant number of studies involving phenols, and examples of these PCET reactions have been shown to occur *via* concerted (where electron transfer and proton transfer occur simultaneously),[6-16] and *via* consecutive (where electron transfer and proton transfer occur separately)[17-19] mechanisms. In this chapter the kinetic and electrochemical parameters of a series of chemically reversible PCET reactions of a biological molecule, Riboflavin, in its free (non-protein bound) form have been evaluated.

Scheme 2.1. Riboflavin (vitamin B_2).

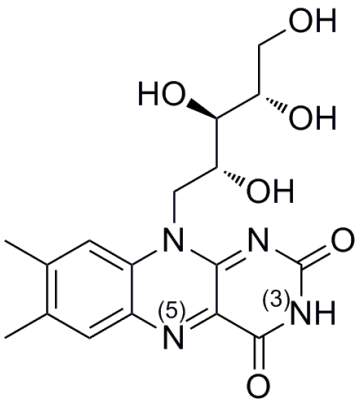

Flavin mononucleotide (FMN) and flavin adenine dinucleotide (FAD) are cofactors of enzymes which are involved in the catalysis of many redox reactions in biological systems, as flavins are able to accept electron pairs from many functional groups. These redox reactions include the dehydrogenation of NADPH and D-amino acids.[20-24] Flavin cofactors (FMN and FAD) are more versatile than nicotinamide coenzymes (NAD and NADP) because they can undergo either one- or two-electrons, while nicotinamides can only undergo two-electron processes. In fact, in many flavoproteins, the flavin cofactor accepts an electron pair from NADH, NADPH or other two-electron donors, and transfers them to a large variety of electron acceptors. One-electron acceptors include heme Fe, molecular oxygen, flavodoxin (a flavoprotein) or even another flavin cofactor within the same flavoprotein (diflavin reductases).[20-24] Their unique reactivity with oxygen also enables flavins to take part in important aerobic processes.[20] Riboflavin (Figure 2.1) is the primary redox active component of FAD and FMN.

It is well established that in protic and buffered aqueous media, the fully-oxidized flavin (Fl) is directly reduced to the fully-reduced flavin (FlH_2) in a two-electron and two-proton process, without being able to observe the flavosemiquinone radical.[25-34] While this is useful for modeling systems of flavoproteins that catalyze two-electron processes (e.g. assimilatory nitrate reductase,[35] microsomal NADH-cytochrome b_5 reductase[36]), it is not relevant for those flavoproteins (e.g. flavodoxin[37,38]) where the second electron transfer does not occur, and the flavosemiquinone radical form is observed after reduction. Therefore, an aprotic organic environment is more suitable to model the one-electron processes. Riboflavin is poorly soluble in most solvents suitable for electrochemistry, except for dimethyl sulfoxide where it is soluble up to approximately 4 mM.

Studies by Tatwawadi *et al.*[39] and Sawyer *et al.*[40] on riboflavin in DMSO showed separately using cyclic voltammetry (CV) the presence of a reduction process on the

forward scan and at least two oxidation waves when the scan direction was reversed. Tatwawadi *et al*. observed that one mol of electrons were transferred per mol of riboflavin during electrolysis, and it was concluded that the reduction wave corresponds to a single electron transfer to form the anionic radical, similar to observed for the reduction of quinones in aprotic solvents.[41-45]

Niemz *et al*.[24] discovered that when the imide proton at N3 (Figure 2.1) was substituted by a methyl group, cyclic voltammetry showed the reduction was reversible, with only one oxidation wave, indicating no chemical reactions had occurred. Addition of a proton donor (DH) resulted in the appearance of an additional oxidation wave. It was concluded that DH donated a proton to the radical anion ($Fl^{\bullet -}$), to form the neutral radical ($FlH^{\bullet}$). $FlH^{\bullet}$ was immediately further reduced to FlH^{-}, which is the species being oxidized in the additional oxidation wave.

In this chapter, we will discuss the electrochemical reduction of riboflavin in DMSO without an additional proton source, determine whether the fully-oxidized flavin acts as a proton donor to the reduced species and discuss the long-term chemical reversibility of the reduction process. The species responsible for each of the voltammetric peaks detected during the forward and reverse scans were identified *via* variable scan rate cyclic voltammetry experiments over a range of concentrations, and by spectroscopic monitoring of the reduction and reoxidation processes *via* UV-vis and EPR spectroscopies. The detected species include the dianion (Fl^{2-}) and the deprotonated oxidized flavin (Fl^{-}), which have not been reported previously. The detailed electron transfer mechanism of free flavin in an aprotic organic media involves a series of chemically reversible PCET reactions, which was modeled using digital simulation techniques, enabling the calculation of the associated electrochemical and kinetic parameters.

2.2. Experimental

2.2.1. Chemicals

n-Bu_4NPF_6 was prepared by reacting equal molar amounts of a 40% aqueous solution of *n*-Bu_4OH with a 65% aqueous solution of HPF_6, washing the precipitate with hot water, recrystallising three times from hot ethanol and then drying under vacuum for 24 hours at 140 ^oC. Solutions for electrochemical experiments were prepared by adding DMSO (Tedia) and the correct concentration of *n*-Bu_4NPF_6 to pre-dried 3Å molecular sieves (Fluka) (dried under vacuum at 140 °C for 6 hours in a Büchi Glass Oven B-585) and leaving the DMSO/electrolyte in a glass vacuum syringe under a nitrogen atmosphere for at least 36 hours. Riboflavin was reagent grade and obtained from Alfa Aesar. ^1H NMR experiments confirmed that riboflavin exists in its protonated form in DMSO, since an imide peak was detected at 11.34 ppm. (See Figure A2.1 in appendix)

2.2.2. Electrochemical Procedures

Cyclic voltammetry (CV) experiments were conducted with a computer-controlled Eco Chemie Autolab PGSTAT 100 with an ADC fast scan generator. Working electrodes used were 0.01 mm, 0.02 mm, 0.05 mm, and 1 mm diameter planar Pt disks, used in conjunction with a Pt auxiliary electrode and a silver wire (0.5 M Bu_4NPF_6 in CH_3CN) reference electrode. Accurate potentials were obtained using ferrocene as an internal standard. The electrochemical cells were dried at 110 °C for a least one hour prior to use. Solutions of riboflavin (1 mM, 0.5 M *n*-Bu_4NPF_6 in DMSO) for voltammetric analysis were deoxygenated by purging with high purity argon gas and all voltammetric experiments were conducted at 22 (±2) °C in a Faraday cage. Karl Fischer coulometric titrations indicated that the analyte solutions contained 25 mM of H_2O when they were added to the electrochemical cell (DMSO is difficult to be kept dry below this level when

placed in an electrochemical cell). Digital simulations of the CV data were performed using the DigiElch 6 software package purchased from Gamry Instruments.

Controlled potential electrolysis was performed in a two-compartment electrolysis cell using Pt mesh as the working and auxiliary electrodes and a silver wire as the reference electrode (separated from the working electrode compartment with a glass membrane containing a solution of 0.5 M *n*-Bu_4NPF_6 in CH_3CN).[17]

2.2.3. Spectroscopic Experiments

In situ electrochemical UV-vis spectra were obtained using an optically semi-transparent thin layer electrochemical (OSTLE) cell at 22 (±2) °C and recorded on a Perkin Elmer Model Lambda 750 UV-vis-NIR spectrophotometer.[17] EPR spectra were obtained by electrolyzing solutions of riboflavin in DMSO at 22 (±2) °C in an electrolysis cell, transferring the electrolyzed solutions under nitrogen to a quartz flat cell and recording continuous wave X-band spectra with a Bruker ELEXSYS E500 EPR spectrometer.

2.3. Results and Discussion

2.3.1. Cyclic voltammetry

As was observed in previous voltammetric studies of free flavins in aprotic media, we were likewise able to observe two oxidation processes (wave 2 and wave 3) upon reversal of the scan direction after the first reduction process (wave 1). (Figure 2.1(*a*))

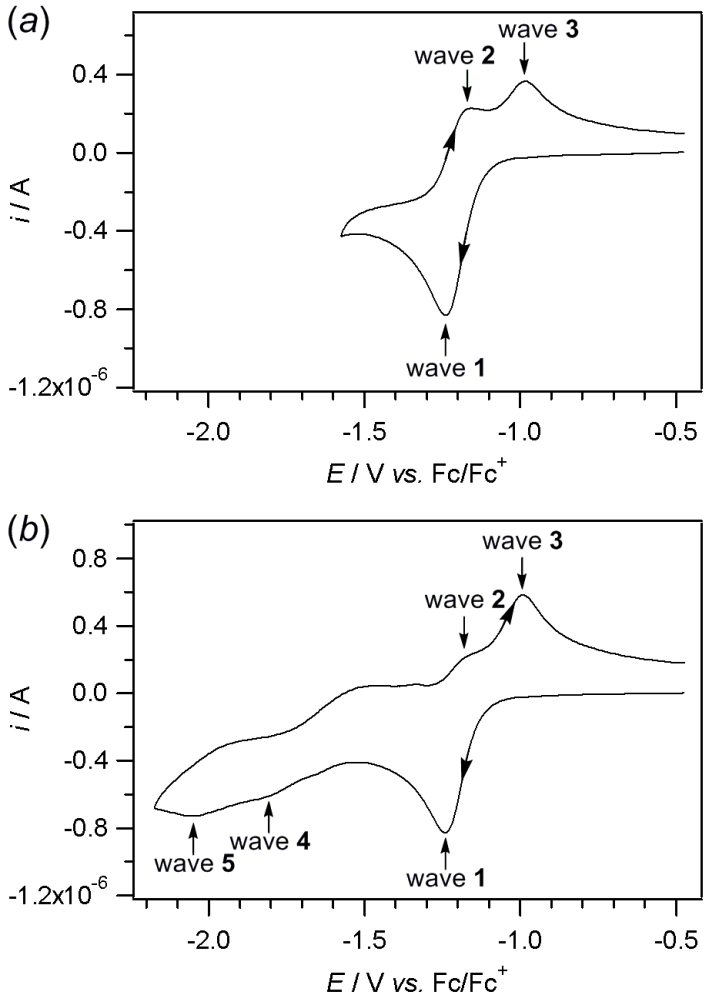

Figure 2.1. Cyclic voltammograms of the reduction of 1 mM riboflavin at a 1 mm diameter planar Pt electrode in DMSO with 0.5 M *n*-Bu_4NPF_6, and at scan rate 0.1 V s^{-1}. (*a*) Scan direction reversed at 1.6 V *vs.* Fc/Fc^+. (*b*) Scan direction reversed at –2.2 V *vs.* Fc/Fc^+.

Figure 2.2 – 2.4 show variable scan rate cyclic voltammograms of 1 mM – 3.6 mM riboflavin in DMSO, where the current scale has been normalized by multiplying by $\nu^{-0.5}$ (ν = the scan rate in V s^{-1}). It can be observed that as the scan rate increases, wave 2 increases in magnitude while wave 3 diminishes in magnitude. The change in relative size of waves 2 and 3 can be explained by the reactions in eqs 1 – 4 (either the ECE (eqns 1–3) or DISP1 (eqns 1,2 and 4) mechanisms)[46], where the reduction process (wave 1) produces the protonated anion (FlH^-), which can then be oxidized back to fully-oxidized flavin (wave 3) when the scan direction is reversed. As the scan rate is increased, the protonation reaction of the initially formed radical anion (eq 2) is outrun. The amount of the radical anion ($Fl^{\bullet-}$) increases with respect to the amount of FlH^- hence wave 2 that is associated with oxidation of the radical anion (the reverse of eq 1) increases in magnitude while wave 3 decreases in magnitude.

$$Fl + e^- \rightleftharpoons Fl^{\bullet-} \quad (1)$$

$$Fl^{\bullet-} + DH \rightleftharpoons FlH^{\bullet} + D^- \quad (2)$$

$$FlH^{\bullet} + e^- \rightleftharpoons FlH^- \quad (3)$$

$$Fl^{\bullet-} + FlH^{\bullet} \rightleftharpoons FlH^- + Fl \quad (4)$$

For the experiments in this study, no additional proton donor was added. Therefore, the proton source is likely to be the fully-oxidized flavin (Fl), as was first postulated by Niemz *et al.*,[24] which reacts to form the deprotonated oxidized flavin, Fl^- according to eq 5. Controlled potential electrolysis experiments by Tatwawadi *et al.*[39] in DMSO (and repeated in this present study) confirmed that the overall reaction occurred by one-electron per molecule, which is consistent with half of the Fl molecules being reduced by

two-electrons and the other half acting as proton donors (thereby being unavailable for further reduction at this applied potential). Therefore, although wave 1 occurs *via* two-electrons, the total charge transferred during bulk electrolysis of the entire reaction solution would average out to indicate that one-electron was transferred per molecule of fully-oxidized riboflavin. Trace water present in the solution is potentially an alternative source of protons, although in this instance is considered to be an unlikely donor for several reasons. Firstly, the anionic radical is not a strong enough base to deprotonate water. Furthermore, although DMSO is extremely difficult to dry,[47] it has been shown that the water in DMSO is relatively unreactive because it DMSO undergoes strong hydrogen-bonding with water.[44,45] The pK_a of water in DMSO is 32, indicating the acidity is significantly decreased in DMSO, making it less likely to act as a proton donor. It was found that the addition of 0.5 M of water to the DMSO did not increase the size of wave 3 relative to wave 2 (at a fixed scan rate) during CV experiments, which supports the hypothesis that water was not acting as a proton donor during the reduction reaction.

$$Fl^{\bullet-} + Fl \rightleftharpoons FlH^{\bullet} + Fl^{-} \quad (5)$$

$$Fl^{\bullet-} + e^{-} \rightleftharpoons Fl^{2-} \quad (6)$$

$$Fl^{2-} + Fl \rightleftharpoons FlH^{-} + Fl^{-} \quad (7)$$

$$Fl^{-} + e^{-} \rightleftharpoons Fl^{2-\bullet} \quad (8)$$

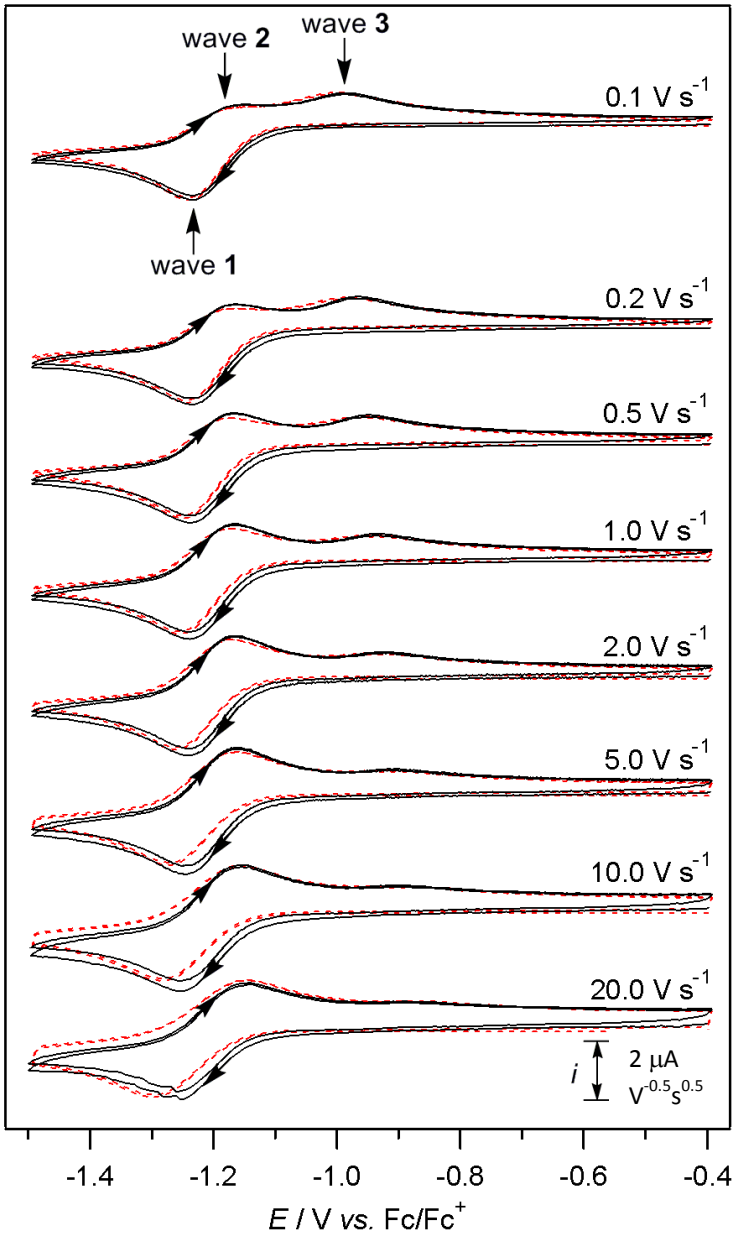

Figure 2.2. (Black lines) Variable scan rate CVs of 2 consecutive scans of 1 mM riboflavin in DMSO with 0.5 M *n*-Bu_4NPF_6, recorded at a 1 mm Pt electrode at 22 (±2) ^{o}C, where the scan direction was reversed at –1.5 V *vs.* Fc/Fc^+. (Red dashed lines) Digital simulations of the CV data based on the mechanism in Scheme 2.2 and parameters given in Tables 2.1 and 2.2. The current data were scaled by multiplying by $\nu^{-0.5}$.

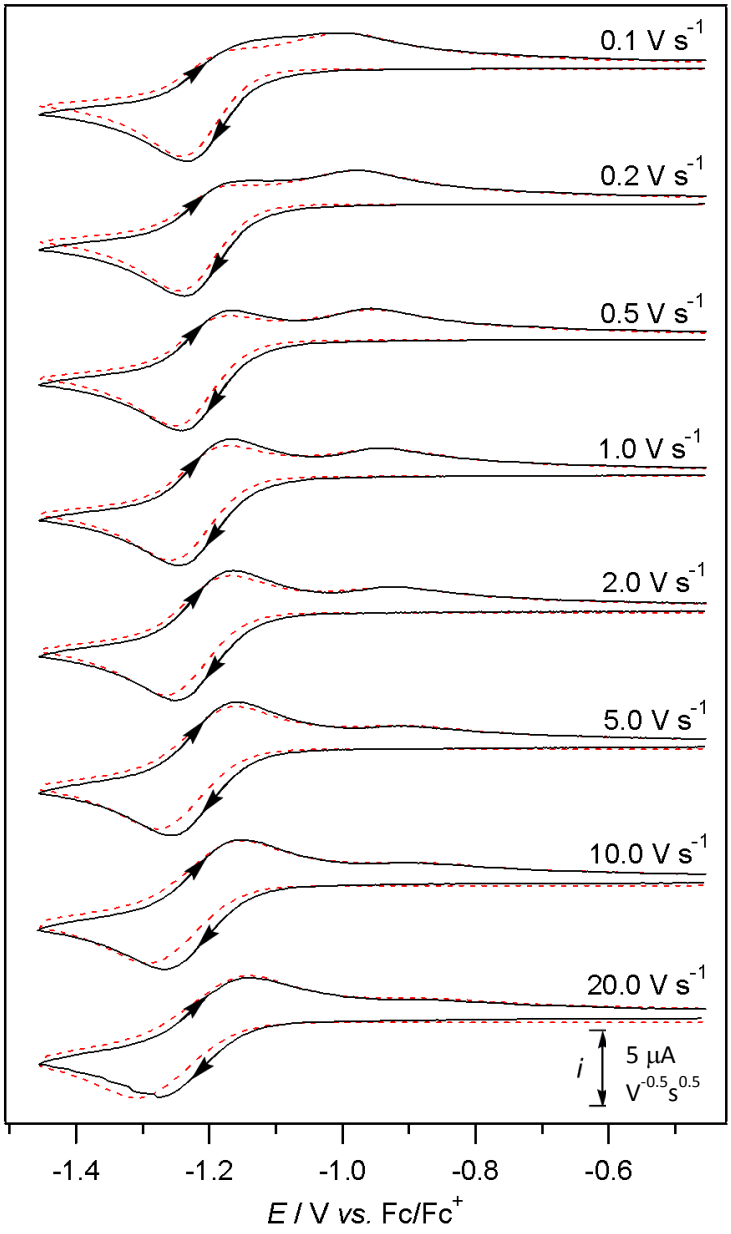

Figure 2.3. (Black line) Variable scan rate cyclic voltammograms of 2 mM riboflavin in DMSO with 0.5 M *n*-Bu_4NPF_6, recorded at a 1 mm Pt electrode at 22 (±2) ^oC, where the scan direction was reversed at -1.45 V *vs.* Fc/Fc^+. (Red dashed line) Digital simulations of the CV data based on the mechanism in Scheme 2.2 and parameters given in Table 2.1 and 2.2. The current data were scaled by multiplying by $v^{-0.5}$.

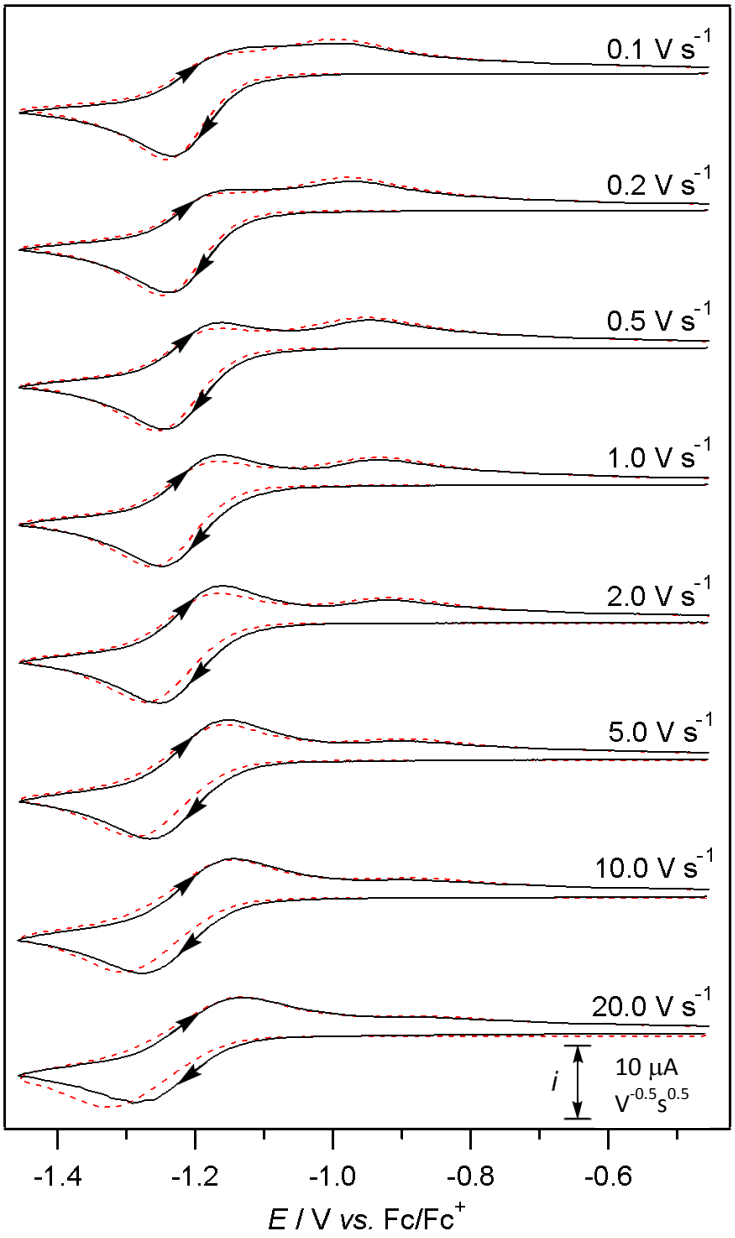

Figure 2.4. (Black line) Variable scan rate cyclic voltammograms of 3.6 mM riboflavin in DMSO with 0.5 M *n*-Bu_4NPF_6, recorded at a 1 mm Pt electrode at 22 (±2) ^{o}C, where the scan direction was reversed at -1.45 V *vs.* Fc/Fc^{+}. (Red dashed line) Digital simulations of the CV data based on the mechanism in Scheme 2.2 and parameters given in Table 2.1 and 2.2. The current data were scaled by multiplying by $\nu^{-0.5}$.

Variable scan rate voltammetric experiments were performed at planar electrodes between 10 μm and 1 mm diameter. (Figures 2.2, 2.5 and 2.6) It was found that at the fastest scan rate (20 V s^{-1}) the anodic (E_p^{ox}) to cathodic (E_p^{red}) peak-to-peak separation (ΔE_{pp}) were similar at the smallest and largest electrode (both were around 100 mV). The effects of uncompensated solution resistance are expected to be the highest at the electrode with a large surface area and at the fastest scan rate.[48] Therefore, if the ΔE_{pp}-values at the 10 μm and 1 mm diameter electrodes are similar at the higher scan rate of 20 V s^{-1}, the increasing ΔE_{pp}-values shown in Figure 2.2 with increasing scan rates are due to a relatively slow heterogeneous electron transfer rate (k_s) rather than solely due to uncompensated solution resistance. Experiments performed on ferrocene at varying scan rates (where it is assumed that the heterogeneous electron transfer rate is fast, $k_s \geq 1$)[49] under identical conditions showed significantly smaller ΔE_{pp}-values at high scan rates compared to those obtained for riboflavin, eliminating the likelihood of uncompensated solution resistance (which would also affect ferrocene), and supporting a relatively slow rate of heterogeneous electron transfer for riboflavin at a Pt electrode surface in DMSO.

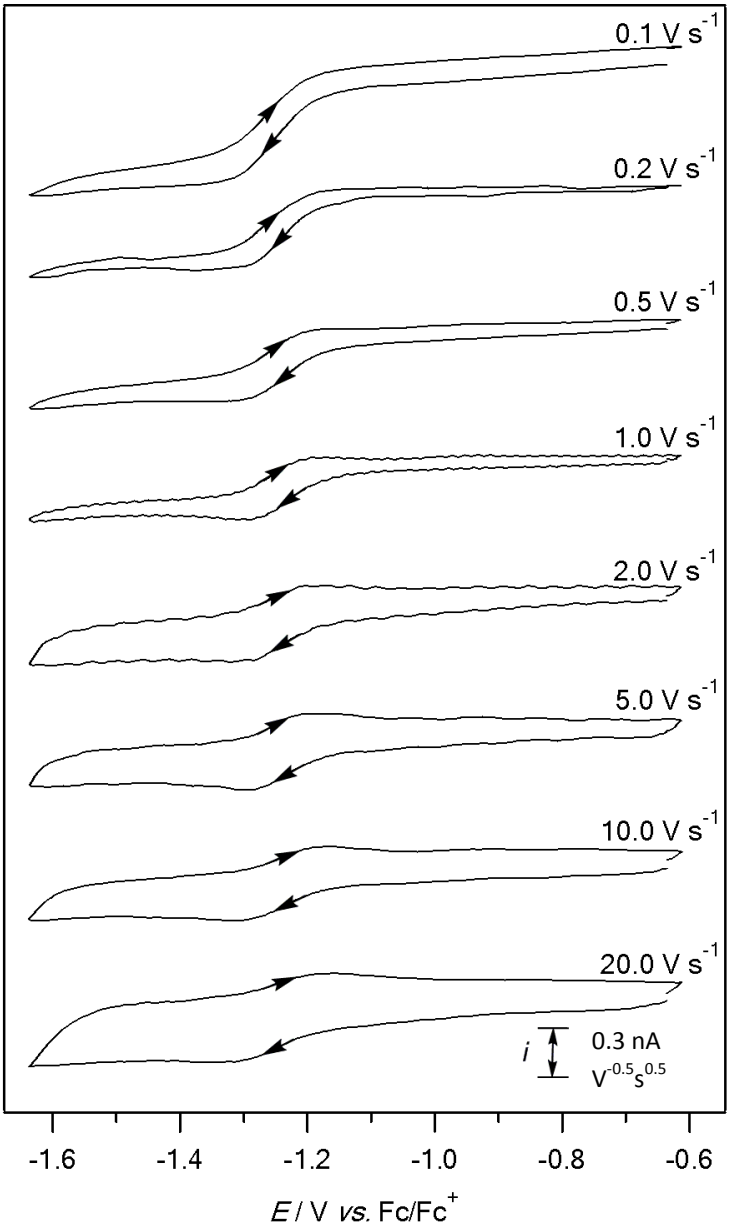

Figure 2.5. Variable scan rate cyclic voltammograms of 1 mM riboflavin in DMSO with 0.5 M *n*-Bu_4NPF_6, recorded at a 0.01 mm Pt electrode at 22 (±2) ^oC, where the scan direction was reversed at -1.65 V *vs.* Fc/Fc^+. The current data were scaled by multiplying by $\nu^{-0.5}$.

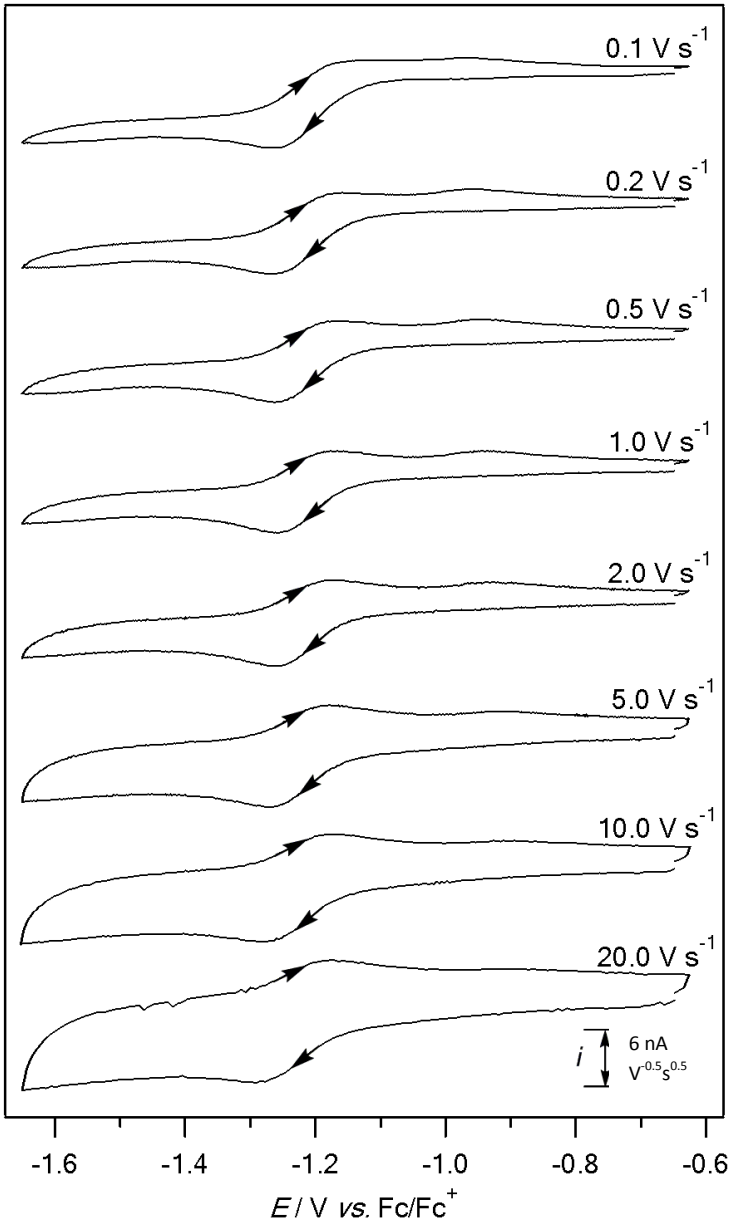

Figure 2.6. Variable scan rate cyclic voltammograms of 1 mM riboflavin in DMSO with 0.5 M *n*-Bu_4NPF_6, recorded at a 0.05 mm Pt electrode at 22 (±2) ^oC, where the scan direction was reversed at -1.65 V *vs.* Fc/Fc^+. The current data were scaled by multiplying by $\nu^{-0.5}$.

When the scan was extended to more negative potentials, additional reduction waves 4 and **5** were observed at approximately –1.8 V and –2.0 V *vs.* Fc/Fc^{+}, respectively (Figures 2.1(*b*) and 2.7 – 2.9). Wave 2 was observed to be significantly smaller when the scan direction was reversed just after wave 5 (at –2.2 V *vs.* Fc/Fc^{+}) compared to when the scan direction was reversed just after wave 1 (at –1.5 V *vs.* Fc/Fc^{+}) (compare Figures 2.1(*a*) and 2.1(*b*)). In contrast, wave 3 was observed to increase in size if the forward scan direction was extended past wave 5. Therefore, it is apparent that the electron transfer reactions occurring during wave 5 result in an increase in the amount of species responsible for wave 3.

It can be observed in Figures 2.7 – 2.9 that the current magnitude of wave 5 increases as the scan rate increases, whilst wave 4 decreases in current magnitude as the scan rate increases. Therefore, it is proposed that wave 5 is associated with further one-electron reduction of $Fl^{\bullet-}$ to form the dianion (Fl^{2-}) according to eq 6. Fl^{2-} is then able to rapidly gain a proton from an intermolecular exchange with Fl to form FlH^{-} (eq 7), which can then be oxidized in wave 3 (the reverse of eq 3). The position of wave 5 is consistent to what is often observed during the reduction of semiquinones in aprotic organic media, where the second electron transfer step (1 e^{-} reduction of the anionic radical to form the dianion) occurs several hundred mV more negative than the first electron transfer step (1 e^{-} reduction of the fully-oxidized quinone to form the anion radical).[41–45] The assignment of wave 5 as associated with one-electron reduction of $Fl^{\bullet-}$, negates the possibility that wave 1 occurs *via* a direct two-electron reduction to form the dianion, and the relatively small size of wave 5 as compared to wave 1 indicates that the anionic radical undergoes a chemical step to form another species.

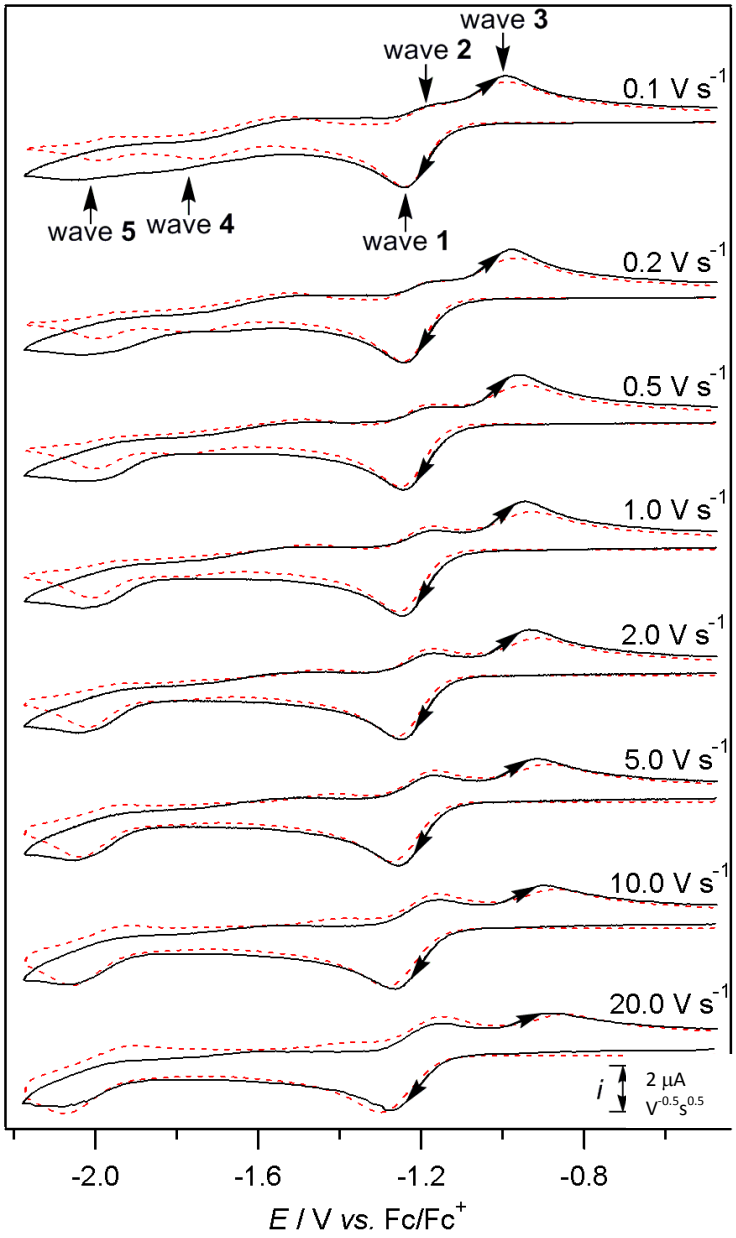

Figure 2.7. (Black lines) Variable scan rate CVs of 1 mM riboflavin in DMSO with 0.5 M *n*-Bu_4NPF_6, recorded at a 1 mm Pt electrode at 22 (±2) ^{o}C, where the scan direction was reversed at –2.2 V *vs.* Fc/Fc^{+}. (Red dotted lines) Digital simulations of the CV data based on the mechanism in Scheme 2.2 and parameters given in Tables 2.1 and 2.2. The current data were scaled by multiplying by $\nu^{-0.5}$.

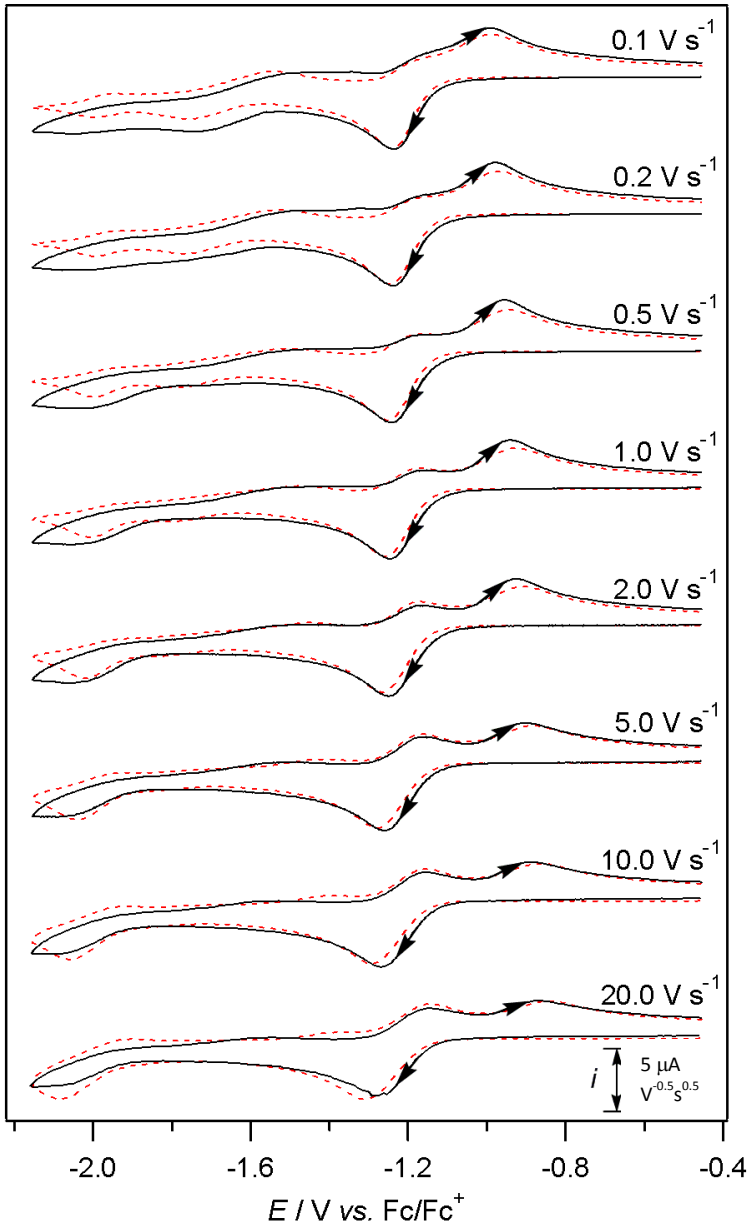

Figure 2.8. (Black line) Variable scan rate cyclic voltammograms of 2 mM riboflavin in DMSO with 0.5 M *n*-Bu_4NPF_6, recorded at a 1 mm Pt electrode at 22 (±2) ^oC, where the scan direction was reversed at -2.15 V *vs.* Fc/Fc^+. (Red dashed line) Digital simulations of the CV data based on the mechanism in Scheme 2.2 and parameters given in Table 2.1 and 2.2. The current data were scaled by multiplying by $v^{-0.5}$.

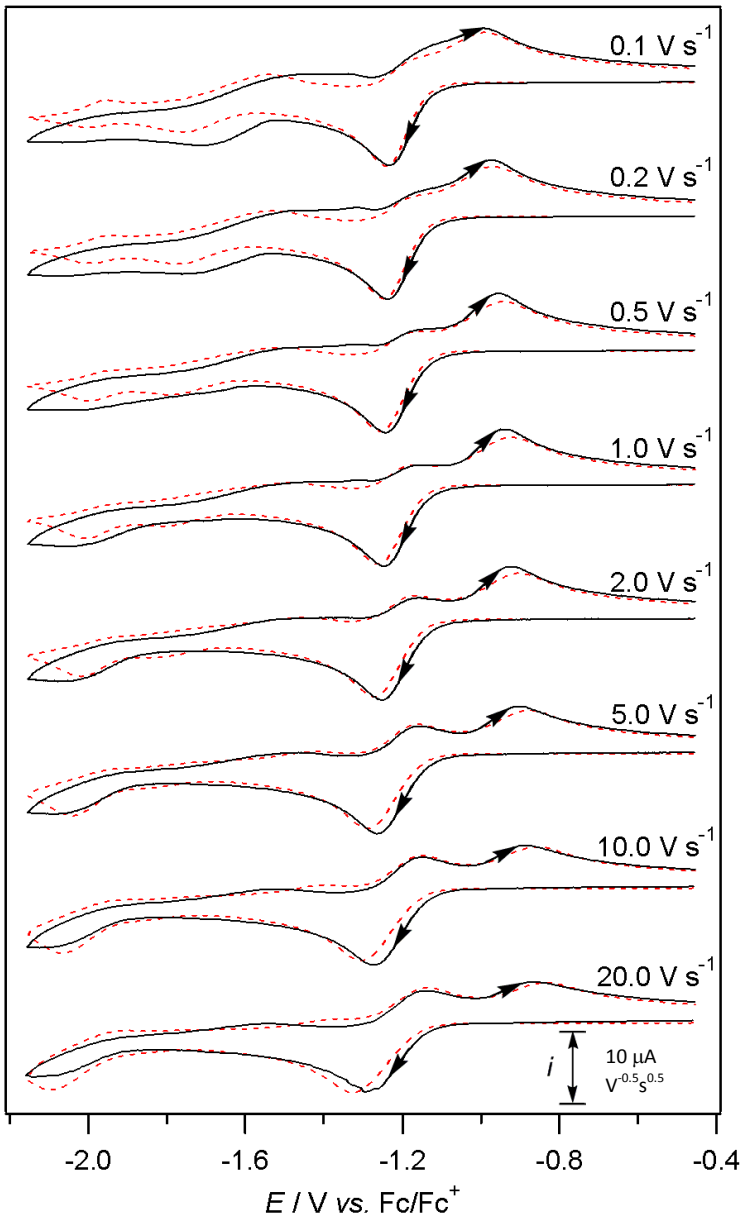

Figure 2.9. (Black line) Variable scan rate cyclic voltammograms of 3.6 mM riboflavin in DMSO with 0.5 M *n*-Bu_4NPF_6, recorded at a 1 mm Pt electrode at 22 (±2) ^{o}C, where the scan direction was reversed at -2.15 V *vs.* Fc/Fc^+. (Red dashed line) Digital simulations of the CV data based on the mechanism in Scheme 2.2 and parameters given in Table 2.1 and 2.2. The current data were scaled by multiplying by $\nu^{-0.5}$.

Because the species responsible for waves 4 and 5 are present at the electrode surface at lower concentrations than the starting material, wave 4 and 5 are easily overlooked, which is the reason these voltammetric waves have not yet been discussed in any detail. Species that exist in low concentrations are more easily detected using a differential voltammetric scanning technique such as square-wave voltammetry. In Figure 2.10, we observe that wave 4 and 5 are much more prominent. We can more confidently say that wave 4 is associated with the reduction of a flavin species despite the fact that wave 4 is only observed at very slow scan rate for cyclic voltammograms of riboflavin.

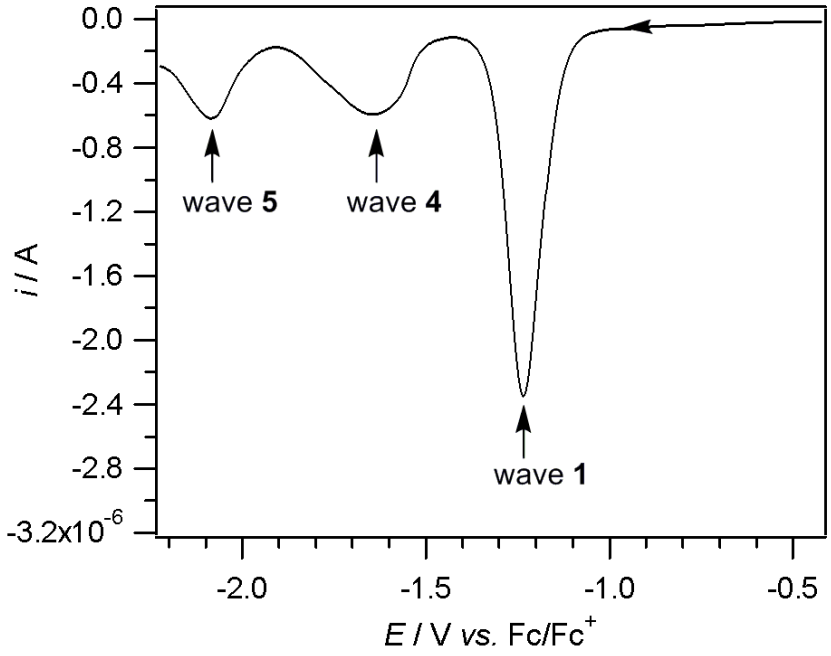

Figure 2.10. Square wave voltammogram obtained during the reduction of 2 mM riboflavin in DMSO with 0.5 M *n*-Bu_4NPF_6 at a 1 mm Pt electrode at 22 (±2) ^oC, recorded with a pulse period (τ) = 25 Hz, a potential step = 2 mV and a pulse amplitude = 20 mV.

Wave 4 is only noticeable at slow scan rates (ν < ~0.2 V s^{-1}) and can be observed to decrease in magnitude proportionally to wave 2 increasing in magnitude as the scan rate is increased. As the scan rate increases, the reaction between Fl and $Fl^{\bullet-}$ is outrun (eq 5), hence the amount of Fl^{-} at the electrode surface would also diminish. Although the formation of Fl^{-} has been suggested by Niemz et al.,[24] there has not yet been substantial proof that this species has been formed. It is, however, expected to be able to be electrochemically reduced at potentials more negative than wave 1, as Fl^{-} is expected to be harder to reduce than the neutral oxidized flavin (Fl) due to the negative charge on the isoalloxazine ring, which is where the redox reactions occur in the flavin. Therefore, wave 4 has been assigned as due to the reduction of Fl^{-} (eq 8). Wave 4 is also observed to be drawn out over a larger potential range when compared to wave 1, which can be accounted for by the process involving a slower heterogeneous electron transfer than the reduction of fully-oxidized flavin. Assigning wave 4 to the reduction of Fl^{-} would also help to explain the increase in relative size of wave 4 for increasing riboflavin concentrations at the same scan rate. As the concentration of riboflavin is increased, the chemical reaction between Fl and $Fl^{\bullet-}$ to form Fl^{-} and $FlH^{\bullet}$ would be pushed towards the product, and more Fl^{-} would exist in solution leading to a larger relative size of wave 4.

In order to show that wave 4 is indeed associated with the reduction of Fl^{-}, one equivalent of the strong base *n*-Bu_4NOH (40% in water) was added to a solution of 1.5 mM riboflavin in DMSO, where *n*-Bu_4NO^{-} is expected to deprotonate the imide proton on the isoalloxazine ring. It was observed that upon addition of base, the bright yellow colored solution immediately changed into a dark brown colored solution. The resulting solution was analyzed *via* cyclic voltammetry and it was observed that while wave 1 had completely disappeared, the current magnitude of wave 4 had increased (Figure 2.11), indicating that Fl had completely reacted with the base, and wave 4 is likely to be associated with the reduction of deprotonated fully-oxidized flavin Fl^{-}.

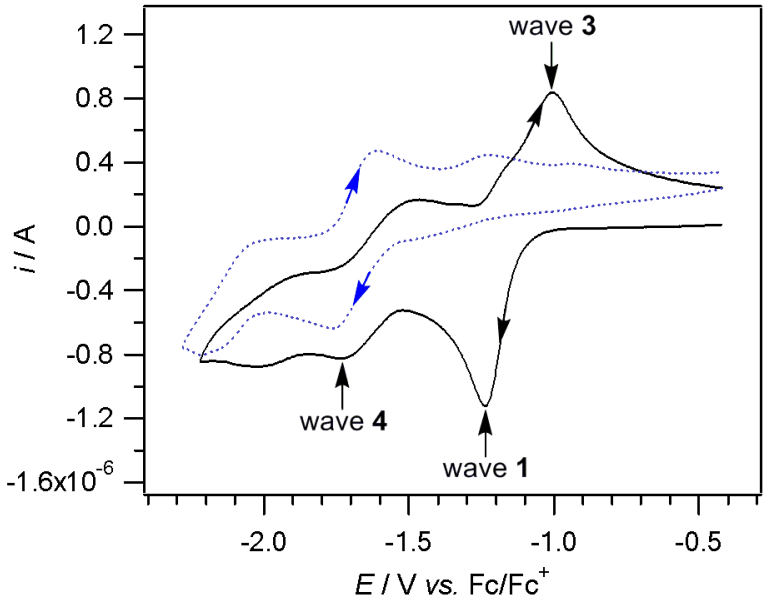

Figure 2.11. Cyclic voltammograms of 1.5 mM riboflavin in DMSO with 0.5 M *n*-Bu_4NPF_6, recorded at a 1 mm Pt electrode at 22 (±2) ^oC and at a scan rate of 0.1 V s^{-1}: (Black line) before addition of *n*-Bu_4NOH; (Dotted blue line) after addition of *n*-Bu_4NOH.

2.3.2. Controlled potential electrolysis

Bulk controlled-potential electrolysis and coulometry experiments were carried out in order to determine the number of electrons transferred during the bulk reduction and to estimate the lifetime of the reduced flavin species. The applied potential was set at –1.0 V *vs.* Ag wire (the reference electrode was separated from the test solution with a salt bridge containing 0.5 M *n*-Bu_4NPF_6 in CH_3CN), which was approximately –0.2 V more negative than the reduction peak (E_p^{red}). While the electrolysis experiment was in progress, the color of the solution was observed to change from bright yellow to reddish-brown. In Figure 2.12(*a*), the CV obtained in the working electrode compartment of the electrolysis cell (at a 1 mm diameter Pt electrode) prior to the electrolysis (black solid line) and the CV obtained at the completion of the electrolysis (blue dotted line) can be compared. It is significant to observe that the position of zero current in the CV obtained after the

completion of the electrolysis has shifted upwards when compared to the CV obtained before electrolysis. This indicates that the reduced species exists in a negatively charged state that can undergo oxidation by applying a potential more positive than –0.6 V *vs.* Ag wire (0.5 M *n*-Bu_4NPF_6 in CH_3CN).

In Figure 2.12(*b*), the current *vs.* time trace obtained during the electrolysis (black solid line) is shown, together with the corresponding charge (the integrated current *vs.* time) that has been manipulated to express the number of electrons transferred per molecule (red dotted line). The coulometry data confirm that close to one electron (0.95) was transferred per riboflavin molecule during the bulk reduction. In order to determine if the reduced species is sufficiently long-lived in this media and if the reduction is reversible, an oxidizing potential of –0.5 V *vs.* Ag wire (0.5 M *n*-Bu_4NPF_6 in CH_3CN) was applied to the working electrode, which resulted in the transfer of 0.85 electrons per molecule of riboflavin and the regeneration of the fully-oxidized flavin. It has been previously observed that the reverse electrolysis process does not always quantitatively regenerate the initial oxidized species (even if the reduced species is indefinitely long-lived) due to the diffusion of a portion of the reduced species into the other compartment of the electrolysis cell and can no longer get oxidized at the working electrode.[17] The resultant CV obtained upon completion of the reverse electrolysis was identical to the CV of fully-oxidized riboflavin, and the color of the solution turned from reddish-brown back to bright yellow, indicating that riboflavin is recovered upon oxidation on electrolysis timescales (hours) and confirming that its reduced forms are long-lived in DMSO solution.

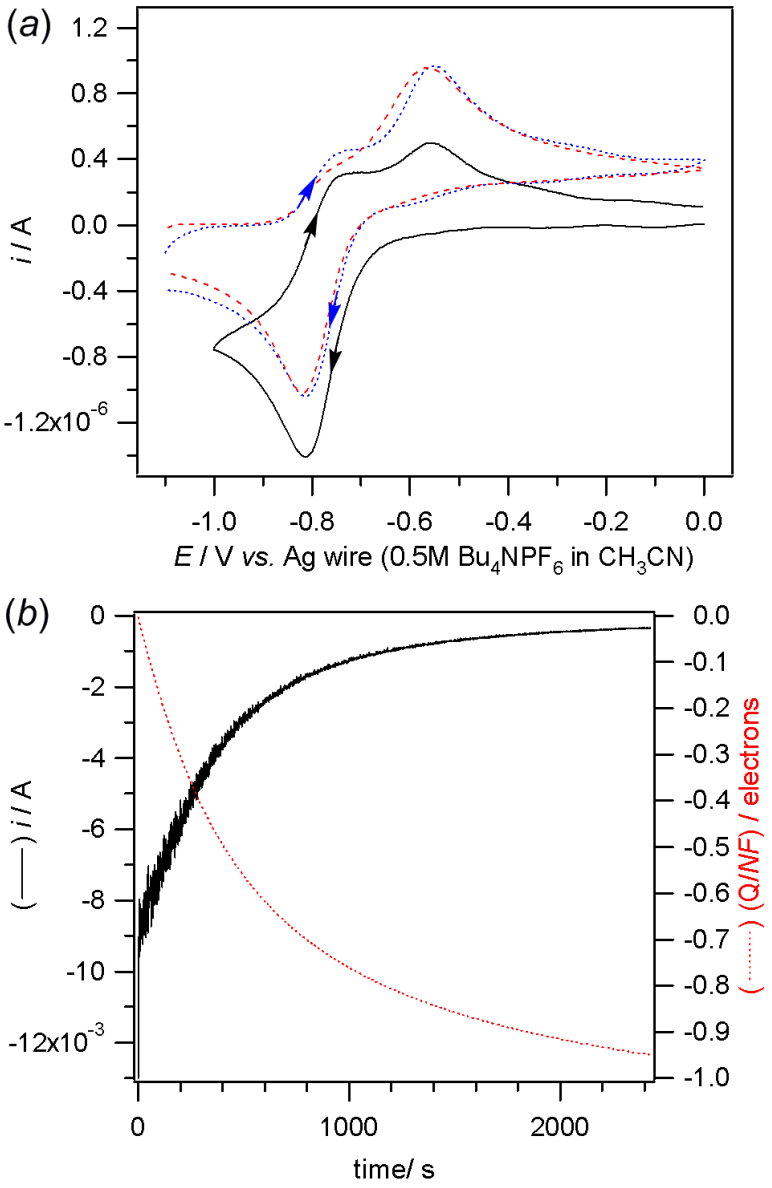

Figure 2.12. Voltammetric and coulometric data obtained at 22 (±2) ^{o}C during the controlled potential electrolysis of 2 mM riboflavin in DMSO with 0.5 M *n*-Bu_4NPF_6. (*a*) Cyclic voltammograms recorded at a scan rate of 0.1 V s^{-1} with a 1 mm diameter planar Pt electrode: (Black line) before the bulk reduction of riboflavin; (Blue dotted line) after the exhaustive reduction of riboflavin; (Red dashed line) simulated voltammogram according to the reaction in Scheme 2.2 and parameters in Tables 2.1 and 2.2. (*b*) Current/coulometry *vs.* time data obtained during the exhaustive reduction of riboflavin at –1.0 V *vs.* Ag wire (0.5 M *n*-Bu_4NPF_6 in CH_3CN).

2.3.3. UV-vis experiments

Although the cyclic voltammograms obtained during the bulk reduction and bulk re-oxidation suggests that majority of the fully-oxidized flavin could be regenerated, approximately 10% of the initial amount had been lost. While there is sufficient reason to suspect diffusion into the counter electrode compartment, the possibility of decomposition or other irreversible chemical reactions should not be disregarded. In order to spectroscopically confirm that the reduced species ($Fl^{\bullet -}$ and FlH^{-}) could be oxidized back into fully-oxidized riboflavin without forming any decomposition products, *in situ* electrochemical UV-vis spectroscopic experiments were performed in an OSTLE cell.[17] In this experiment, electrolysis occurs in a thin layer cell with a pathlength of 0.67 mm with a thin Pt wire mesh as the working electrode, and UV-vis spectra are continuously collected during electrolysis. As the amount of riboflavin in the thin layer cell is many times less than in a regular electrolysis experiment, no stirring or agitation of the solution is required for all the riboflavin molecules to undergo reduction, and the diffusion within and out from the thin layer occurs extremely slowly. Figure 2.13(*a*) shows the spectra obtained during the forward bulk reduction, Figure 2.13(*b*) shows the spectra obtained during the reverse bulk oxidation and Figure 2.13(*c*) shows the spectra obtained before bulk reduction (black line), and after the reduced compound had been oxidized (dotted blue line). The overlap of the spectra shown in Figure 2.13(*c*) confirms the complete regeneration of the fully-oxidized riboflavin after electrolysis, which means that the reduced species ($Fl^{\bullet -}$ and FlH^{-}) are long-lived within the time scale of this experiment (approximately 1 h).

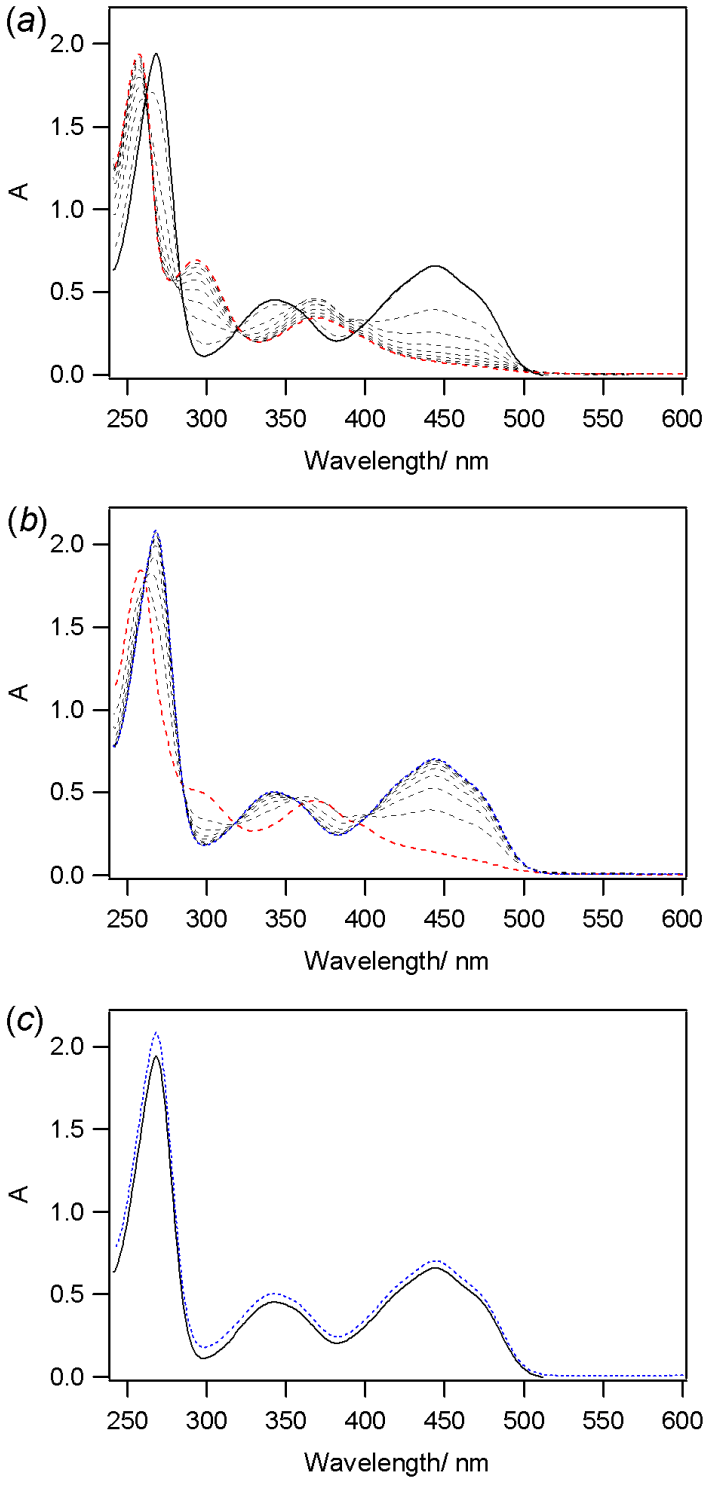

Figure 2.13. *In situ* electrochemical UV-vis spectra of 1 mM riboflavin in DMSO containing 0.5 M *n*-Bu_4NPF_6. (*a*) Obtained during the reduction of riboflavin. (*b*) Obtained during the reoxidation of the reduced forms of riboflavin ($Fl^{\bullet -}$ and FlH^-). (*c*) A comparison of (black line) riboflavin and (dotted blue line) after the reduced compound had been oxidized back to the starting material.

During the bulk reduction of riboflavin, the UV-visible peaks with absorption maxima at 268 nm, 343 nm and 445 nm were observed to decrease, concomitantly to the appearance and increase in size of peaks with absorption maxima at 257 nm and 370 nm. The anionic radical $Fl^{\bullet-}$ has characteristic absorption maxima at around 370 nm and a smaller peak at approximately 478 nm, as shown by Niemz *et al.*[24] using a modified *N*-methylated flavin that is able to undergo reduction to obtain radical anion $Fl^{\bullet-}$ quantitatively. When one equivalent of a suitable proton donor was added to this modified *N*-methylated flavin, the fully-oxidized flavin was reduced to form purely FlH^{-}, with only a shoulder absorption around 360 nm.[24] In comparison, our UV-vis spectra depicted a shoulder (rather than a clear peak) at 478 nm and a significantly smaller peak at 370 nm, as FlH^{-} and $Fl^{\bullet-}$ were both formed during the reduction. We also did not observe a bright red color after electrolysis, but a dull reddish-brown, likely to be a mixture of the red $Fl^{\bullet-}$ and the dull yellow FlH^{-}.

2.3.4. EPR experiments

EPR experiments were performed by electrochemically reducing solutions of riboflavin in DMSO in an electrolysis cell and transferring an aliquot of the reduced solution into a silica flat cell under a nitrogen atmosphere. A radical signal with a *g*-value of 2.0048 was detected (Figure 2.14(*a*)), with the same splitting pattern as has been previously observed during the reduction of riboflavin in DMSO.[34] The EPR signal showed no change in intensity over a period of at least 3 hours, indicating that the detected radical was long-lived. The CV and electrolysis experiments conducted on riboflavin indicate that 2 reduced flavin species are formed during the electrochemical reduction step, FlH^{-} and $Fl^{\bullet-}$, existing together with the deprotonated oxidized flavin Fl^{-}. Therefore, the detection of a long-lived radical can be accounted for by an equilibrium between FlH^{-} and Fl^{-} to produce 2 molecules of $Fl^{\bullet-}$ (eq 9).

$$FlH^- + Fl^- \rightleftharpoons 2\ Fl^{\bullet -} \quad (9)$$

Provided that the equilibrium constant in eq 9 is low, $Fl^{\bullet -}$ will appear to exist as a long-lived radical, albeit with a lower EPR signal intensity if reduced by one electron directly to the anionic radical. Quantitative EPR experiments were conducted by over-modulating the EPR signal obtained after the bulk electrochemical reduction of fully-oxidized riboflavin and comparing the signal intensity with the long-lived anionic radical produced during the one-electron reduction of vitamin K_1 (VK_1),[44] under identical instrumental and experimental conditions. Figure 2.14(*b*) shows that the anionic radical signal of reduced vitamin K_1 ($VK_1^{\bullet -}$) is significantly more intense than that of $Fl^{\bullet -}$. The integrated EPR signal intensity of $Fl^{\bullet -}$ was found to be 40% of the integrated signal intensity of $VK_1^{\bullet -}$, with the two solutions produced by electrolysis and the EPR spectra recorded under identical instrumental conditions. These data support the assignment of the anionic radical produced during the reduction of fully-oxidized riboflavin as a product formed by a secondary equilibrium process (eq 9) instead of a direct one-electron reduction.

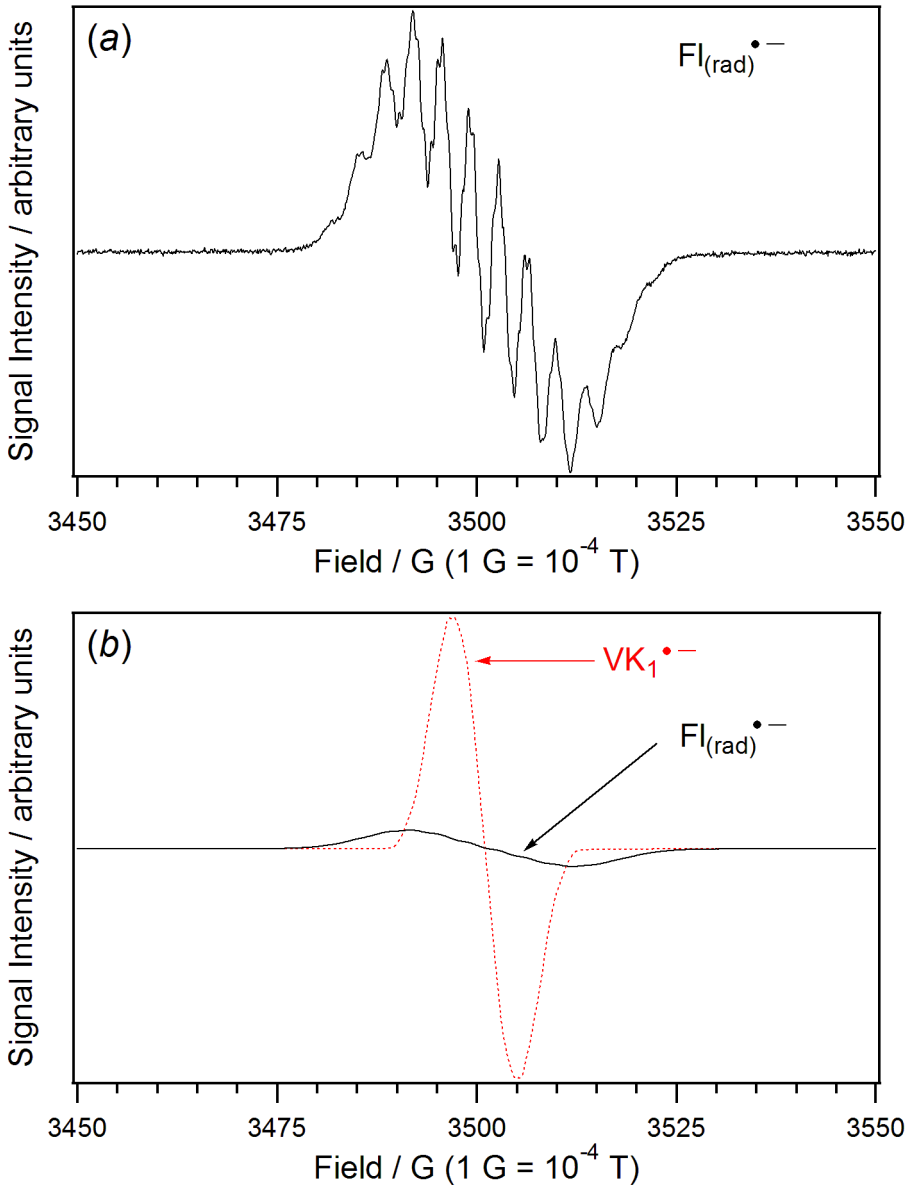

Figure 2.14. (*a*) Continuous wave X-band EPR spectrum of a 2 mM solution of riboflavin that had been exhaustively reduced in DMSO containing 0.5 M *n*-Bu_4NPF_6 *via* controlled potential electrolysis by one-electron per molecule to partially form [$Fl^{\bullet -}$] according to Scheme 2.2. Modulation amplitude = 0.2 G, T = 22 (±2) ^{o}C. (*b*) Continuous wave X-band EPR spectra of separate solutions of 2 mM riboflavin and 2 mM vitamin K_1 in DMSO containing 0.5 M *n*-Bu_4NPF_6 that had been exhaustively reduced *via* controlled potential electrolysis by one-electron per molecule to form $Fl^{\bullet -}$ (plus FlH^-) and $VK_1^{\bullet -}$, respectively. Modulation amplitude = 10 G, T = 22 (±2) ^{o}C.

2.3.5. Digital simulation of CV data

There have been many reports of both inorganic and organic compounds that undergo reversible structural changes (including proton transfer reactions and ligand substitutions about a metal ion) before, during, or after the electron transfer steps. When the electron transfer steps and reversible chemical transformations occur in a consecutive manner, the mechanism can be represented as a square-scheme.[50–62] The complete electrochemical reduction mechanism of riboflavin in DMSO is given in Scheme 2.2, based on the results and analysis of the electrochemical and spectroscopic data. The electrochemical reduction mechanism comprises a number of square schemes involving several proton transfer and electron transfer reactions. It is known that the presence of the imide proton on N3 on the flavin isoalloxazine ring (or the addition of a proton source) is critical to the observation of wave 3,[24] hence the imide proton must be involved in the coupled chemical reactions. Thus, the proposed reactions include the intermolecular proton transfer of the imide proton (N3–H) of the fully-oxidized flavin Fl to the N5 atom of other reduced flavin species as shown in Scheme 2.2.

For slow scan rates and a low switching potential of –1.6 V *vs.* Fc/Fc^+, fully-oxidized riboflavin (Fl) is first reduced by one electron to form the anionic radical $Fl^{\bullet-}$ ($E^0_{f(1)}$), which receives a proton from another fully oxidized flavin to form the neutral radical $FlH^\bullet$ and the deprotonated oxidized flavin (Fl^-) (eq 5). Since the $E^0_{f(3)}$ (–1.05 V *vs.* Fc/Fc^+) for the reduction of $FlH^\bullet$ to FlH^- is less negative than the $E^0_{f(1)}$ (–1.22 V *vs.* Fc/Fc^+) for the reduction of Fl to $Fl^{\bullet-}$, the neutral radical $FlH^\bullet$ will be immediately reduced to FlH^- at that applied potential (or can react *via* a disproportionation reaction according to eq 4). The Fl^- and FlH^- species can then undergo a comproportionation reaction (involving an electron and proton exchange) to form two molecules of the anionic radical $Fl^{\bullet-}$ (eq 9). As the comproportionation is an equilibrium reaction, $Fl^{\bullet-}$, Fl^- and FlH^- would exist in equilibrium. When the scan direction is reversed, we observe the oxidation of both $Fl^{\bullet-}$

(wave 2) and FlH^- (wave 3). At fast scan rates, the rate constant of the proton transfer step (eq 5) is outrun and only wave 2 (one-electron oxidation of $Fl^{\bullet-}$ back to Fl) is observed when the scan direction is reversed.

For slow scan rates and a more negative switching potential of –2.2 V *vs.* Fc/Fc^+, two additional reduction waves are observed (waves 4 and 5). Wave 4 is associated with the reduction of the deprotonated oxidized flavin Fl^- ($E^0_{f(4)}$) and wave 5 is associated with the reduction of the anionic radical $Fl^{\bullet-}$ ($E^0_{f(2)}$). As the scan rate increases, wave 4 becomes smaller (less Fl^- produced as eq 5 is outrun), while wave 5 becomes larger (as eq 5 is outrun, $Fl^{\bullet-}$ does not get protonated, so there is more $Fl^{\bullet-}$ able to undergo further reduction). The dianion Fl^{2-} can be converted into FlH^- according to equation 7. $Fl^{\bullet-}$ is in equilibrium with $Fl^{2\bullet-}$ according to eq 10, and the deprotonation of fully oxidized flavin (shown on the left of Scheme 2.2) can occur *via* eqs 5, 7 and 10.

$$Fl^{2-\bullet} + Fl \rightleftharpoons Fl^{\bullet-} + Fl^- \qquad (10)$$

Digital simulations were performed on the cyclic voltammetric data that were obtained at scan rates between 0.1 – 20 V s^{-1}, for concentrations of riboflavin between 1 mM – 3.6 mM, and at a Pt working electrode with a diameter of 1 mm. The data were modeled according to the entire mechanism in Scheme 2.2. A simulation program Digielch was used, which predicts voltammograms based on the E^0 and k_s of the electron transfer reactions and the K_{eq} and rate constants of the chemical reactions that were input into the program. Using this program, we used a trial and error process with no fixed paramters to obtain a set of parameters that could give us a good fit to experimental data when the scan rates, switching potential and concentrations were changed. The trial and error process typically required estimating the E^0 and changing the parameters until the trends with increasing scan rates at both switching potentials could be observed, before tweaking the E^0 and k_s and once again changing the kinetic parameters until the trends were observed.

This process is repeated until a good fit to experimental data was obtained. One set of electrochemical and kinetic parameters that was able to simulate the CVs of varying scan rates for 2 switching potentials for all concentrations of riboflavin was obtained. The electrochemical and kinetic parameters obtained by the simulations are given in Tables 2.1 and 2.2. The simulated voltammograms for 1 mM riboflavin (Figures 2.2, 2.7 and 2.12), 2 mM riboflavin (Figures 2.3 and 2.8) and 3.6 mM riboflavin (Figures 2.4 and 2.9) are shown as dashed red lines.

The simulations were based on the ECE mechanism (eqs 1 – 3) rather than the DISP1 mechanism (eqs 1,2 and 4). Due to the large number of steps involved in the reaction, it is very challenging to be able to distinguish between these two possibilities. Also, the electron transfer steps and homogeneous reactions were modeled based on consecutive pathways, instead of concerted pathways, as it is also very difficult to differentiate with the large number of homogeneous steps involved.

The simulations use exactly the same electrochemical and kinetic parameters for all of the scan rates and concentrations of riboflavin. A good match between the experimental and simulated voltammograms could be obtained, which indicates the proposed mechanism is theoretically possible, and supports the assignment of the overall reaction given in Scheme 2.2. It can also be observed in Figure 2.12 that the simulation of the CV that was obtained after electrolysis (that contains FlH^{-} and $Fl^{\bullet -}$) using the same parameters also matched the experimentally obtained CV, which also supports the overall mechanism.

Scheme 2.2. Voltammetrically induced proton-coupled electron transfer reduction mechanism of riboflavin in DMSO studied by cyclic voltammetry over a range of scan rates and concentrations.[a]

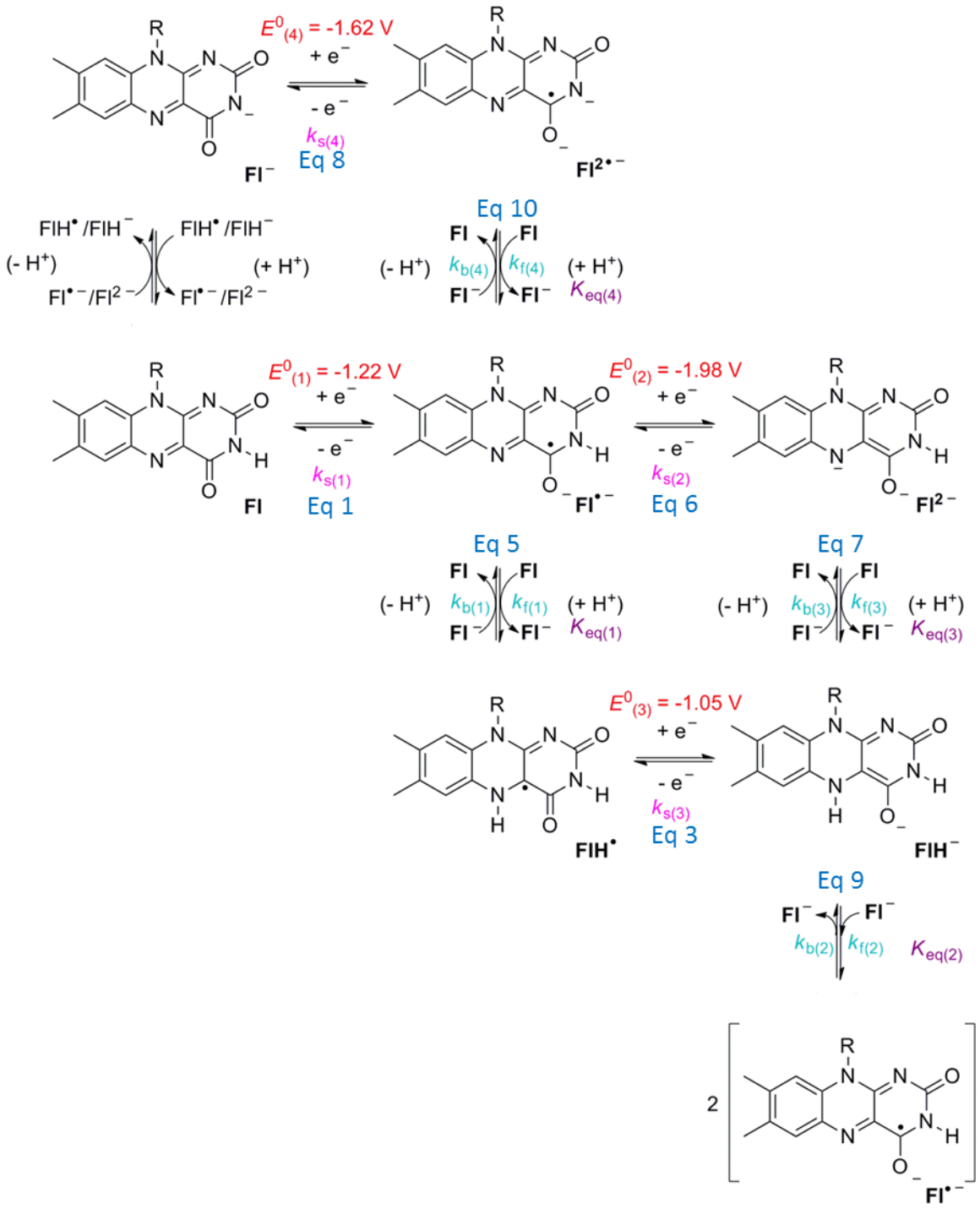

[a]Electrochemical, equilibrium and kinetic values associated with the heterogeneous electron transfer steps ($E^0_{f(1)} - E^0_{f(4)}$) (eqs 1, 3, 6 and 8) and homogeneous chemical steps (eqs 5, 7, 9 and 10) are given in Tables 2.1 and 2.2. Only one resonance structure is given

for each compound and the counterions for the charged species are either the supporting electrolyte cation (n-Bu_4N^+) or anion (PF_6^-).

Table 2.1. Electrochemical parameters obtained by digital simulation of CV[a] data for the reaction mechanism given in Scheme 2.2.

10^{-6} D / cm^2 s^{-1}	R / Ω	Eq 1 $Fl + e^- \rightleftharpoons Fl^{\bullet-}$		Eq 6 $Fl^{\bullet-} + e^- \rightleftharpoons Fl^{2-}$		Eq 3 $FlH^{\bullet} + e^- \rightleftharpoons FlH^-$		Eq 8 $Fl^- + e^- \rightleftharpoons Fl^{2-\bullet}$	
		$E^0_{(1)}$[b] / V	$k_{s(1)}$/ cm s^{-1}	$E^0_{(2)}$[b] / V	$k_{s(2)}$ / cm s^{-1}	$E^0_{(3)}$[b] / V	$k_{s(3)}$/cm s^{-1}	$E^0_{(4)}$[b] / V	$k_{s(4)}$/cm s^{-1}
1.6	1000	-1.22	0.02	-1.98	0.01	-1.05	0.001	-1.62	0.0004

[a]CV data recorded in DMSO at 22 (±2) [o]C with 0.5 M n-Bu_4NPF_6 as the supporting electrolyte with a 1 mm diameter planar Pt working electrode and at scan rates between 0.1 – 20 V s^{-1}. [b]Formal potential *vs.* Fc/Fc^+ (add 0.43 V to convert to *vs.* SCE[67]).

Table 2.2. Equilibrium and rate constants obtained by digital simulation of CV data for the reaction mechanism given in Scheme 2.2 obtained in DMSO containing 0.5 M Bu_4NPF_6 at 22 (±2) ^oC.

Eq 5 $Fl^{\bullet-} + Fl \rightleftharpoons FlH^{\bullet} + Fl^-$			Eq 9 $FlH^- + Fl^- \rightleftharpoons 2\,Fl^{\bullet-}$			Eq 7 $Fl^{2-} + Fl \rightleftharpoons FlH^- + Fl^-$			Eq 10 $Fl^{2-\bullet} + Fl \rightleftharpoons Fl^{\bullet-} + Fl^-$		
$K_{eq(1)}$	$k_{f(1)}$ / L mol^{-1} s^{-1}	$k_{b(1)}$ / L mol^{-1} s^{-1}	$K_{eq(2)}$	$k_{f(2)}$ / L mol^{-1} s^{-1}	$k_{b(2)}$ / L mol^{-1} s^{-1}	$K_{eq(3)}$	$k_{f(3)}$ / L mol^{-1} s^{-1}	$k_{b(3)}$ / L mol^{-1} s^{-1}	$K_{eq(4)}$	$k_{f(4)}$ / L mol^{-1} s^{-1}	$k_{b(4)}$ / L mol^{-1} s^{-1}
8.00 × 10^{-3}	1.00 × 10^6	1.25 × 10^8	1.67 × 10^{-1}	2.00 × 10^2	1.19 × 10^3	4.17 × 10^{13}	≥ 1.00 × 10^6	2.40 × 10^{-8}	5.76 × 10^6	1.00 × 10^4	1.74 × 10^{-3}

All the electrochemical and kinetic parameters reported in Tables 2.1 and 2.2 were input into the simulation of each cyclic voltammogram, although the effects of the different equilibrium and rate constants are not always noticeable at a single scan rate, and a wide range of values could be used to match the cyclic voltammogram at a particular scan rate. As we continue to use these parameters to simulate the cyclic voltammograms at different scan rates, the range of values is narrowed down, as the parameters would have to reflect the trends observed at different scan rates. Thus, the simulations need to match over a range of scan rates in order to obtain the optimal kinetic values. Matching the simulations to different concentrations of riboflavin would narrow down the range of values of the kinetic parameters, giving a more accurate set of kinetic

values. The thermodynamic nature of the square scheme means that the equilibrium constants and formal potentials of species in the square scheme are interrelated. Thus, if two formal potentials (e.g. $E^0_{f(2)}$ and $E^0_{f(3)}$) and only one equilibrium constant (e.g. $K_{eq(1)}$) are known, then the second equilibrium constant in the square scheme (i.e. $K_{eq(3)}$) is interrelated and can be calculated.[63,64]

It is crucial to note that the estimated formal potentials reported in Table 2.1 are given *vs.* the ferrocene$^{0/+}$ (Fc/Fc^+) redox couple, which is the recommended reference standard for non-aqueous solvents.[65,66] In order to convert the reported formal potential to the saturated calomel electrode (SCE) scale, 0.43 V can be added to the values reported in Table 2.1.[66,67] Also, the forward rate constant of eq 7 in Table 2 is reported as the minimum value which provided a good fit to the experimental data, although it could possibly approach the diffusion limited maximum (~1×10^{10} L mol^{-1} s^{-1}). The heterogeneous electron transfer rate for eq 8 ($k_{s(4)}$) appeared to be particularly low; 2 orders of magnitude less than the heterogeneous electron transfer rate for the initial electron transfer step ($k_{s(1)}$). The Marcus Microscopic model of electron transfer predicts that electron transfer reactions involving large structural changes would have a slower rate of heterogeneous electron transfer, thus the low $k_{s(4)}$-value could indicate that the transformation between Fl^- and $Fl^{2-\bullet}$ involves a comparatively large structural change.[48] Surface/solute interactions may also be important, since it was found that when glassy carbon (GC) rather than Pt was used as the electrode surface, the voltammetric waves became more drawn out, suggesting even slower heterogeneous electron transfer rates.

2.3.6. Relevance of electrochemical results to flavoproteins

It has been established that many flavins in flavoproteins undergo reduction *via* a hydride transfer, directly reducing fully-oxidized flavin (Fl) to FlH^-.[68–69] In this study, FlH^- is formed *via* PCET reactions instead of a direct hydride transfer. In our system of

free flavins, several oxidation states of flavin can coexist, and FlH^- undergoes additional chemical reactions. However, proton-coupled electron transfer steps have also been observed in some flavoproteins. For example, the crystal structure of flavodoxin suggests that after one-electron reduction, N5 undergoes protonation by a nearby amide proton of the protein backbone.[70–72] While we have proposed that $FlH^{\bullet}$ of free riboflavin in aprotic media would immediately be reduced as it is formed because it is easier to reduce than the fully-oxidized flavin, it has been proposed that the reduction potential of the neutral radical ($FlH^{\bullet}$) in flavodoxin is more negative than in free FMN by 300 – 400 mV, due to stabilization of the $FlH^{\bullet}$ by H-bonding interactions of N5–H with a carbonyl oxygen in the flavoprotein.[72] Therefore, after the anionic radical $Fl^{\bullet-}$ is protonated to form the neutral radical $FlH^{\bullet}$, it does not undergo further reduction, as occurs in this study. This indicates the importance of the protein structure in stabilizing the different forms of the flavoquinones, and if a slight conformation change or mutation occurs, the reduction potentials and electron transfer mechanism may also vary significantly.

Due to the role of a neighboring Fl acting as a proton donor to $Fl^{\bullet-}$, this study has more significance for flavoproteins containing two or more flavin cofactors, such as hepatic NADPH-cytochrome P-450 reductase (a diflavin reductase), as well as Na^+-pumping NADH-ubiquinone oxidoreductase. For Na^+-pumping NADH-ubiquinone oxidoreductase, which has two covalently bound FMN cofactor, one non-covalently bound FAD cofactor and one non-covalently bound riboflavin cofactor, it has recently been shown that the radical anion ($Fl^{\bullet-}$) was present in the fully reduced enzyme,[73–74] although this phenomena is not well understood. It is believed that this study may provide insights on the mechanisms of similar enzymes, provided that the two flavin cofactors are well positioned to interact with each other.

2.4. Conclusions

Bulk controlled potential electrolysis and spectroscopic experiments indicated that the net electrochemical reduction of riboflavin in DMSO occurred by one-electron per molecule and was completely chemically reversible on the hours timescale at 22 (±2) ^{o}C, indicating that both the anionic radical ($Fl^{\bullet-}$) and the further reduced and protonated anion (FlH^{-}) were very long-lived. Quantitative EPR experiments led to the estimation that $Fl^{\bullet-}$ existed in approximately 40% yield based on the exhaustive electrolysis of the starting material. However, CV experiments and associated digital simulations indicated that the persistent existence of $Fl^{\bullet-}$ in the bulk solution (produced during controlled potential electrolysis experiments) was a result of the homogeneous reaction between FlH^{-} and the deprotonated oxidized flavin Fl^{-} to form 2 molecules of $Fl^{\bullet-}$ (eq 9) rather than by direct one-electron reduction of fully-oxidized flavin to form $Fl^{\bullet-}$. While the EPR spectroscopic experiments are only sensitive to the existence of radicals, the UV-vis spectrum of the reduced solution indicated that a mixture of both $Fl^{\bullet-}$ and FlH^{-} exists after reduction. CV experiments confirmed the existence of the deprotonated oxidized flavin (Fl^{-}) and the dianion (Fl^{2-}) *via* the identification of their voltammetric waves, which allowed the assignment of their standard redox potentials.

2.5. References

1. Huynh, M. H. V.; Meyer, T. J. *Chem. Rev.* **2007**, *107*, 5004–5064.

2. Costentin, C. *Chem. Rev.* **2008**, *108*, 2145–2179.

3. Costentin, C.; Robert, M.; Savéant, J.-M. *Acc. Chem. Res.* **2010**, *43*, 1019–1029.

4. Warren, J. J.; Tronic, T. A.; Mayer, J. M. *Chem. Rev.* **2010**, *110*, 6961–7001.

5. Bonin, J.; Robert, M. *Photochem. Photobiol.* **2011**, *87*, 1190–1203.

6. Rhile, I. J.; Mayer, J. M. *J. Am. Chem. Soc.* **2004**, *126*, 12718–12719.

7. Costentin, C.; Robert, M.; Savéant, J.-M. *J. Am. Chem. Soc.* **2006**, *128*, 4552–4553.

8. Rhile, I. J.; Markle, T. F.; Nagao, H.; DiPasquale, A. G.; Lam, O. P.; Lockwood, M. A.; Rotter, K.; Mayer, J. M. *J. Am. Chem. Soc.* **2006**, *128*, 6075–6088.

9. Costentin, C.; Robert, M.; Savéant, J.-M. *J. Am. Chem. Soc.* **2006**, *128*, 8726–8727.

10. Markle, T. F.; Mayer, J. M. *Angew. Chem. Int. Ed.* **2008**, *47*, 738–740.

11. Costentin, C.; Louault, C.; Robert, M.; Savéant, J.-M. *J. Am. Chem. Soc.* **2008**, *130*, 15817–15819.

12. Costentin, C.; Louault, C.; Robert, M.; Savéant, J.-M. *PNAS*, **2009**, *106*, 18143–18148.

13. Costentin, C.; Robert, M.; Savéant, J.-M. *Phys. Chem. Chem. Phys.* **2010**, *12*, 11179–11190.

14. Bonin, J.; Costentin, C.; Louault, C.; Robert, M.; Savéant, J.-M. *J. Am. Chem. Soc.* **2011**, *133*, 6668–6674.

15. Mayer, J. M. *Acc. Chem. Res.* **2011**, *44*, 36–46.

16. Bonin, J.; Costentin, C.; Robert, M.; Savéant, J.-M. *Org. Biomol. Chem.* **2011**, *9*, 4064–4069.

17. Williams, L. L.; Webster, R. D. *J. Am. Chem. Soc.* **2004**, *126*, 12441–12450.

18. Webster, R. D. *Acc. Chem. Res.* **2007**, *40*, 251–257.

19. Yao, W. W.; Peng, H. M.; Webster, R. D.; Gill, P. M. W. *J. Phys. Chem. B* **2008**, *112*, 6847–6855.

20. Walsh, *C. Acc. Chem. Res.* **1980**, *13*, 148–155.

21. Ghisla, S; Massey, V. *Eur. J. Biochem.* **1989**, *181*, 1–17.

22. Bruice, T. C. *Isr. J. Chem.*, **1984**, *24*, 54-61.

23. Mueller, F. In *Topics in Current Chemistry*; Boschke, F. L., Ed.; Springer-Verlag: Berlin, 1983; Vol. 108, pp 71–108.

24. Niemz, A.; Imbriglio, J.; Rotello, V. M. *J. Am. Chem. Soc.* **1997**, *119*, 887–892.

25. Janik, B.; Elving, P. J. *Chem. Rev.* **1968**, *68*, 295–319.

26. Michaelis, L.; Schwarzenbach, G. *J. Biol. Chem.* **1938**, *123*, 527–542.

27. Draper, R. D.; Ingaham, L. L. *Arch. Biochem. Biophys.* **1968**, *125*, 802–808.

28. Hartley, A. M.; Wilson, G. S. *Anal. Chem.* **1966**, *38*, 681–687.

29. Lowe, H. J.; Clark, W. M. *J. Biol. Chem.* **1956**, *220*, 983–992.

30. Wei, H.; Omanovic, S. *Chem. Biodiv.* **2008**, *5*, 1622–1639.

31. Cable, M.; Smith, E. T. *Anal. Chim. Acta.* **2005**, *537*, 299–306.

32. Ksenzhek, O. S.; Petrova, S. A. *Bioelectrochem. Bioenerg.* **1983**, *11*, 105–127.

33. Diculescu, V. C.; Militaru, A.; Shah, A.; Qureshi, R.; Tugulea, L.; Brett, A. M. O. *J. Electroanal. Chem.* **2010**, *647*, 1–7.

34. Male, R.; Samotowka, M. A.; Allendoerfer, R. D. *Electroanalysis* **1989**, *1*, 333–339.

35. Kay, C. J.; Solomonson, L. P.; Barber, M. J. *Biochemistry* **1990**, *29*, 10823–10828.

36. Iyanagi, T. *Biochemistry* **1977**, *16*, 2725–2730.

37. Heering, H. A.; Hagen, W. R. *J. Electroanal. Chem.* **1996**, *404*, 249–260.

38. Paulsen, K. E.; Stankovich, M. T.; Stockman, B. J.; Markley, J. L. *Arch. Biochem. Biophys.* **1990**, *280*, 68–73.

39. Tatwawadi, S. V.; Santhanam, K. S. V.; Bard, A. J. *J. Electroanal. Chem.* **1968**, *17*, 411–420.

40. Sawyer, D. T.; McCreery, R. L. *Inorg. Chem.* **1972**, *11*, 779–782.

41. Hammerich, O.; Svensmark, B. In *Organic Electrochemistry,* 3rd ed.; Lund, H., Baizer, M. M., Eds.; Marcel Dekker: New York, 1991; Chapter 16.

42. Gupta, N.; Linschitz, H. *J. Am. Chem. Soc.* **1997**, *119*, 6384–6391.

43. Quan, M.; Sanchez, D.; Wasylkiw, M. F.; Smith, D. K. *J. Am. Chem. Soc.* **2007**, *129*, 12847–12856.

44. Hui, Y.; Chng, E. L. K.; Chng, C. Y. L.; Poh, H. L.; Webster, R. D. *J. Am. Chem. Soc.* **2009**, *131*, 1523–1534.

45. Hui, Y.; Chng, E. L. K.; Chua, L. P.-L.; Liu, W. Z.; Webster, R. D. *Anal. Chem.* **2010**, *82*, 1928–1934.

46. Amatore, C.; Savéant, J.-M. *J. Electroanal. Chem.* **1977**, *85*, 27–46.

47. Hui, Y.; Webster, R. D. *Anal. Chem.* **2011**, *83*, 976–981.

48. Bard, A. J.; Faulkner, L. R. *Electrochemical Methods: Fundamentals and Applications*, 2nd ed.; Wiley: New York, 2001.

49. Bond, A. M.; Henderson, T. L. E.; Mann, D. R.; Mann, T. F.; Thormann, W.; Zoski, C. G. *Anal. Chem.* **1988**, *60*, 1878–1882.

50. Geiger, W. E. *Prog. Inorg. Chem.* **1985**, *33*, 275–352.

51. Evans, D. H.; O'Connell, K. M. *Electroanal. Chem.* **1986**, *14*, 113–207.

52. Evans, D. H. *Chem. Rev.* **1990**, *90*, 739–751.

53. Araki, K.; Shu, C-F.; Anson, F. C. *Inorg. Chem.* **1991**, *30*, 3043–3047.

54. Bond, A. M.; Feldberg, S. W.; Greenhill, H. B.; Mahon, P. J.; Colton, R.; Whyte, T. *Anal. Chem.* **1992**, *64*, 1014–1021.

55. Richards, T. C.; Geiger, W. E.; *J. Am. Chem. Soc.* **1994**, *116*, 2028–2033.

56. Hecht, M.; Schultz, F. A.; Speiser, B. *Inorg. Chem.* **1996**, *35*, 5555–5563.

57. Pierce, D. T.; Hatfield, T. L.; Billo, E. J.; Ping, Y. *Inorg. Chem.* **1997**, *36*, 2950–2955.

58. Hong, S. H.; Evans, D. H.; Nelson, S. F.; Ismagilov, R. F. *J. Electroanal. Chem.* **2000**, *486*, 75–84.

59. Batchelor, R. J.; Einstein, F. W. B.; Gay, I. D.; Gu, J-H.; Mehta, S.; Pinto, B. M.; Zhou, X-M. *Inorg. Chem.* **2000**, *39*, 2558–2571.

60. Galijasevic, S.; Krylova, K.; Koenigbauer, M. J.; Jaeger, G. S.; Bushendorf, J. D.; Heeg, M. J.; Ochrymowycz, L. A.; Taschner, M. J.; Rorabacher, D. B. *J. Chem. Soc., Dalton Trans.* **2003**, 1577–1586.

61. Shaw, M. J.; Hyde, J.; White, C.; Geiger, W. E. *Organometallics*, **2004**, *23*, 2205–2208.

62. Kuan, S. L.; Leong, W. K.; Goh, L. Y.; Webster, R. D. *Organometallics*, **2005**, *24*, 4639–4648.

63. Hong, S. H.; Evans, D. H.; Nelsen, S. F.; Ismagilov, R. F. *J. Electroanal. Chem.* **2000**, *486*, 75–84.

64. Rudolph, M.; Reddy, D. P.; Feldberg, S. W. *Anal. Chem.* **1994**, *66*, 589A–600A.

65. Gritzner, G.; Kuta, J. *Pure Appl. Chem.* **1984**, *56*, 461–466.

66. Connelly, N. G.; Geiger, W. E. *Chem. Rev.* **1996**, *96*, 877–910.

67. Chang, J. P.; Fung, E. Y.; Curtis, J. C. *Inorg. Chem.* **1986**, *25*, 4233–4241.

68. Nishida, H.; Inaka, K.; Yamanaka, M.; Kaida, S.; Kobayashi, K.; Miki, K. *Biochemistry*, **1995**, *34*, 2763–2767.

69. Iyanagi, T. *Biochemistry*, **1977**, *16*, 2725–2730.

70. Stockman, B. J.; Westler, W. M.; Mooberry, E. S.; Markley, J. L. *Biochemistry*, **1988**, *27*, 136–142.

71. Burkhart, B. M.; Ramakrishnan, B.; Yan, H.; Reedstorm, R. J.; Markley, J. L.; Straus, N. A.; Sundaralingam, M. *Acta. Cryst. Section D*, **1995**, *51*, 318–330.

72. Paulsen, K. E.; Stankovich, M. T.; Stockman, B. J.; Markley, J. L. *Arch. Biochem. Biophys.* **1990**, *280*, 68–73.

73. Barquera, B.; Morgan, J. E.; Lukoyanov, D.; Scholes, C. P.; Gennis, R. B.; Nilges, M. J. *J. Am. Chem. Soc.* **2003**, *125*, 265–275.

74. Barquera. B.; Ramirez-Silva, L.; Morgan, J. E.; Nilges, M. J. *J. Biol. Chem.* **2006**, *281*, 36482–36491.

Chapter 3

Differences in Proton-Coupled Electron Transfer Reactions of Flavin Mononucleotide (FMN) and Flavin Adenine Dinucleotide (FAD) between Buffered and Unbuffered Aqueous Solutions.

3.1. Introduction

Flavins such as flavin adenine dinucleotide (FAD) and flavin mononucleotide (FMN) are versatile cofactors as they can exist in 3 redox states, the fully-oxidized quinone, the semiquinone as well as the fully-reduced hydroquinone. Some flavoproteins have the ability to stabilize the semiquinone state such that it can undergo one-electron processes as well as two-electron processes.[1-9] While a number of flavoproteins have been studied extensively and their protein structure and mechanism well-established, a large number of flavoprotein mechanisms are still widely debated despite the fact that the protein structure has already been elucidated.

Different flavoproteins undergo different reactions due to the difference in the protein structure, leading to different intermolecular interactions of the flavin cofactor with the protein as well as bound water molecules. Also, protein structure influences whether the flavin cofactor is accessible by solvent or buried in a hydrophobic environment. For example, the isoalloxazine ring of the flavin cofactor in NADH-cytochrome b_5 reductase is situated in a large crevice between the two domains of the flavoprotein,[10] and can be accessed by water molecules when NAD^+ is not bound. When NAD^+ is bound, changes in

intermolecular interactions causes it to be able to stabilize the flavosemiquinone form, making it possible to donate to one-electron acceptors.[8]

Scheme 3.1. Riboflavin (vitamin B_2), flavin mononucleotide (FMN) and flavin adenine dinucleotide (FAD).

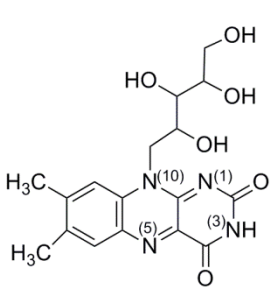

Riboflavin

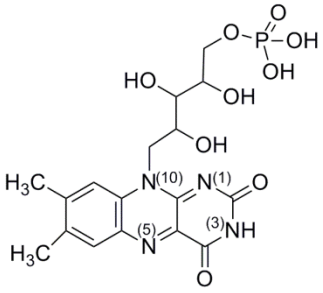

Flavin mononucleotide (FMN)

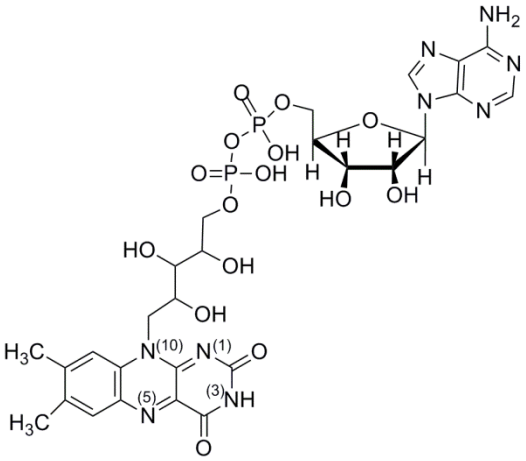

Flavin adenine dinucleotide (FAD)

In the previous chapter, the proton-coupled electron transfer (PCET) mechanism of riboflavin in the aprotic organic solvent dimethyl sulfoxide (DMSO) was discussed.[11] However, the PCET reactions that occur in DMSO is unlikely to be similar with what occurs within flavoproteins where the flavin cofactor is accessible by a network of water molecules. Many electrochemical studies have been conducted on flavins in buffered aqueous solutions, and there is consensus that in buffered aqueous media the fully-oxidized flavin (Fl) is reduced to the flavohydroquinone (FlH_2) in "one step" in a $2e^-/2H^+$ reduction (by one step it is meant that the individual electron transfer and proton transfer steps occur in one observable voltammetric process i.e. only one reduction wave is observed).[12-21]

While this is most definitely true for flavins in low pH buffered environments, the mechanism might be less straightforward for flavins in higher pH environments (where there are fewer protons available) and/ or a decreased buffer capacity, where different intermediates and products are possible. This hypothesis is strengthened by some phenomena observed during the voltammetric reduction of quinones. Quinones (Q), whose electrochemical properties are similar to flavins, undergo two one-electron reduction processes in aprotic organic solvents to form first the semiquinone anion radicals ($Q^{\bullet-}$) and then the dianions (Q^{2-}), but without the quinone donating an electron to one of its reduced species. Two clear reduction waves would be observed several hundred mV apart. However, recent studies have shown that when water is added to an organic solution containing quinones, the two reduction waves shift towards less negative potentials, with the second reduction wave shifting more than the first until the two reduction waves eventually merge. This phenomenon was attributed to the hydrogen-bonding interactions with water stabilizing the negative charge on the quinone, with a stronger effect of stabilization on the dianion (Q^{2-}). Thus, when the concentration of water is high enough, the quinone is directly reduced to the hydrogen-bonded dianion [$Q^{2-}(H_2O)_x$] in one two-electron process.[22] This emphasizes that we should not be too quick to generalize that the observation of only one reduction wave equates to a $2e^-/2H^+$ reduction.

In a related study of quinones in unbuffered aqueous solutions,[23] it was argued that when the proton concentration is lower than the quinone concentration, the oxidized quinone (Q) would undergo a $2e^-$ reduction directly to the strongly hydrogen-bonded dianion ($Q^{2-}(H_2O)_x$), much like in an organic media with high water concentration, as described in the previous study. It was suggested that the reduced species, however, will exist as a mixture of Q^{2-}, QH^-, and QH_2, as the dianion is basic enough to deprotonate

water molecules. Similarities between flavins and quinones has led us to believe that this mechanism could be extended to flavins in unbuffered aqueous solutions as well as flavins in buffered aqueous solutions of very high pH, where proton concentration is similarly lower than the flavin concentration.

In order to better understand the electron transfer mechanism in flavoproteins where the flavin cofactor can be accessed by water molecules, this study has investigated the importance of hydrogen-bonding in buffered and unbuffered aqueous solutions, the pH dependence of the reaction mechanisms, and the likely mechanism at different pHs. In order to determine which reduced species have been formed, it is important to ensure that molecular oxygen is not available in solution to react with the reduced flavin to form the oxidized flavin or a flavin-oxygen intermediate. Thus, all voltammetric experiments were conducted under an argon atmosphere to avoid such complications. The electrochemical data obtained in unbuffered solutions were carefully modeled using digital simulation techniques in order to explain the appearance of all the detected voltammetric peaks.

3.2. Experimental

3.2.1. Chemicals

Flavin mononucleotide (FMN) and flavin adenine dinucleotide (FAD) were analytical reagent grade and obtained from Alfa Aesar. Potassium chloride (KCl) was obtained from Goodrich Chemical Enterprise. Acetic acid, phosphoric acid and boric acid used in the Britton-Robinson buffers were analytical reagent grade and obtained from Sinopharm Chemical Reagent Co., Ltd.

3.2.2. Electrochemical Procedures

Cyclic voltammetry (CV) experiments were conducted with a computer-controlled Eco Chemie Autolab PGSTAT 100 with an ADC fast scan generator. The working electrode was a 1 mm diameter planar glassy carbon (GC) disk that was polished frequently with 1 μm alumina powder, and used in conjunction with a Pt wire auxiliary electrode and an Ag/AgCl reference electrode. Unbuffered solutions were prepared by making a solution of FMN or FAD in 0.4 M KCl in deionized water and adjusting the pH using carefully diluted solutions of HCl and NaOH. Buffered solutions were prepared by adding an equal volume of acetic acid, phosphoric acid and boric acid (0.04 mol L^{-1}), followed by adjusting to the desired pH using an NaOH solution (0.2 mol L^{-1}). This solution was then added to FMN to form a 1 mM FMN solution in Britton-Robinson buffer. Solutions of FMN (1 mM FMN in Britton-Robinson buffer and 1 – 5 mM FMN and 0.4 M KCl in deionized water) for voltammetric analysis were deoxygenated by purging with high purity argon gas and all voltammetric experiments were conducted at 22 (±2) °C in a Faraday cage. Digital simulations of the CV data were performed using the DigiElch 6 software package purchased from Gamry Instruments.

Controlled potential electrolysis was performed in a two-compartment electrolysis cell using a GC rod as the working electrode, Pt mesh as the auxiliary electrode and an Ag/AgCl (3 M KCl) reference electrode.

3.2.3 Spectroscopic Experiments

UV-vis spectra were obtained using a thin layer quartz cell at 22 (±2) °C and recorded on a Perkin Elmer Model Lambda 750 UV-vis-NIR spectrophotometer.

3.3. Results and Discussion

3.3.1. 1 mM FMN in buffered aqueous solutions

3.3.1.1. Cyclic voltammetry

Cyclic voltammetry experiments were performed at variable scan rates between 0.1 V s^{-1} and 20 V s^{-1} in buffered solutions of 1 mM FMN (pH 3 – 11) (Figure 3.1). Between pH 3 – 5, the initial species in solution is likely to be FMN, as the p*K*a of FMN is approximately 10,[13–14,16,19,27–33] and so it will not lose its imide proton at this pH. In this pH range, only one reduction wave (and one oxidation wave during the reverse scan) is observed. (Figure 3.2) Simple pH calculations tell us that $[H^+] \geq [FMN]$, thus the acid concentration in the buffer solution is sufficient to donate one or two protons to the analyte, and it is likely that FMN undergoes a two-electron/two-proton reduction to form the fully reduced flavin $FMNH_2$. The shift of approximately 60 mV per pH unit in this pH range is indicative of a reduction with an equal number of electrons and protons transferred. Controlled potential electrolysis with coulometry enabled the determination that two electrons were transferred per flavin molecule, which also indicates that two protons were transferred during the reduction wave.

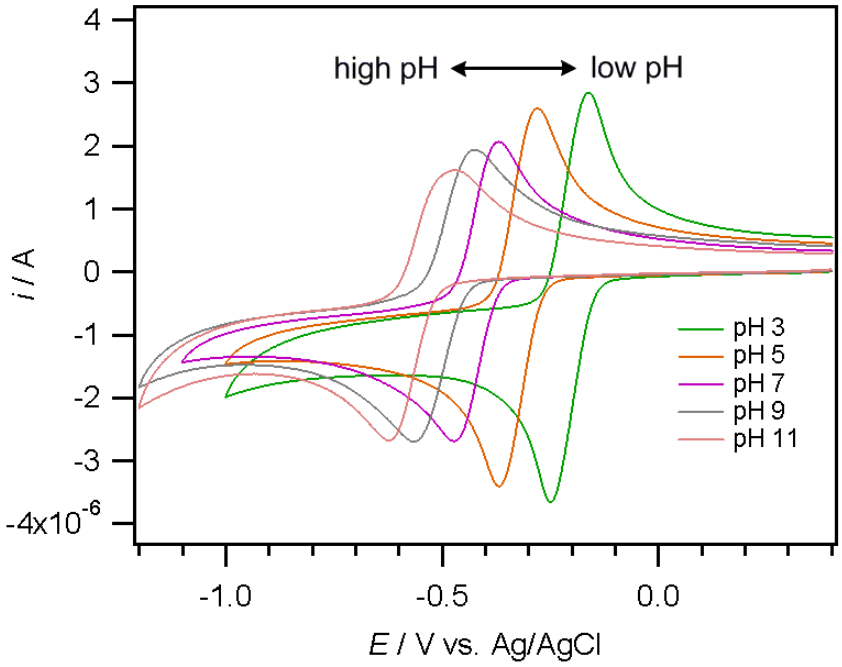

Figure 3.1. Cyclic voltammograms of 1 mM FMN in buffered solutions of pH 3 – 11, at 0.1 Vs^{-1} using a 1 mm diameter planar GC electrode.

Between pH 7 – 9, the fully-oxidized species is still FMN, but as the proton concentration is much lower than the analyte concentration, its reduced forms may not immediately undergo a protonation reaction, as we have observed for flavins in buffered acidic media. In a previous study regarding the reduction of quinones in organic media of varying water concentration, when the water level was significantly high, strong hydrogen-bonding interactions with the dianion caused the two reduction waves to merge and the fully-oxidized quinones would be reduced by 2 electrons directly to the dianion in one observable reduction wave.[22] Thus, it is postulated that in this aqueous environment of neutral to moderately basic pH, FMN is similarly electrochemically reduced by 2 electrons to FMN^{2-} which undergoes stronger hydrogen-bonding interactions with water. The hydrogen-bonded dianion (subsequently written as $FMN^{2-}(H_2O)_x$ to emphasize its

stronger hydrogen-bonding interactions with water) then extracts a proton from the buffer molecules to form $FMNH^{\bullet}$.[23] It was observed that the shift per pH unit in this pH range was significantly lower than 60 mV. However, a shift of 30 mV per pH unit was not expected due to the formation of different species rather than a direct $2e^{-}/H^{+}$ reduction. In the cyclic voltammograms at high scan rates, two distinct oxidation waves can be detected, indicating that two different reduced flavin species were being oxidized. $FMNH^{\bullet}$ and the hydrogen-bonded dianion ($FMN^{2-}(H_2O)_x$) can undergo oxidation at slightly different potentials, giving rise to 2 oxidative peaks during the reverse scan (I_{ox} and II_{ox} in Figure 3.3). The actual ratio of each species present depends on the rate and equilibrium constants of the protonation and hydrogen-bonding reactions. The two overlapping oxidative peaks are only observed at high scan rates at pH 9, although it is likely that two oxidative peaks were also present at lower scan rates. An explanation for the visible separation of peaks at higher scan rates could be due to a relatively slow equilibrium between the hydrogen bonded dianion and the $FMNH^{\bullet}$, resulting in both species only being voltammetrically detectable at faster scan rates. Another possible explanation could also be the different heterogeneous electron transfer rates of the two reduced species, and the species with the slower heterogeneous electron transfer rate would have a comparatively larger peak-to-peak separation as scan rate increases, leading to a visible separation.

At pH 11, the pH > p*K*a of the imide proton on the isoalloxazine ring of FMN, thus the initial species present before electrochemical reduction is FMN^{-} (FMN with the N3 deprotonated). After a 2-electron reduction and various hydrogen-bonding and protonation reactions, a mixture of hydrogen-bonded dianion FMN^{2-} and $FMNH^{-}$ are formed. Similar to pH 9, the CVs conducted at pH 11 shows two separate oxidation peaks

at higher scan rates, while at lower scan rates, the oxidation peak was especially broad, indicating the possibility that it could be comprised of two oxidation peaks (Figure 3.4).

It is postulated that for higher pH values (pH 9 – 11) and at low scan rates, the major reduced species present is $FMNH^{-}$. As the scan rates increases, the protonation reaction of the hydrogen-bonded dianion ($FMN^{2-}(H_2O)_x$) is outrun, hence more of the $FMN^{2-}(H_2O)_x$ species (oxidized during I_{ox}) and less of $FMNH^{-}$ (oxidized during II_{ox}) will be available for oxidation when the scan direction is reversed. While differences are not noticeable at slow scan rates, when the cyclic voltammograms recorded at scan rates between 5 – 20 V s^{-1} are examined and compared, it can be observed that the first oxidation peak (I_{ox}) increases in size and the second oxidation peak (II_{ox}) decreases in size as the scan rate increases.

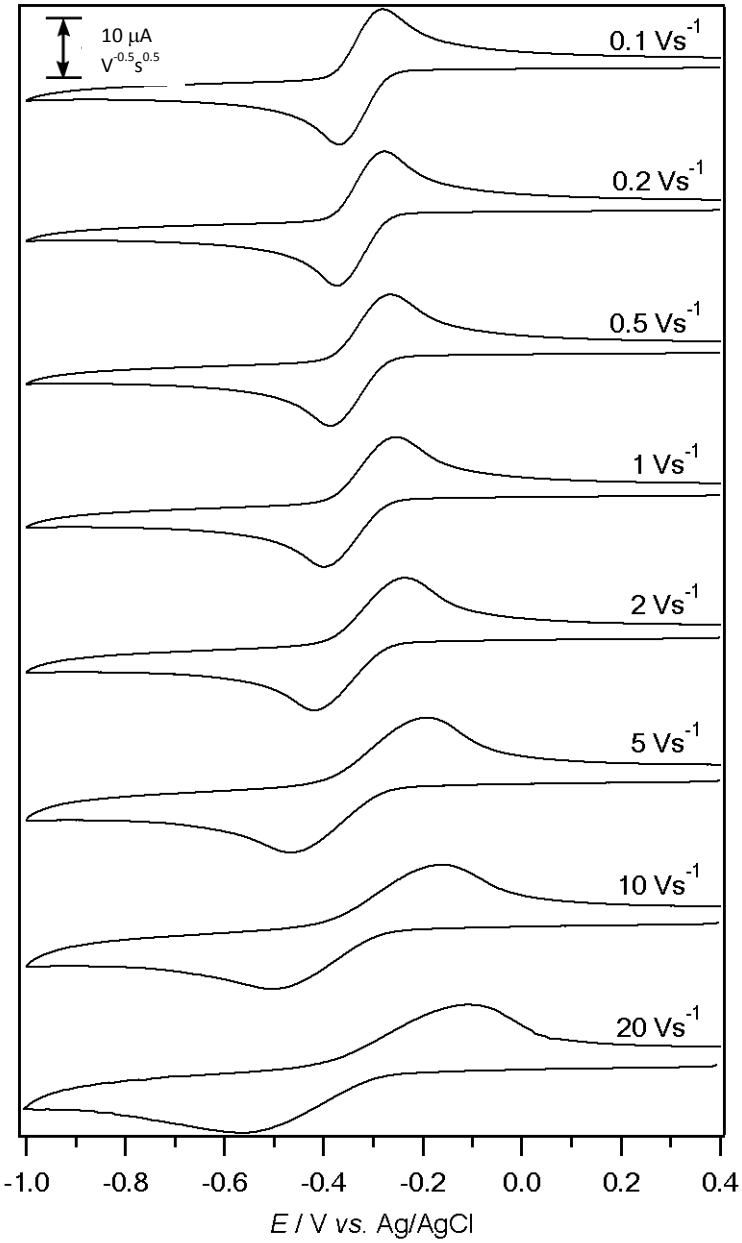

Figure 3.2. Variable scan rate cyclic voltammograms of 1 mM FMN in a buffered aqueous solution of pH 5, recorded at a 1 mm GC electrode at 22 (±2). The current data were scaled by multiplying by $\nu^{-0.5}$.

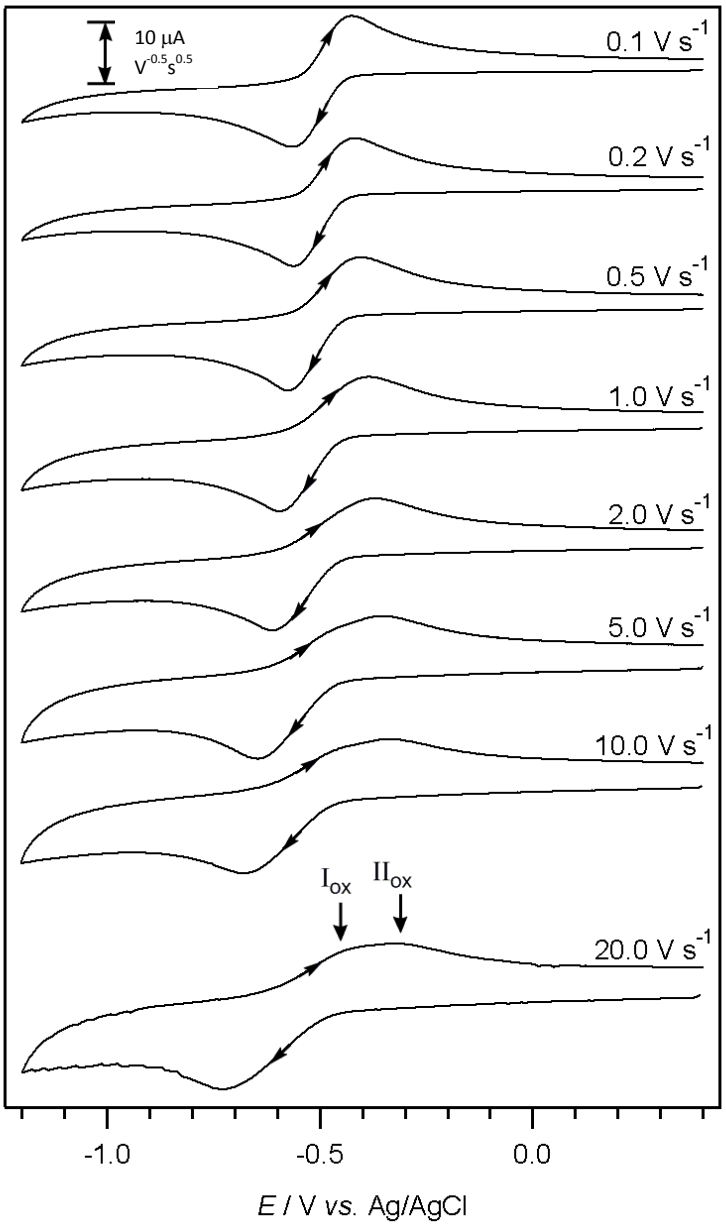

Figure 3.3. Variable scan rate cyclic voltammograms of 1 mM FMN in a buffered solution of pH 9, using a 1 mm diameter planar GC electrode. The current data were scaled by multiplying by $v^{-0.5}$.

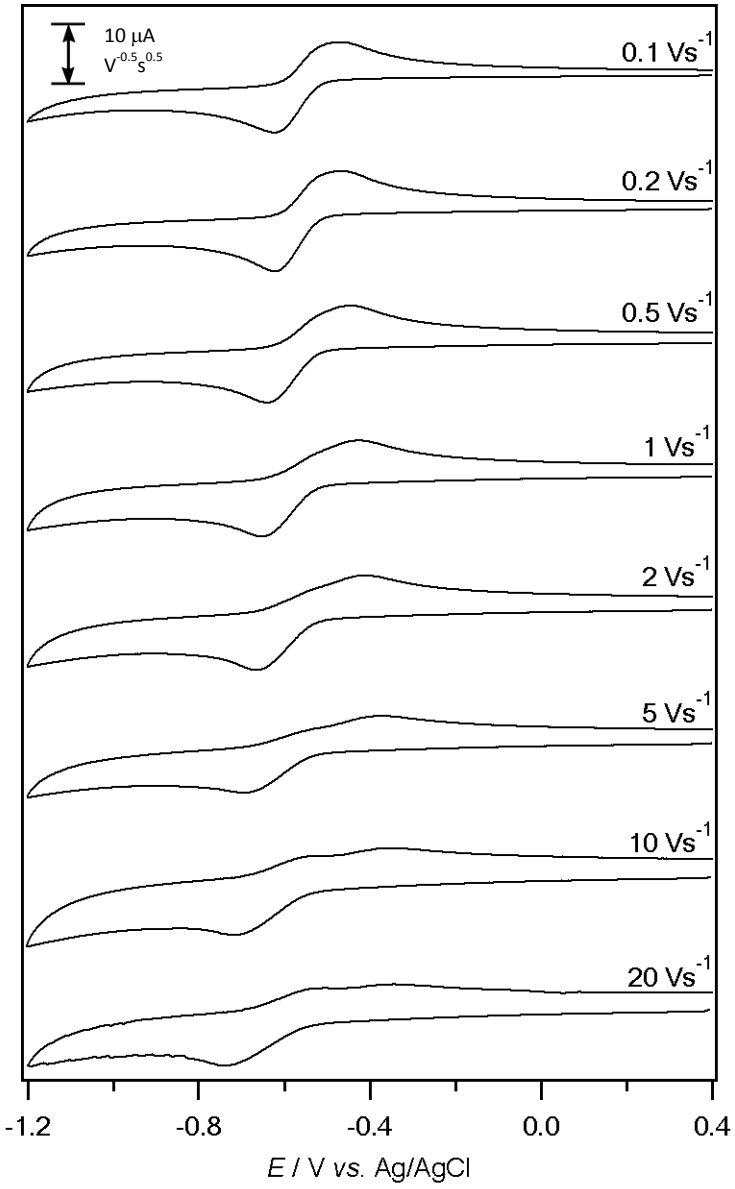

Figure 3.4. Variable scan rate cyclic voltammograms of 1 mM FMN in a buffered aqueous solution of pH 11, recorded at a 1 mm GC electrode at 22 (±2). The current data were scaled by multiplying by $\nu^{-0.5}$.

3.3.1.2. Controlled potential electrolysis

In order to determine the main species present in solution after bulk reduction, as well as to find out if the pH of the solution affects the identity of the final reduced species, a series of bulk electrolysis experiments were conducted. Controlled potential bulk electrolysis was performed for 2 mM FMN in buffered aqueous solutions at pH 3, 5, 7, 9 and 11. At each pH, coulometry measurements indicated that 2 electrons were transferred per molecule over the long electrolysis timescale.

It is interesting to note the differences between the coulometry results of flavins in buffered aqueous media and that of flavins in aprotic organic media, in that two electrons were calculated to be transferred per flavin molecule in buffered aqueous media while it was calculated that one electron was transferred per flavin molecule in aprotic organic media, despite the fact that the initial voltammetric wave is assigned to a $2e^-$ reduction. It was then established that the donation of the imide proton of oxidized flavin to the N5 of a flavosemiquinone and the subsequent comproportionation reaction led to a "false" reading by coulometry. It is important to note that in buffered aqueous media at this pH range, the reduced species are much more likely to take one of the abundant protons in the buffer solution rather than to take the imide proton from another flavin. In fact, there is also no evidence of such a reaction occurring at high pH values.

At acidic pH, the color changed from fluorescent yellow (FMN) to a greenish-brown to an orangey-brown and gradually lightening as the reduction process approached completion (two electrons transferred per FMN molecule). However, at basic pH, the color change was not as obvious, gradually changing from a fluorescent yellow to a dull yellow after two electrons were transferred per FMN molecule. It has been previously reported that $FMNH^-$ is a dull yellow color, while the anionic radical $FMN^{\bullet -}$ is red and

the neutral radical $FMNH^{\bullet}$ is blue.[24] Although the observed color change does not provide a definite proof of a different reduction pathway, subsequent UV-vis experiments are able to qualify this visible color change, and will be discussed in the following section.

Cyclic voltammograms were recorded using a 1 mm diameter planar GC electrode at three points during each experiment: once before bulk electrolysis, once after one electron was transferred per FMN molecule, and lastly after two electrons were transferred per FMN molecule. It was observed for each pH that after one electron had been transferred, the initial current reading at the starting point of the cyclic voltammograms (+0.4 V vs. Ag/AgCl), shifted upwards to positive currents, indicative of a reduced flavin species existing in the solution that can be oxidized at any potential more positive than approximately –0.4 V *vs.* Ag/AgCl. After the transfer of two electrons per FMN molecule, the current at the same starting point shifted further upwards, showing that more of the reduced species had been formed. However, because the CV scans commenced from a potential that was positive enough to oxidize the reduced species back to fully oxidized FMN, the CVs obtained still appeared largely similar to that of the fully oxidized FMN, the only difference being the position of zero current. Therefore, with reference with the CV data and coulometry data obtained for pH 3 – 5, FMN goes through a chemically reversible $2e^{-}/2H^{+}$ reduction to form $FMNH_2$ [Figure 3.5(*a*)].

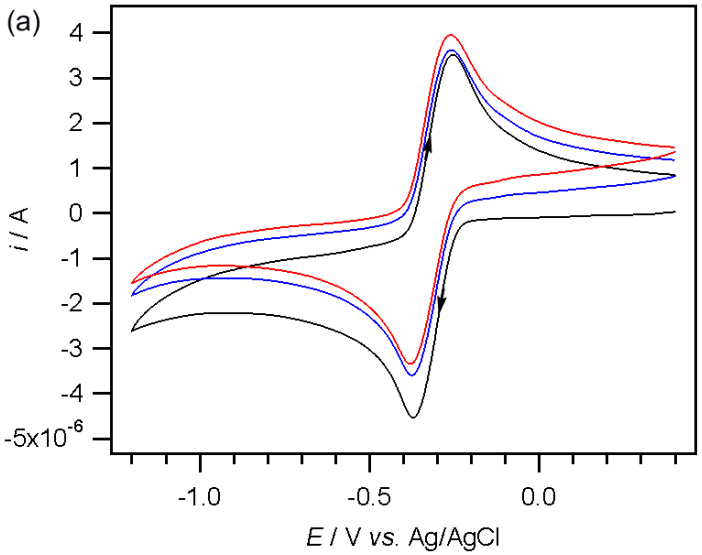
(a)
4
3
2
1
0
-1
-2
-3
-4
-5x10-6
i / A
-1.0
-0.5
0.0
E / V vs. Ag/AgCl

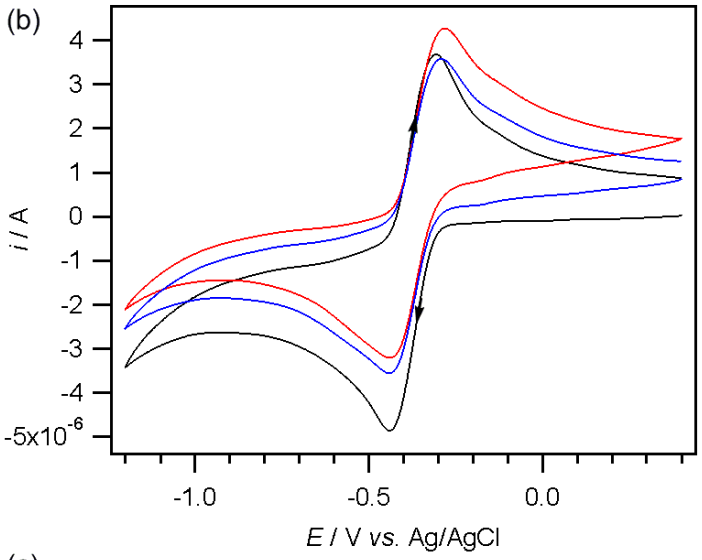
(b)
4
3
2
1
0
-1
-2
-3
-4
-5x10-6
i / A
-1.0
-0.5
0.0
E / V vs. Ag/AgCl

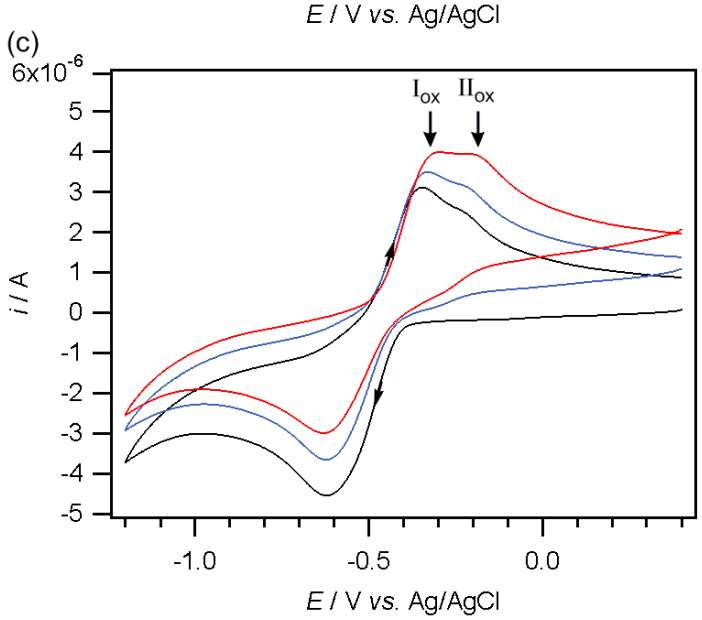
(c)
6x10-6
5
4
3
2
1
0
-1
-2
-3
-4
-5
Iox
IIox
i / A
-1.0
-0.5
0.0
E / V vs. Ag/AgCl

Figure 3.5. Cyclic voltammograms of 2 mM FMN at 0.1 Vs^{-1} using a 1 mm diameter planar GC electrode, before electrolysis (black line), after one electron has been transferred per molecule (blue line), and after two electrons have been transferred per molecule (red line), in a buffered aqueous solution of (*a*) pH 5, (*b*) pH 7 and (*c*) pH 9.

However, for pH 7 – 9, the cyclic voltammograms recorded after 2 electrons were transferred per FMN molecule showed the appearance of two closely-spaced reduction and oxidation peaks (I_{ox} and II_{ox}) [Figure 3.5(*b*) and (*c*)]. In this pH range, the concentration of free protons is much lower than the concentration of flavins, and thus FMN is not likely to follow the same reduction pathway as it does in highly acidic buffer solutions. We postulate that the observation of two closer spaced reduction and oxidation peaks is due to the basicity of the flavin dianion and its ability to take a proton from the buffer solution, and as the time scale of the electrolysis experiment is long (> 1 h), the proton transfer reaction has time to take place and reach equilibrium, and the existence of two voltammetric waves are more pronounced than in the CV before bulk reduction.[23] This will give rise to an equilibrium of FMN^{2-}, $FMNH^{-}$ and $FMNH_2$, and the major species present depends on the pH of the solution and the pK_a of each of the species.[23] When a CV scan is performed after the two electron electrolysis at pH = 9, a very broad reduction process is detected with a shoulder and two clear oxidation peaks are detected when the scan direction is reversed, due to a number of reduced species existing in the bulk solution [Figure 3.5(*c*)].

The observation of FMN^{2-}, $FMNH^{-}$ and $FMNH_2$ in the bulk solution after electrolysis is further substantiated by the UV-vis spectra obtained of the 2-electron reduced species at each pH, as shown in the following section.

3.3.1.3. UV-vis spectroscopy

UV-vis spectra were collected before and after the bulk electrolysis experiment, in order to determine if any structural changes occurred within the chromophore and to identify the species present in the bulk solution. Extra care was taken to ensure that the solution from the electrolysis cell was transferred in an oxygen-free environment to the UV-vis cell, from which ambient air was also purged and replaced by nitrogen gas. This was done to ensure accurate UV-vis results, as the reduced flavin is easily oxidized by molecular oxygen.

The UV-vis spectra of fully-oxidized FMN at pH 3 – 9 were identical, with peaks at 446 nm, 370 nm and 265 nm but the UV-vis spectrum of fully-oxidized FMN at pH 11 was slightly shifted, with peaks at 444 nm, 355 nm and 265 nm. (Figure 3.6) This indicates that at pH 11, FMN likely exists with its imide proton deprotonated (FMN^{-}), as the pK_a of FMN is close to 10.[13–14,16,19,24–33] UV-vis data of the different flavin species obtained by chemical methods, collected by Hemmerich *et al.*[25] and Dudley *et al.*,[26] further substantiates the hypothesis that at pH 3 – 9, the initial species is FMN, while at pH 11, the initial species is likely to be FMN^{-}.[24-26]

After bulk electrolysis, where two electrons were transferred to each FMN molecule, significant differences between the 2-electron-reduced compounds at each pH could be observed. For pH 3 – 5, two shoulder absorbances with maxima at around 400 nm and 280 nm, as well as a large peak at 245 nm were observed. However, for pH 7 – 11, a small peak at 350 nm, a large peak at 255 nm as well as a shoulder absorbance at approximately 290 nm were observed. This indicates that after two electrons were transferred, the species after reduction at pH 3 – 5 and at pH 7 – 11 are different.

The UV-vis spectra of the species after 2 e^- electrolysis at pH 3 – 5 is similar to the spectra obtained by Dudley *et al.*[26] and Hemmerich *et al.*[25] for $FMNH_2$, and the spectra of $FADH_2$ obtained by Malinowski *et al.*[34] which has an identical chromophore. On the other hand, the spectra obtained after 2 e^- electrolysis at pH 7 – 11 resembles the spectrum reported for $FMNH^-$ instead.[24] This not only substantiates the hypothesis that the final product at pH 3 – 5 is $FMNH_2$ and that at pH 7 – 11 is $FMNH^-$, but agrees with prior data regarding the p*K*a of $FMNH_2$ to be between 5 and 7, with data collected by Hemmerich *et al.* indicating that the p*K*a of $FMNH_2$ is around 6.2.[25]

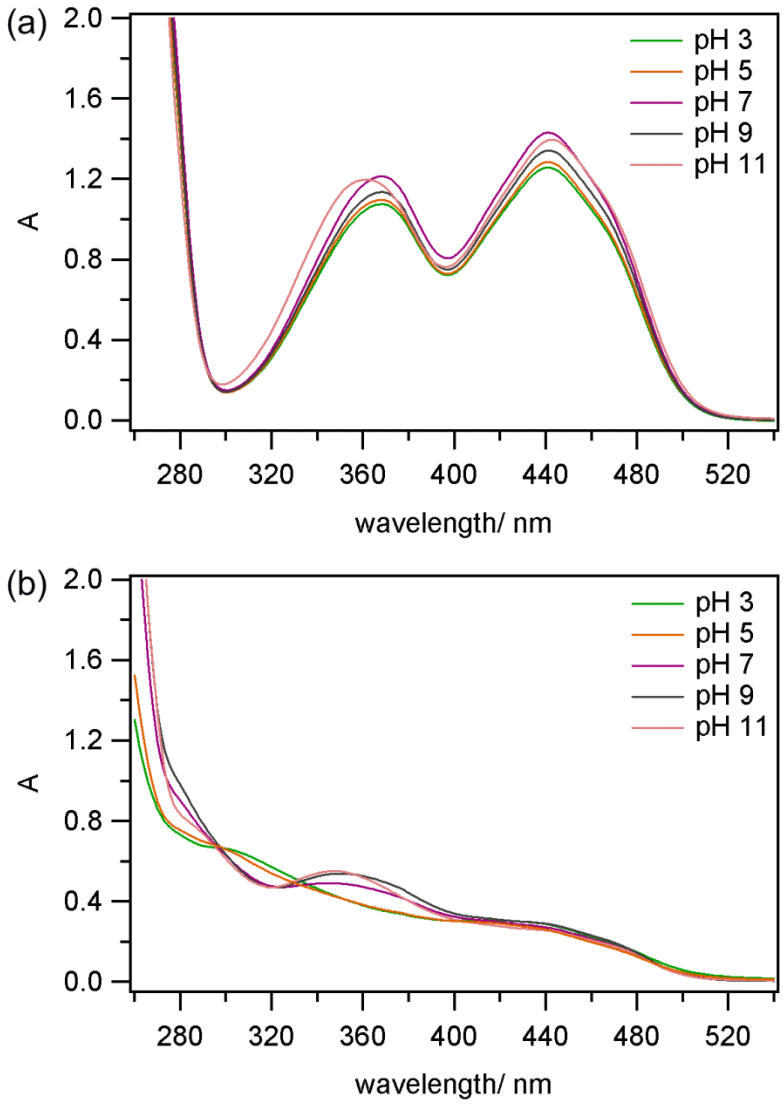

Figure 3.6. UV-vis spectra of 2 mM FMN in buffered aqueous solutions of pH 3 – 11, (*a*) before bulk electrolysis and (*b*) after 2 electrons were transferred per molecule of FMN during bulk electrolysis.

3.3.1.4. Electron Transfer Mechanism of FMN in buffered aqueous solutions

The reduction mechanism of FMN in buffered aqueous media is proposed based on voltammetric and spectroscopic data collected. For acidic aqueous environment of pH 3 – 5, FMN undergoes a $2e^-/2H^+$ reduction to $FMNH_2$ at all scan rates (Scheme 3.2). A UV-vis spectrum of the 2 e^- reduced species confirmed its identity as $FMNH_2$, having a good agreement with previous UV-vis studies of the different flavin species.[24] The intense colors observed during the bulk reduction suggest that some of the intermediate radical compounds may have been formed but with a finite lifetime (possibly due to comproportion reactions between $FMNH_2$ and fully-oxidized FMN) before being eventually converted to $FMNH_2$ as the electrolysis approaches completion.

Scheme 3.2. Voltammetrically induced proton-coupled electron transfer reduction mechanism of FMN in buffered aqueous solutions of pH 3 – 5, studied by cyclic voltammetry over varying scan rates and concentrations.

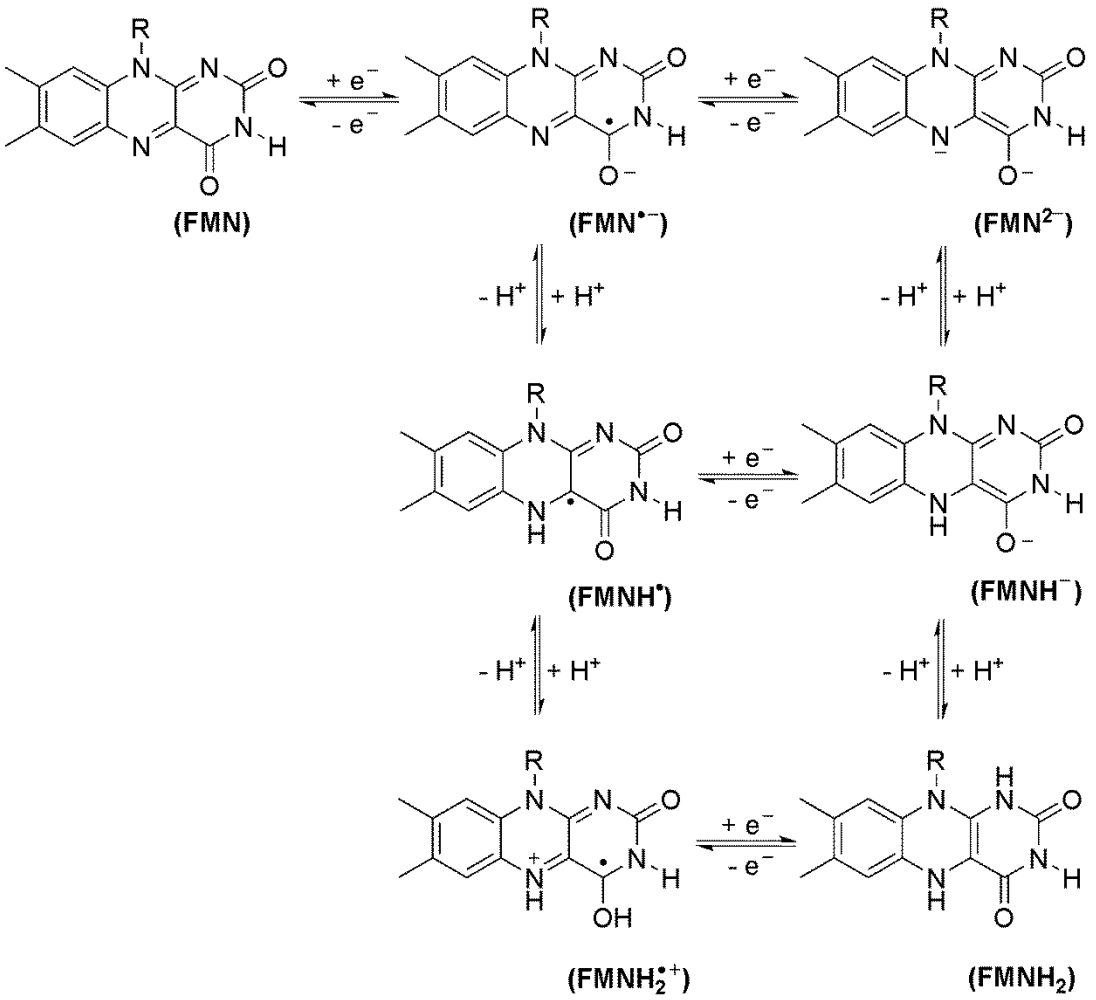

Scheme 3.3. Voltammetrically induced proton-coupled electron transfer reduction mechanism of FMN in buffered aqueous solutions of pH 7 – 11, studied by cyclic voltammetry over varying scan rates and concentrations.

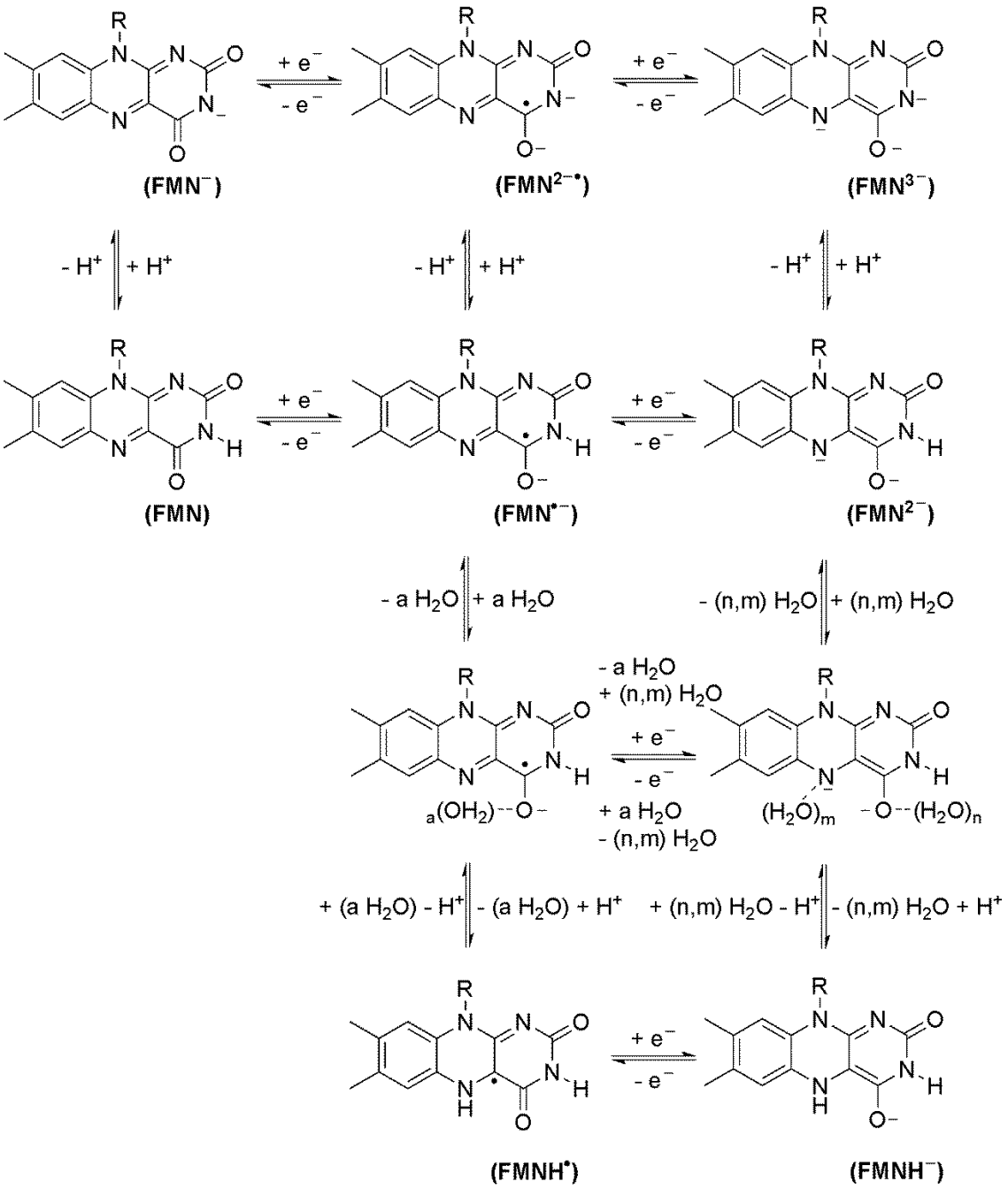

For a neutral to basic aqueous environment between pH 7 – 9 (Scheme 3.3), the pH is lower than the pK_a of FMN, thus the species before reduction is still the neutral fully-oxidized flavin FMN. Bulk electrolysis has confirmed that 2 electrons were transferred to each FMN molecule, and the lack of large color changes suggested that FMN was reduced by 2 electrons to the dianion FMN^{2-}. During electrolysis, the time scale is long enough for the dianion to extract a proton from the buffer molecules, forming $FMNH^-$.

Nevertheless, the time scale of each cyclic voltammetry scan is much shorter than for an electrolysis environment and different reduction species were observed. For slow scan rates between pH 7 – 9, there is sufficient time for the proton transfer reaction to take place after the dianion is formed but as the scan rate increases, the time scale of the scan would decrease and the proton transfer reaction takes place to a smaller extent, and the reverse oxidation wave is observed to be split into two processes, assigned to the hydrogen-bonded dianion ($FMN^{2-}(H_2O)_x$) and $FMNH^-$.

For the highly basic aqueous environment of pH 11, the pH is higher than the pK_a of FMN, thus the flavin species at pH 11 before reduction is the deprotonated fully-oxidized flavin FMN^-, as confirmed by comparing its UV-vis spectra to the spectra at lower pH values as well as the spectra of the different flavin species collected previously. The reduced species present after bulk electrolysis is the same as the other basic solutions, $FMNH^-$.

3.3.2. 1 mM FMN, 5 mM FMN and 1 mM FAD in unbuffered aqueous solutions

3.3.2.1. Rationale behind detailed investigation of flavins in unbuffered aqueous solutions

For experiments in unbuffered aqueous media, the proton concentration and thus the pH surrounding the electrode surface is expected to change significantly during the cyclic voltammetry scans. This is especially true for flavins as the electrochemical reduction of flavins in aqueous buffered media has showed a series of proton-coupled electron transfer (PCET) reactions that take up a proton from the solution. Therefore, it was not expected that the same trends would be observed for unbuffered solutions as for the buffered solutions.[23] It is possible that flavoproteins in a biological environment which have the flavin isoalloxazine ring exposed to water might not always exist in a position that enables unhindered access of buffer molecules. For example, the bowl-shaped surface near the FMN-binding site in microsomal NADPH-cytochrome *c* reductase has an opening approximately 6Å wide, while the active site containing the flavin cofactor in ferrodoxin- $NADP^+$- oxidoreductase and monomine oxidase A are more open.[35–38] Water molecules in contact with the flavin isoalloxazine ring can also be physically bound by the flavoprotein, which eliminates the possibility of a well-buffered flavin binding site. Although it has been reported that the cytoplasm, mitochondrial-cytosol and endocytotic vesicles in cells are well buffered by proteins and the H_2CO_3/ HCO_3^- system, a small crevice 6 Å wide where the flavin cofactor is bound is not necessarily equally well-buffered since both water and other molecules in the crevice are unable to diffuse away freely and be replenished at the active sites. Therefore, the biological environment of some flavin cofactors could resemble that of an unbuffered aqueous solution during cyclic

voltammetry measurements, where the solution around the electrode surface rapidly changes in pH, while the pH in the bulk solution remains unchanged. Furthermore, protein buffering, rather than H_2CO_3/ HCO_3^- buffering, is considered to be dominant in cells.[39] It is important to note that it could be difficult to classify the environment of the flavin cofactor as completely well-buffered, totally unbuffered, or even completely hydrophobic, and in some cases we might observe an "intermediate" environment.

3.3.2.2. Cyclic voltammetry (1 mM FMN in unbuffered aqueous solutions)

Variable scan rate cyclic voltammetry experiments were conducted of unbuffered 1 mM FMN solutions at a range of pH values from pH 2.13 – 11.03, as shown in Figure 3.7, using small quantities of HCl or NaOH to vary the pH of the solution.

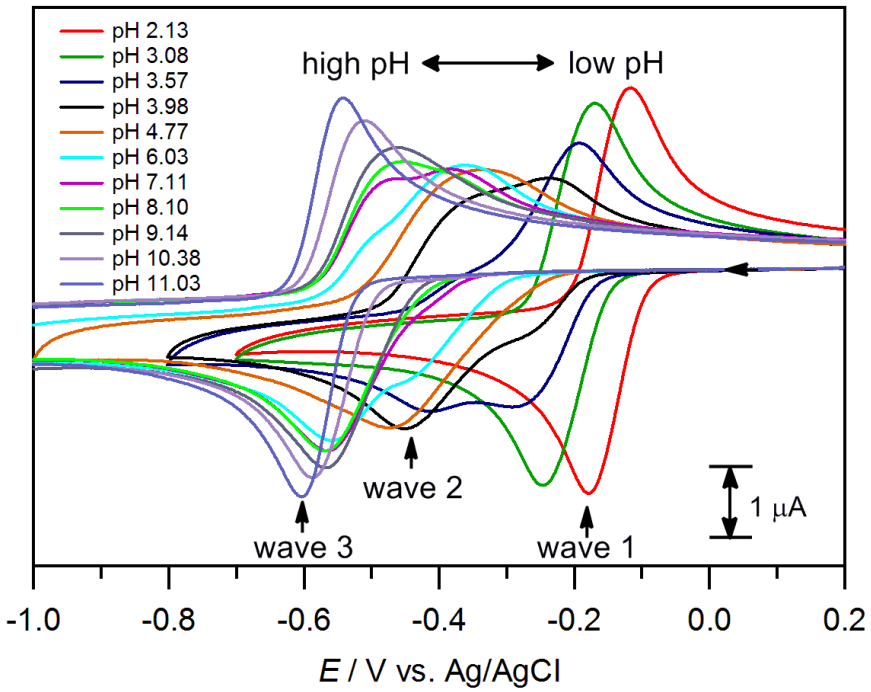

Figure 3.7. Cyclic voltammograms of 1 mM FMN in unbuffered aqueous solutions containing 0.4 M KCl between pH 2 – 11, using a 1 mm diameter planar GC electrode at a scan rate of 0.1 V s^{-1}.

At the scan rate of 0.1 V s^{-1} and low pHs (pH 2.13 – 3.08), only one distinctive redox wave is observed at approximately E^0 = -0.15 V (wave 1) and with the ratio of the oxidative and reductive peak currents (i_p^{ox}/ i_p^{red}) equal to unity, indicating a chemically and electrochemically reversible reaction (Figure 3.7). Wave 1 becomes broader when the pH increases from pH 2.13 to pH 3.08. It can also be observed that wave 1 shifts by approximately -59 mV/ ΔpH as the pH increases from pH 2.13 to pH 3.08, as expected for a *n* H^+, *n* e^- redox couple. Wave 1 is thus proposed to be a $2e^-$/ $2H^+$ reduction, forming $(FMNH_2)H^-$ as there are sufficient protons present for this reaction at low pH (for the abbreviated names of the different flavin species, the H^- outside of the parenthesis indicates the protonation state of the phosphate groups of the side chain as shown in Scheme 3.4.).

As pH 3.57, the size of wave 1 decreases while another wave (wave 2) starts appearing at a more negative potential (E^0 = –0.40 V). As the pH increases, wave 1 continues to decrease in size while wave 2 increases in size, which indicates that the fully-oxidized FMN would be reduced via wave 2 instead of wave 1 as pH increases. Wave 2 starts appearing at pH 3.57, at which the concentration of protons added is around 0.27 mM, approximately a third of the concentration of FMN in the solution (1.0 mM). As there are not enough protons for all the flavins to undergo $2e^-$/ $2H^+$ or $2e^-$/ H^+ reduction, the remainder of the fully-oxidized $(FMN)H^-$ will be reduced without any proton transfer step. This is substantiated by the observation that the peak potentials of wave 2 vary by less than 50 mV over the intermediate pHs (from pH 3.98 to pH 7.11), indicating that wave 2 is unlikely to be a proton-coupled electron transfer reaction. Initially, it was suspected that wave 2 was a one-electron reduction (as the peak height appears significantly smaller than wave 1 and wave 3), where the fully-oxidized $(FMN)H^-$ was reduced to the anionic flavin radical, $(FMN^{\bullet -})H^-$. However, it was observed that wave 2

was broader and larger than expected for a one-electron reduction, which suggested the possibility of a two-electron reduction but with a very slow heterogeneous electron transfer rate. Further experimentation with a rotating disk electrode confirmed the two electron transfer, and will be discussed in section 3.3.2.4.

Since the reduction potential of wave 2 shifts by a much smaller amount between pH 4 – 7 than expected for a $2e^-/ 2H^+$ or $2e^-/ H^+$ reduction, it suggests that wave 2 does not involve the reduced flavin species getting protonated by a free acid, and is therefore independent of pH change. Wave 2 is therefore postulated to be a $2e^-$ reduction process via an EE mechanism, forming the dianion $(FMN^{2-})H^-$, which is likely to undergo further hydrogen-bonding interactions with H_2O like it does in buffered aqueous solutions. Similarly, due to the basicity of the dianion $(FMN^{2-})H^-$, it could extract a proton from either a nearby water molecule or possibly even another flavin molecule, which could be assisted by the π-stacking interactions of the flavin isoalloxazine ring in aqueous solutions at concentrations above 50 μM.[40–41]

At pH 3.98, waves 1 and 2 both occur because there are sufficient protons available for the $2e^-/ 2H^+$ reduction for some of the FMN molecules, but the remaining FMN molecules will be reduced in a direct $2e^-$ reduction process, and two different reduced flavin species would exist together in solution. At pH 4.77, the pH dependent wave 1 is no longer observed. At this pH, only one very broad and drawn-out process (wave 2) was observed, believed to be associated with the direct $2e^-$ reduction of the fully-oxidized $(FMN)H^-$ to the dianion $(FMN^{2-})H^-$. While the protonation of the dianion by free acid is unlikely to occur at this pH, hydrogen bonding of the dianion to water molecules is highly likely. The extensive hydrogen-bonding network that is formed between the flavin dianion and water molecules increases the possibility that the dianion would deprotonate a water

molecule to form $(FMNH^{-})H^{-}$. The E^{0} of $(FMN)H^{-}$ / $(FMN^{\bullet-})H^{-}$ and that of $(FMN^{\bullet-})H^{-}$ / $(FMN^{2-})H^{-}$ are likely to be close enough to merge into a single voltammetric wave, as was observed for quinones in organic solvents containing sufficiently large amounts of water.[22] This is because the dianion is more strongly stabilized in water due to hydrogen-bonding interactions, which facilitates the easier addition of an electron to it. Wave 2 is observed to be associated with slower heterogeneous electron transfer reactions as it becomes broader and more spread out at higher scan rates.

At the pH range where wave 1 and wave 2 are observed in a single CV scan, wave 1 can be observed to decrease in magnitude proportionally to wave 2 increasing in magnitude as the scan rate is increased. (Figure 3.8) At fast scan rates, the protonation reaction of the anionic radical $(FMN^{\bullet-})H^{-}$ is outrun, hence $(FMN^{\bullet-})H^{-}$ will undergo the second electron transfer step, forming the dianion $(FMN^{2-})H^{-}$.

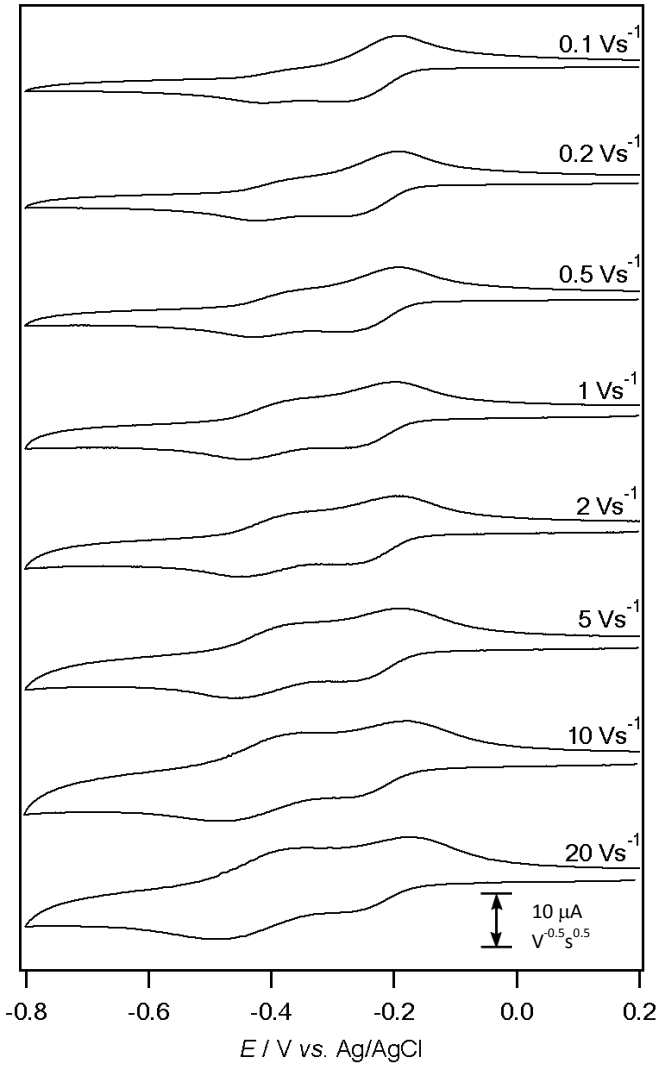

Figure 3.8. Variable scan rate cyclic voltammograms of 1 mM FMN with 0.4 M KCl in an unbuffered aqueous solution of pH 3.57, recorded at a 1 mm GC electrode at 22 (±2) ^{o}C. The current data were scaled by multiplying by $\nu^{-0.5}$.

At pH 6.03, the peak current of wave 2 decreases in magnitude while another chemically reversible wave (wave 3) begins to form at approximately E^0 = –0.52 V. From pH 6.03 to pH 9.14, wave 2 decreases in size while concomitantly wave 3 increases in size. The similarity between the peak heights of wave 3 at high pHs (where only wave 3 is observed) with that of wave 1 at very low pHs (where only wave 1 is observed) suggests that wave 3 is also a two-electron reduction process. Further investigations using rotating

disk electrode voltammetry confirmed the two-electron transfer. Wave 3 is not observed to shift with changes in the pH of the solution, indicating that it is also not a proton-coupled electron transfer reaction.

3.3.2.3. Cyclic voltammetry (5 mM FMN in unbuffered aqueous solutions)

Cyclic voltammetry experiments were also performed in solutions of 5.0 mM FMN to understand the effect of concentration of FMN on the voltammetric responses over the entire pH range. While the voltammetric response of the 5 mM FMN solution showed a similar trend to the 1 mM FMN solution, larger changes were observed in the range of pH 2 – 4, as shown in Figure 3.9.

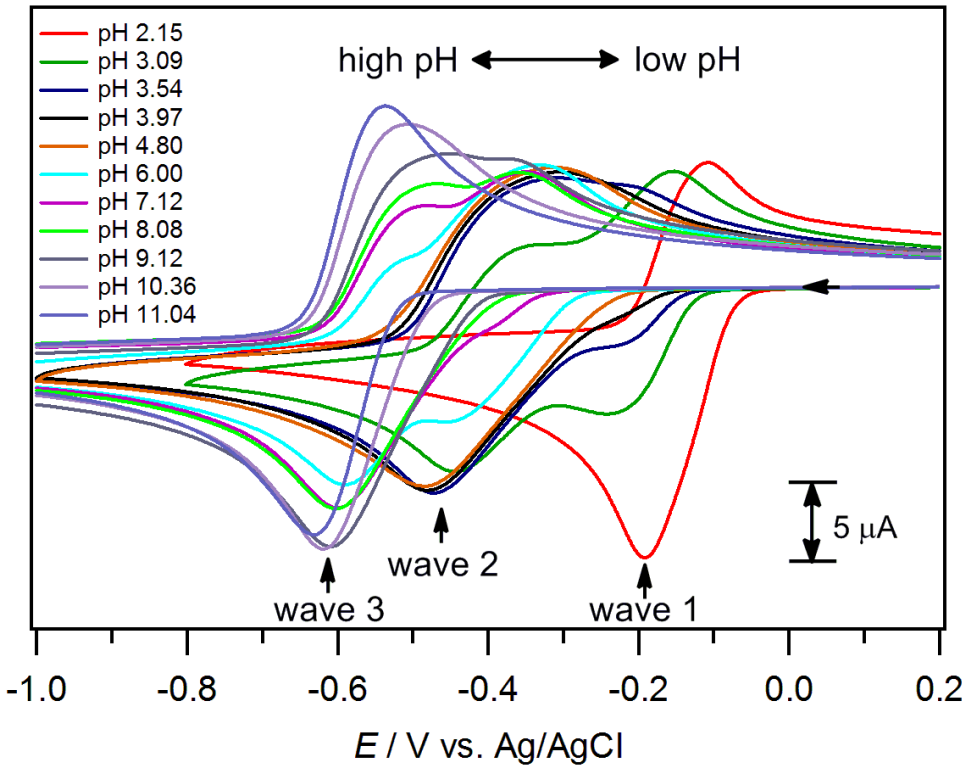

Figure 3.9. Cyclic voltammograms of 5 mM FMN in unbuffered aqueous solutions containing 0.4 M KCl between pH 2 – 11, using a 1 mm diameter planar GC electrode at a scan rate of 0.1 V s^{-1}.

In a 5 mM FMN solution, the amount of protons required in the proton-coupled electron transfer (PCET) is five times higher than required in a 1 mM FMN solution. Therefore, when the voltammograms of the 5 mM FMN solution were compared with the voltammograms of the 1 mM FMN solution obtained at identical pH values, wave 1 was significantly smaller for the higher concentration FMN solution, while wave 2 was significantly larger. This meant that wave 2 first appeared at a lower pH of 3.09 (compared to pH 3.57 in 1 mM FMN solution), because the concentration of FMN (5 mM) had already exceeded the concentration of free protons in the solution, but for the 1.0 mM FMN solution there were still sufficient free protons for the proton-couple electron transfer reaction at pH 3.09. The sensitivity of wave 1 to the ratio of the concentration of FMN and protons in solution further supported the hypothesis that wave 1 is a $2e^{-}/2H^{+}$ reduction process. It was observed that increasing the concentration of FMN in solution mainly affected the voltammetric response of FMN at low pH values, where wave 1 was originally observed. However, when comparing the cyclic voltammograms of 1 mM and 5 mM FMN at each of the pH values above pH 5, it is observed that they are almost identical [Figures 3.7 and 3.9]. This also supports the hypothesis that wave 2 and wave 3 are proton-independent electron transfers.

3.3.2.4. Rotating Disk Electrode Voltammetry (1 mM FMN in unbuffered aqueous solutions)

Unlike FMN in buffered aqueous solutions, electrolysis experiments could not be performed in unbuffered aqueous solutions due to of the large change in pH during the electrolysis that renders the results of such experiments inaccurate. After electrolysis of 1.0 mM of FMN solution at pH 3.57, the final pH of the solution was found to be much higher at 10.36 due to the flavin taking a proton from the solution as it is being reduced.

Therefore, rotating disk electrode (RDE) voltammetry would be a more accurate method in order to determine the number of electrons transferred to FMN in unbuffered solutions at different pH values.

RDE voltammetry was performed at a scan rate of 0.02 V s^{-1}, at which the noise level was minimal and current leveled off completely (Figure 3.10). In the RDE voltammetry, reduction of FMN gives very similar limiting current values at the three chosen pH values: pH 2.20 (only wave 1 observed), pH 4.80 (only wave 2 observed), and pH 9.13 (only wave 3 observed). As it was previously established that wave 1 is a proton-coupled $2e^-$ reduction, it gives substantial evidence that wave 2 and wave 3 are similarly two-electron reduction processes.[23] At all pH values, the limiting current is proportional to the square root of rotational velocity. It is observed that the slope of the graph at pH 4.80 is not as steep as that of pH 2.20 and pH 9.13, suggesting that wave 2, which contributes to the peak observed at pH 4.80 has a slower heterogeneous electron transfer step(s). From these experiments, the diffusion coefficient of FMN was determined using the Koutecký-Levich plots, by plotting the reciprocal of the limiting current against reciprocal of square root rotational velocity, using eqs 1 and 2,[42]

$$\frac{1}{I_c} = \frac{1}{0.62nF\pi r^2 D_A^{2/3} \upsilon^{-1/6} C_A^b} \bullet \frac{1}{\omega^{1/2}} + \frac{1}{nF\pi r^2 k_h C_A^b} \qquad (1)$$

$$D_A = \left[\frac{1}{0.62nF\pi r^2 \upsilon^{-1/6} C_A^b} \bullet \frac{1}{\text{gradient}} \right]^{3/2} \qquad (2)$$

where I_c is the limiting current (A), n is the number of electrons transferred (eq mol^{-1}), F is the Faraday constant (96,487 C eq^{-1}), πr^2 is the geometric disc area (cm^2), D_A is the diffusion coefficient of the species of interest (in cm^2 s^{-1}), υ is the kinematic viscosity (cm^2 s^{-1}), C^b_A is the bulk concentration of electroactive species (in mol cm^{-3}), ω is the rotational velocity (rad s^{-1}) and k_h is the heterogeneous rate constant of electron transfer (cm s^{-1}).

The plots at all three pH values show linear relationships between the reciprocal of limiting current and reciprocal of rotational velocity (Figure 3.11). The gradient of the Koutecky-Levich plots can be used to calculate the diffusion coefficient of the species of interest using eq 2.

By using the plot at pH 2.20, the diffusion coefficient of FMN was determined to be 3.80×10^{-6} cm^2 s^{-1} and was close to the value obtained later by digital simulation of CV data.

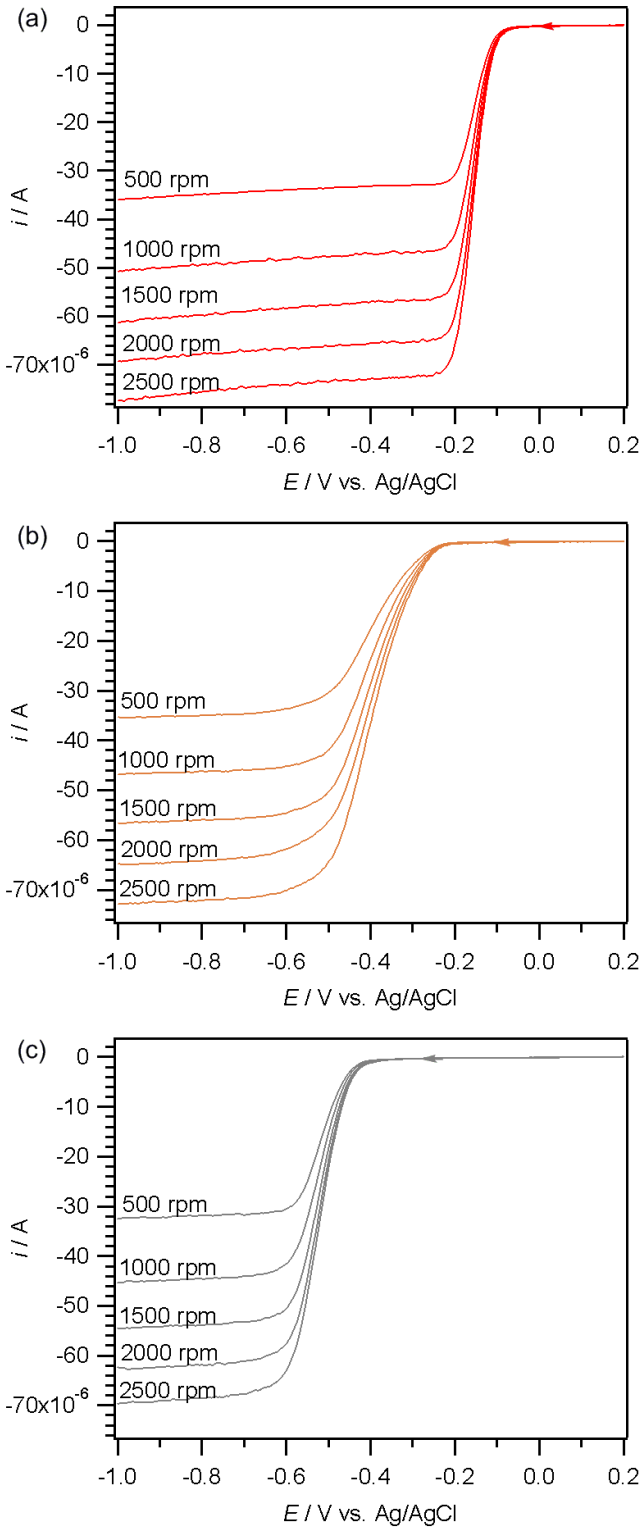

Figure 3.10. RDE voltammograms of 1.0 mM FMN in unbuffered 0.2 M KCl solution, recorded at 3 mm GC electrode at variable rotational velocities (500 – 2500 rpm) and 0.02 V s^{-1} scan rate, at (*a*) pH 2.20, (*b*) pH 4.80 and (*c*) pH 9.13.

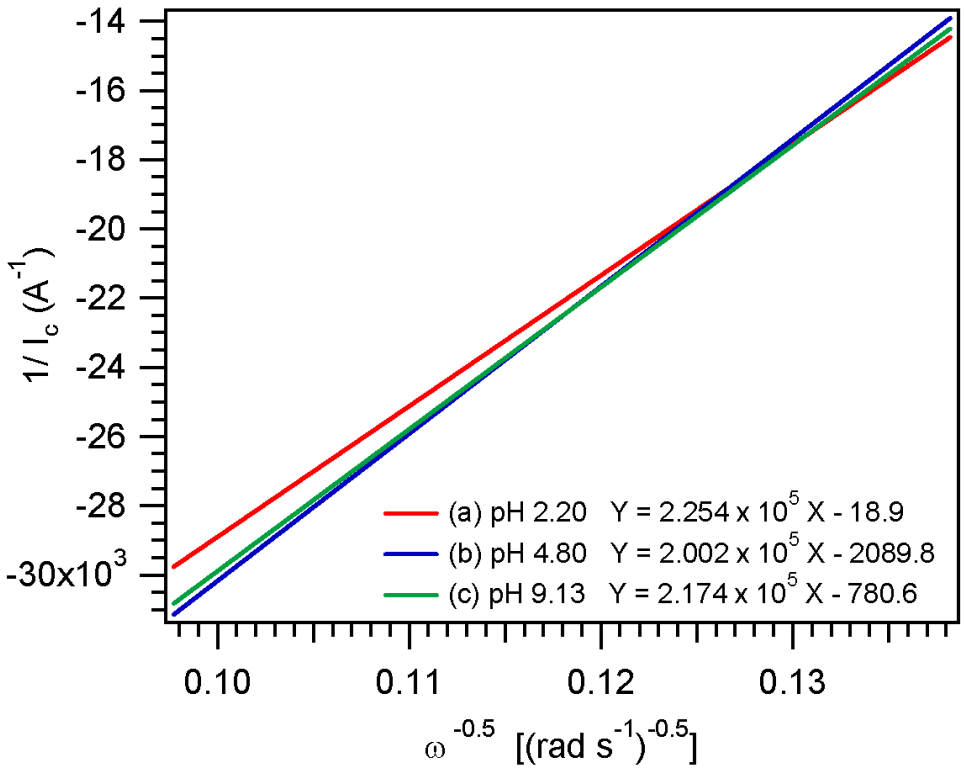

Figure 3.11. Koutecký-Levich plots of the RDE voltammograms at pH 2.20, pH 4.80 and pH 9.13.

3.3.2.5. Possible involvement of phosphate group in mechanism and the identification of wave 3

Wave 1 is currently assigned to the $2e^-/2H^+$ reduction of fully-oxidized $(FMN)H^-$ to the flavohydroquinone $(FMNH_2)H^-$ (proton dependent), and wave 2 is assigned to the $2e^-$ reduction of fully-oxidized $(FMN)H^-$ to the dianion $(FMN^{2-})H^-$ (proton independent) which is only observed when there are insufficient protons in solution to form $(FMNH_2)H^-$. It has been proven from the rotating disc electrode voltammetry that all 3 waves involve the transfer of the same number of electrons (two electrons). However, the experiments conducted did not enable the identification of the reactions occurred and

reduced species formed in wave 3, and gave no additional information other than that wave 3 is a two-electron reduction process.

A 1.0 mM FMN (in 0.4 M KCl) solution has a pH = 5.7 before adjustment to more acidic or basic values. During the preparation of the unbuffered solution, it was observed that a significantly larger amount of NaOH was required to change the pH to more basic levels than the amount of HCl required to change the pH to more acidic levels. The exact amount of NaOH (mmoles) required to obtain solutions of each pH value was tabulated, and it was observed that a 1.0 mM FMN solution required just under 1 equivalent of NaOH to change the pH from 5.7 to 6.0. As the final amount of NaOH added to obtain a solution of pH 6.0 was much higher than it should be, the similarity of the concentrations of FMN and OH^- suggested that OH^- was reacting with $(FMN)H^-$ in a 1:1 ratio to form a different oxidized flavin species. The pK_a of the phosphate group on the flavin side chain was found to be 6.20, which coincides with the pH of the solution where base had to be added to adjust to the desire pH levels.[29,43]

Scheme 3.4. Chemical structures of flavin mononucleotide at different protonation states of the phosphate group.

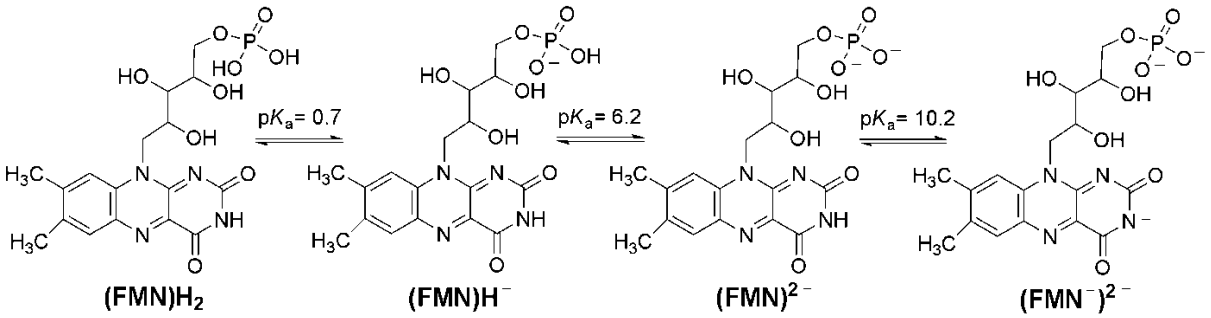

Therefore, a plausible reason why close to 1 equivalent of NaOH (as compared to FMN) had to be added to effect such a small pH change from pH 5.7 to 6.0, is that the OH^- added reacts with the protons that are released by the phosphate groups around pH 6.2.

It was then postulated that at the pH range of 6.03 – 9.14, the oxidized FMN with the phosphate group fully deprotonated ($(FMN)^{2-}$), is the species which undergoes reduction in wave 3 to form $(FMN^{\bullet-})^{2-}$ and subsequently $(FMN^{2-})^{2-}$ in the same voltammetric wave. The dianion $(FMN^{2-})^{2-}$ formed in wave 3 would similarly form hydrogen-bonding with the water molecules, and possibly gain a proton from a water molecule, just as postulated for the dianion $(FMN^{2-})H^-$ formed in wave 2. For the experiments performed in buffered solutions, $(FMN)^{2-}$ is also present at sufficiently high pH, but the shift in voltammetric peak potentials over the pH range is controlled by the equilibrium expression in the Nernst equation involving the free acid as well as protonation reactions of reduced flavins with the buffer electrolyte.

At pH 10.38 and pH 11.03, a slight shift in the reduction potential for wave 3 was observed. At this pH range, the pH of the solution is higher than the pK_a of the imide proton on the FMN isoalloxazine ring. Therefore, before reduction takes place, oxidized FMN exists as a mixture of $(FMN)^{2-}$ and the deprotonated $(FMN^-)^{2-}$. The ratio of the concentration of $(FMN)^{2-}$ and $(FMN^-)^{2-}$ at high pHs can be calculated using the Henderson-Hasselbalch equation (eq 3), and calculated values are reported in Table 3.1.

$$\mathrm{pH} = \mathrm{p}K_a + \log \frac{[(\mathrm{FMN}^-)^{2-}]}{[(\mathrm{FMN})^{2-}]} \qquad (3)$$

The pK_a of FMN has been investigated by several laboratories and a range of values have been reported, ranging from 9.65 to 10.40.[13–14,16,19,27–33] The pK_a of FMN used in this

study to calculate the ratio of the two species was 10.2, the value which was obtained by P. Cerletti using titration, fluorescence and absorption methods.[29] The increased negative charge on the deprotonated flavin would cause the deprotonated flavin to be harder to reduce than the protonated form, thus shifting the reduction potential to more negative potentials. Thus at pH 11, the hydrogen-bonded $(FMN^{3-})^{2-}$ is initially formed. All the reduced species formed (regardless of pH of the solution) are expected to undergo hydrogen-bonding interactions with water molecules as observed in buffered solutions and for quinones in similar media, and given sufficient time, the fully-reduced species $(FMN^{3-})^{2-}$ would be protonated to form $(FMNH^{2-})^{2-}$.

Table 3.1. Concentration of $(FMN)^{2-}$ and $(FMN^{\cdot-})^{2-}$ at different pHs, calculated from pK_a $(FMN)^{2-}$ = 10.20.

pH	$[(FMN)^{2-}]$/ mM	$[(FMN^{\cdot-})^{2-}]$/ mM
pH 9.14	0.920	0.080
pH 10.38	0.398	0.602
pH 11.03	0.148	0.852

In order to find out if number of negative charges on the side chain would in fact affect the electrochemical behavior of FMN, despite being a fair distance away from the electroactive center, we repeated the cyclic voltammetry experiments at pH 2 – 11 using FAD, which also contains two phosphate groups which can be doubly deprotonated (Scheme 3.1).

3.3.2.6. Cyclic Voltammetry (1 mM FAD in unbuffered aqueous solutions)

The comparison of the voltammograms of 1 mM FMN (Figure 3.7) with that of 1 mM FAD (Figure 3.12), allowed for the observation of 2 noticeable differences. The immediate difference was that the lowest pH that wave 3 was observed was pH 4 (for FAD), rather than pH 6 (for FMN). Another difference was that wave 2 is only observed at pH 4 for FAD, and not significant at other pH values. As the pK_a's of the phosphate groups of FAD are 2.06 and 3.69,[44] at pH 2 – 3, oxidized FAD will consist mainly of $(FAD)H^-$ which would be reduced to $(FADH_2)H^-$ due to sufficient number of protons at that pH. At pH 4, FAD will consist of a mixture of flavins with completely deprotonated ($(FAD)^{2-}$) and singly-protonated phosphate groups ($(FAD)H^-$). Thus, $(FAD)H^-$ would be reduced to $(FADH_2)H^-$ in wave 1 until insufficient protons are available to allow further reduction via this reduction pathway, and the remaining $(FAD)H^-$ will undergo reduction via an EE mechanism to $(FAD^{2-})H^-$ in wave 2, and flavins with the phosphate groups completely deprotonated ($(FAD)^{2-}$) will undergo reduction via an EE mechanism to $(FAD^{2-})^{2-}$ in wave 3. The observation of wave 3 appearing after the phosphate groups are both deprotonated (pH 4 and higher for FAD), is in good agreement with our cyclic voltammograms from FMN, where wave 3 occurs only when the phosphate group is completely deprotonated (pH 6 and higher), giving further evidence that the charge on the phosphate group affects the electrochemistry of the flavins.

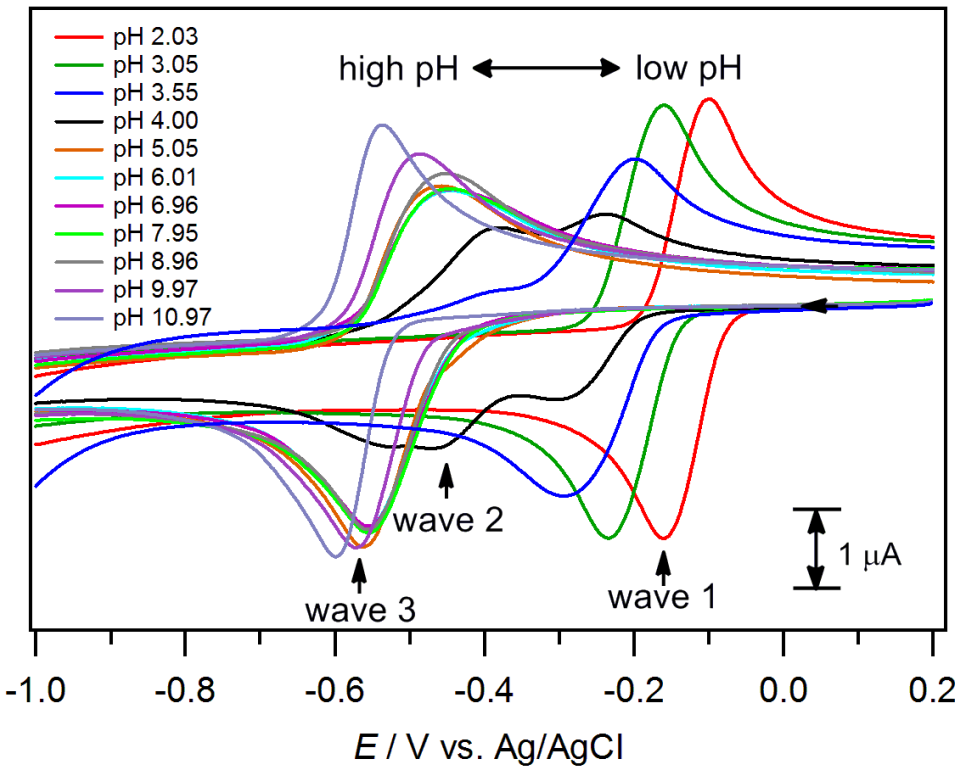

Figure 3.12. Cyclic voltammograms of 1 mM FAD in unbuffered aqueous solutions containing 0.4 M KCl between pH 2 – 11, using a 1 mm diameter planar GC electrode at a scan rate of 0.1 V s^{-1}.

The negative charge on the phosphate group could possibly affect the electrochemistry of the flavins, because of ion-dipole interactions of the highly negatively charged phosphate group with a positive dipole at the electroactive isoalloxazine ring, forming a partial negative charge at the electroactive center. This increased negative charge at the electroactive isoalloxazine ring would cause the flavin to be harder to reduce (wave 3 occurs at more negative potentials than wave 2).

3.3.2.7. Electron Transfer Mechanism of FMN in unbuffered aqueous solutions

The electrochemical reduction mechanisms of FMN in unbuffered aqueous solutions from pH 2 – 11 are given in Schemes 3.5 – 3.7, based on the results of the cyclic

voltammetry experiments conducted with 1 – 5 mM of FMN in solution with 0.4 M of KCl as electrolyte. The mechanisms, as well as the electrochemical and kinetic parameters in Schemes 3.5 – 3.7 were refined by performing digital fitting of the voltammetric data obtained at the different pH values using the commercially available DigiElch software, in a trial and error process where each individual parameter is varied while keeping the other parameters constant, and the process repeated until the simulation parameters (equilibrium constants, rate constants and electrode potentials) allowed simulated voltammograms that closely matched the experimental voltammograms at each pH value (Figure 3.13). In Tables 2 and 3, the optimized parameters used in the digital simulations for the mechanisms in Schemes 3.5 – 3.7 are reported. The concentrations of H^+ and OH^- used in the simulations were set according to the amount of added acid (hydrochloric acid) or base (sodium hydroxide) during the experiment to adjust the pH from the initial pH of 1 mM FMN in 0.4 M KCl (pH 5.7).

A good match between the simulated and experimental voltammograms were obtained by using parameters reported in Tables 2 and 3, with the simulated and experimental voltammograms shown in Figure 3.13 (1 mM FMN) and Figure 3.14 (5 mM FMN).

For wave 1, both the shift in peak potential and decrease in peak height from pH 2.13 to pH 4.77 were observed. $(FMN)H^-$ was first reduced by one electron to form $(FMN^{\bullet -})H^-$ at a potential E^0 = -0.345 V, then receives a proton to form $(FMNH^{\bullet})H^-$. The protonated radical $[(FMNH^{\bullet})H^-]$ is then reduced at a less negative potential (E^0 = -0.0125 V), forming $(FMNH^-)H^-$. This anionic species and its protonated form $(FMNH_2)H^-$, depend on the amount of protons available in the solution. The reactions in eqs 1, 8, 3 and 9 (Scheme 3.5) give rise to wave 1.

Wave 2 appears at pH 3.57 and starts increasing in size as the pH increases. When there are minimal protons in the solution, $(FMN^{\bullet-})H^{-}$ will be further reduced to $(FMN^{2-})H^{-}$ (likely to be hydrogen-bonded and could be eventually protonated), as shown by eqs 1 and 2 in Schemes 3.5 and 3.6. While we believe that the dianion is likely to undergo protonation in unbuffered aqueous solutions at intermediate to high pH values, as it does in buffered aqueous solutions at high pH, the closely spaced reduction waves of fully-oxidized FMN and the anionic radical $(FMN^{\bullet-})H^{-}$ makes it difficult to observe the formation of $(FMNH^{-})H^{-}$ during the reverse scan. This is because in aprotic organic solvents, the oxidation of FlH^{-} occurs at slightly more positive potentials than $Fl^{\bullet-}$, while the reduction of Fl and $Fl^{\bullet-}$ are separated by close to 0.8 V. In comparison, in buffered aqueous solutions, the reduction of Fl and $Fl^{\bullet-}$ are so closely spaced they are observed in a single voltammetric wave, so the oxidation of FlH^{-} (if any present) would be buried within a single oxidation wave.

Wave 3 is formed at high pHs, where we postulate that $(FMN)^{2-}$ (with the phosphate group fully deprotonated) undergoes $2e^{-}$ reduction as in eqs 4 and 5 in Scheme 3.6, and where the $(FMN^{-})^{2-}$ (with the phosphate group fully deprotonated) undergoes $2e^{-}$ reduction as in eqs 6 and 7 in Scheme 3.7. It is important to note that while Scheme 3.6 and 3.7 showed the dianion (or dianion with the imide proton deprotonated) as the final reduction product at higher pH ranges, hydrogen bonding of water to the dianion and further protonation by a water molecule are reactions that are highly possible as well. In fact, at high scan rates, another oxidation wave was observed like in buffered aqueous solutions at high pH. (Variable scan rate cyclic voltammograms given in figures A3.1 – A3.36 in appendix.) However, unlike for buffered aqueous solutions where there are no competing waves within the same voltammogram, results are not conclusive as there can be complications from wave 2 that could be occurring at the same pH.

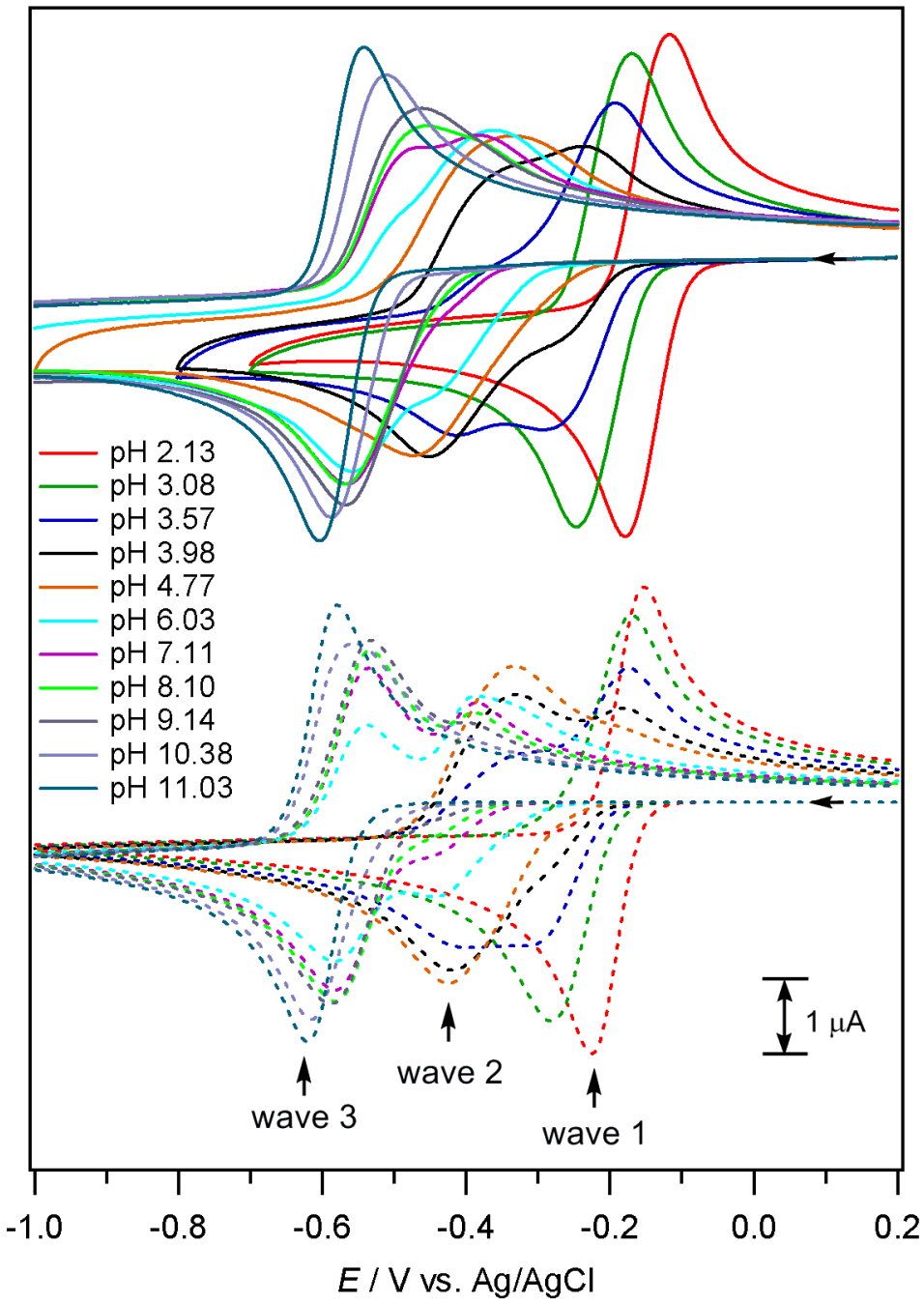

Figure 3.13. CVs of 1.0 mM FMN in 0.4 M KCl recorded at 1 mm GC electrode (solid lines) and digital simulations of the CV data based on the mechanism in Schemes 3.5 – 3.7 and parameters given in Table 3.2 and 3.3 (dotted lines).

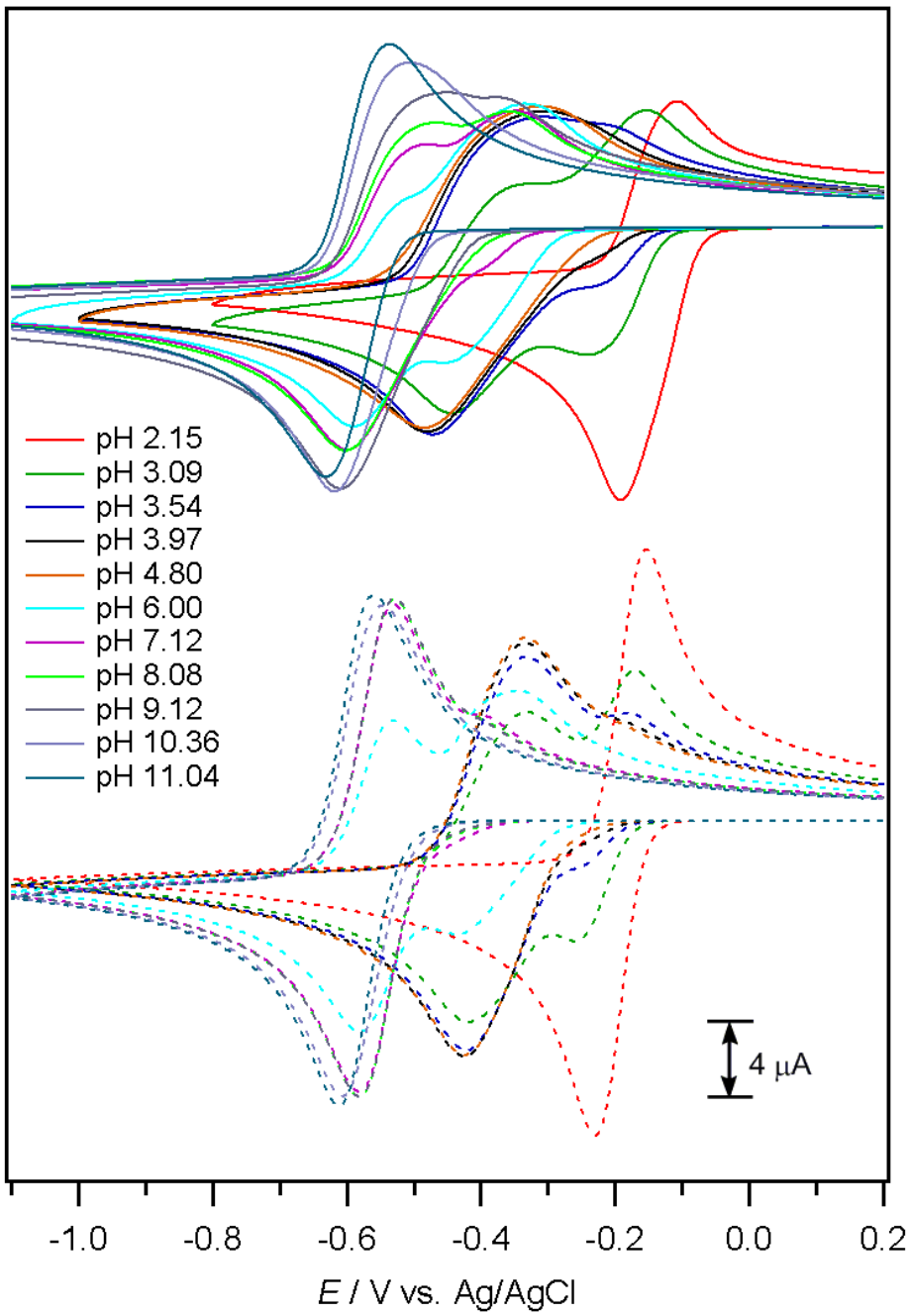

Figure 3.14. CVs of 5.0 mM FMN in 0.4 M KCl recorded at 1 mm GC electrode (solid lines) and digital simulations of the CV data based on the mechanism in Schemes 3.5 – 3.7 and parameters given in Table 3.2 and 3.3 (dotted lines).

Scheme 3.5. Voltammetrically induced proton-coupled electron transfer reduction mechanism of FMN in unbuffered aqueous solution of pH 2.13 − 6.03 over a range of scan rates.

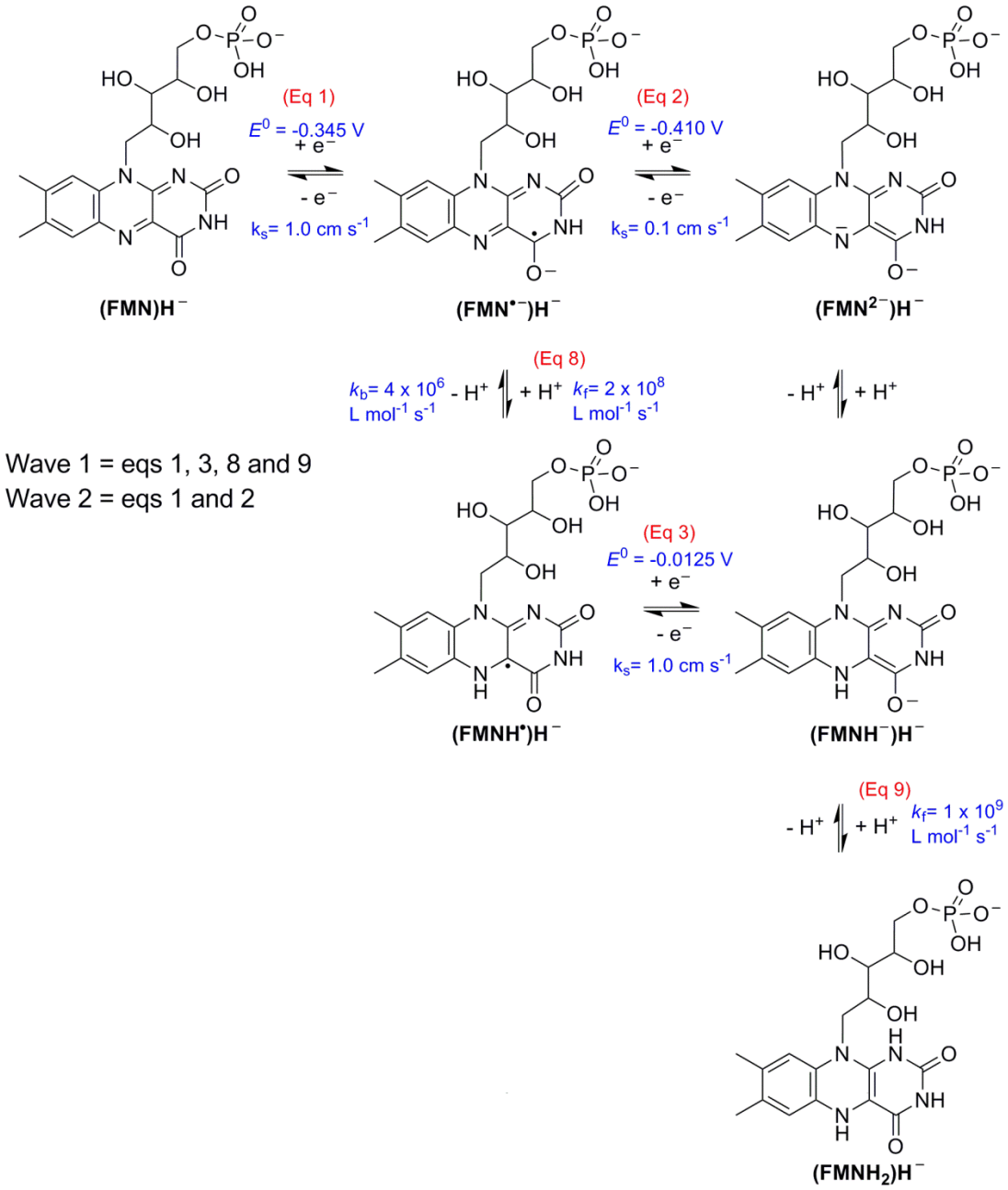

Scheme 3.6. Voltammetrically induced electron transfer reduction mechanism of FMN in unbuffered aqueous solution of pH 6.03 – 9.14 over a range of scan rates.

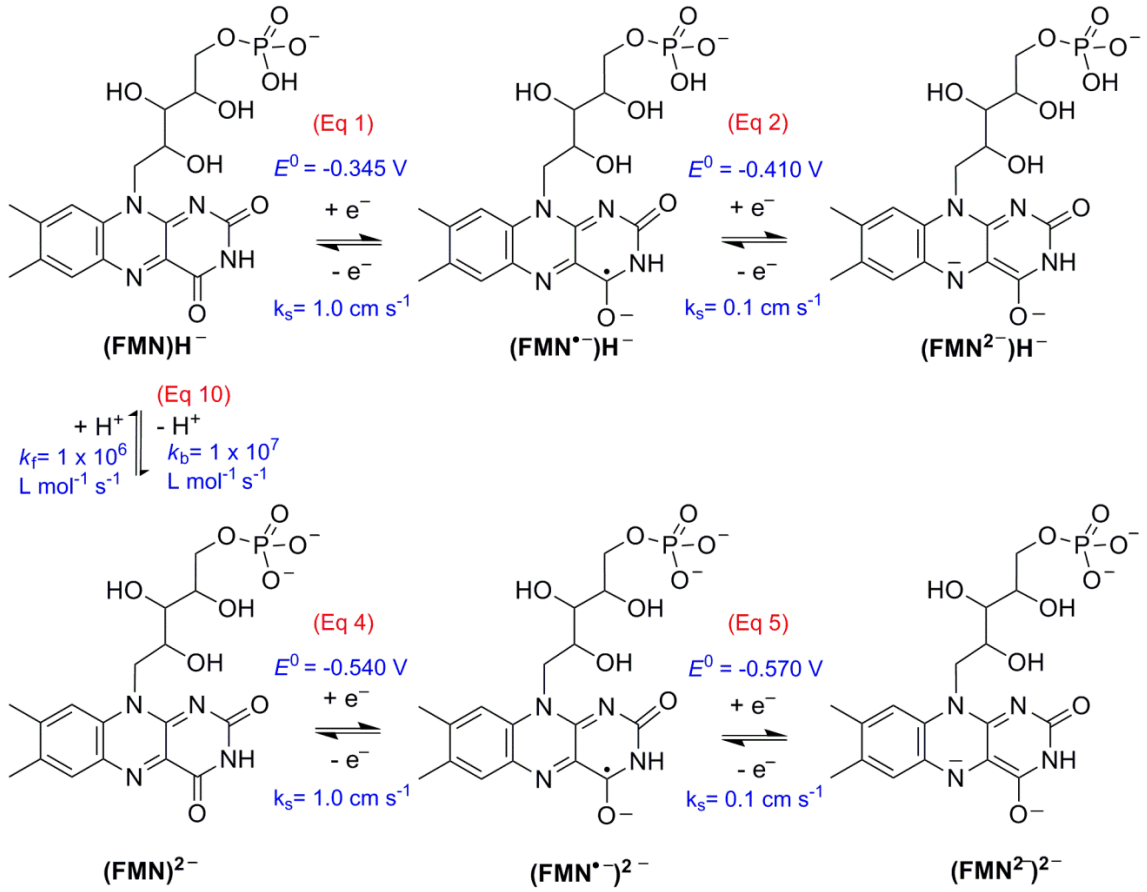

Wave 3 = eqs 4, 5 and 10

Scheme 3.7. Voltammetrically induced electron transfer reduction mechanism of FMN in unbuffered aqueous solution of pH 10.38 – 11.03 over a range of scan rates.

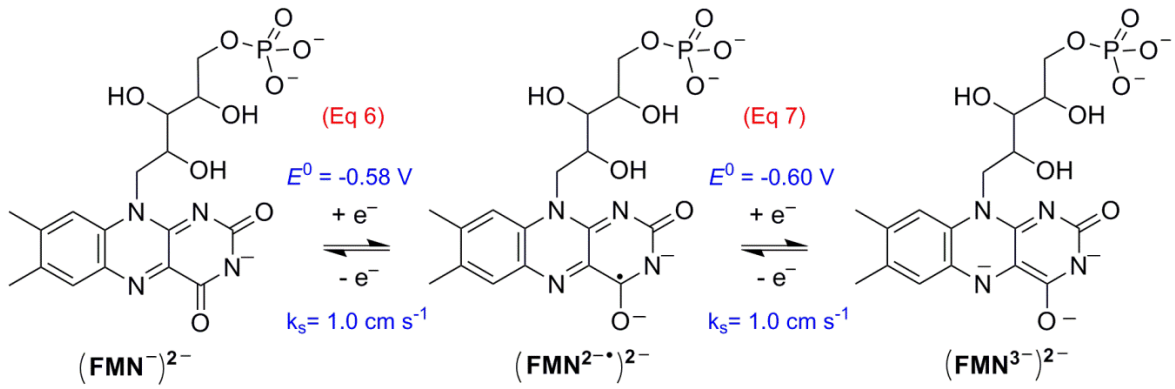

Wave 3 = eqs 6 and 7

Table 3.2. Electrochemical parameters obtained by digital simulation of CV[a] data for the reaction mechanism given in Schemes 3.5 – 3.7.

10^{-6} D / cm^2 s^{-1}	**Eq 1** $(FMN)H^-$ + e^- ⇌ $(FMN^{\bullet-})H^-$		**Eq 2** $(FMN^{\bullet-})H^-$ + e^- ⇌ $(FMN^{2-})H^-$		**Eq 3** $(FMNH^{\bullet})H^-$ + e^- ⇌ $(FMNH^-)H^-$		**Eq 4** $(FMN)^{2-}$ + e^- ⇌ $(FMN^{-\bullet})^{2-}$		**Eq 5** $(FMN^{-\bullet})^{2-}$ + e^- ⇌ $(FMN^{2-})^{2-}$		**Eq 6** $(FMN^-)^{2-}$ + e^- ⇌ $(FMN^{2-\bullet})^{2-}$		**Eq 7** $(FMN^{2-\bullet})^{2-}$ + e^- ⇌ $(FMN^{3-})^{2-}$	
	$E^0_{(1)}$ / V	$k_{s(1)}$ / cm s^{-1}	$E^0_{(2)}$ / V	$k_{s(2)}$ / cm s^{-1}	$E^0_{(3)}$ / V	$k_{s(3)}$ / cm s^{-1}	$E^0_{(4)}$ / V	$k_{s(4)}$ / cm s^{-1}	$E^0_{(5)}$ / V	$k_{s(5)}$ / cm s^{-1}	$E^0_{(6)}$ / V	$k_{s(6)}$ / cm s^{-1}	$E^0_{(7)}$ / V	$k_{s(7)}$ / cm s^{-1}
3.0	-0.345	1	-0.41	0.1	-0.0125	1	-0.54	1	-0.57	1	-0.60	1	-0.60	1

[a]CV data recorded in unbuffered aqueous solutions at 22 (±2) °C with 0.4 M KCl as the supporting electrolyte with a 1 mm diameter planar GC working electrode and at scan rate of 0.1 V s^{-1}. E^0 = formal reduction potential, k_s = heterogeneous electron transfer rate constant and D = diffusion coefficient.

Table 3.3. Equilibrium (K_{eq}) and forward (k_f) and backward (k_b) rate constants, obtained by digital simulation of CV data for the reaction mechanism given in Schemes 3.5 – 3.7 obtained in unbuffered aqueous solution containing 0.4 M KCl at 22 (±2) °C.

Eq 8 $(FMN^{\bullet-})H^- + H^+$ ⇌ $(FMNH^{\bullet})H^-$			**Eq 9** $(FMNH^-)H^- + H^+$ ⇌ $(FMNH_2)H^-$			**Eq 10** $(FMN)H^-$ ⇌ $(FMN)^{2-} + H^+$			**Eq 11** H_2O ⇌ $H^+ + OH^-$		
$K_{eq(1)}$	$k_{f(1)}$ / L mol^{-1} s^{-1}	$k_{b(1)}$ / L mol^{-1} s^{-1}	$K_{eq(2)}$	$k_{f(2)}$ / L mol^{-1} s^{-1}	$k_{b(2)}$ / L mol^{-1} s^{-1}	$K_{eq(3)}$	$k_{f(3)}$ / L mol^{-1} s^{-1}	$k_{b(3)}$ / L mol^{-1} s^{-1}	$K_{eq(4)}$	$k_{f(4)}$ / L mol^{-1} s^{-1}	$k_{b(4)}$ / L mol^{-1} s^{-1}
50	2.00×10^8	4.00×10^6	50	1.00×10^9	2.00×10^7	1.00×10^{-7}	500	5.00×10^{-9}	1.00×10^{-14}	1.00×10^6	1.00×10^{20}

3.3.3. Relevance of electrochemical results to flavoproteins and further applications

Based on current results, the mechanisms and redox properties of flavins are highly sensitive towards the physical environment that the flavin is located, which is one of the unique advantages of flavin as a cofactor as it allows different flavoproteins to undergo different processes and thus have different functions. The behavior of free flavins has been shown to vary when they are in an aprotic hydrophobic media, a buffered aqueous media, or an unbuffered aqueous media. Past research has shown that the behavior of the flavin cofactor in each flavoprotein also differs depending on the intermolecular interactions between flavin cofactor and protein backbone. For example, binding of NAD^+ to cytochrome b_5 reductase causes changes in the protein such that it changes intermolecular interactions between the flavoprotein and $FADH_2$ in such a way that stabilizes the flavosemiquinone form, thus allowing the donation of an electron to one-electron acceptors.[8] The rate of electron shuttling to the electrode surface for the two-electron redox process of free-flavins is increased when the flavin is bound in OM c-Cyt, which promotes a one-electron redox process forming a flavosemiquinone.[45]

It would appear to be simpler to analyze each flavoprotein separately, however, the distance between the flavin binding site to the surface of the protein as well as how open the flavin binding site is to solution would affect the electron transfer rate between the electrode transfer rate and the flavin bound in the protein. In most cases, the heterogeneous electron transfer rate is slow for flavins bound within a flavoprotein, thus causing difficulties in finding the detailed electron transfer mechanism in that flavoprotein. Thus, deductions can be formed based on the closest model. For flavoproteins with flavins situated in a solvent-accessible site, care must be exercised when considering if the active site of the flavoprotein is as well buffered as the cell

cytoplasm, considering the differences in the electrochemical reduction mechanism between flavins in buffered and unbuffered aqueous solutions.

The crystal structure of the flavoprotein (whether the flavin cofactor is buried in a totally hydrophobic environment, freely accessible to solvent molecules, when access to solvent molecules is controlled by the protein structure, or if the flavin binding site has any charged species) is useful to decipher which mechanism would be most applicable to each flavoprotein.

3.4. Conclusion

The electrochemical reduction of FMN in buffered aqueous solutions between pH 3 – 11 occurs by two electrons per molecule, as proven by bulk controlled potential electrolysis experiments. UV-vis spectroscopy of the solution after bulk reduction showed that the main reduced species present in the bulk solution for pH 3 – 5 is $FMNH_2$ while the main reduced species for pH 7 – 10 is $FMNH^-$. Cyclic voltammetry experiments performed at high pH and slow scan rates showed a significantly broadened oxidation peak, which separated into two oxidation peaks at faster scan rates, indicating that both processes might occur even at slow scan rates. The second oxidation peak also decreased in size as scan rate increased, indicating that the protonation reaction of the hydrogen-bonded dianion $FMN^{2-}(H_2O)_x$ to form $FMNH^-$ was outrun.

FMN in unbuffered aqueous solutions had significantly different results than in buffered aqueous solutions, showing that differences in the buffer capacity in the flavin binding sites of flavoproteins could lead to different mechanisms and reduction potentials. Three different voltammetric waves were observed over the entire pH range: wave 1 is dominant when $[H^+] \geq [FMN]$; wave 2 appears at a mid-range pH generally between pH

3.5 – 6 (where the lower point of the pH range is dependent on the concentration of FMN and the upper point of the pH range is dependent on the pK_{a2} of the phosphate group); and wave 3 is dominant when the pH is higher than the pK_{a2} of the phosphate group. Rotating disc electrode voltammetry confirmed that all 3 waves involve a 2 electron reduction. Comparisons of the CVs of 1 mM FMN and 5 mM FMN at different pH values confirmed that wave 1 was a proton-dependent electron transfer, while waves 2 and 3 were proton-independent electron transfers. Comparisons of the CVs of 1 mM FMN and 1 mM FAD indicated that wave 3 occurs only when the phosphate groups are completely deprotonated forming a highly negative charge on the side chain, which can form ion-dipole interactions with the isoalloxazine ring in free flavins.

3.5. References

1. Walsh, *C. Acc. Chem. Res.* **1980**, *13*, 148–155.

2. Ghisla, S; Massey, V. *Eur. J. Biochem.* **1989**, *181*, 1–17.

3. Bruice, T. C. *Isr. J. Chem.*, **1984**, *24*, 54-61.

4. Mueller, F. In *Topics in Current Chemistry*; Boschke, F. L., Ed.; Springer-Verlag: Berlin, 1983; Vol. 108, pp 71–108.

5. Niemz, A.; Imbriglio, J.; Rotello, V. M. *J. Am. Chem. Soc.* **1997**, *119*, 887–892.

6. Massey, V.; Hemmerich, P. *Biochem. Soc. Trans.* **1980**, *8*, 246–257.

7. Paulsen, K. E.; Stankovich, M. T.; Stockman, B. J.; Markley, J. L. *Arch. Biochem. Biophys.* **1990**, *280*, 68–73.

8. Iyanagi, T. *Biochemistry*, **1977**, *16*, 2725–2730.

9. Iyanagi, T.; Watanabe, S.; Anan, K. F. *Biochemistry*, **1984**, *23*, 1418–1425.

10. Nishida, H.; Inaka, K.; Yamanaka, M.; Kaida, S.; Kobayashi, K.; Miki, K. *Biochemistry*, **1995**, *34*, 2763–2767.

11. Tan, S. L. J.; Webster, R. D. *J. Am. Chem. Soc.* **2012**, *134*, 5954–5964.

12. Janik, B.; Elving, P. J. *Chem. Rev.* **1968**, *68*, 295–319.

13. Michaelis, L.; Schwarzenbach, G. *J. Biol. Chem.* **1938**, *123*, 527–542.

14. Draper, R. D.; Ingraham, L. L. *Arch. Biochem. Biophys.* **1968**, *125*, 802–808.

15. Hartley, A. M.; Wilson, G. S. *Anal. Chem.* **1966**, *38*, 681–687.

16. Lowe, H. J.; Clark, W. M. *J. Biol. Chem.* **1956**, *220*, 983–992.

17. Wei, H.; Omanovic, S. *Chem. Biodiv.* **2008**, *5*, 1622–1639.

18. Cable, M.; Smith, E. T. *Anal. Chim. Acta.* **2005**, *537*, 299–306.

19. Ksenzhek, O. S.; Petrova, S. A. *Bioelectrochem. Bioenerg.* **1983**, *11*, 105–127.

20. Diculescu, V. C.; Militaru, A.; Shah, A.; Qureshi, R.; Tugulea, L.; Brett, A. M. O. *J. Electroanal. Chem.* **2010**, *647*, 1–7.

21. Male, R.; Samotowka, M. A.; Allendoerfer, R. D. *Electroanalysis* **1989**, *1*, 333–339.

22. Hui, Y.; Chng, E. L. K.; Chng, C. Y. L.; Poh, H. L.; Webster, R. D. *J. Am. Chem. Soc.* **2009**, *131*, 1523–1534.

23. Quan, M.; Sanchez, D.; Wasylkiw, M. F.; Smith, D. K. *J. Am. Chem. Soc.* **2007**, *129*, 12847–12856.

24. Nöll, G. *J. Photochem. Photobiol. A,* **2008**, *200*, 34–38.

25. Hemmerich, P.; Veeger, C.; Wood, H. C. S. *Angew. Chem.* **1965**, *77*, 699–716.

26. Dudley, K. H.; Ehrenberg, A.; Hemmerich, P.; Müller, F. *Helv. Chim. Acta.* **1964**, *47*, 1354–1383.

27. Mayhew, S. G. *Eur. J. Biochem.* **1999**, *265*, 698–702.

28. Ke, B. *Arch. Biochem. Biophys.* **1957**, *68*, 330–340.

29. Cerletti, P. *Anal. Chim. Acta.* **1959**, *20*, 243–250.

30. Michaelis, L.; Schubert, M. P.; Smythe, C. V. *J. Biol. Chem.* **1936**, *116*, 587–607.

31. Albert, A. *Biochem. J.* **1953**, *54*, 646–654.

32. Heelis, P. F. *Chem. Soc. Rev.* **1982**, *11*, 15–39.

33. Stare, F. J. *J. Biol. Chem.* **1935**, *112*, 223–229.

34. Malinowski, E. R.; Barber, M. J.; Whitaker, G. T.; Smith, E. T. *J. Chemometrics.* **2007**, *21*, 520–528.

35. Bruns, C.M.; Karplus, P. A. *J. Mol. Biol.* **1995**, *247*, 125–145.

36. Mattevi, A. *Trends Biochem. Sci.* **2006**, *31*, 276–283.

37. Edmondson, D. E.; Binda, C.; Mattevi, A. *NeuroToxicology,* **2004**, *25*, 63–72.

38. Edmondson, D. E.; Binda, C; Wang, J.; Upadhyay A. K.; Mattevi, A. *Biochemistry,* **2009**, *48*, 4220–4230.

39. Durand, T.; Vidal, G.; Canioni, P.; Gallis, J.-L. *Cyrobiology,* **1998**, *36*, 269–278.

40. Müller, F.; Mayhew, S. G.; Massey V. *Biochemistry,* **1973**, *12*, 4654–4662.

41. Sarma, R. H.; Dannies, P.; Kaplan, N. O. *Biochemistry,* **1968**, *7*, 4359–4367.

42. Treimer, S.; Tang, A.; Johnson, D. C. *Electroanalysis*, **2002**, *14*, 165–171.

43. Tsentalovich, Y. P.; Lopez, J. J.; Sagdeev, R. Z. *Spectrochim. Acta* **2002**, *58*, 2043–2050.

44. Bidwell, J.; Thomas, J.; Stuehr, J. *J. Am. Chem. Soc.* **1986**, *108*, 820-825.

45. Okamoto, A.; Hashimoto, K.; Nealson, K. H.; Nakamura, R. *Proc. Natl. Acad. Sci. USA*, **2013**, *110*, 7856–7861.

Chapter 4

Proton-Coupled Electron Transfer Reactions of Flavins in Aprotic Organic Solvents and the Effects of Trace Water.

4.1. Introduction

Flavins are versatile coenzymes because they can undergo one- or two-electron processes, as well as accept electrons from a large variety of functional groups, and catalyze a large number of redox reactions in biological systems.[1–12] The ability of flavins to undergo different processes in different flavoproteins indicates the importance of the immediate environment of the flavin (e.g. the isoalloxazine ring of the flavin buried in a hydrophobic region[13–14], or accessible by solvent[15–16] and/ or molecular oxygen[5]), and intermolecular interactions between the flavin and the flavoprotein (e.g. π–stacking[17] and H–bonding[18–21]).

In an electrochemical study conducted in an aprotic organic solvent, Niemz et al[11] reported that the imide proton could act as a proton donor, causing significant difference in the electron transfer mechanism between a flavin with the N3-H group, and a flavin with an N3-Me group. The flavin with the N3-H group was reduced to the anionic radical ($Fl^{-\bullet}$), but due to the availability of protons from the N3-H group of another flavin molecule, was quickly protonated to $FlH^{\bullet}$ (via an intermolecular proton transfer), which was immediately further reduced to FlH^{-} at the potential applied. The flavin molecules that acted as the proton donor are thus deprotonated, forming Fl^{-}. Fl^{-} was then able to undergo comproportionation with FlH^{-} to form two molecules of $Fl^{-\bullet}$. Upon reversal of the scan direction, the oxidation peaks of $Fl^{-\bullet}$ and FlH^{-} were both observed.[11] The flavin with the N3-Me group was reduced to the anionic radical, and without a suitable proton source available in solution, the anionic radical did not undergo any chemical

transformation, and is oxidized back to fully-oxidized flavin upon reversal of scan direction.

As described in chapter 3, a series of experiments were conducted on riboflavin (vitamin B_2) in dimethyl sulfoxide (DMSO), and the ability of the imide proton of one riboflavin molecule to protonate the anionic radical ($Fl^{-\bullet}$) species of another flavin molecule was confirmed. Additional reduction waves were assigned to the reduction of Fl^- (wave 4) and $Fl^{-\bullet}$ (wave 5), forming $Fl^{2-\bullet}$ and Fl^{2-} respectively. The dianion (Fl^{2-}) was also able to be protonated, presumably by the N3-H of another flavin molecule. At high scan rates, the protonation reaction of $Fl^{-\bullet}$ is outrun, and the electrochemically-induced reduction mechanism resembles that of a flavin with an N3-Me group, as described by Niemz *et. al*. The rate and equilibrium constant values associated with the reactions in the electrochemically-induced reduction mechanism were determined.[22]

In chapter 4, in unbuffered aqueous solutions of varying acidity, it was postulated that the flavin dianion was able to exist in a hydrogen-bonded (with H_2O) state at intermediate and high pHs, at least on the short (CV) timescale of ≤ a few seconds.[23] This is analogous to quinone dianions that can exist in unbuffered aqueous environments or in aqueous-organic mixtures in a fully non-protonated hydrogen-bonded state.[24,25] However, in aqueous solutions the fates of the flavin dianions are difficult to ascertain due to the potentials of the first and second electron transfer steps coinciding so that only one two-electron chemically reversible wave is observed. In contrast, in a non-aqueous environment the first and second electron transfer steps can be separated in the absence of a proton source, which enables the fates of the dianions to be probed. Nevertheless, water is a ubiquitous impurity present in all organic solvents, which leads to the possibility of competing reactions with trace H_2O. Therefore, this study is devoted to examining the effects that trace water has on the voltammetric behavior of flavins in aprotic organic media, to determine whether the anion radical and dianion undergo protonation with

water. The effects of trace water are also relevant to the biological functions of flavins, since many exist naturally within proteins in a lipophilic environment where there are very low amounts of water.

This study required the synthesis of compounds **1** and **2**, which are identical other than the N3 moiety either being attached to hydrogen atom or a methyl group. The hydroxyl-containing ribityl group on N10 in riboflavin/FMN was replaced with an ethyl group in order to improve its solubility in aprotic organic solvents. The role of trace water in the potential protonation of the anion radical and dianion were investigated by comparing the voltammograms of flavins **1** and **2** in the presence and absence of deliberately added water.

Scheme 4.1. Riboflavin (vitamin B_2), Flavin mononucleotide, flavin **1** and flavin **2**.

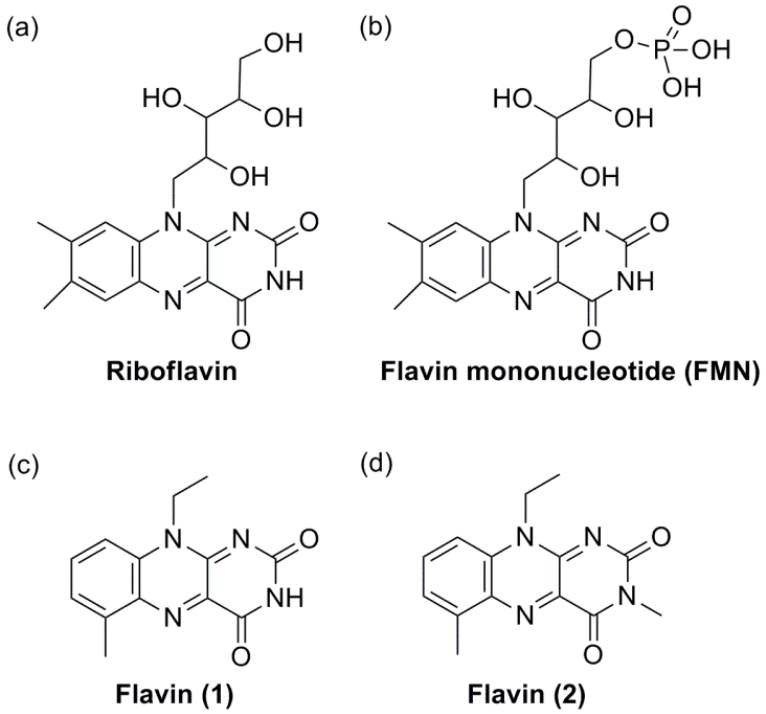

4.2. Experimental

4.2.1. Chemicals

n-Bu_4NPF_6 was prepared by reacting equal molar amounts of a 40% aqueous solution of *n*-Bu_4OH with a 65% aqueous solution of HPF_6, washing the precipitate with hot water, recrystallizing three times from hot ethanol and then drying under vacuum for 24 hours at 140 ^oC.

Flavins **1** and **2** were synthesized based on the procedure by Yoneda et al.[26]

4.2.2. Electrochemical Procedures

Cyclic voltammetry (CV) experiments were conducted with a computer-controlled Eco Chemie Autolab PGSTAT 100 with an ADC fast scan generator. The working electrode was a 1 mm diameter planar Pt or Glassy Carbon (GC) disk, used in conjunction with a silver wire (0.5 M Bu_4NPF_6 in CH_3CN) reference electrode. Accurate potentials were obtained using ferrocene as an internal standard. Solutions of riboflavin (1 mM, 0.5 M *n*-Bu_4NPF_6 in DMSO) for voltammetric analysis were deoxygenated by purging with high purity argon gas and all voltammetric experiments were conducted at 22 (±2) °C in a Faraday cage. Karl Fischer coulometric titrations indicated that the analyte solutions contained 100 mM of H_2O when they were added to the electrochemical cell.

Controlled potential electrolysis was performed in a two-compartment electrolysis cell using Pt mesh as the working and auxiliary electrodes and a silver wire as the reference electrode (separated from the working electrode compartment with a glass membrane containing a solution of 0.5 M *n*-Bu_4NPF_6 in CH_3CN).[27]

4.2.3 Spectroscopic Experiments

In situ electrochemical UV-vis spectra were obtained using an optically semi-transparent thin layer electrochemical (OSTLE) cell at 22 (±2) °C and recorded on a Perkin Elmer Model Lambda 750 UV-vis-NIR spectrophotometer.[27]

4.3. Results and Discussion

4.3.1 Cyclic voltammetry

Cyclic voltammograms of 1 mM flavin **1** were run at variable scan rates of 0.1 V s^{-1} to 20 V s^{-1} in DMSO with 0.2 M *n*-Bu_4NPF_6 at 22 (±2) ^{o}C (Figure 4.1), which are closely related in appearance to previous reports on riboflavin.[11,16,28–29] Similar experiments conducted in acetonitrile yielded comparable results (Figures A4.1 and A4.2 in appendix). Subsequent experiments focused on the use of DMSO as the solvent in order for a more accurate comparison with riboflavin results, as riboflavin is poorly soluble in most organic solvents. When the scan direction was reversed after the first reduction peak (wave 1), two oxidation peaks were observed (waves 2 and 3). When the scan direction was reversed after the second reduction peak (wave 5), the size of wave 3 increased with the corresponding decrease in the size of wave 2. As the scan rate was increased and the scan direction reversed just after wave 1, it was observed that the size of wave 2 increased and the size of wave 3 decreased (Figure 4.1).

The initial wave (wave 1) is a one-electron reduction of Fl to form $Fl^{\bullet-}$ (eq 1), followed by protonation by the N3H of another flavin molecule forming $FlH^{\bullet}$ (eq 2a), and the immediate further one-electron reduction to form FlH^{-} (eq 3). A comproportionation reaction between FlH^{-} and Fl^{-} occurs, forming 2 molecules of the anionic radical $Fl^{-\bullet}$ (eq 4). During the reverse scan, the oxidation peaks of both $Fl^{-\bullet}$ (wave 2) as well as FlH^{-}

(wave 3) are observed. When the scan rate is increased sufficiently to outrun the proton transfer reaction (eq 2a), only eq 1 is observed in the forward and reverse scans.[22]

When the scan direction is reversed after the second reduction peak, additional processes occur after the initial eqs 1, 2a, 3 and 4. At slow scan rates $Fl^{-\bullet}$, which was formed by eq 4, is reduced to the dianion Fl^{2-} (eq 5), which is then protonated by another Fl to form FlH^- and deprotonated Fl^- (eq 6a). During the reverse scan, the oxidation peaks of FlH^- as well as $Fl^{-\bullet}$ are observed. As the scan rate is increased sufficiently to outrun eq 2a, all the flavin is reduced to $Fl^{-\bullet}$ in the first reduction wave, and subsequently reduced to Fl^{2-} in the second reduction wave. Fl^{2-} is similarly protonated to form FlH^-. At faster scan rates FlH^- is subsequently oxidized during the reverse scan with little $Fl^{-\bullet}$ being present.[22]

$$Fl + e^- \rightleftharpoons Fl^{\bullet-} \quad (1)$$

$$Fl^{-\bullet} + Fl \rightleftharpoons FlH^{\bullet} + Fl^- \quad (2a)$$

$$FlH^{\bullet} + e^- \rightleftharpoons FlH^- \quad (3)$$

$$FlH^- + Fl^- \rightleftharpoons 2\ Fl^{-\bullet} \quad (4)$$

$$Fl^{-\bullet} + e^- \rightleftharpoons Fl^{2-} \quad (5)$$

$$Fl^{2-} + Fl \rightleftharpoons FlH^- + Fl^- \quad (6a)$$

Some notable differences in the cyclic voltammograms of flavin **1** and riboflavin are that wave 2 and wave 3 are more closely spaced for flavin **1** than in riboflavin. This causes wave 2 and wave 3 to be merged at a scan rate of 0.1 Vs^{-1}.

For riboflavin, when the potential was scanned past the second electron transfer step in order to produce the dianion, it was observed that wave 2 increased in size and wave 3 decreased in size as the scan rate increased.[22] However, for flavin **1**, it was observed that wave 2 decreased in size and wave 3 increased in size as the scan rate was increased (when the potential was extended to sufficiently negative potentials to produce the

dianion). Riboflavin is larger in size and likely undergoes stronger hydrogen-bonding interactions with DMSO (due to the hydroxyl groups), thus the decreased mobility makes it easier to outrun eq 6a as the scan rate increases. In contrast, flavin **1** has a smaller size, undergoes weaker interactions with DMSO and has increased mobility, and at 20 Vs^{-1}, eq 6a cannot be outrun. Instead, the products of eq 6a can also undergo a comproportionation reaction to form the anionic radical $Fl^{-\bullet}$ (eq 4), and it is this reaction that is outrun as the scan rate increases. Thus, as the scan rate increases, wave 2 decreases in size (less $Fl^{-\bullet}$) and wave 3 increases in size (more FlH^-).

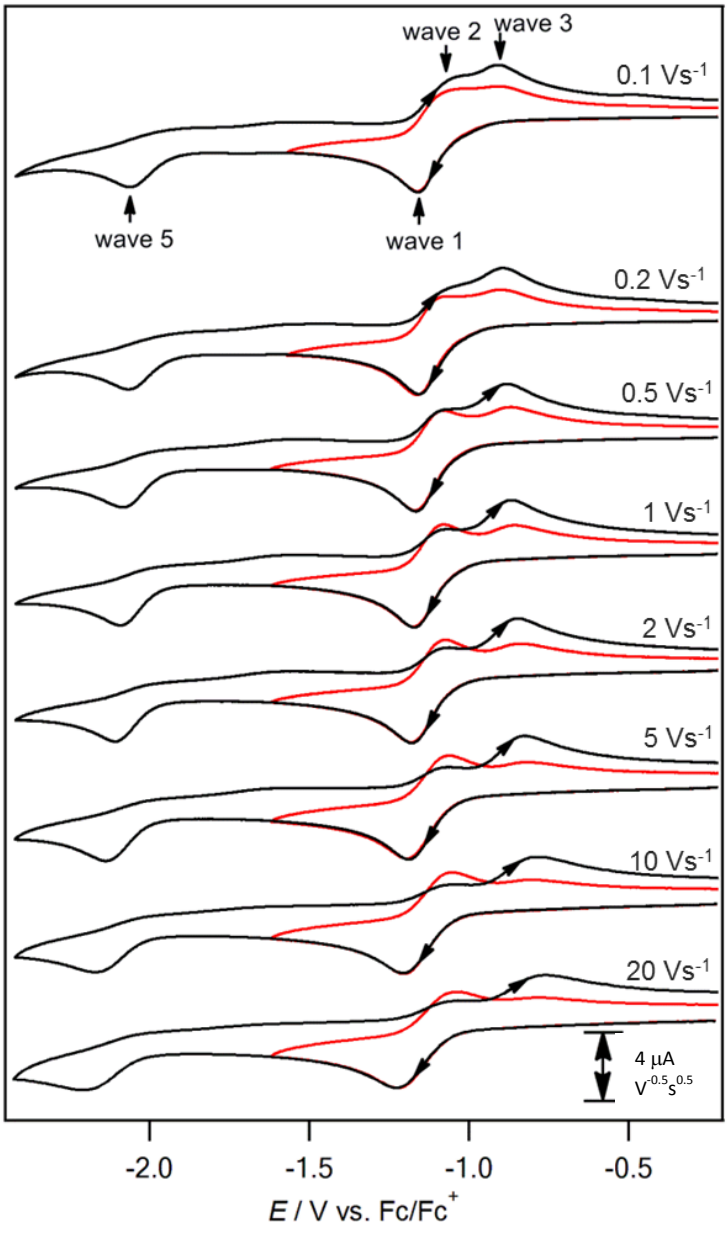

Figure 4.1. Variable scan rate cyclic voltammograms of the reduction of 1 mM flavin **1** at a 1 mm diameter planar Pt electrode in DMSO with 0.2 M *n*-Bu_4NPF_6 at 22 (±2) ^oC. The current data were scaled by multiplying by $\nu^{-0.5}$.

As previously reported, for the N3-methylated flavin such as flavin **2**, there is only one oxidation peak observed when the scan direction was reversed after the first reduction peak (Figure 4.2).

The N3-H of flavins acts as a proton donor to the radical anion, thus in the case of N3-methylated flavins, there is no proton source to protonate the radical anion to the neutral radical species. Therefore, after the N3-methylated flavin (Fl) is reduced by one-electron to form the radical anion $Fl^{-\bullet}$ (eq 1), no further chemical steps should take place, so that when the scan direction is reversed, the oxidation of $Fl^{-\bullet}$ back to Fl is observed.

However, it can be observed that if the scan direction is reversed after the second reduction peak of flavin **2**, waves 2 and 3 are detected during the reverse scan. In the second reduction process, $Fl^{-\bullet}$ is reduced by one-electron to form the dianion Fl^{2-} (eq 5). The appearance of wave 3 indicates that a suitable proton donor is available and the dianion Fl^{2-} is protonated to form FlH^- (eq 6b), which is then oxidized back to Fl in wave 3. Although no water was deliberately added to solution, the concentration of water naturally present in the DMSO solution as measured by Karl-Fischer titration was found to be to be approximately 100 mM, which is far greater than the concentration of flavin in solution (1 mM). The ratio of water molecules to analyte molecules increases the probability of water acting as a proton donor.

$$Fl^{2-} + H_2O \rightleftharpoons FlH^- + OH^- \qquad (6b)$$

It is interesting to note that at higher scan rates, the voltammograms of flavin **1** start to resemble that of flavin **2**. This supports the electron transfer mechanism for flavin **1**, as

when scan rate is sufficiently high to outrun the proton transfer reaction (eq 2a), the mechanistic pathway of flavin **1** will indeed be almost identical to that of flavin **2**. The only difference would be that the flavin **2** dianion would be protonated only by water, while the flavin **1** dianion could extract a proton from another flavin molecule. Also, the observation that wave 3 is larger at higher scan rates, indicates that the protonation reaction (eq 6b) occurs very quickly.

When the scan rates were increased and the potential was extended past the second reduction process, the size of wave 2 decreased while the size of wave 3 increased (for both flavins **1** and **2**) (Figures 4.1 and 4.2). It is postulated that at slow scan rates, as Fl^{2-} is being oxidized to $Fl^{-\bullet}$, FlH^- in solution has more time to convert back to Fl^{2-} via eq 6b (providing the equilibrium constant favors the back reaction), which would then be oxidized to $Fl^{-\bullet}$ (eq 5). This in turn would push the equilibrium of eq 5 towards the reactants, as long as the scan rate is slow enough for the reaction to occur. $Fl^{-\bullet}$ is then oxidized to Fl in wave 2, with little wave 3 observed. At fast scan rates, FlH^- has less time to equilibrate; FlH^- is then directly oxidized to Fl in wave 3, and wave 3 is correspondingly larger.

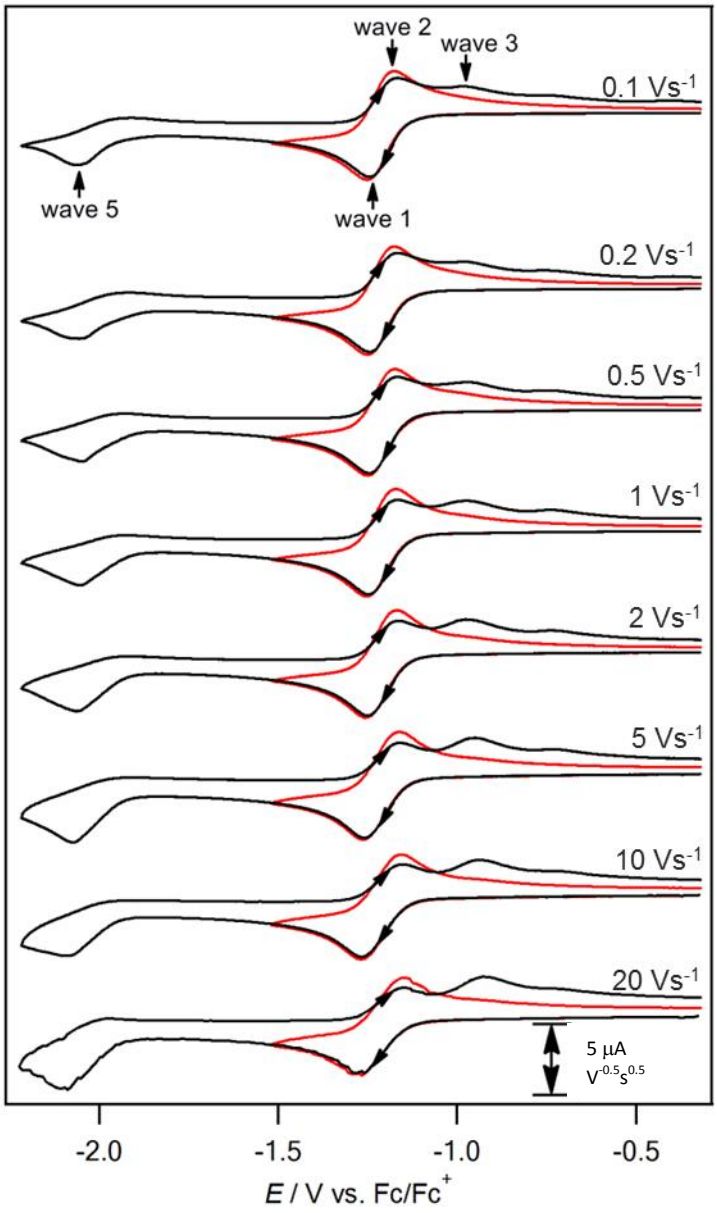

Figure 4.2. Variable scan rate cyclic voltammograms of the reduction of 1 mM flavin **2** at a 1 mm diameter planar Pt electrode in DMSO with 0.2 M *n*-Bu_4NPF_6 at 22 (±2) ^oC. The current data were scaled by multiplying by $\nu^{-0.5}$.

4.3.2 Effects of water on voltammetric processes of flavins

For FMN in unbuffered aqueous solutions at intermediate to high pH, where insufficient protons are available in solution, it was previously postulated that the dianion is able to form strong hydrogen bonding interactions with water molecules, before it is

subsequently protonated.[23] However, in unbuffered aqueous solutions, we were unable to prove that protonation did in fact occur due to the reduction of Fl to $Fl^{-\bullet}$ and the reduction of $Fl^{-\bullet}$ to Fl^{2-} having merged into one observable voltammetric wave, disallowing the observation of the oxidation of the FlH^- species if it was in fact formed. The rapid change in pH during electrolysis experiments in unbuffered aqueous solutions (solutions became very basic as protons are taken up from the bulk solution) also rendered any spectroelectrochemical experiments (e.g. UV-vis spectroscopy) unhelpful. Also, we were unable to ascertain whether the dianion extracted a proton from water or the N3-H of another flavin molecule, as it is impractical to physically eliminate either one of the possible proton sources. Therefore, the addition of water to solutions of flavin in aprotic organic solvents would not just be useful in understanding systems where trace water is present in a mostly hydrophobic environment, but would also provide insights regarding the processes in unbuffered aqueous solutions.

For the experiment of flavin **2** in DMSO (Figure 4.2), the only likely source of protons for the protonation of the dianion is the trace amount of water already present in the DMSO solution as flavin **2** is N3-methylated. In order to substantiate this hypothesis, additional water was progressively added to the solution, and cyclic voltammograms were recorded after each addition. Since water can also be reduced at the platinum working electrode, which caused the second reduction peak to be concealed, the following discussion relates to the first process.

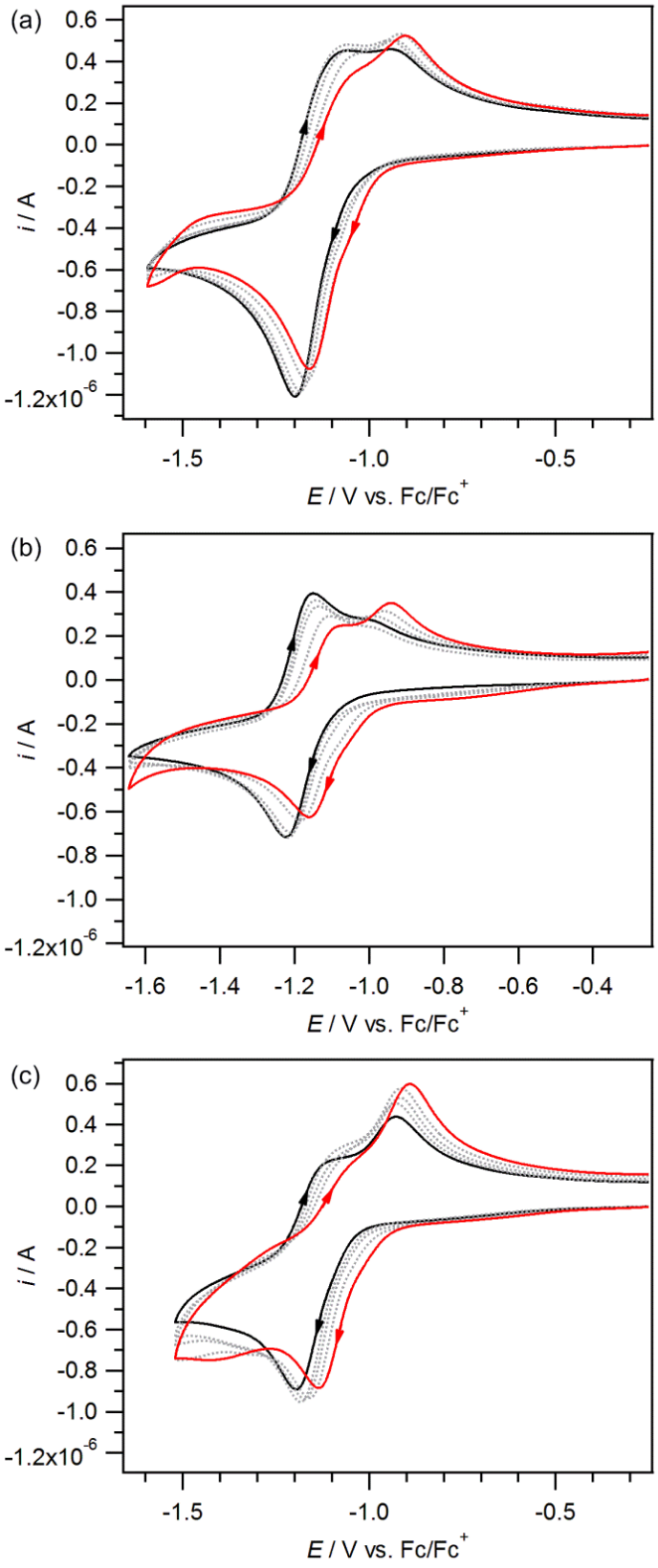

Figure 4.3. Cyclic voltammograms of the reduction of (a) 1 mM flavin **1**, (b) 1 mM flavin **2**, and (c) 1 mM riboflavin at a 1 mm diameter planar Pt electrode in DMSO with

0.2 M *n*-Bu_4NPF_6 at 22 (±2) ^oC, before addition of water, [H_2O] = 100 mM (black line) and after addition of 500μL of water, [H_2O] = 5 M (red line), at the scan rates of 0.1 Vs^{-1}.

Figure 4.3b shows the CVs obtained when relatively large amounts of water was added to the DMSO solution containing flavin **2**. A shift of the waves to less negative potentials can be interpreted as due to hydrogen bonding interactions, which is a phenomenon observed in the reduction of quinones in organic solvents as the water content is increased.[30–31] Another interesting observation was the change in the ratio of the oxidation peaks as more water was added to the solution. As water is added, wave 3 increases in size and wave 2 decreases in size. These results give further proof that water can indeed play a role in the electron transfer mechanism of flavins in aprotic organic solvents, either as a hydrogen-bond donor or a proton donor. After the initial electron transfer step (eq 1), $Fl^{\bullet-}$ reacts with water in an equilibrium reaction that strongly favors the reactants. However, with the addition of a large amount of water, the equilibrium was shifted towards the products based on Le Chatelier's principle. This effect is more prominent for Fl^{2-} than for $Fl^{-\bullet}$, as the former is more basic and thus more able to take a proton from water, even without the deliberate addition of water to solution. Nevertheless, $Fl^{-\bullet}$ could still be protonated by water if sufficient water is present (eq 2b).

$$Fl^{-\bullet} + H_2O \rightleftharpoons FlH^{\bullet} + OH^{-} \qquad (2b)$$

A similar increase in height of wave 3 and decrease in height of wave 2 was observed for flavin **1** (Figure 4.3a) and riboflavin (Figure 4.3c), indicating that even when a stronger proton donor is available, water still plays a role in the electron transfer mechanism. Eq 2a and 2b are expected to occur simultaneously during the reduction of flavin **1**, with eq 2b insignificant in solutions of low water concentrations, and increasing in importance as the concentration of water is increased.

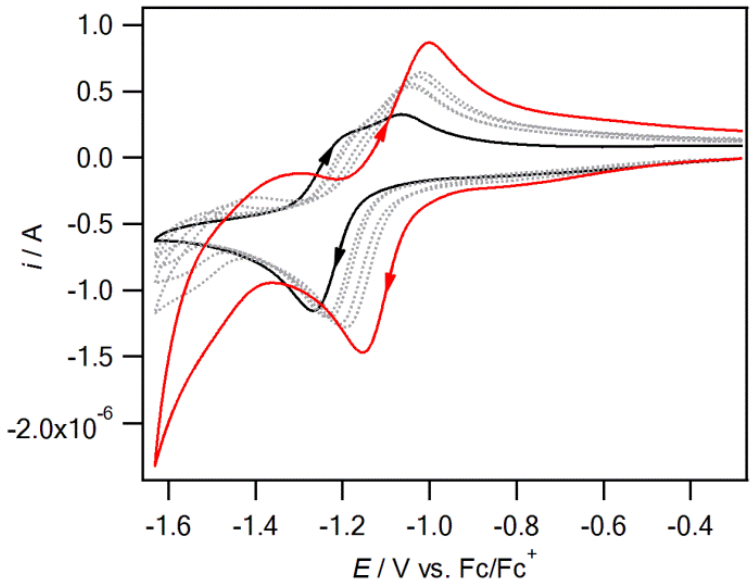

Figure 4.4. Cyclic voltammograms of the reduction of 1 mM flavin **1** at a 1 mm diameter planar Pt electrode in acetonitrile with 0.2 M *n*-Bu_4NPF_6 at 22 (±2) ^oC, before addition of water, [H_2O] = 50 mM (black line) and after addition of 100μL of water, [H_2O] = 1 M (red line), at the scan rates of 0.1 Vs^{-1}.

When the solvent used for electrochemistry was changed to acetonitrile instead of DMSO, a significantly lesser amount of water was required to observe a change in the ratio of oxidative peaks for flavin **1**, and even the complete disappearance of wave 2 (Figure 4.4). This difference is expected, as water itself undergoes stronger hydrogen-bonding interactions with DMSO than acetonitrile, and thus more water is required to affect any changes in the reaction.[30]

4.3.3 Electrolysis Experiments

Bulk electrolysis of 1 mM of flavin **1**, flavin **2** and riboflavin were carried out in DMSO.

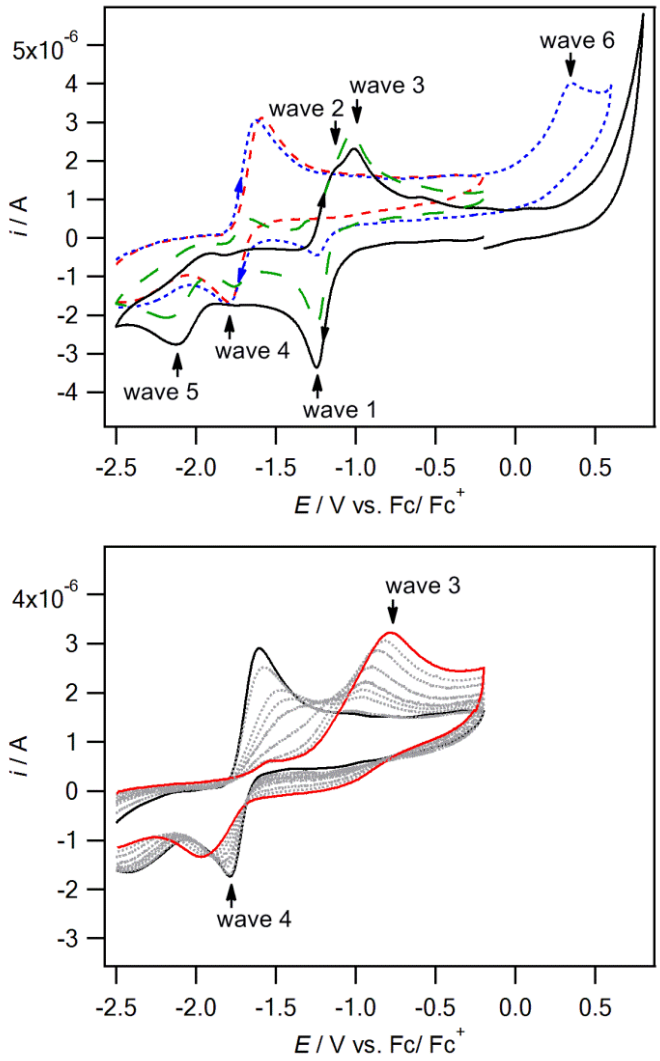

Figure 4.5. Voltammetric data obtained at 22 (±2) ^{o}C during the controlled potential electrolysis of 1 mM flavin **1** in DMSO with 0.2 M *n*-Bu_4NPF_6. (*a*) Cyclic voltammograms recorded at a scan rate of 0.1 V s^{-1} with a 1 mm diameter planar Pt electrode: (Black line) before the bulk reduction of flavin **1**; (Green dashed line) after the exhaustive 1 electron reduction of flavin **1**; (Blue dotted line) after the exhaustive 2 electron reduction of flavin **1** when the scan direction was reversed at 1 V; (Red dashed line) after the exhaustive 2 electron reduction of flavin **1** when the scan direction was

reversed at 0.3 V. (*b*) Variable scan rate cyclic voltammograms from 0.1 V s^{-1} (black line) to 20 V s^{-1} (red line), of flavin **1** after 2 e^- bulk reduction. The current data were scaled by multiplying by $\nu^{-0.5}$.

Flavin **1**, which has the N3-H moiety the same as riboflavin, was expected to undergo reductive electrolysis via a similar mechanism. After 1 e^- was transferred per molecule of flavin **1** (a potential of -1.4 V vs. Fc/Fc^+ was applied), a mixture of Fl^- and FlH^- was present in solution, as well as some $Fl^{\bullet-}$ due to a comproportionation reaction between Fl^- and FlH^- (eq 4) (Figure 4.5a, green dashed line). In order to investigate the major products formed after $2e^-$ reduction, the application of -2.15 V vs. Fc/Fc^+ allowed a second e^- to be transferred per molecule of flavin **1**. From the voltammograms obtained after $2e^-$ reduction (Figure 4.5a, red dashed line), an oxidation wave is detected at ~ -1.7 V vs. Fc/Fc^+, which likely corresponds to the oxidation of $Fl^{2-\bullet}$ to Fl^- (eq 7). When the scan direction was reversed, the corresponding reduction wave of Fl^- is detected, with no wave 1 observed.

It is also observed that a new chemically irreversible oxidation wave is observed at ~ 0.8V, and when the scan direction is reversed, wave 1 was once again observed in the voltammogram. This indicates that the new oxidation wave is associated with the conversion of the fully reduced species back to the fully-oxidized flavin (Fl). It is proposed that this additional oxidation wave corresponds to the oxidation of FlH_2 to Fl, as it occurs around the same potential as when a hydroquinone is reduced to a quinone (where there is also a very wide potential separation between the forward and reverse processes in the absence of acid).

It can be postulated that when the second electron was transferred, $Fl^{-\bullet}$ was reduced to Fl^{2-} (eq 5), which could be protonated to form FlH^- (eq 6b). It is likely that the flavin exists mainly in the state of FlH^- after $2e^-$ reduction. (Further evidence can also be

observed from the *in situ* electrochemical UV-vis experiments (Figure 4.8), as discussed in the next section.) At fast scan rates, FlH^- is oxidized to Fl in wave 3, and Fl is deprotonated by FlH^- to form FlH_2 and Fl^- (which is reduced in wave 4 in the reverse scan) via eq 10, and almost no wave 1 in the reverse scan (indicating no Fl, as Fl has been deprotonated), if the scan direction was reversed prior to wave 6. If the scan direction was reversed after wave 6, and at fast scan rates, FlH^- is oxidized to Fl in wave 3, and Fl is deprotonated by FlH^- to form FlH_2 (which gets oxidized in wave 6) and Fl^- (which is reduced in wave 4 in the reverse scan) via eq 10, and since FlH_2 has been oxidized back to Fl in wave 6 via eq 13, wave 1 would once again be observed in the reverse scan.

At relatively slow scan rates, FlH^- is converted to Fl^{2-} via eq 6a or 6b as Fl^{2-} is oxidized to $Fl^{-\bullet}$, and the oxidation wave 2 can be observed to appear. At even slower scan rates, $Fl^{-\bullet}$ would have sufficient time and subsequently gets deprotonated to form $Fl^{2-\bullet}$ (the reverse of eq 11 or 12), which is oxidized in wave 4 (the reverse of eq 7). Importantly, all the reactions are completely chemically reversible on the electrolysis timescale such that the starting material can be regenerated from the reduced products by the application of 1 V *vs.* Fc/Fc^+ (Figure A4.3 – A4.5 in appendix).

$$Fl^- + e^- \rightleftharpoons Fl^{2-\bullet} \quad (7)$$

$$Fl^- + \text{"}H^+\text{"} \rightleftharpoons Fl \quad (8)$$

$$Fl^{2-\bullet} + \text{"}H^+\text{"} \rightleftharpoons Fl^{-\bullet} \quad (9)$$

$$FlH^- + Fl \rightleftharpoons FlH_2 + Fl^- \quad (10)$$

$$Fl^{2-\bullet} + H_2O \rightleftharpoons Fl^{-\bullet} + OH^- \quad (11)$$

$$Fl^{2-\bullet} + FlH^- \rightleftharpoons Fl^{-\bullet} + Fl^{2-} \quad (12)$$

$$FlH_2 \rightleftharpoons Fl + 2H^+ + 2e^- \quad (13)$$

Flavin **2**, which has N3-Me instead of an N3-H, is expected to behave differently from flavin **1** as well as riboflavin. After exhaustive 1e$^-$ reduction, the voltammogram showed only wave 2 in the oxidative scan, which corresponds to the oxidation of $Fl^{-\bullet}$ to Fl (eq 1) (Figure 4.6a, blue dotted line). The application of a potential of -2 V *vs.* Fc/Fc^+ allowed a second e$^-$ to be transferred per molecule of flavin, reducing the $Fl^{-\bullet}$ in solution to Fl^{2-} (eq 2). An equilibrium reaction occurs, with Fl^{2-} extracting a proton from surrounding water molecules (eq 6b), thus a mixture of Fl^{2-} and FlH^- is present in solution. Indeed, a small amount of wave 3 was detected at the completion of the electrolysis, corresponding to the oxidation of FlH^- to Fl, as shown in the voltammogram in Figure 4.6a (red dashed line). The remaining Fl^{2-} would then be oxidized to $Fl^{-\bullet}$ (eq 5), and further reduced to Fl (eq 1) in wave 2. When variable scan rate cyclic voltammetry was performed after bulk 2 e$^-$ electrolysis of flavin **2**, two different oxidation waves were observed at different scan rates, indicative of an equilibrium reaction occurring (Figure 4.6b). At slow scan rates, wave 2 was observed, where the anionic radical $Fl^{-\bullet}$ was oxidized back to Fl. When the scan rate was increased, the size of wave 2 decreased while the size of wave 3 increased until at a scan rate of 20 V s^{-1}, only wave 3 was detected, associated with oxidation of FlH^-. At slow scan rates, as Fl^{2-} is being oxidized to $Fl^{-\bullet}$, the depletion of Fl^{2-} causes the equilibrium reaction (eq 6b) to shift towards Fl^{2-}, forming more $Fl^{-\bullet}$, thus the size of wave 2 will predominate at slow scan rates. As the scan rate is increased, as Fl^{2-} is being oxidized to $Fl^{-\bullet}$, insufficient time is available for the equilibrium to shift towards Fl^{2-}, and the majority of the flavin will remain in solution as FlH^-, which is oxidized in wave 3 back to Fl. It is interesting to note that unlike flavin 1, wave 1 was observed in the reverse scan, indicating that Fl is present in this case. This is because eq 10 cannot occur due to the lack of an N(3) proton to act as a proton source for FlH^- (in the bulk solution), and since eq 10 cannot occur, Fl will remain present during the reverse scan to once again be reduced in wave 1.

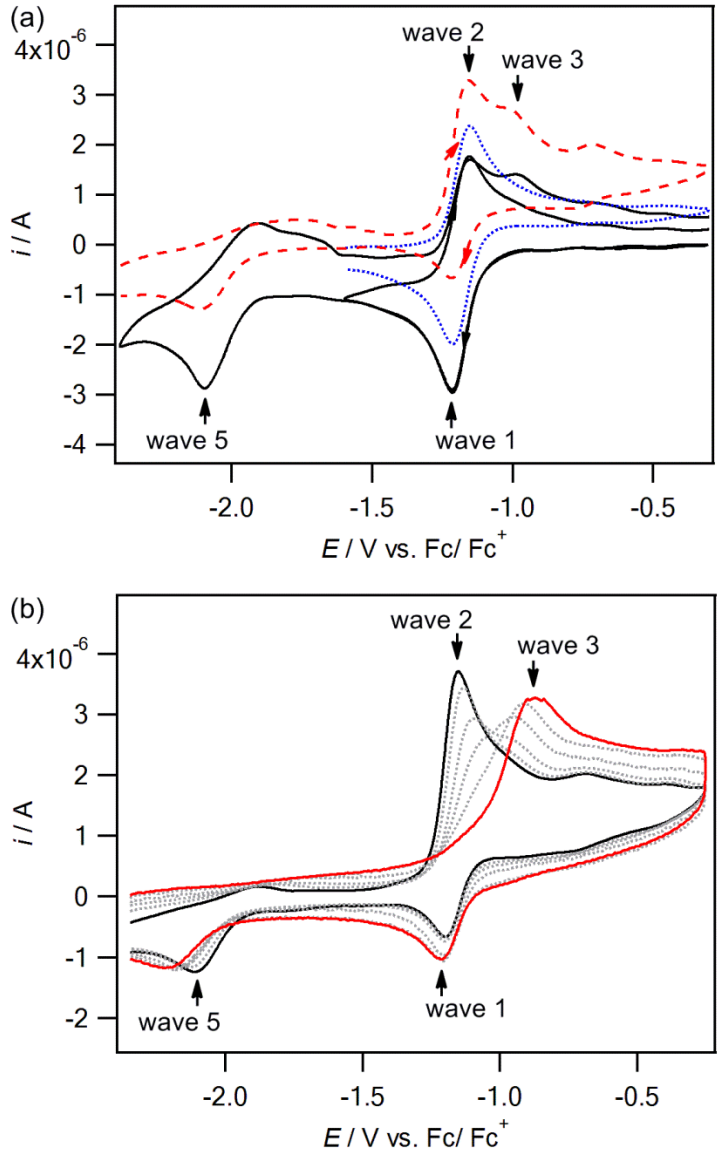

Figure 4.6. Voltammetric data obtained at 22 (±2) °C during the controlled potential electrolysis of 1 mM flavin **2** in DMSO with 0.2 M *n*-Bu_4NPF_6. (*a*) Cyclic voltammograms recorded at a scan rate of 0.1 V s^{-1} with a 1 mm diameter planar Pt electrode: (Black line) before the bulk reduction of flavin **2**; (Blue dotted line) after the exhaustive 1 electron reduction of flavin **2**; (Red dashed line) after the exhaustive 2 electron reduction of flavin **2**. (*b*) Variable scan rate cyclic voltammograms from 0.1 V s^{-1} (black line) to 20 V s^{-1} (red line), of flavin **2** after 2 e^- bulk reduction. The current data were scaled by multiplying by $\nu^{-0.5}$.

For riboflavin, we obtained a similar result as flavin **1**, including the additional oxidation wave at ~1.0 V which reforms Fl and the appearance of reduction wave 1 in the reverse scan. This additional oxidation wave likely corresponds to the oxidation of FlH_2 to Fl (Figure 4.7).

One significant difference between the electrolysis results of flavin **1** and that of riboflavin is that the wave associated with oxidation of $Fl^{2-\bullet}$ is barely detected for reduced riboflavin. (Figure 4.5b and Figure A4.6 in appendix) This could be due to differences in the mobility between riboflavin and flavin **1**, causing a difference in the composition of species present in solution. The conversion from FlH^- to Fl^{2-} is slower, and thus the majority of the species remain as FlH^- even at slow scan rates.

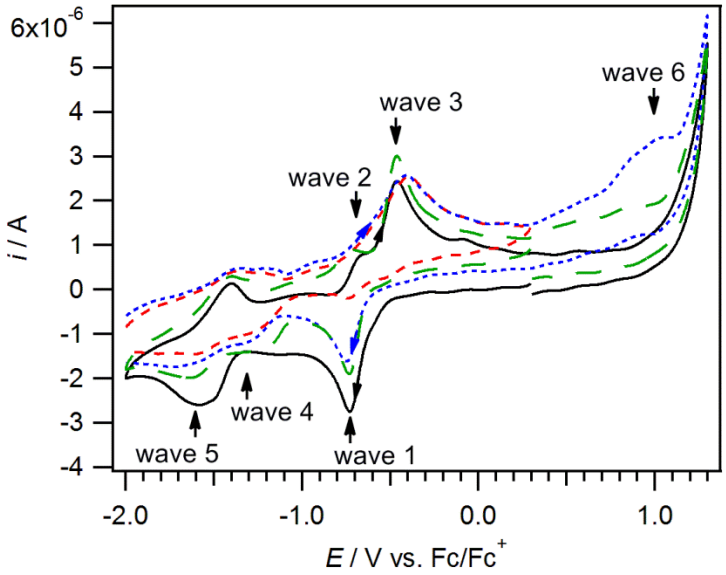

Figure 4.7. Cyclic voltammograms obtained during the controlled potential electrolysis of 1 mM riboflavin in DMSO with 0.2 M *n*-Bu_4NPF_6, recorded at a scan rate of 0.1 V s^{-1} with a 1 mm diameter planar Pt electrode at 22 (±2) ^oC: (Black line) before the bulk reduction of riboflavin; (Green dashed line) after the exhaustive 1 electron reduction of riboflavin; (Blue dotted line) after the exhaustive 2 electron reduction of riboflavin when the scan direction was reversed at 1.3 V; (Red dashed line) after the

exhaustive 2 electron reduction of riboflavin when the scan direction was reversed at 0.3 V.

4.3.4 In situ electrochemical UV-vis Experiments

In situ electrochemical UV-vis spectra of flavins **1** and **2** were collected before, during and after electrolysis (Figure 4.8).

Before electrolysis, peaks of the fully oxidized flavin were observed at ~340 and 430 nm. After 1 e^- reduction, some differences between the UV-vis spectra of reduced flavins **1** and **2** were observed. A peak appeared at ~375 nm for both flavins, however the size of the peak was dramatically larger for flavin **2** as compared to flavin **1**. This difference is not surprising, as the peak at 375 nm is indicative of the flavin anion radical ($Fl^{-\bullet}$).[32–33] For flavin **2**, all of the flavin is reduced to $Fl^{-\bullet}$ in a simple 1 e^- reduction (eq 1). However, for flavin **1**, Fl is reduced to $Fl^{-\bullet}$ (eq 1), which is protonated by Fl to form $FlH^{\bullet}$ (eq 2a), which is then further reduced to FlH^- (eq 3). The $Fl^{-\bullet}$ present after 1e^- bulk reduction is due to a comproportionation reaction between FlH^- and the deprotonated fully oxidized flavin Fl^- (eq 4), and the amount of $Fl^{-\bullet}$ formed is considerably less than for flavin **2**. The 1 e^- reduction product could be completely converted back to fully oxidized flavin upon oxidation for both flavin **1** and **2**.

When a potential more negative than the second reduction peak was applied, the reduction reaction first progressed via the 1 e^- reduction product and later further reduced to the 2 e^- reduction product. The UV-vis spectra of the 2 e^- reduction product for flavins **1** and **2** were strikingly similar and it can be concluded that after 2 e^- reduction, flavins **1** and **2** exist as the same species (FlH^- and Fl^{2-}). The 2 e^- reduction product could also be completely converted back to fully oxidized flavin upon oxidation, despite the apparent complexity of the voltammograms shown in Figures 4.5 – 4.7. This indicates that both the

1 e^- reduction product and the 2 e^- reduction product are stable for the duration of the experiment in deoxygenated conditions (at least one hour).

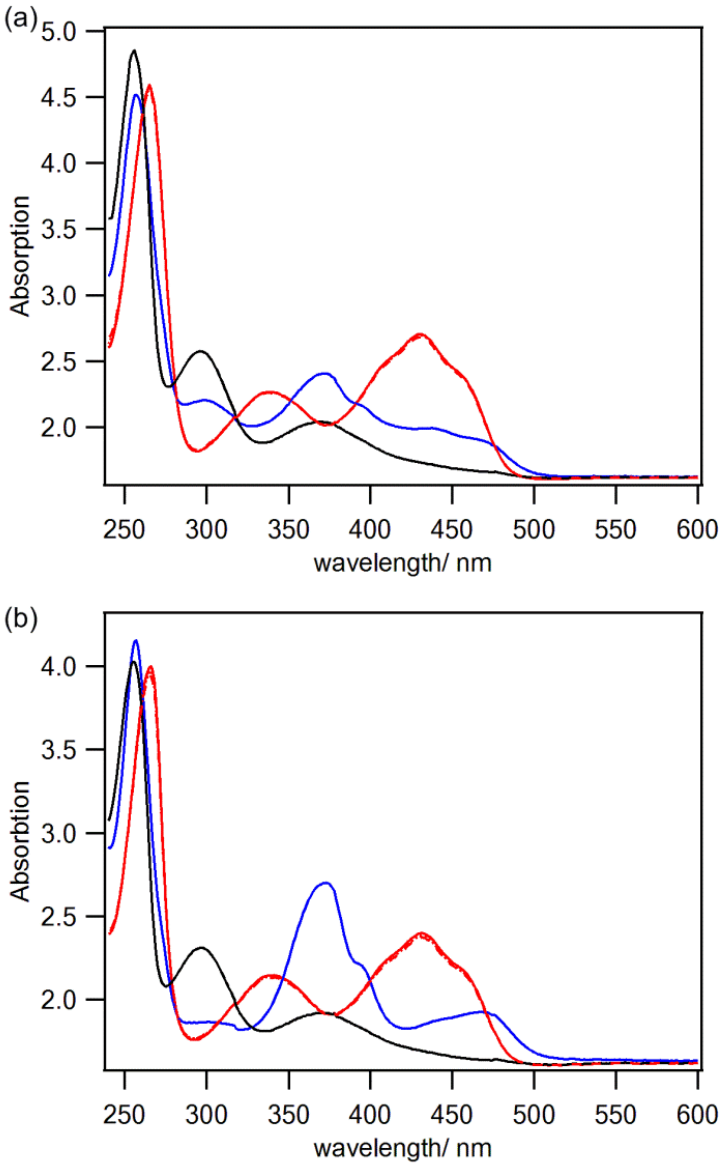

Figure 4.8. *In situ* electrochemical UV-vis spectra of (a) 1 mM flavin **1** and (b) 1 mM flavin **2** in DMSO containing 0.2 M *n*-Bu_4NPF_6, before bulk reduction (red line), after the flavin has been reduced by 1 electron (blue line), after the 1 electron reoxidation (red dotted line), after the flavin has been reduced by 2 electrons (black line) and after the 2 electron reoxidation back to the starting state (red dashed line).

4.3.5 Electron Transfer mechanisms

Based on the electrochemical and in situ spectroscopic experiments performed, two different mechanisms for flavin **1** which has an N3H group, and flavin **2** which has an N3Me group can be deduced.

For flavin **1**, the mechanism is very similar to that of riboflavin, as riboflavin also has an N3H group. For cyclic voltammetry at slow scan rates, a fully-oxidized flavin is reduced by 1 electron to the anionic radical $Fl^{-\bullet}$ (eq 1), which extracts a proton from another fully-oxidized flavin to form the neutral radical $FlH^{\bullet}$ and the deprotonated fully-oxidized flavin Fl^{-} (eq 2a and 8). As the reduction potential of $FlH^{\bullet}$ is less negative than that of the fully oxidized flavin, $FlH^{\bullet}$ is immediately reduced to FlH^{-} (eq 3). FlH^{-} then undergoes a comproportionation reaction with the deprotonated Fl^{-} to form 2 molecules of the anionic radical $Fl^{-\bullet}$ (eq 4). Upon reversal of the scan direction, the oxidation peaks of both $Fl^{-\bullet}$ (wave 2) and FlH^{-} (wave 3) are observed due the equilibrium reaction. When the voltammogram was scanned to more negative potentials before reversal of scan direction, two additional reduction waves are detected; a small wave 4 which corresponds to the reduction of Fl^{-} (eq 7), and a large wave 5 which corresponds to the reduction of the anionic radical $Fl^{-\bullet}$ to the dianion Fl^{2-} (eq 5). The dianion Fl^{2-} is then protonated to FlH^{-} (eq 6a), presumably by another flavin molecule (but if the water content is high then it can also act as a proton donor in competition with the flavin). Comproportionation could once again occur if the proton was extracted from another flavin molecule, as long as the scan rate is slow enough for it to occur. Upon reversal of scan direction, the oxidation peaks of both $Fl^{-\bullet}$ (wave 2) and FlH^{-} (wave 3) are observed.

As the scan rate is increased sufficiently to outrun the protonation reaction (eq 2a), the mechanism becomes similar to that of flavin **2.** A fully-oxidized flavin is reduced by 1 electron to the anionic radical $Fl^{-\bullet}$ (eq 1), and upon reversal of scan direction, the

oxidation of $Fl^{-\bullet}$ back to Fl is observed. When the voltammogram was scanned to more negative potentials, $Fl^{-\bullet}$ was then reduced to the dianion Fl^{2-} (eq 5), which is protonated by another molecule of Fl to FlH^- (eq 6a) while forming the deprotonated Fl^-. The resultant species FlH^- and Fl^- undergo comproportionation with each other to form 2 molecules of $Fl^{-\bullet}$ (eq 4). Upon scan reversal, as the scan rate increases, wave 3 becomes larger (more FlH^- available for oxidation) and wave 2 becomes smaller (less $Fl^{-\bullet}$ available for oxidation) as the forward reaction of eq 4 is outrun.

For riboflavin, it is eq 6a that is outrun as the scan rate increases, so an increase in wave 2 (more $Fl^{-\bullet}$ available for oxidation) and a decrease in wave 3 (less FlH^- available for oxidation) is observed.

Controlled potential electrolysis also gave insights on the mechanism of flavin **1** after bulk 2 e^- reduction. A new oxidative wave (wave 6) was detected at 0.8 V vs. Fc/Fc^+, and the application of a potential slightly more positive resulted in the regeneration of the starting material. It is believed that after 2 e^- reduction, a portion of the flavin is converted to FlH_2, which is oxidized back to Fl in wave 6. Upon reversal of scan direction, Fl is once again reduced to $Fl^{-\bullet}$/ FlH^- in wave 1. The same oxidative wave at 0.8 V is also observed after the bulk 2 electron reduction of riboflavin. Although FlH_2 could be formed by protonation of FlH^-, it is more likely that disproportionation of FlH^- is taking place; this wave is only observed after bulk electrolysis and not during cyclic voltammetry.

Scheme 4.2. Voltammetrically induced proton-coupled electron transfer reduction mechanism of flavins with an N3-H moiety such as riboflavin and flavin **1**, in aprotic organic solvents, studied by variable scan rate cyclic voltammetry and controlled potential electrolysis.[a]

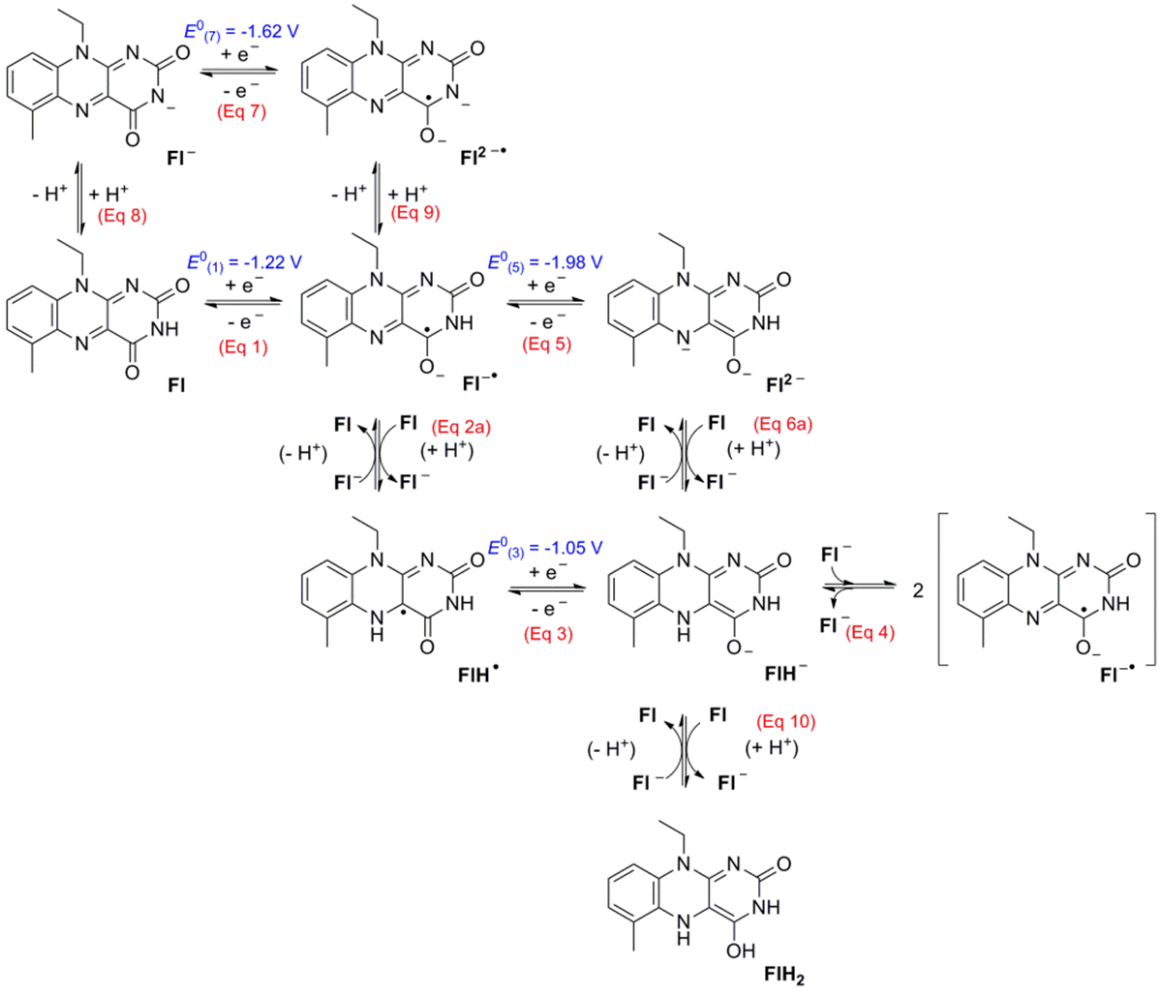

[a] Electrochemical values reported are based on riboflavin.

Scheme 4.3. Voltammetrically induced proton-coupled electron transfer reduction mechanism of flavin **2** in aprotic organic solvents, studied by variable scan rate cyclic voltammetry and controlled potential electrolysis.

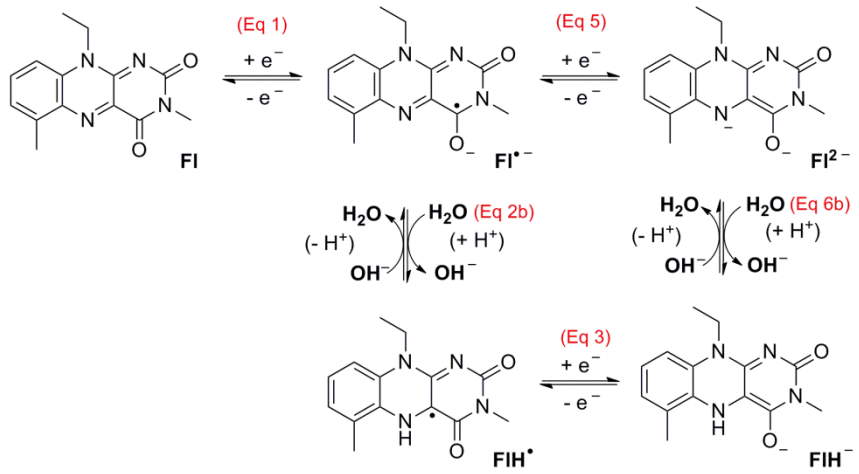

Flavin **2** undergoes a comparatively simpler mechanism, but despite the fact that flavin **2** is unable to donate a proton to its anionic radical $Fl^{-\bullet}$, it is still able to form FlH^- as long as a suitable proton donor (such as trace water in organic solvents or a substrate in a flavoprotein) is present.

When the scan direction was reversed after the first reduction wave (wave 1), the reduction of Fl to $Fl^{-\bullet}$ is detected in wave 1, and the corresponding oxidation wave in the reverse scan. No difference in the wave shape is detected when scan rate is increased, other than an increased peak-to-peak separation (due to resistance effects), as any chemical reaction occurring is negligible.

When the potential was applied up to the second electron transfer step, the reduction of Fl to $Fl^{-\bullet}$ is detected in wave 1, and the reduction of $Fl^{-\bullet}$ to Fl^{2-} in wave 5. Fl^{2-} then takes a proton from a surrounding water molecule to form FlH^- in an equilibrium reaction (eq 6b). When the scan rate is slow, as Fl^{2-} is reduced back to $Fl^{-\bullet}$ on the reverse scan, the equilibrium (eq 6b) is pushed towards Fl^{2-}, which can be also reduced to $Fl^{-\bullet}$. As the scan

rate is increased, less time is available for the equilibrium to be pushed towards Fl^{2-}, and FlH^- is the main reduced species present, and is thus oxidized in wave 3. This trend shows that eq 6b occurs quickly to form FlH^-, and is the reason why more FlH^- is seen at high scan rates. If eq 6b occurs sufficiently slowly such that it could be outrun, a larger wave 2 and smaller wave 3 at fast scan rates would be observed.

A similar effect was noticed when running variable scan rate cyclic voltammetry after the 2 e^- per molecule bulk electrolysis of flavin molecule, where it is similarly believed that the major species formed was FlH^-, in equilibrium with Fl^{2-}. Only when an applied potential is used to oxidize Fl^{2-} back to the anionic radical $Fl^{-\bullet}$, does the equilibrium shift towards Fl^{2-}, forming a larger wave 2 and smaller wave 3 at slow scan rates, as well as a smaller wave 2 and larger wave 3 at fast scan rates.

The formation of FlH_2 after the bulk 2 e^- per molecule electrolysis of flavin **2** was not significant as it was for flavin **1** or riboflavin, which indicates the possible involvement of the N3-H in the formation of the fully reduced FlH_2.

4.3.6 Relevance of electrochemical results to flavoproteins and further applications

These results have shown that even for N3 methylated flavins, or flavins in flavoproteins that have a strong hydrogen bonding on N3-H, they are able to undergo reactions similar to N3-protonated flavins such as riboflavin, as long as a suitable proton donor is available. Flavoproteins which contain more than one flavin cofactor, such as hepatic NADPH-cytochrome P-450 reductase and Na^+-pumping NADH-ubiquinone oxidoreductase[34–35] could undergo the more complicated reactions as depicted in Scheme 4.2. Flavoproteins which have the flavin cofactor accessible by water are expected to undergo reactions via Scheme 4.3 or via the schemes depicted in chapter 3, depending on the pH of the solution and its buffering capacity.

A more detailed understanding of the electrochemistry of flavins could also contribute to the improvement of man-made systems, where redox chemistry has been applied in synthetic methods, molecular shuttles,[36] logic gates,[37] switches[38] and wires.[39] Flavins are also potential molecules for electron-transporting devices such as organic solar cells, organic field effect transistors as well as organic light-emitting diodes, due to their electron-deficient nature and reversible electrochemistry.[40–41] As we continue to better understand flavin electrochemistry in various media, it would be desirable to be able to modify the redox, optical and electronic properties of flavins as required.

4.4. Conclusion

A comparison of variable scan rate cyclic voltammograms of flavin **1** and **2** provided insights into the similarities and differences between the electron transfer mechanism of the two flavins. For flavin **1**, when the scan was reversed after the first reduction wave, Fl was reduced to $Fl^{-\bullet}$ and protonated by the N3-H of another flavin molecule, followed by reduction and comproportionation forming a mixture of Fl^{-}, FlH^{-} and $Fl^{-\bullet}$. As the scan rate is increased, the protonation is outrun and the mechanism becomes similar to that of flavin **2**, which is the reversible reduction of Fl to $Fl^{-\bullet}$. If the scan was reversed after the second reduction wave, FlH^{-} was observed for both flavins **1** and **2**. FlH^{-} is formed by the protonation of Fl^{2-}, although the proton sources were different. For flavin **1**, the dianion is protonated by another Fl molecule, forming FlH^{-} and Fl^{-}, which undergo comproportionation with each other to form $Fl^{-\bullet}$. For flavin **2**, the dianion extracts a proton from the trace water found in the organic solvent. Variable scan rate cyclic voltammetry indicates that the protonation reaction occurs quickly and forms FlH^{-} to a large extent.

The ability of water to donate a proton to flavin was investigated by adding increasing amounts of water to a flavin solution, and analyzing the resultant cyclic voltammograms. It was observed that when a sufficient amount of water was added, even the anionic radical $Fl^{-\bullet}$ could be protonated to form $FlH^{\bullet}$.

In-situ electrochemical UV-vis spectroscopy and controlled potential electrolysis demonstrated that the 1 e^- reduced species and 2 e^- reduced species for all flavins were stable on the time scale of the experiment (> 1 h), and gave further confirmation of the comproportionation reaction occurring for flavin **1**. It was also observed that the 2 e^- reduced species for flavins **1** and **2** had a similar UV-vis spectrum and is likely to be mainly due to FlH^-. Variable scan rate experiments performed on fully reduced solutions of flavins indicated that the several species existed in a complex chemical equilibrium. Despite the equilibrium reactions, the starting materials could be completed regenerated by the application of an oxidizing potential indicated that the reduced species were long-lived (for at least several hours) in DMSO solution.

4.5. References

1. Lienhart, W.-D.; Gudipati, V.; Macheroux, P. *Arch. Biochem. Biophys.* **2013**, *535*, 150–162.

2. Guengerich, F. P.; Munro, A. W. *J. Biol. Chem.* **2013**, *288*, 17065–17073.

3. Mansoorabadi, S. O.; Thibodeaux, C. J.; Liu, H-W. *J. Org. Chem.* **2007**, *72*, 6329–6342.

4. Medina, M. *FEBS J.* **2009**, *276*, 3942–3958.

5. Dijkman, W. P.; de Gonzalo, G.; Mattevi, A.; Fraaije, M. W. *Appl. Microbiol. Biotechnol.* **2013**, *97*, 5177–5188.

6. Iyanagi, T.; Watanabe, S.; Anan, K. F. *Biochemistry*, **1984**, *23*, 1418–1425.

7. Walsh, *C. Acc. Chem. Res.* **1980**, *13*, 148–155.

8. Ghisla, S; Massey, V. *Eur. J. Biochem.* **1989**, *181*, 1–17.

9. Bruice, T. C. *Isr. J. Chem.*, **1984**, *24*, 54-61.

10. Mueller, F. In *Topics in Current Chemistry*; Boschke, F. L., Ed.; Springer-Verlag: Berlin, 1983; Vol. 108, pp 71–108.

11. Niemz, A.; Imbriglio, J.; Rotello, V. M. *J. Am. Chem. Soc.* **1997**, *119*, 887–892.

12. Massey, V.; Hemmerich, P. *Biochem. Soc. Trans.* **1980**, *8*, 246–257.

13. Heering, H. A.; Hagen, W. R. *J. Electroanal. Chem.* **1996**, *404*, 249–260.

14. Paulsen, K. E.; Stankovich, M. T.; Stockman, B. J.; Markley, J. L. *Arch. Biochem. Biophys.* **1990**, *280*, 68–73.

15. Iyanagi, T. Redox Properties of microsomal reduced nicotinamide adenine dinucleotide-cytochrome b_5 reductase and cytochrome b_5. *Biochemistry* **1977**, *16*, 2725–2730.

16. Nishida, H.; Inaka, K.; Yamanaka, M.; Kaida, S.; Kobayashi, K.; Miki, K. *Biochemistry*, **1995**, *34*, 2763–2767.

17. Nandwana, V.; Samuel, I.; Cooke, G.; Rotello, V. M. *Acc. Chem. Res.* **2013**, *46*, 1000–1009.

18. Burkhart, B. M.; Ramakrishnan, B.; Yan, H.; Reedstorm, R. J.; Markley, J. L.; Straus, N. A.; Sundaralingam, M. *Acta. Cryst. Section D*, **1995**, *51*, 318–330.

19. Correll, C. C.; Batie, C. J.; Ballou, D. P.; Ludwig, M. L. *Science*, **1992**, *258*, 1604–1610.

20. Bruns, C. M.; Karplus, P. A. *J. Mol. Biol.* **1995**, *247*, 125–145.

21. Nascimento, A. S.; Catalano-Dupuy, D. L.; Bernardes, A.; Neto, M. O.; Santos, M. A. M.; Ceccarelli, E. A.; Polikarpov, I. *BMC Struct. Biol.* **2007**, *7*, 69–80.

22. Tan, S. L. J.; Webster, R. D. *J. Am. Chem. Soc.* **2012**, *134*, 5954–5964.

23. Tan, S. L. J.; Kan, J. M.; Webster, R. D. *J. Phys. Chem. B* **2013**, *117*, 13755–13766.

24. Quan, M.; Sanchez, D.; Wasylkiw, M. F.; Smith, D. K. *J. Am. Chem. Soc.* **2007**, *129*, 12847–12856.

25. Lim, Z. H.; Chng, E. L. K.; Hui, Y.; Webster, R. D. *J. Phys. Chem. B* **2013**, *117*, 2396–2402.

26. Akiyama, T.; Simeno, F.; Murakami, M.; Yoneda, F. *J. Am. Chem. Soc.* **1992**, *114*, 6613–6620.

27. Williams, L. L.; Webster, R. D. *J. Am. Chem. Soc.* **2004**, *126*, 12441–12450.

28. Tatwawadi, S. V.; Santhanam, K. S. V.; Bard, A. J. *J. Electroanal. Chem.* **1968**, *17*, 411–420.

29. Sawyer, D. T.; McCreery, R. L. *Inorg. Chem.* **1972**, *11*, 779–782.

30. Hui, Y.; Chng, E. L. K.; Chng, C. Y. L.; Poh, H. L.; Webster, R. D. *J. Am. Chem. Soc.* **2009**, *131*, 1523–1534.

31. Tessensohn, M. E.; Hirao, H.; Webster, R. D. *J. Phys. Chem. C* **2013**, *117*, 1081–1090.

32. Massey, V.; Palmer, G. *Biochemistry*, **1966**, *5*, 3181–3189.

33. Dudley, K. H.; Ehrenberg, A.; Hemmerich, P.; Mueller, F. *Helv. Chim. Acta* **1964**, *47*, 1354–1383.

34. Barquera, B.; Morgan, J. E.; Lukoyanov, D.; Scholes, C. P.; Gennis, R. B.; Nilges, M. J. *J. Am. Chem. Soc.* **2003**, *125*, 265–275.

35. Barquera. B.; Ramirez-Silva, L.; Morgan, J. E.; Nilges, M. J. *J. Biol. Chem.* **2006**, *281*, 36482–36491.

36. Fioravanti, G.; Haraszkiewicz, N.; Kay, E. R.; Mendoza, S. M.; Bruno, C.; Marcaccio, M.; Wiering, P. G.; Paolucci, F.; Rudolf, P.; Brouwer, A. M.; Leigh, D. A. *J. Am. Chem. Soc.* **2008**, *130*, 2593–2601.

37. de Silva, A. P.; McClenaghan, N. D. *Chem. Eur. J.* **2004**, *10*, 574–586.

38. Richmond, C. J.; Parenty, A. D. C.; Song, Y. F.; Cooke, G.; Cronin, L. *J. Am. Chem. Soc.* **2008**, *130*, 13059–13065.

39. Cruz, A. V. B.; Mishra, A. K.; Schmickler, W. *Chem. Phys.* **2010**, *371*, 10–15.

40. Toogood, H. S.; Leys, D.; Scrutton, N. S. *FEBS J.* **2007**, *274*, 5481–5504.

41. Legrand, Y. M.; Gray, M.; Cooke, G.; Rotello, V. M. *J. Am. Chem. Soc.* **2003**, *125*, 15789–15795.

Chapter 5

Summary/ Conclusions

The electrochemical behaviour of flavins have often been considered analogous to quinones over the past few decades, as they behave similarly in buffered aqueous solutions and are both able to form a long-lived radical anion. Hence, flavin electrochemical terminology has been based on quinones, with its radicals (neutral and anionic) commonly referred to as semiquinones, and the fully-reduced flavin species referred to as hydroquinones. However, in this thesis, we have shown using electrochemical methods that, in non-aqueous aprotic media, flavin chemistry can be much more complex than quinone chemistry due to the reactivity of the N5 on the flavin isoalloxazine ring. Further investigation has also led to the understanding of flavin chemistry in intermediate systems, which will be more apt in modelling biological flavin systems, where the flavin is bound by a protein.

As discussed in chapter 2, electrochemical studies were conducted on riboflavin (vitamin B_2) in DMSO, an aprotic organic solvent, in order to examine the electrochemical behavior of flavins in non-aqueous media, especially at potentials more negative than the first reduction wave (wave 1). At varying concentrations of riboflavin, two additional reduction waves were observed at –1.6 V (wave 4) and –2.0 V (wave 5) vs. Fc/Fc^{+}. The first reduction wave (wave 1) was shown to be a proton-coupled electron transfer reaction, where Fl is reduced to $Fl^{\bullet -}$ (E step), which becomes protonated by the imide proton of another flavin molecule to form $FlH^{\bullet}$ (C step), which then is further reduced by another electron to form FlH^{-} (E step). Variable scan rate cyclic voltammetry enabled the understanding of the kinetics of the reactions occurring as during the reduction of Fl, as it

is observed that the protonation of $Fl^{\bullet-}$ to $FlH^{\bullet}$ would not occur if the time scale of the scan was too short (at fast scan rates). Wave 5 was significant only at high scan rates, and was shown to be the reduction of $Fl^{\bullet-}$ to the dianion Fl^{2-}. Cyclic voltammetry of Fl^{-} (Fl deprotonated by a strong base) allowed the assignment of wave 4 to the reduction of deprotonated oxidized flavin. Electrolysis experiments held in conjunction with cyclic voltammetry, UV-vis and EPR spectroscopy, showed that the anionic radical was formed due to the comproportionation of FlH^{-} and Fl^{-}, and not by direct reduction of Fl. Digital simulations of all voltammetric data allowed for the kinetic and electrochemical parameters of all chemical and electrochemical steps involved.

In biological systems, while protein-bound flavins are unlikely to take a proton from other flavin molecules, they almost always form FlH^{-} during the reductive half reaction, which was also the species formed voltammetrically during wave 1. FlH^{-} is formed in flavoproteins by direct (H^{-}) or indirect (e^{-}, H^{+}, e^{-}) hydride transfer to the reactive flavin N5, while in the present studies, this species is formed via proton-coupled electron transfer reactions (e^{-}, H^{+}, e^{-}). Comproportionation between 2 flavin species forms the anionic radical, and the reduction mechanism becomes more complicated than is often observed for flavins in biological systems. However, with the recent discoveries of exceptions to common flavoprotein mechanisms, extra care should be taken when considering flavoprotein mechanisms. Comproportionation reactions cannot be ruled out for flavoproteins that contain more than one flavin cofactor, such as the diflavin reductases where FAD and FMN are known to transfer electrons between them, and Na^{+}-pumping NADH-ubiquinone oxidoreductase. In particular, the presence of the anionic radical in the fully-reduced flavoproteins, as observed for Na^{+}-pumping NADH-ubiquinone oxidoreductase, could be an indication of the comproportionation observed in this study.

In biological systems, intermolecular interactions with the flavin cofactor could lead to stabilization of either flavin radical as reduction potentials are affected. The system described in chapter 2 would most resemble Class 1 flavoproteins (ignoring comproportionation), as both do not show thermodynamic stabilization of either radical.

In chapter 3, the electrochemically-induced reduction mechanism of FMN in buffered aqueous solutions was reexamined. At pH 3 – 5, UV-vis spectroscopy of the bulk reduced flavin showed that $FMNH_2$ was formed, while $FMNH^-$ was the main reduced species at pH 7 – 11, as was expected due to the pK_a of the fully-reduced flavin. Cyclic voltammetry data at slow scan rates, agreed with previous studies that a reversible $+2e^-/2H^+$ reduction was observed in one voltammetric wave at low pH, while a $+2e^-/H^+$ reduction was observed at high pH. However, at high pH and high scan rates, the oxidative wave appeared to split into two separate waves, assigned to the reduction of $FMNH^-$ and the hydrogen-bonded dianion $FMN^{2-}(H_2O)_x$, where the two species are likely to exist in equilibrium.

The electrochemical reduction of FMN and FAD in unbuffered aqueous solutions was also discussed in chapter 3, where 3 reduction waves were observed at different pH ranges. Rotating disk electrode voltammetry indicated all 3 reduction waves corresponded to 2 e^- reductions. At extremely low pH values (where the exact pH value is dependent on the concentration of flavin), a reversible $+2e^-/2H^+$ reduction was observed in one voltammetric wave (wave 1), similar to the reaction in buffered solutions. However, at higher pH values, insufficient free protons in solution led to a 2 e^- reduction to the dianion Fl^{2-} (wave 2), likely to be stabilized by hydrogen-bonding interactions with water. The proposed existence of the hydrogen-bonded flavin dianion was based on a comparison of the voltammetry of quinones, where the dianion is known to exist in a non-protonated form in aqueous media in the absence of acid and in organic solutions in the

presence and absence of water. While we expected that the dianion would deprotonate water or the flavin N3 to form FlH^-, this could not be experimentally proven as electrolysis was not possible for unbuffered solutions if the pH of the solution is required to be constant throughout the experiment. Thus, spectroscopic methods such as UV-vis would not yield accurate results. Cyclic voltammetry would also prove unhelpful in differentiating the reduction of Fl^{2-} and FlH^- as their reduction potentials were too similar to observe a clear separation between peaks, made more complicated with wave 1 and 3 appearing in the same voltammogram. As the phosphate group/s at the flavin side chain undergoes a deprotonation to form a dianion, wave 3 is observed, also corresponding to a direct 2 e^- reduction. It was postulated that the highly negatively charged side chain interacts with the flavin isoalloxazine ring, making the reduction potential of the (side-chain) deprotonated species more negative (harder to reduce). There have been similar considerations regarding whether this dianion species will be protonated and what was the source of the protons. While two separate oxidation waves were observed at high pH and high scan rates, it could not be considered a definite proof, due to the possibility that the extra oxidation wave was in fact wave 2.

While certain aspects of the electrochemical reduction mechanism were not conclusive, there was sufficient data to show that the mechanism in unbuffered aqueous media was an intermediate of that the mechanisms in buffered aqueous media and non-aqueous aprotic media. While buffered aqueous media had free protons available for protonation, this is often not the case in biological systems, where the flavin is likely to abstract a proton from a substrate or nearby residue. Also, in this chapter, in aqueous solutions with little free protons, the reduction of flavin could occur directly by 2 e^- to the dianion. When the flavin binding site of the protein is freely accessible by solvent molecules, this possible mechanism should not be overlooked.

In chapter 4, the electrochemical reduction of two synthesized flavins (N3-protonated vs. N3-methylated) in aprotic organic media was discussed. Without a suitable proton source, the reductive scan (cyclic voltammetry) of N3-methylated flavin was similar to that of quinones, and the reduction of Fl to the anionic radical was observed to be completely reversible when the scan direction was reversed after wave 1. When the scan direction was reversed after the second reduction peak, a surprising observation was made: some of the dianion has been protonated to FlH^-, despite the fact that the imide proton at N3 was not present for this synthesized flavin. This indicated that the dianion was basic enough to deprotonate trace water in solution. N3-protonated flavin had its dianion protonated to a larger extent than N3-methylated flavin at all scan rates, which was an expected observation as there are two possible proton sources (water and the flavin itself). Bulk reduction of 2 e^- per flavin molecule was performed for both synthesized flavins, and variable scan rate cyclic voltammetry of the reduced solution showed complex equilibrium reactions occurring in both solutions after bulk reduction. While voltammetric waves have not been observed at positive potentials for oxidized flavins, the cyclic voltammogram of the fully-reduced N3-protonated flavin showed the appearance of a new irreversible oxidation wave at ~ +0.4 V *vs.* Fc/Fc^+ (wave 6), and the appearance of wave 1 during the reverse scan. When the scan direction was switched at lower (less positive) potentials than wave 6, wave 1 was also not observed. This result indicated that the species being oxidized in wave 6 would form Fl, the fully-oxidized flavin. The same experiment conducted with riboflavin (N3-protonated) showed similar results, but wave 6 was not observed for the N3-methylated flavin. It was postulated that wave 6 corresponds to the oxidation of the fully-reduced FlH_2 back to Fl, and the imide proton on the flavin N3 plays a role in the formation of FlH_2 in this system.

In chapter 4, water was deliberately added to solutions of both flavins as well as riboflavin in DMSO, and significant hydrogen-bonding interactions were observed, with a similar shift of wave 1 and wave 5 towards less negative potentials, a phenomena that has also been observed in quinones. The hydrogen-bonding interactions stabilize the reduced species, with the most negatively-charged species having the largest degree of stabilization by hydrogen-bonding interactions. However, unlike in flavins bound in flavoproteins which have specific directed hydrogen bonds, the hydrogen-bonding interactions in this system are not specific and could occur at N1, O2, N3-H, O4 and N5, and do not especially stabilize either radical. Thus, the shift in potentials for wave 2 and 3 are approximately equal. While this system is not sufficiently complex to model some flavoproteins (class 2 and 4), results are able to illustrate the effects of hydrogen bonding and show significant thermodynamic stabilization of reduced flavins.

It was also observed that with added water, wave 2 decreased in size concomitantly with the increase in size of wave 3, indicating that with sufficient water in solution, the radical anion of both flavins can be protonated by water at the reactive N5 position to some extent. In this system, where water is deliberately added to aprotic organic media, the electrochemical reduction mechanism is the intermediate between that in pure organic media and unbuffered aqueous solutions. Although the dianion is stabilized by hydrogen-bonding interactions, the stabilization is not enough for Fl to be directly reduced to Fl^{2-}, and an ECE mechanism is favoured. For flavoproteins where no thermodynamic stabilization of either radical have been observed, but with a suitable proton donor nearby (including bound or free water molecules), a similar ECE mechanism is theoretically possible in place of the commonly-observed hydride transfer. For example, in flavodoxins (class 5) which catalyze one-electron transfers, hydride transfer does not occur. Instead, electron transfer is followed by protonation, forming the neutral radical $FlH^{\bullet}$. In this case,

the neutral radical is not reduced as the π-stacking interactions in flavodoxin shifted its reduction potential to more negative potentials.

The results discussed in chapter 4, and particularly the observation of the flavin dianion being protonated to FlH^- by trace water in a largely hydrophobic and aprotic media, provided sufficient proof that the flavin dianion would be protonated in unbuffered aqueous solutions as well, answering some doubts from chapter 3. In comparison, for unbuffered aqueous solutions, hydrogen bonding interactions with the dianion is significant enough such that a direct 2 e^- reduction is observed in a single voltammetric wave via an EE mechanism. As FMN and FAD are both N3-protonated, both the imide proton and water are likely proton sources for the protonation of the dianion. However, in biological systems (excluding multi-flavin proteins), water (or a nearby residue with a suitable pK_a value) is a more likely source. For flavoproteins where the flavin binding site is freely accessible by solvent molecules, and no thermodynamic stabilization of either radical has been observed, an EEC mechanism, where the flavin is first reduced by 2 e^- to the dianion, followed by protonation by water or another suitable proton donor is theoretically possible if hydride attack does not occur.

In conclusion, in this thesis, the electrochemically-induced reduction mechanisms of flavins in different environments have been discussed, bridging the mechanistic gap between aprotic organic media and buffered aqueous media, ranging from the most hydrophobic aprotic organic media, to aprotic organic media with deliberately-added water, to unbuffered aqueous solutions with little free protons, and finally to buffered aqueous solutions where free protons that are used up can be easily regenerated by the buffer solution.

Publications

1. Tan, S. L. J.; Webster, R. D. Electrochemically Induced Chemically Reversible Proton-Couple Electron Transfer Mechanisms of Riboflavin (Vitamin B_2). *J. Am. Chem. Soc.* **2012**, *134*, 5954–5964.

2. Tan, S. L. J.; Kan, J. M.; Webster, R. D. Differences in Proton-Coupled Electron Transfer Reactions of Flavin Mononucleotide (FMN) and Flavin Adenine Dinucleotide (FAD) between Buffered and Unbuffered Aqueous Solutions. *J. Phys. Chem. B,* **2013**, *117*, 13755–13766.

Appendix

List of Equations – Chapter 2

$$Fl + e^- \rightleftharpoons Fl^{\bullet -} \quad (1)$$

$$Fl^{\bullet -} + DH \rightleftharpoons FlH^{\bullet} + D^- \quad (2)$$

$$FlH^{\bullet} + e^- \rightleftharpoons FlH^- \quad (3)$$

$$Fl^{\bullet -} + FlH^{\bullet} \rightleftharpoons FlH^- + Fl \quad (4)$$

$$Fl^{\bullet -} + Fl \rightleftharpoons FlH^{\bullet} + Fl^- \quad (5)$$

$$Fl^{\bullet -} + e^- \rightleftharpoons Fl^{2-} \quad (6)$$

$$Fl^{2-} + Fl \rightleftharpoons FlH^- + Fl^- \quad (7)$$

$$Fl^- + e^- \rightleftharpoons Fl^{2-\bullet} \quad (8)$$

$$FlH^- + Fl^- \rightleftharpoons 2\ Fl^{\bullet -} \quad (9)$$

$$Fl^{2-\bullet} + Fl \rightleftharpoons Fl^{\bullet -} + Fl^- \quad (10)$$

List of Equations – Chapter 3

$(FMN)H^- + e^- \rightleftharpoons (FMN^{\bullet -})H^-$ (1)

$(FMN^{\bullet -})H^- + e^- \rightleftharpoons (FMN^{2-})H^-$ (2)

$(FMNH^{\bullet})H^- + e^- \rightleftharpoons (FMNH^-)H^-$ (3)

$(FMN)^{2-} + e^- \rightleftharpoons (FMN^{-\bullet})^{2-}$ (4)

$(FMN^{-\bullet})^{2-} + e^- \rightleftharpoons (FMN^{2-})^{2-}$ (5)

$(FMN^-)^{2-} + e^- \rightleftharpoons (FMN^{2-\bullet})^{2-}$ (6)

$(FMN^{2-\bullet})^{2-} + e^- \rightleftharpoons (FMN^{3-})^{2-}$ (7)

$(FMN^{\bullet -})H^- + H^+ \rightleftharpoons (FMNH^{\bullet})H^-$ (8)

$(FMNH^-)H^- + H^+ \rightleftharpoons (FMNH_2)H^-$ (9)

$(FMN)H^- \rightleftharpoons (FMN)^{2-} + H^+$ (10)

$H_2O \rightleftharpoons H^+ + OH^-$ (11)

List of Equations – Chapter 4

$Fl + e^- \rightleftharpoons Fl^{\bullet -}$ (1)

$Fl^{-\bullet} + Fl \rightleftharpoons FlH^{\bullet} + Fl^-$ (2a)

$Fl^{-\bullet} + H_2O \rightleftharpoons FlH^{\bullet} + OH^-$ (2b)

$FlH^{\bullet} + e^- \rightleftharpoons FlH^-$ (3)

$FlH^- + Fl^- \rightleftharpoons 2\ Fl^{-\bullet}$ (4)

$Fl^{-\bullet} + e^- \rightleftharpoons Fl^{2-}$ (5)

$Fl^{2-} + Fl \rightleftharpoons FlH^- + Fl^-$ (6a)

$Fl^{2-} + H_2O \rightleftharpoons FlH^- + OH^-$ (6b)

$Fl^- + e^- \rightleftharpoons Fl^{2-\bullet}$ (7)

$Fl^- + "H^+" \rightleftharpoons Fl$ (8)

$Fl^{2-\bullet} + "H^+" \rightleftharpoons Fl^{-\bullet}$ (9)

$FlH^- + Fl \rightleftharpoons FlH_2 + Fl^-$ (10)

$Fl^{2-\bullet} + H_2O \rightleftharpoons Fl^{-\bullet} + OH^-$ (11)

$Fl^{2-\bullet} + FlH^- \rightleftharpoons Fl^{-\bullet} + Fl^{2-}$ (12)

$FlH_2 \rightleftharpoons Fl + 2H^+ + 2e^-$ (13)

Chapter 2

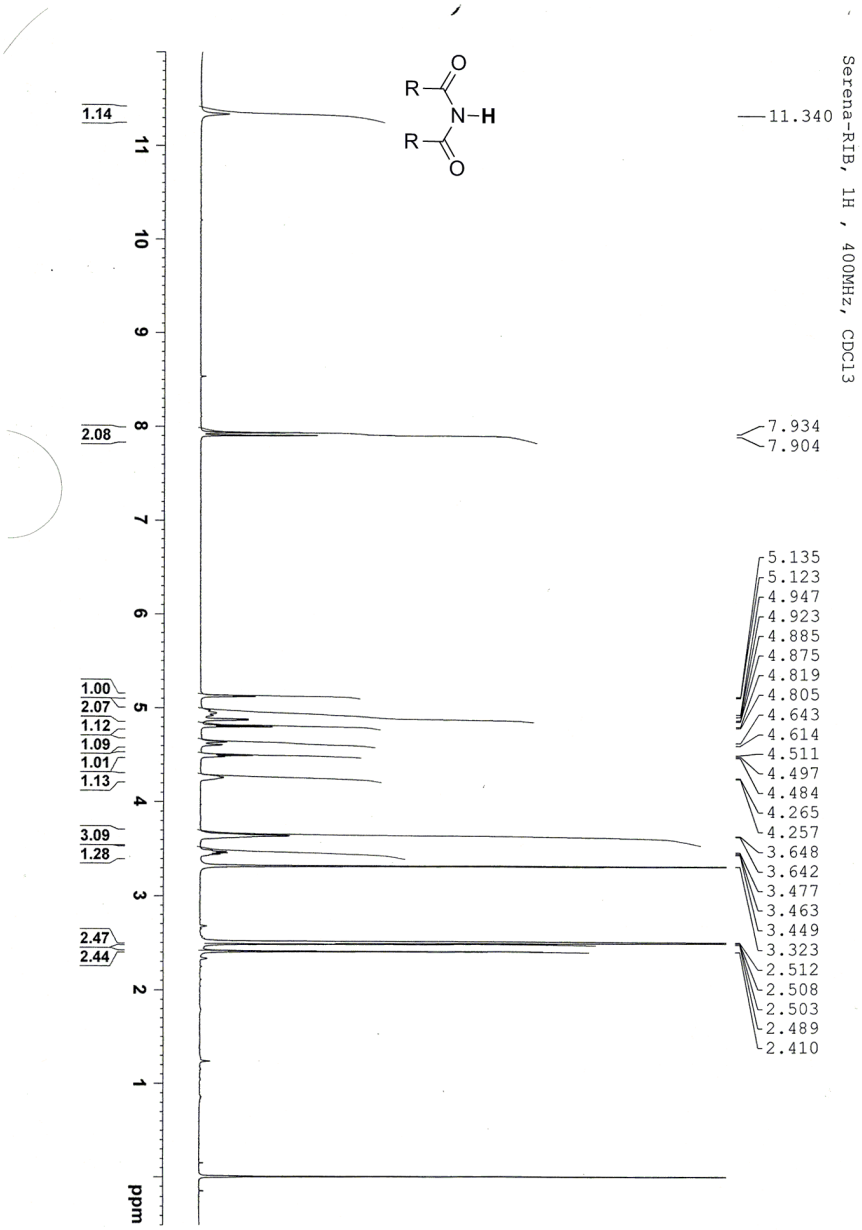

Figure A2.1. 400 MHz ^{1}H NMR spectrum of DMSO-d_6 using a The imide proton is observed at 11.34 ppm, the aromatic protons are at 7.92 ppm, the methyl groups are observed at 3.64 ppm and 2.41 ppm, the protons of the side chain including the O-**H** protons are observed in the range from 2.50 ppm to 5.14 ppm. The large peak at 2.51 ppm belongs to DMSO, while the large peak at 3.32 ppm belongs to residual water.

Chapter 3

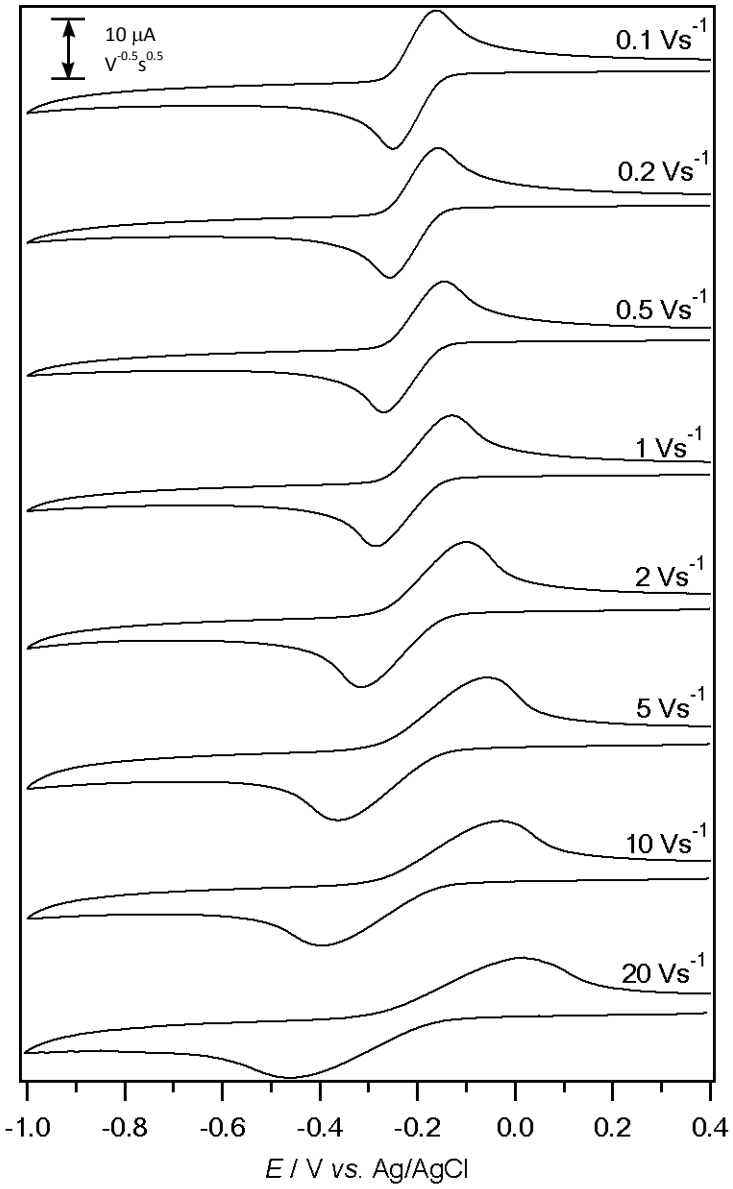

Figure A3.1. Variable scan rate cyclic voltammograms of 1 mM FMN in a buffered aqueous solution of pH 3, recorded at a 1 mm GC electrode at 22 (±2). The current data were scaled by multiplying by $\nu^{-0.5}$.

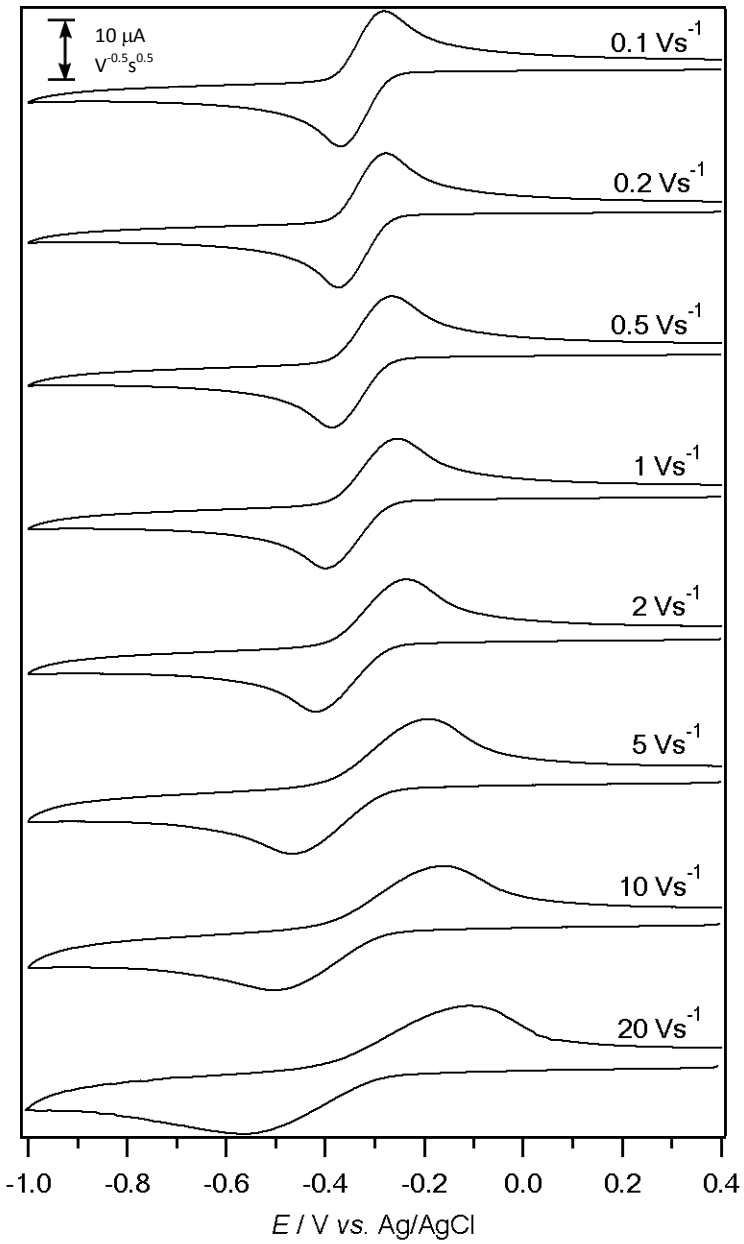

Figure A3.2. Variable scan rate cyclic voltammograms of 1 mM FMN in a buffered aqueous solution of pH 5, recorded at a 1 mm GC electrode at 22 (±2). The current data were scaled by multiplying by $\nu^{-0.5}$.

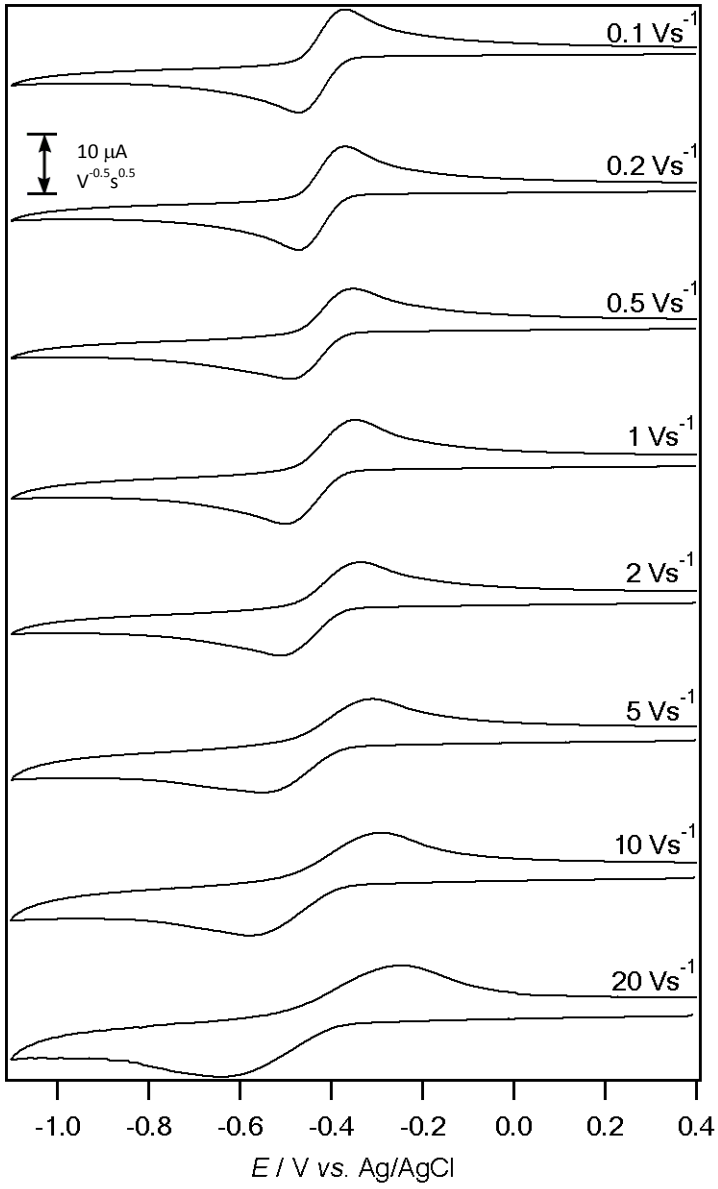

Figure A3.3. Variable scan rate cyclic voltammograms of 1 mM FMN in a buffered aqueous solution of pH 7, recorded at a 1 mm GC electrode at 22 (±2). The current data were scaled by multiplying by $\nu^{-0.5}$.

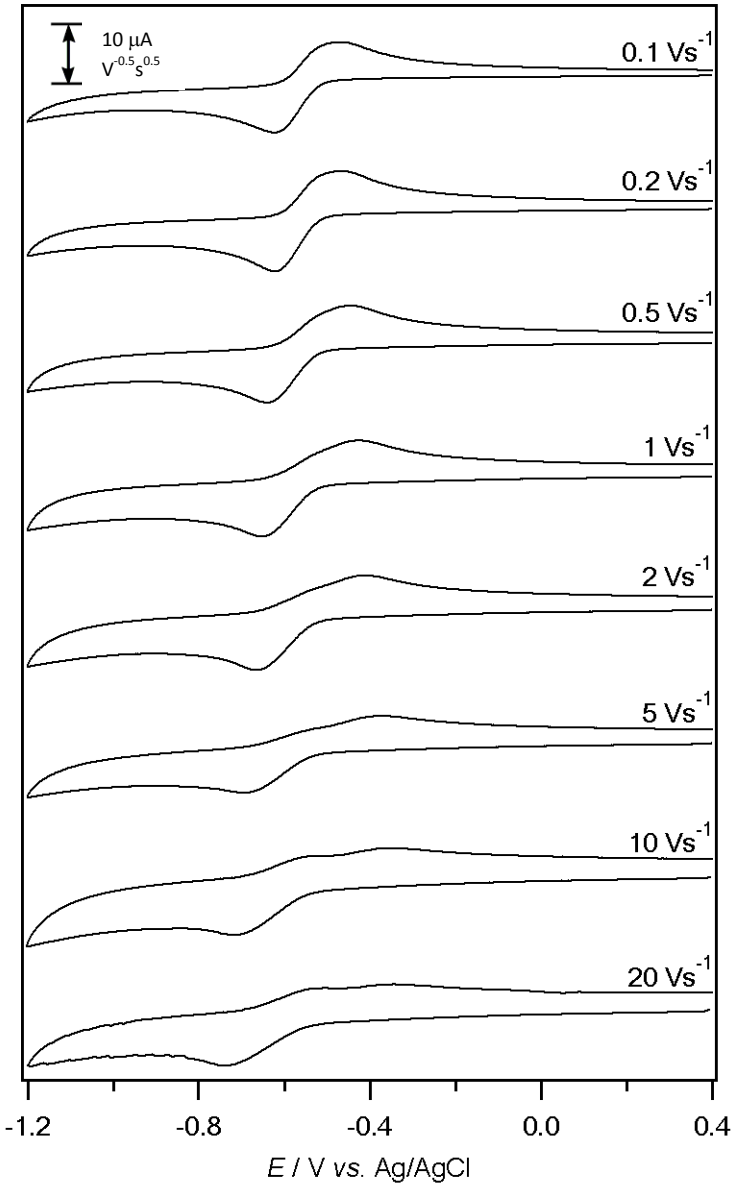

Figure A3.4. Variable scan rate cyclic voltammograms of 1 mM FMN in a buffered aqueous solution of pH 11, recorded at a 1 mm GC electrode at 22 (±2). The current data were scaled by multiplying by $\nu^{-0.5}$.

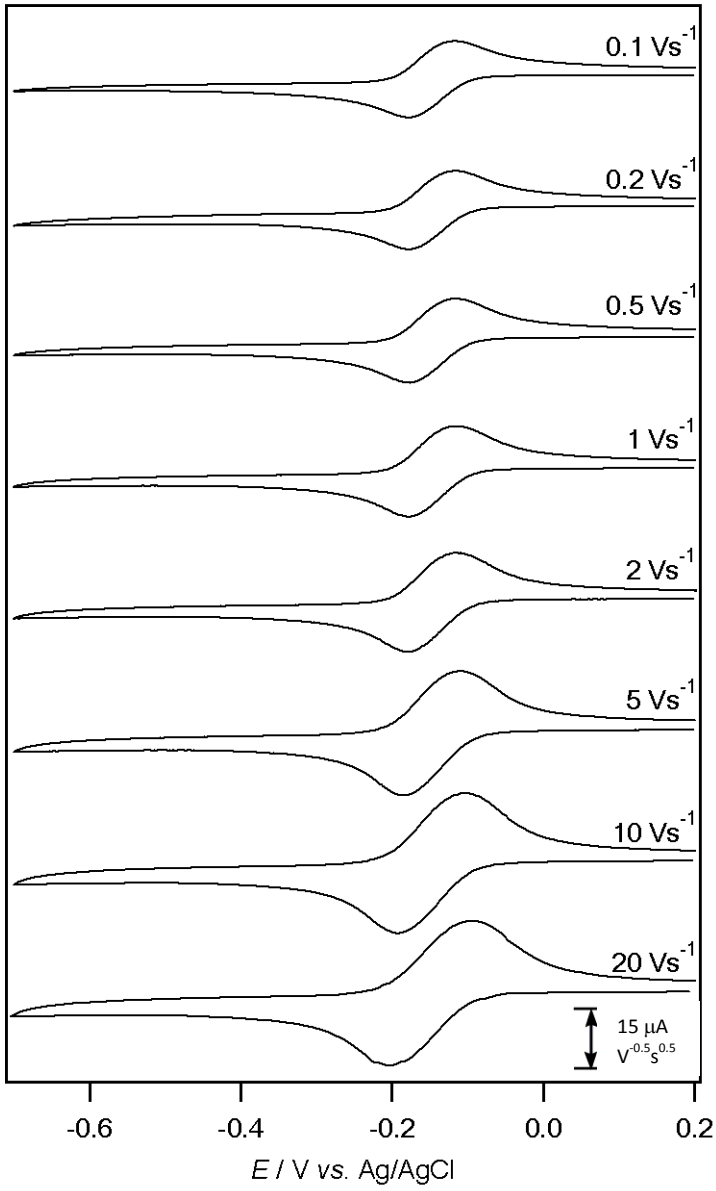

Figure A3.5. Variable scan rate cyclic voltammograms of 1 mM FMN with 0.4 M KCl in an unbuffered aqueous solution of pH 2.13, recorded at a 1 mm GC electrode at 22 (±2) ^{o}C. The current data were scaled by multiplying by $\nu^{-0.5}$.

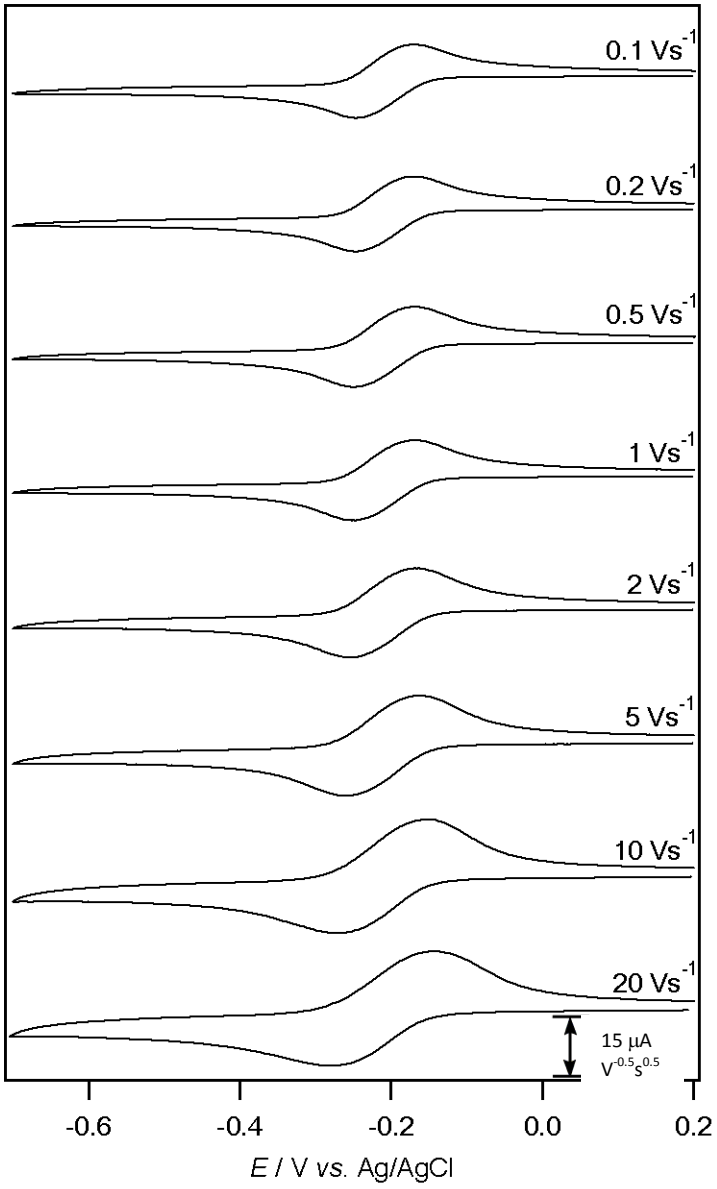

Figure A3.6. Variable scan rate cyclic voltammograms of 1 mM FMN with 0.4 M KCl in an unbuffered aqueous solution of pH 3.08, recorded at a 1 mm GC electrode at 22 (±2) ^{o}C. The current data were scaled by multiplying by $\nu^{-0.5}$.

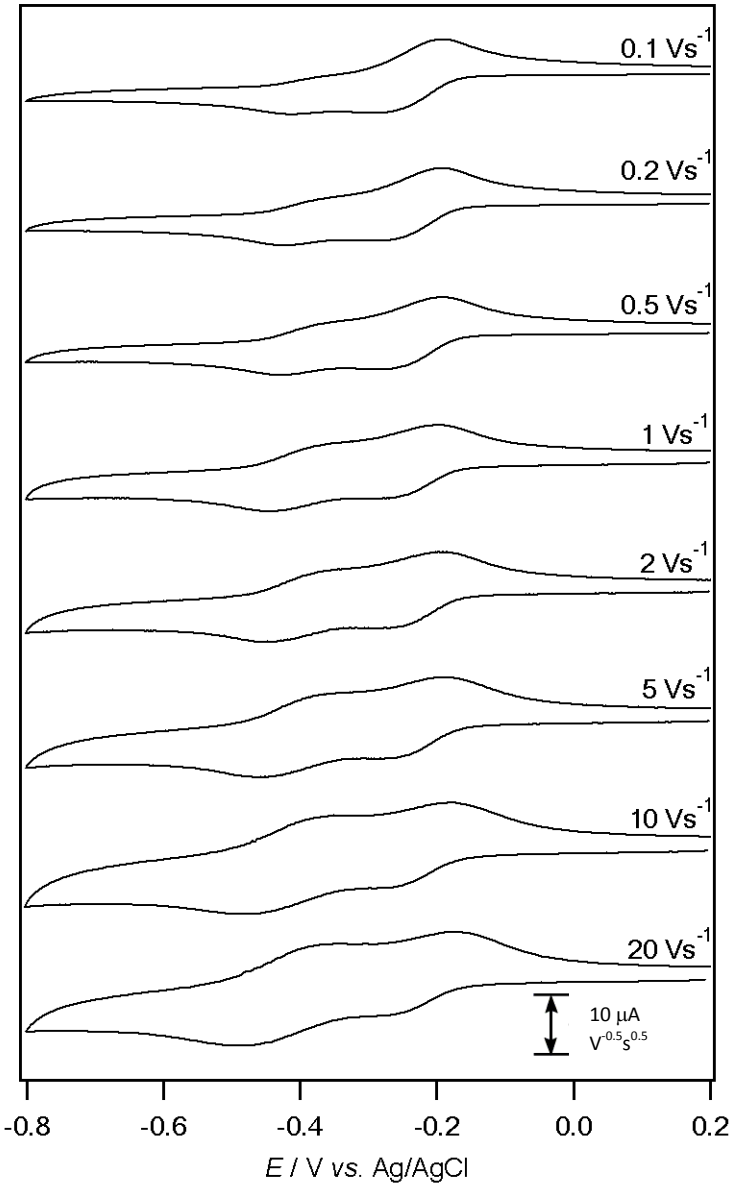

Figure A3.7. Variable scan rate cyclic voltammograms of 1 mM FMN with 0.4 M KCl in an unbuffered aqueous solution of pH 3.57, recorded at a 1 mm GC electrode at 22 (±2) ^{o}C. The current data were scaled by multiplying by $\nu^{-0.5}$.

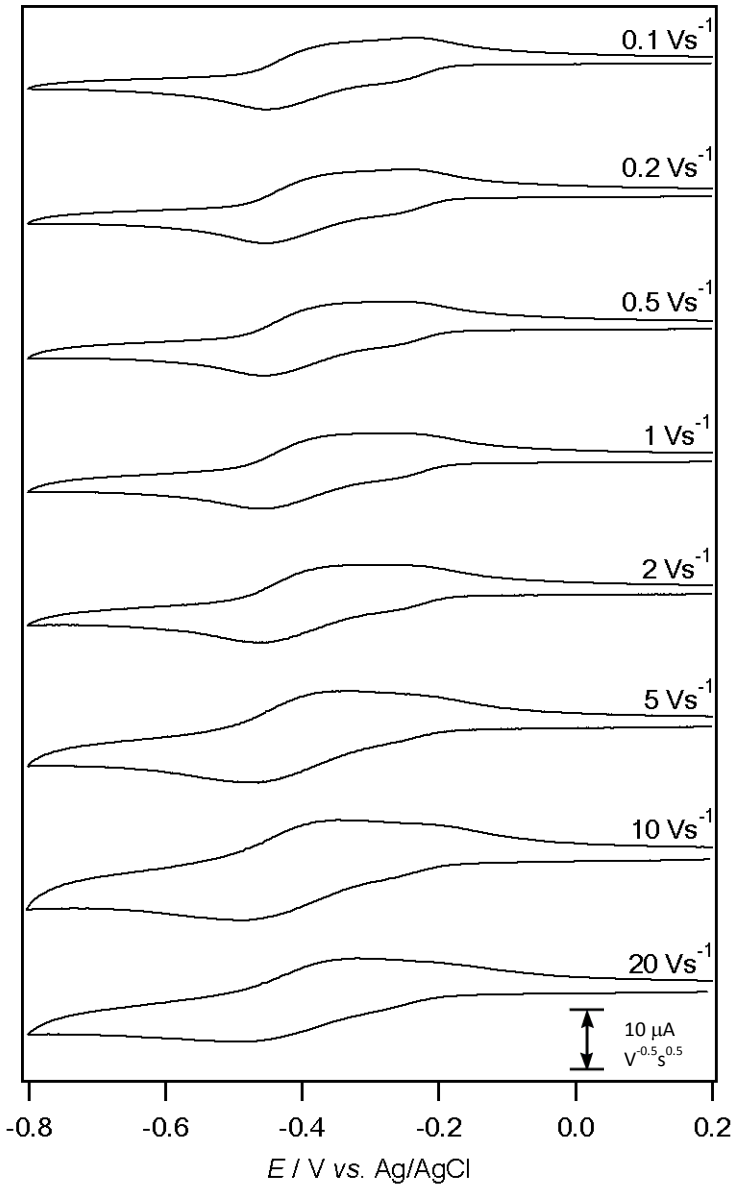

Figure A3.8. Variable scan rate cyclic voltammograms of 1 mM FMN with 0.4 M KCl in an unbuffered aqueous solution of pH 3.98, recorded at a 1 mm GC electrode at 22 (±2) ^{o}C. The current data were scaled by multiplying by $\nu^{-0.5}$.

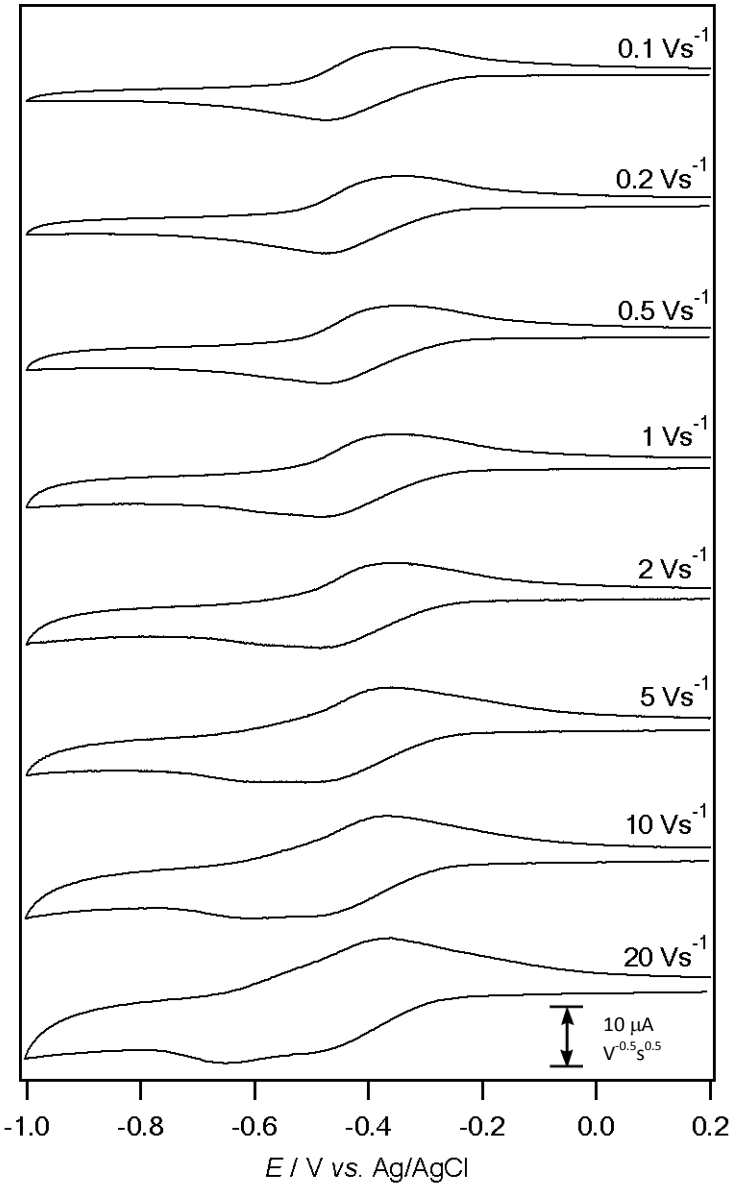

Figure A3.9. Variable scan rate cyclic voltammograms of 1 mM FMN with 0.4 M KCl in an unbuffered aqueous solution of pH 4.77, recorded at a 1 mm GC electrode at 22 (±2) ^{o}C. The current data were scaled by multiplying by $\nu^{-0.5}$.

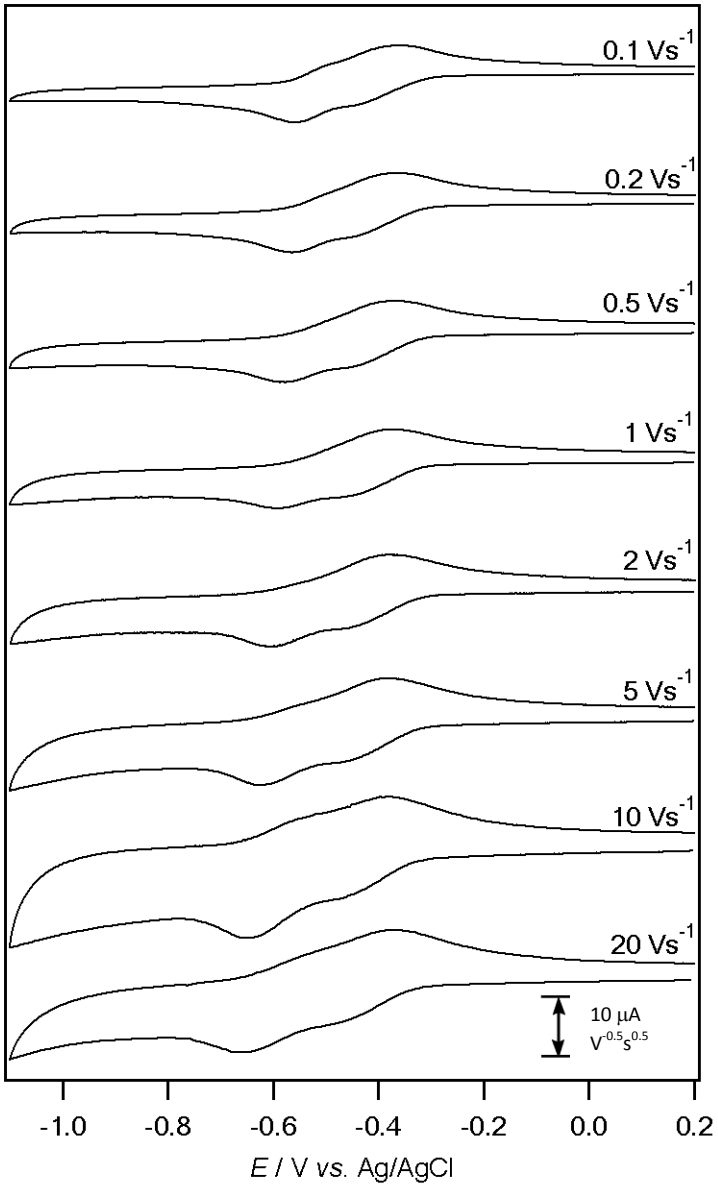

Figure A3.10. Variable scan rate cyclic voltammograms of 1 mM FMN with 0.4 M KCl in an unbuffered aqueous solution of pH 6.03, recorded at a 1 mm GC electrode at 22 (±2) ^{o}C. The current data were scaled by multiplying by $\nu^{-0.5}$.

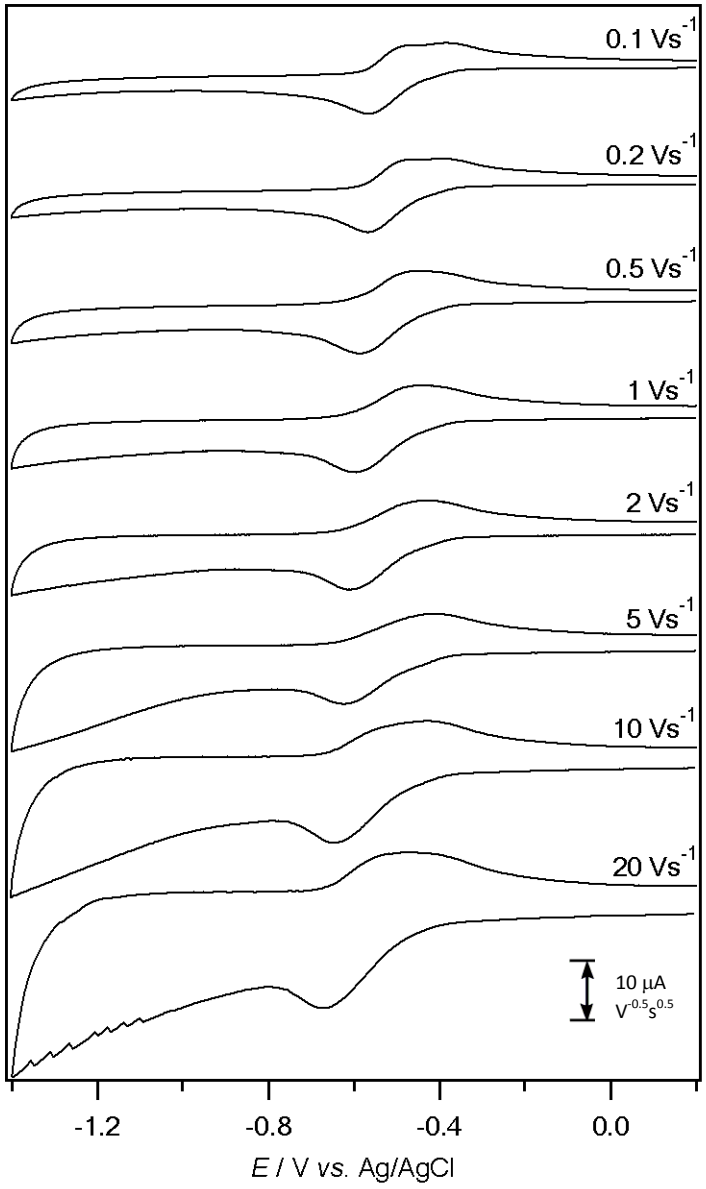

Figure A3.11. Variable scan rate cyclic voltammograms of 1 mM FMN with 0.4 M KCl in an unbuffered aqueous solution of pH 7.11, recorded at a 1 mm GC electrode at 22 (±2) ^{o}C. The current data were scaled by multiplying by $\nu^{-0.5}$.

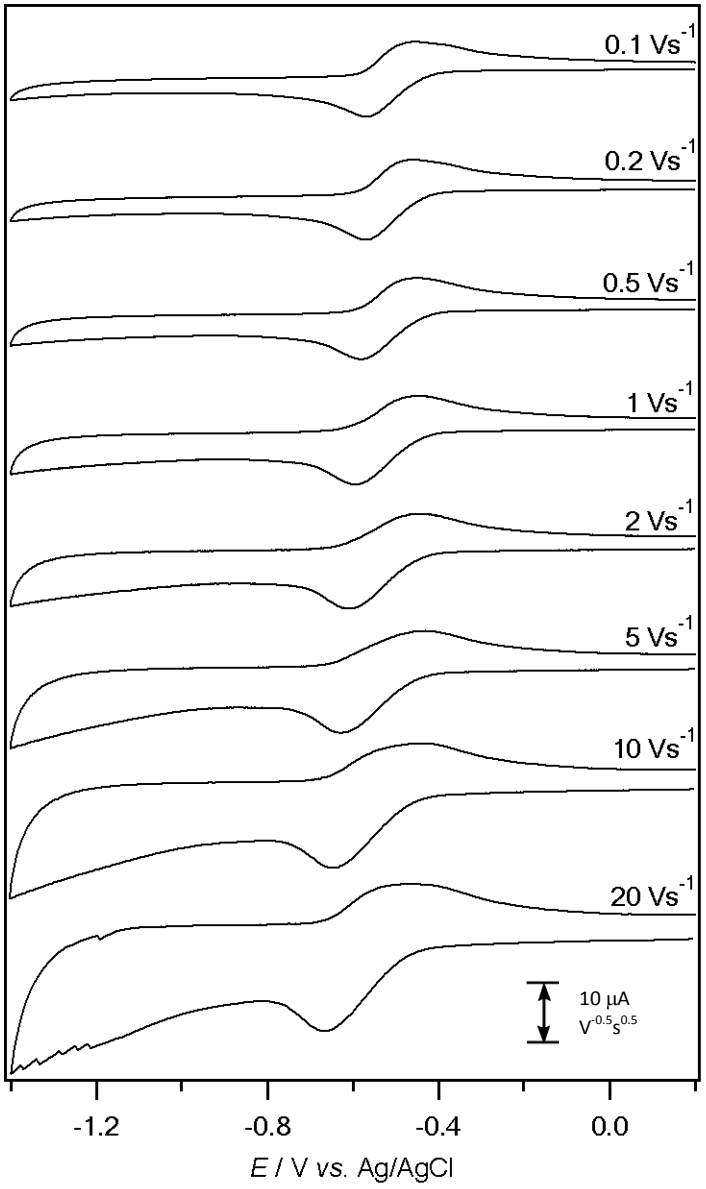

Figure A3.12. Variable scan rate cyclic voltammograms of 1 mM FMN with 0.4 M KCl in an unbuffered aqueous solution of pH 8.10, recorded at a 1 mm GC electrode at 22 (±2) ^{o}C. The current data were scaled by multiplying by $\nu^{-0.5}$.

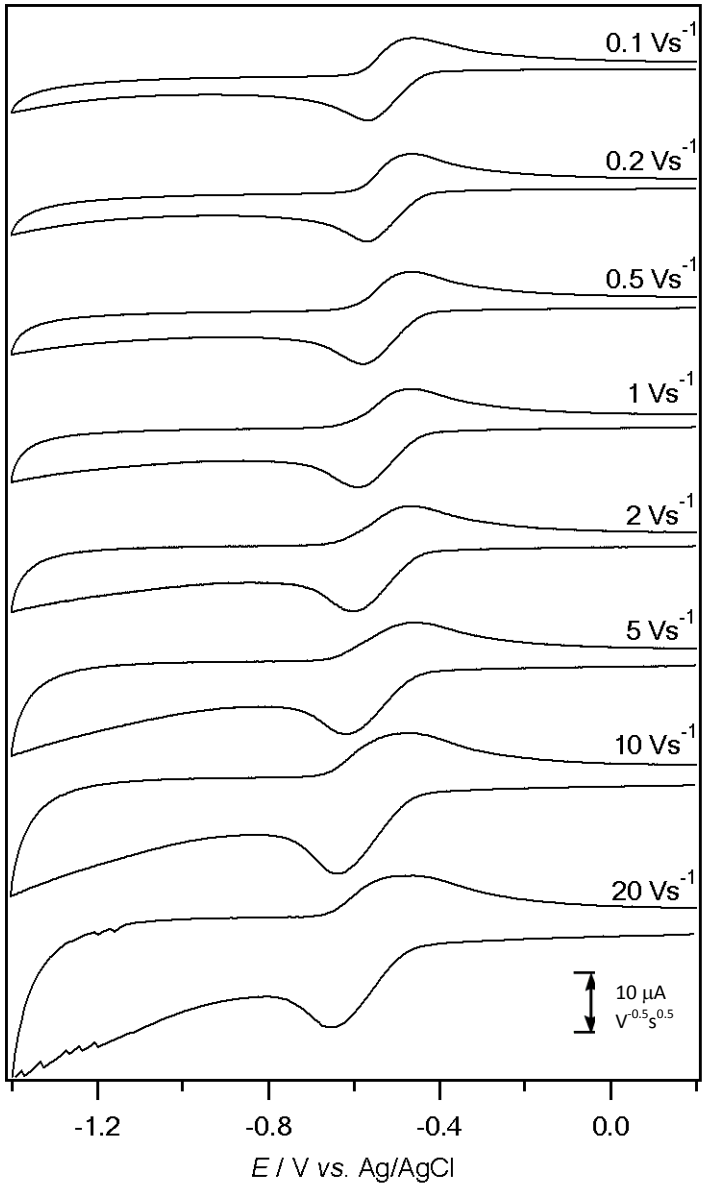

Figure A3.13. Variable scan rate cyclic voltammograms of 1 mM FMN with 0.4 M KCl in an unbuffered aqueous solution of pH 9.14, recorded at a 1 mm GC electrode at 22 (±2) ^{o}C. The current data were scaled by multiplying by $\nu^{-0.5}$.

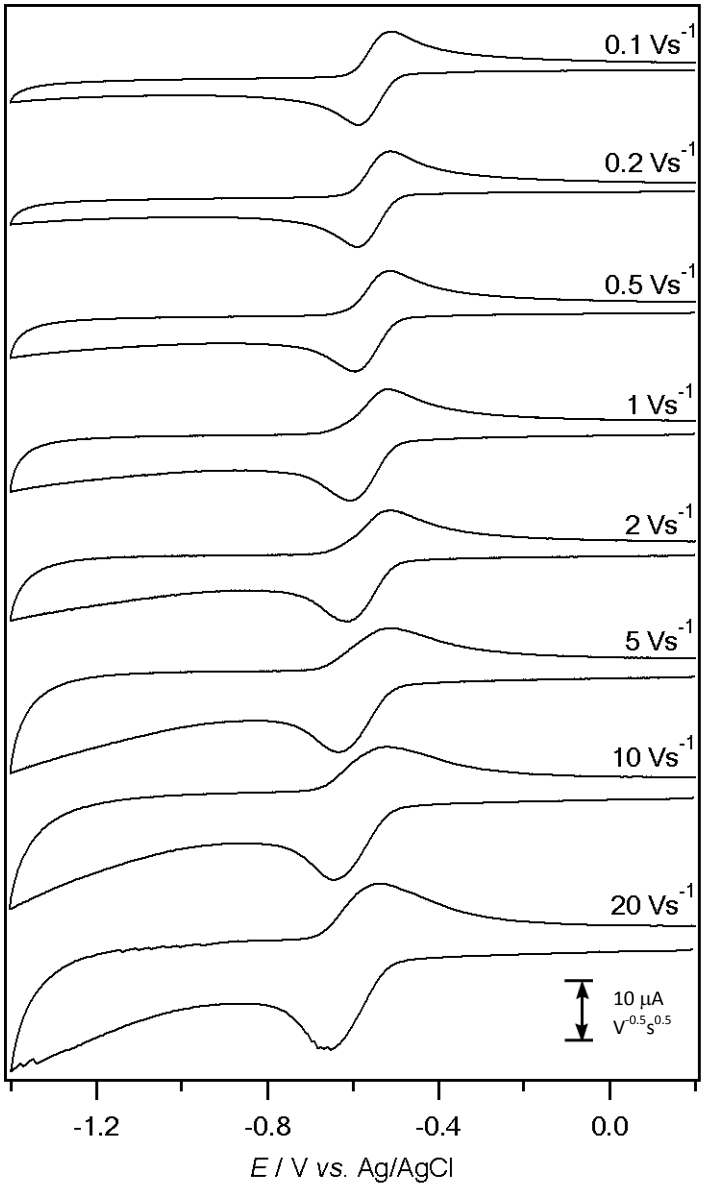

Figure A3.14. Variable scan rate cyclic voltammograms of 1 mM FMN with 0.4 M KCl in an unbuffered aqueous solution of pH 10.38, recorded at a 1 mm GC electrode at 22 (±2) ^{o}C. The current data were scaled by multiplying by $\nu^{-0.5}$.

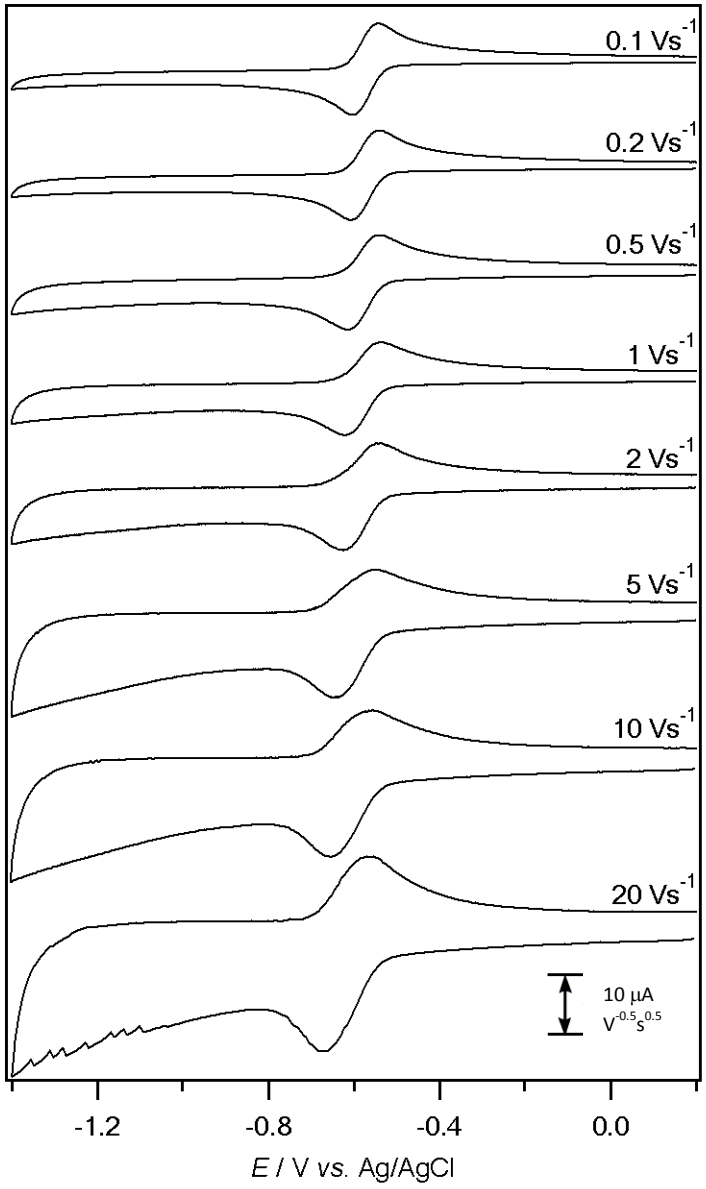

Figure A3.15. Variable scan rate cyclic voltammograms of 1 mM FMN with 0.4 M KCl in an unbuffered aqueous solution of pH 11.03, recorded at a 1 mm GC electrode at 22 (±2) ^{o}C. The current data were scaled by multiplying by $\nu^{-0.5}$.

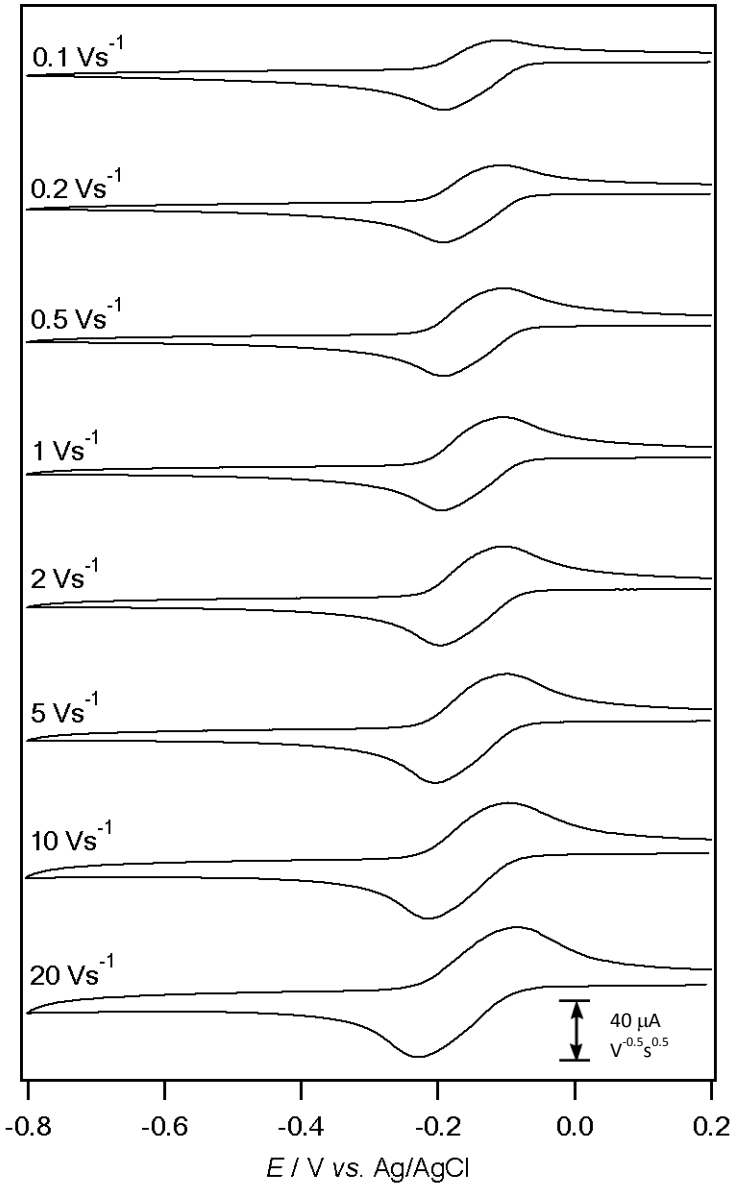

Figure A3.16. Variable scan rate cyclic voltammograms of 5 mM FMN with 0.4 M KCl in an unbuffered aqueous solution of pH 2.15, recorded at a 1 mm GC electrode at 22 (±2) ^{o}C. The current data were scaled by multiplying by $\nu^{-0.5}$.

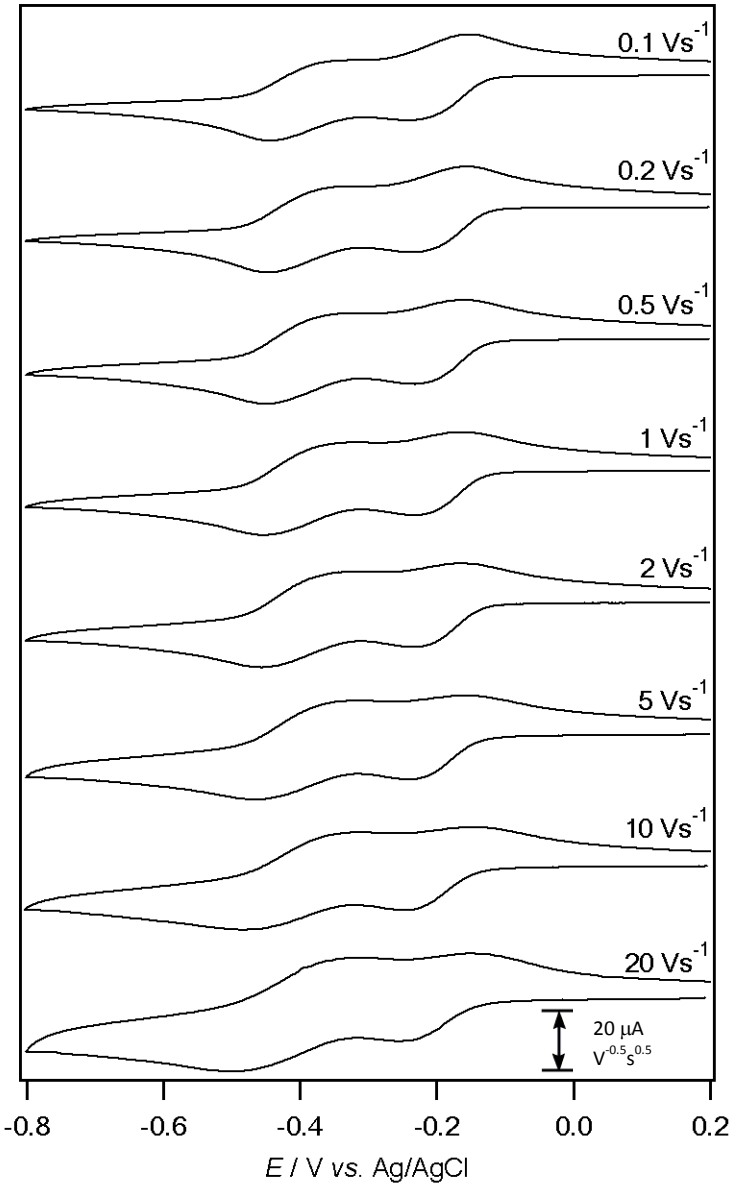

Figure A3.17. Variable scan rate cyclic voltammograms of 5 mM FMN with 0.4 M KCl in an unbuffered aqueous solution of pH 3.09, recorded at a 1 mm GC electrode at 22 (±2) ^{o}C. The current data were scaled by multiplying by $\nu^{-0.5}$.

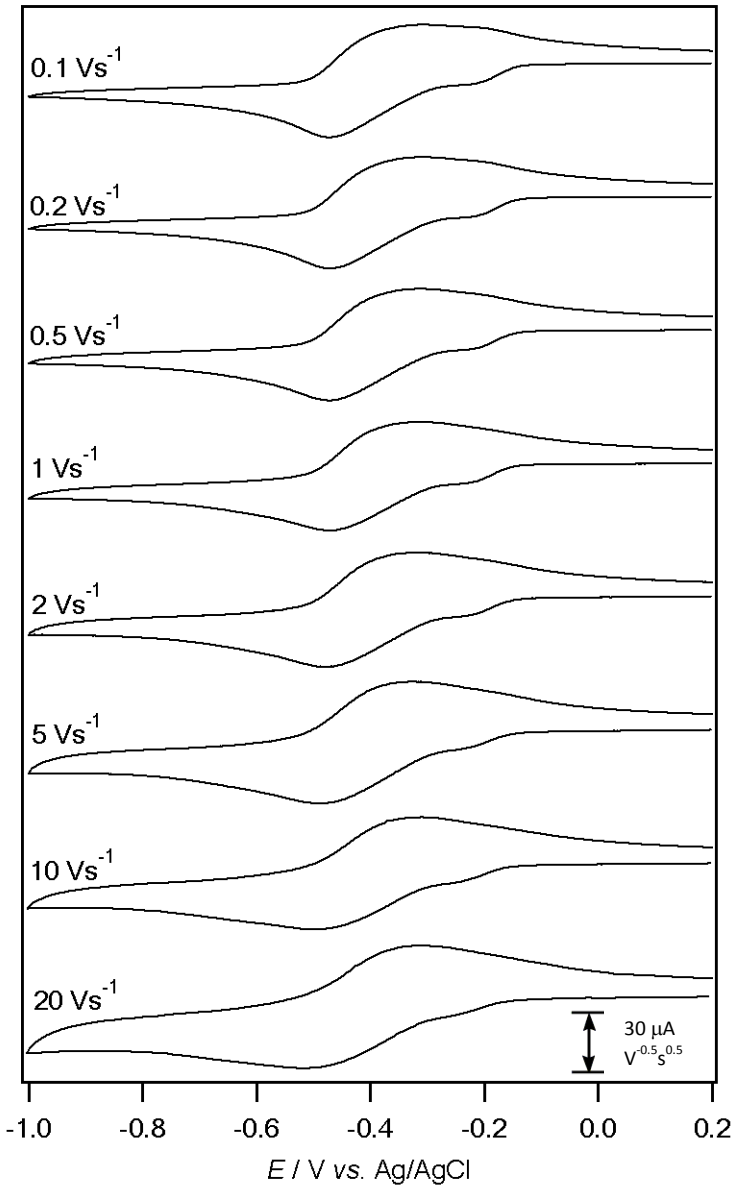

Figure A3.18. Variable scan rate cyclic voltammograms of 5 mM FMN with 0.4 M KCl in an unbuffered aqueous solution of pH 3.54, recorded at a 1 mm GC electrode at 22 (±2) ^{o}C. The current data were scaled by multiplying by $\nu^{-0.5}$.

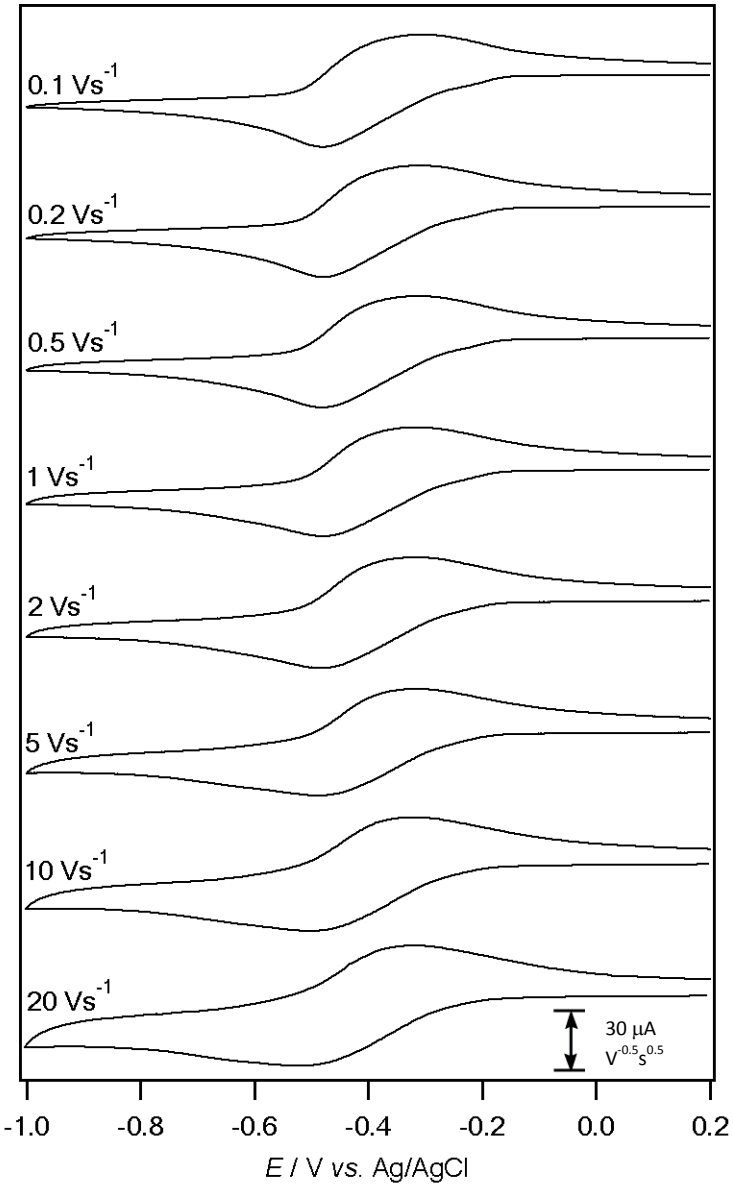

Figure A3.19. Variable scan rate cyclic voltammograms of 5 mM FMN with 0.4 M KCl in an unbuffered aqueous solution of pH 3.97, recorded at a 1 mm GC electrode at 22 (±2) ^{o}C. The current data were scaled by multiplying by $\nu^{-0.5}$.

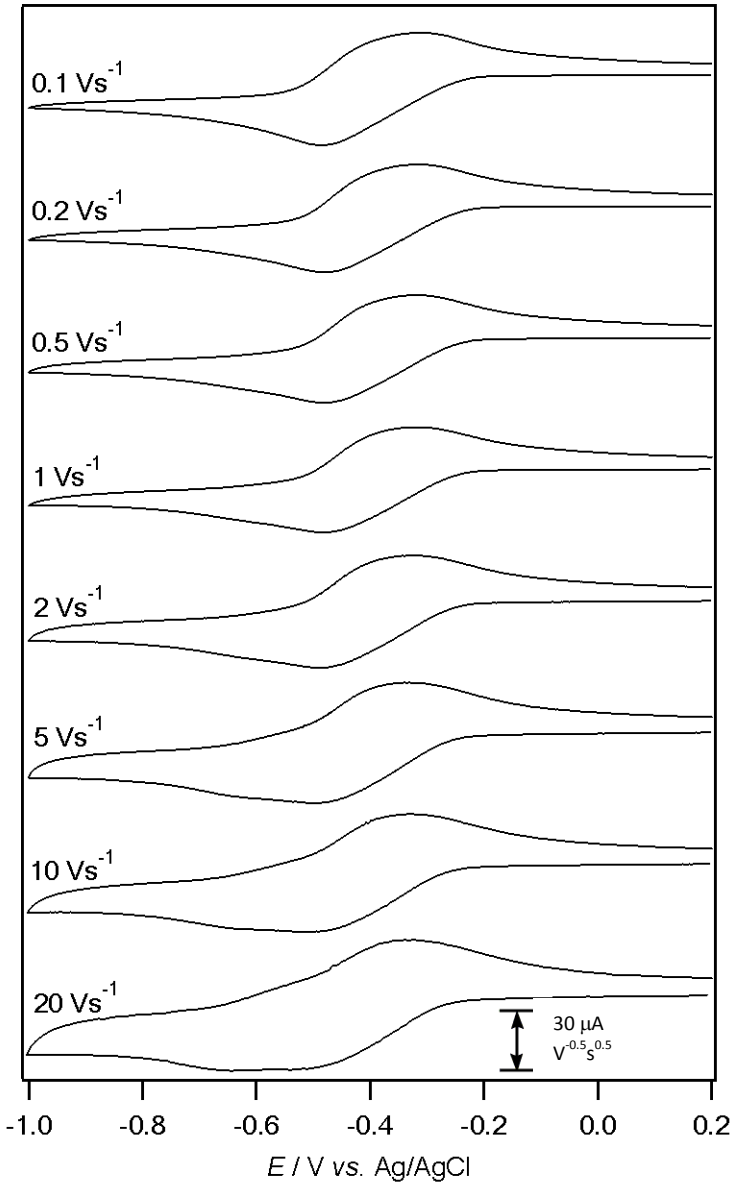

Figure A3.20. Variable scan rate cyclic voltammograms of 5 mM FMN with 0.4 M KCl in an unbuffered aqueous solution of pH 4.80, recorded at a 1 mm GC electrode at 22 (±2) ^{o}C. The current data were scaled by multiplying by $\nu^{-0.5}$.

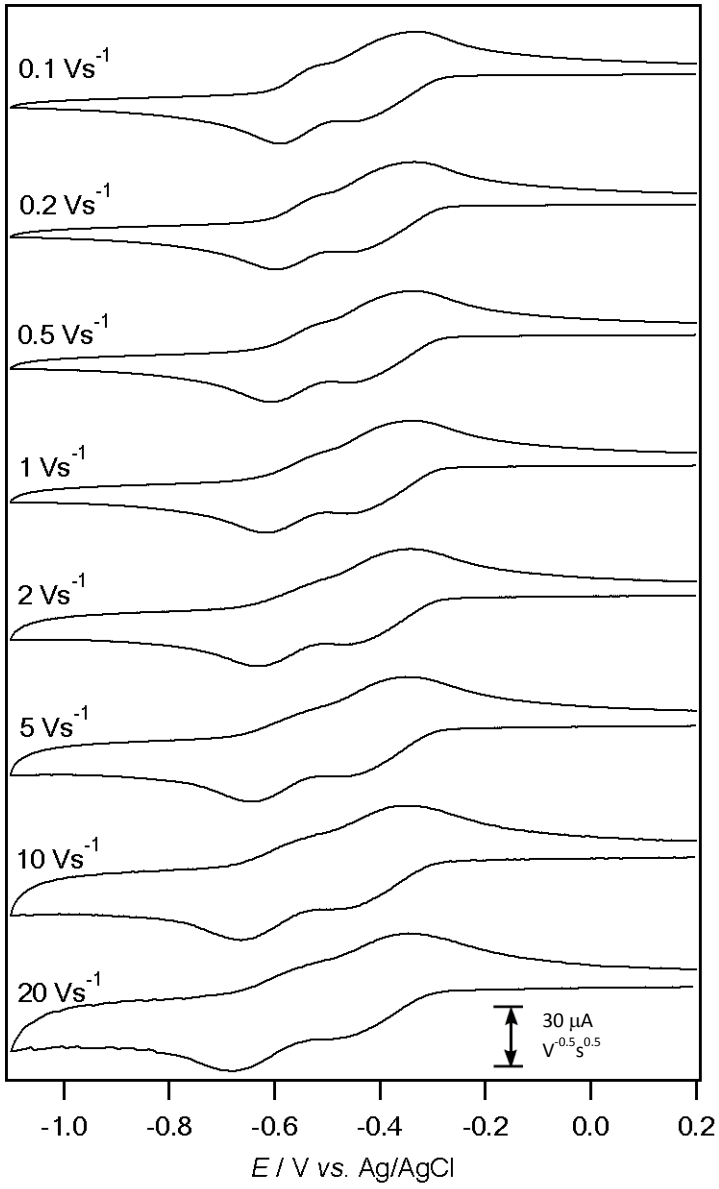

Figure A3.21. Variable scan rate cyclic voltammograms of 5 mM FMN with 0.4 M KCl in an unbuffered aqueous solution of pH 6.00, recorded at a 1 mm GC electrode at 22 (±2) ^{o}C. The current data were scaled by multiplying by $\nu^{-0.5}$.

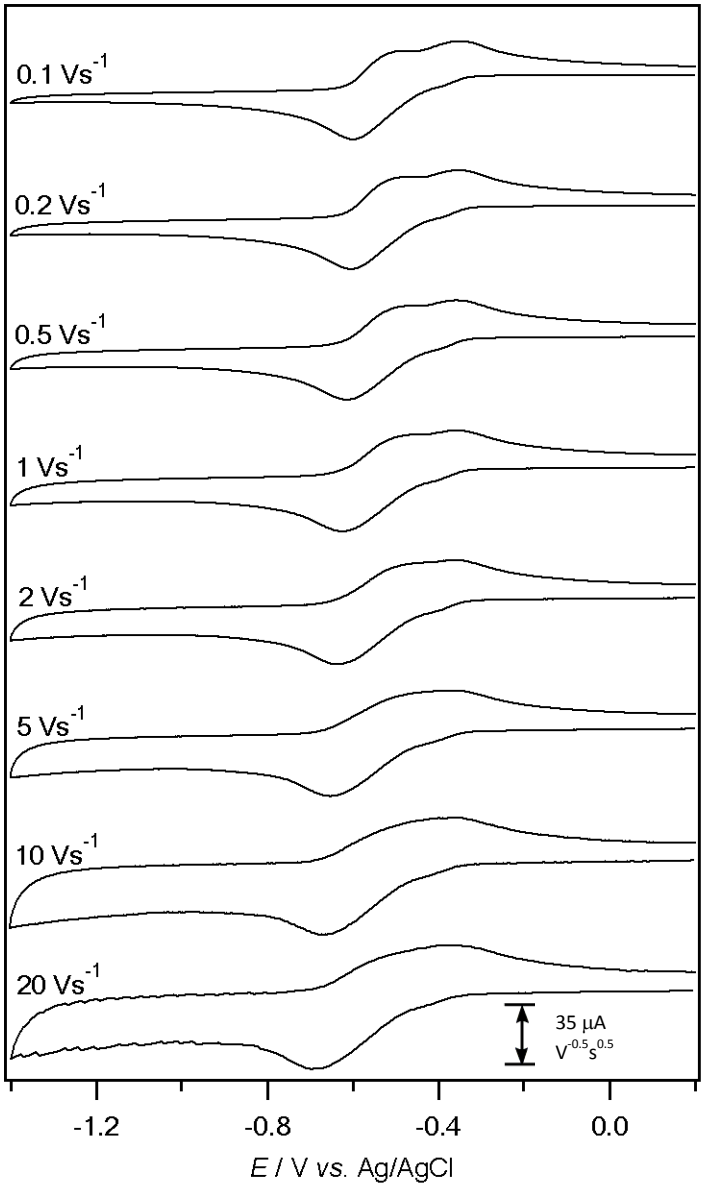

Figure A3.22. Variable scan rate cyclic voltammograms of 5 mM FMN with 0.4 M KCl in an unbuffered aqueous solution of pH 7.12, recorded at a 1 mm GC electrode at 22 (±2) ^{o}C. The current data were scaled by multiplying by $\nu^{-0.5}$.

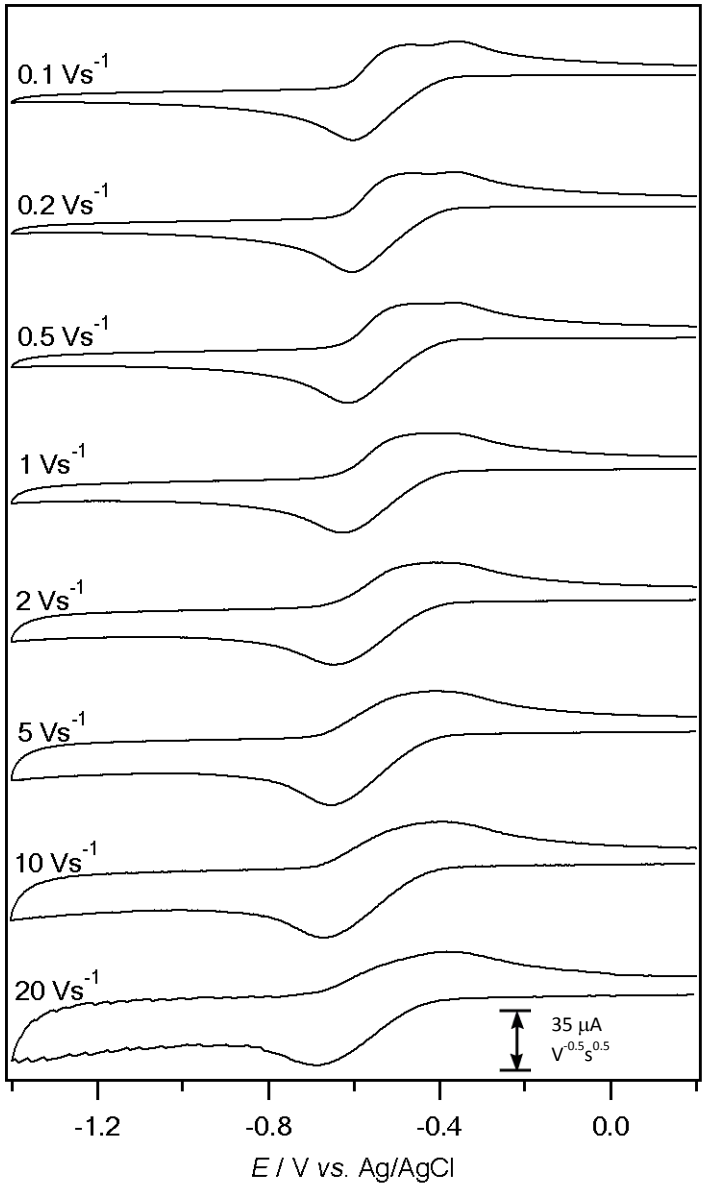

Figure A3.23. Variable scan rate cyclic voltammograms of 5 mM FMN with 0.4 M KCl in an unbuffered aqueous solution of pH 8.08, recorded at a 1 mm GC electrode at 22 (±2) ^{o}C. The current data were scaled by multiplying by $\nu^{-0.5}$.

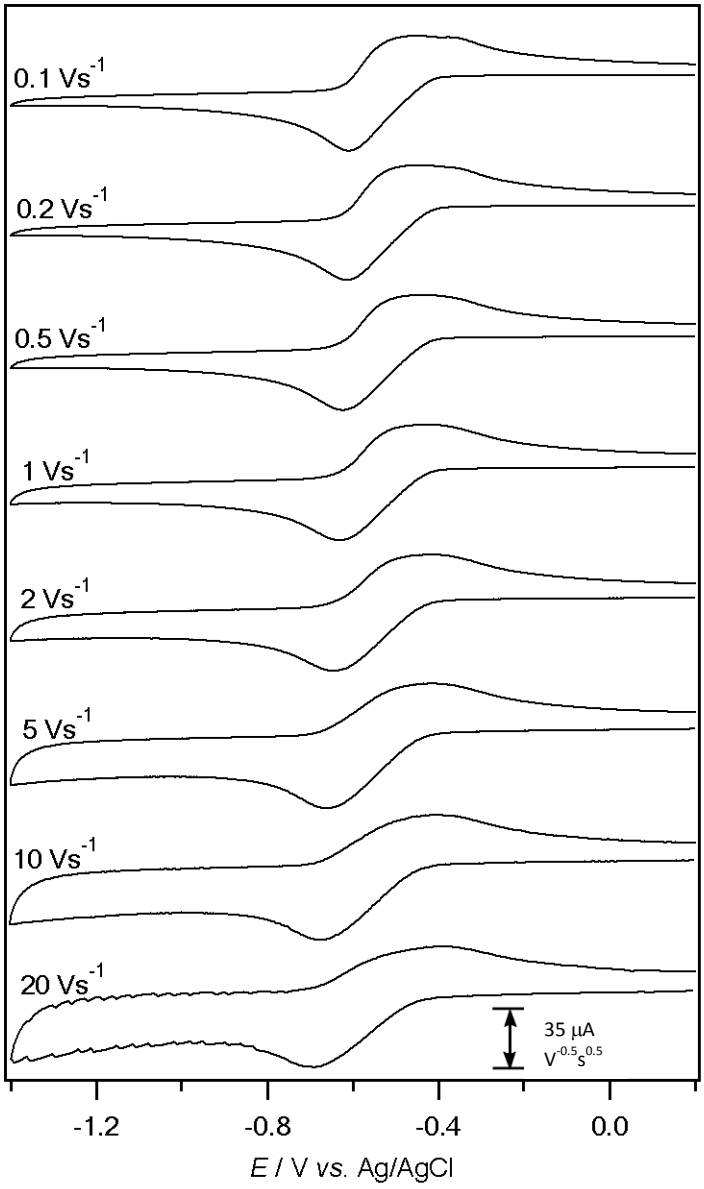

Figure A3.24. Variable scan rate cyclic voltammograms of 5 mM FMN with 0.4 M KCl in an unbuffered aqueous solution of pH 9.12, recorded at a 1 mm GC electrode at 22 (±2) ^{o}C. The current data were scaled by multiplying by $v^{-0.5}$.

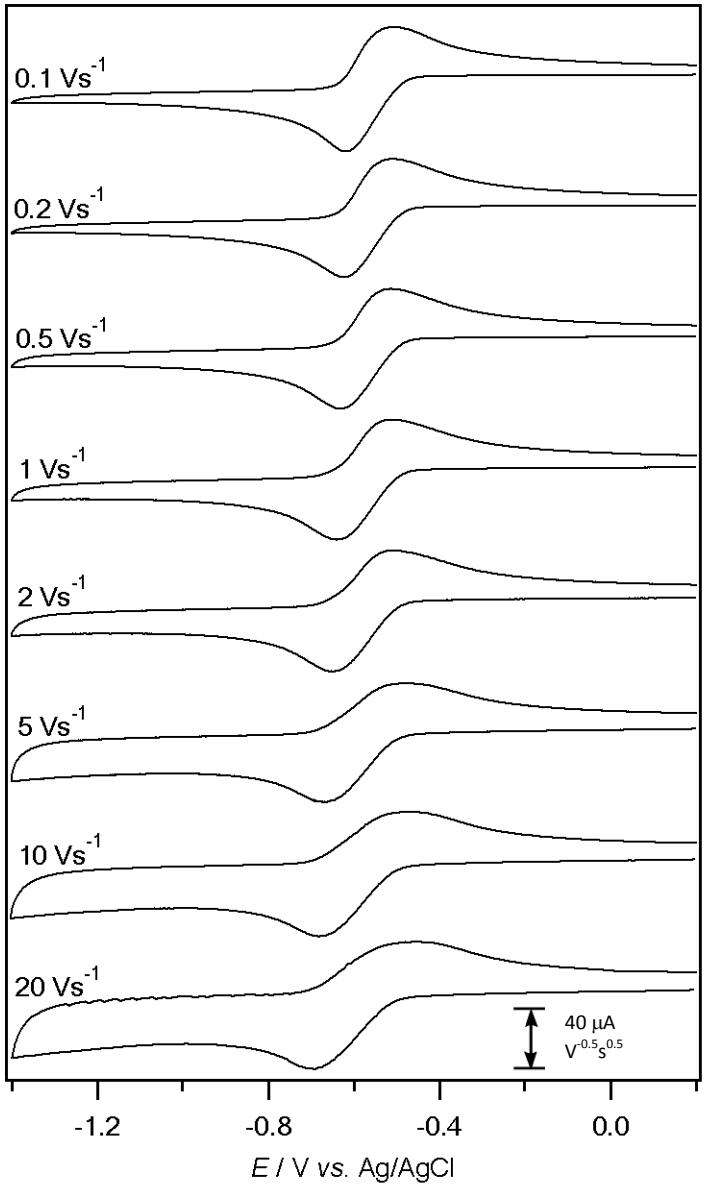

Figure A3.25. Variable scan rate cyclic voltammograms of 5 mM FMN with 0.4 M KCl in an unbuffered aqueous solution of pH 10.36, recorded at a 1 mm GC electrode at 22 (±2) ^{o}C. The current data were scaled by multiplying by $\nu^{-0.5}$.

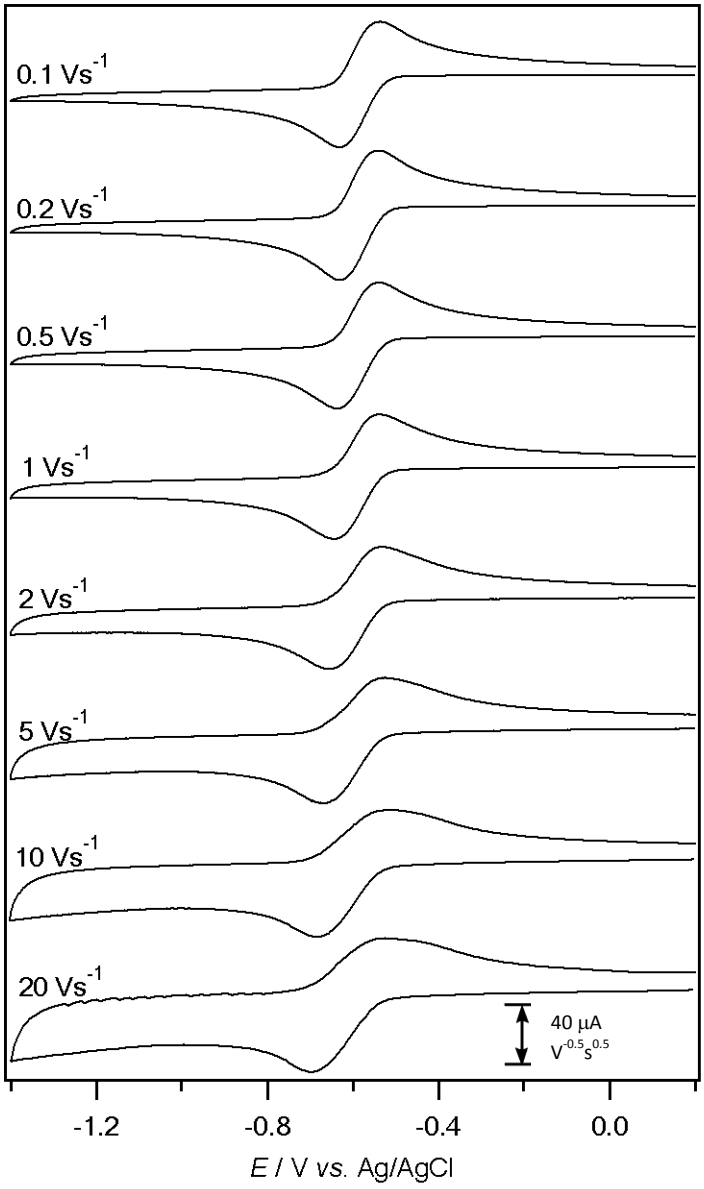

Figure A3.26. Variable scan rate cyclic voltammograms of 5 mM FMN with 0.4 M KCl in an unbuffered aqueous solution of pH 11.04, recorded at a 1 mm GC electrode at 22 (±2) ^{o}C. The current data were scaled by multiplying by $\nu^{-0.5}$.

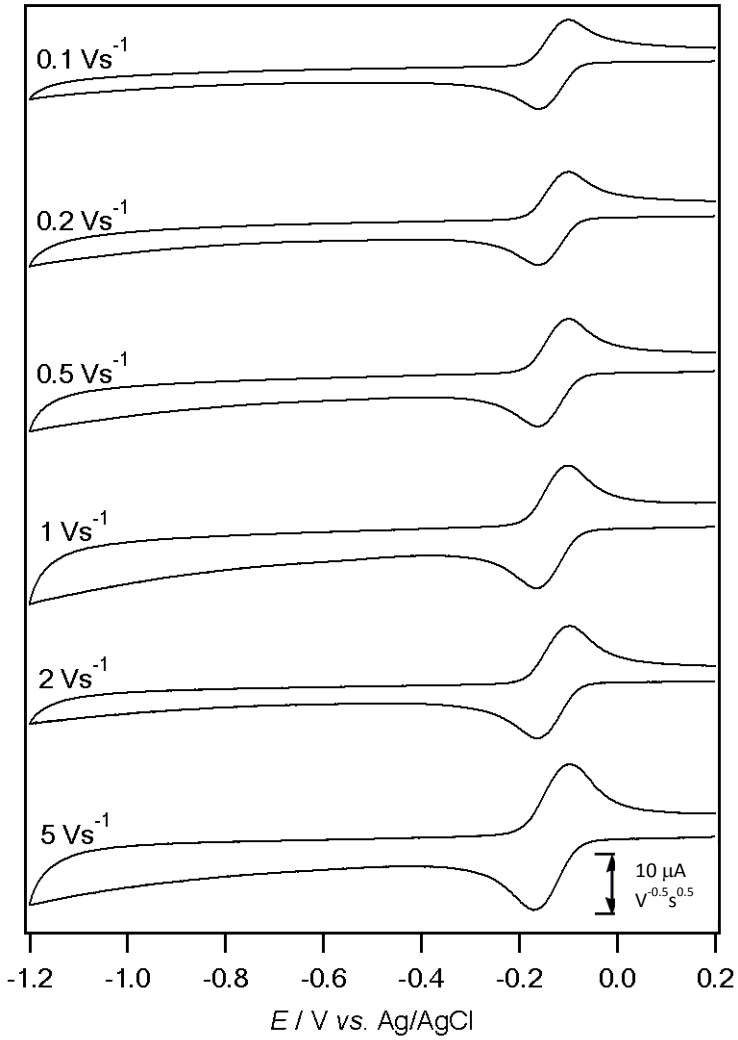

Figure A3.27. Variable scan rate cyclic voltammograms of 1 mM FAD with 0.4 M KCl in an unbuffered aqueous solution of pH 2.03, recorded at a 1 mm GC electrode at 22 (±2) ^{o}C. The current data were scaled by multiplying by $\nu^{-0.5}$.

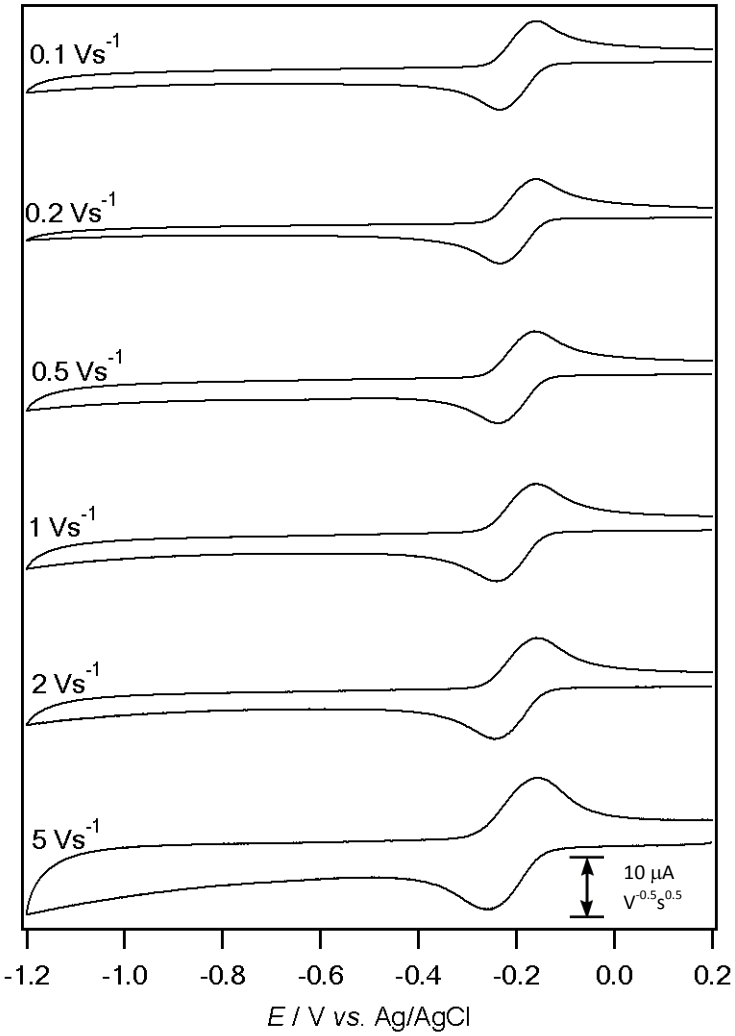

Figure A3.28. Variable scan rate cyclic voltammograms of 1 mM FAD with 0.4 M KCl in an unbuffered aqueous solution of pH 3.05, recorded at a 1 mm GC electrode at 22 (±2) ^{o}C. The current data were scaled by multiplying by $v^{-0.5}$.

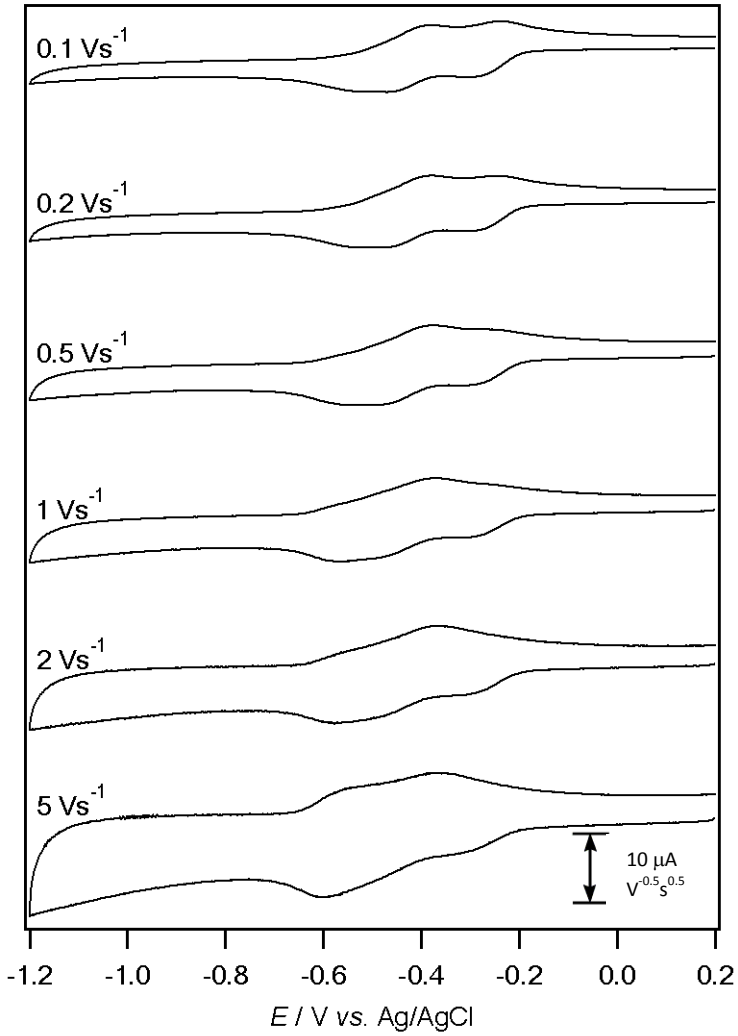

Figure A3.29. Variable scan rate cyclic voltammograms of 1 mM FAD with 0.4 M KCl in an unbuffered aqueous solution of pH 4.00, recorded at a 1 mm GC electrode at 22 (±2) ^{o}C. The current data were scaled by multiplying by $\nu^{-0.5}$.

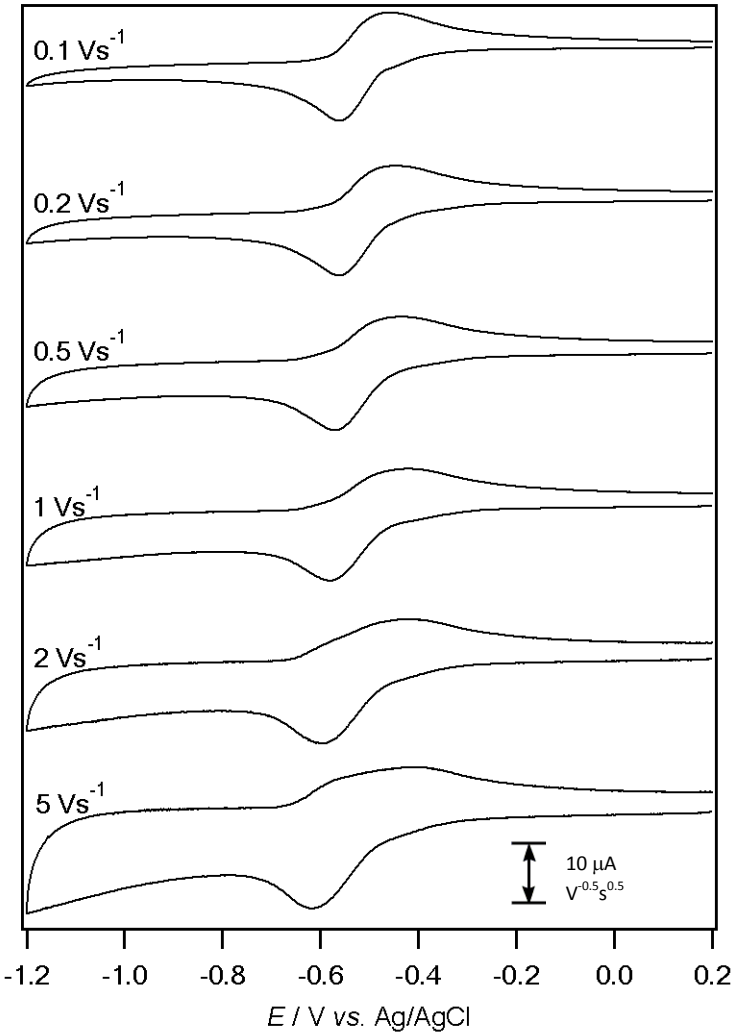

Figure A3.30. Variable scan rate cyclic voltammograms of 1 mM FAD with 0.4 M KCl in an unbuffered aqueous solution of pH 5.05, recorded at a 1 mm GC electrode at 22 (±2) ^{o}C. The current data were scaled by multiplying by $\nu^{-0.5}$.

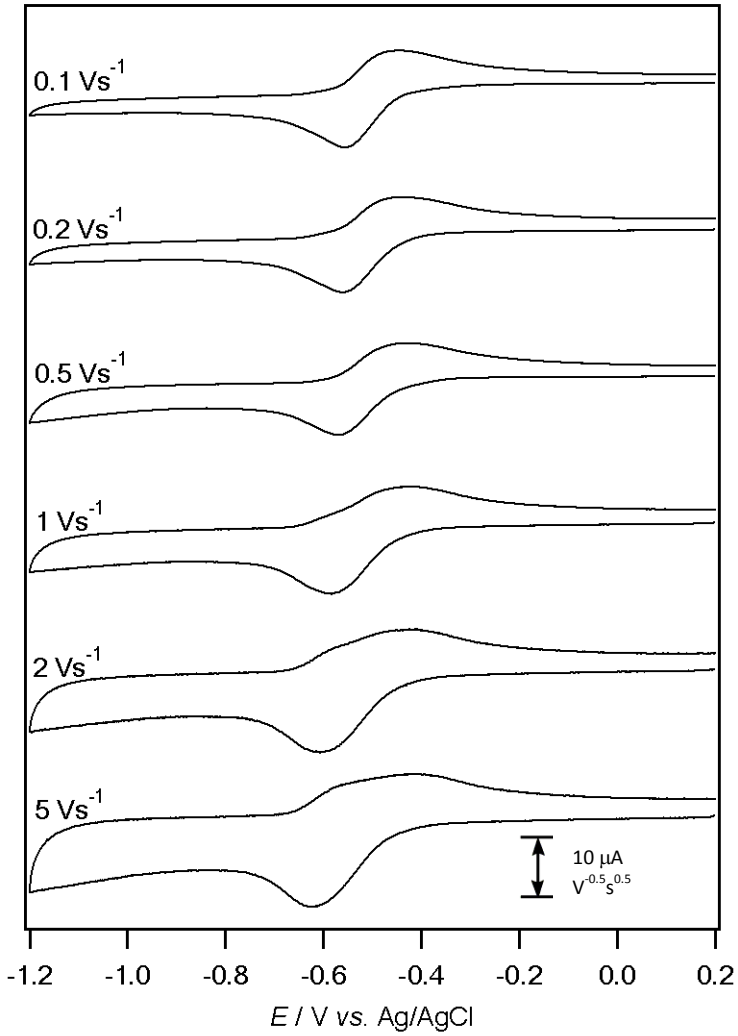

Figure A3.31. Variable scan rate cyclic voltammograms of 1 mM FAD with 0.4 M KCl in an unbuffered aqueous solution of pH 6.01, recorded at a 1 mm GC electrode at 22 (±2) ^{o}C. The current data were scaled by multiplying by $\nu^{-0.5}$.

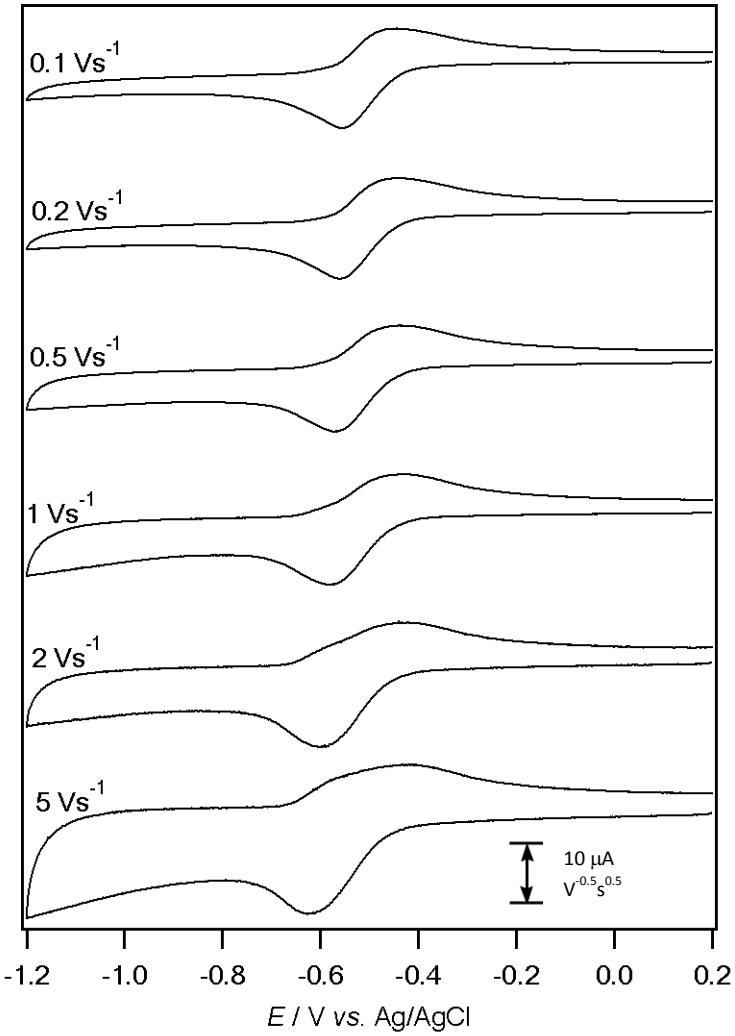

Figure A3.32. Variable scan rate cyclic voltammograms of 1 mM FAD with 0.4 M KCl in an unbuffered aqueous solution of pH 6.96, recorded at a 1 mm GC electrode at 22 (±2) ^{o}C. The current data were scaled by multiplying by $v^{-0.5}$.

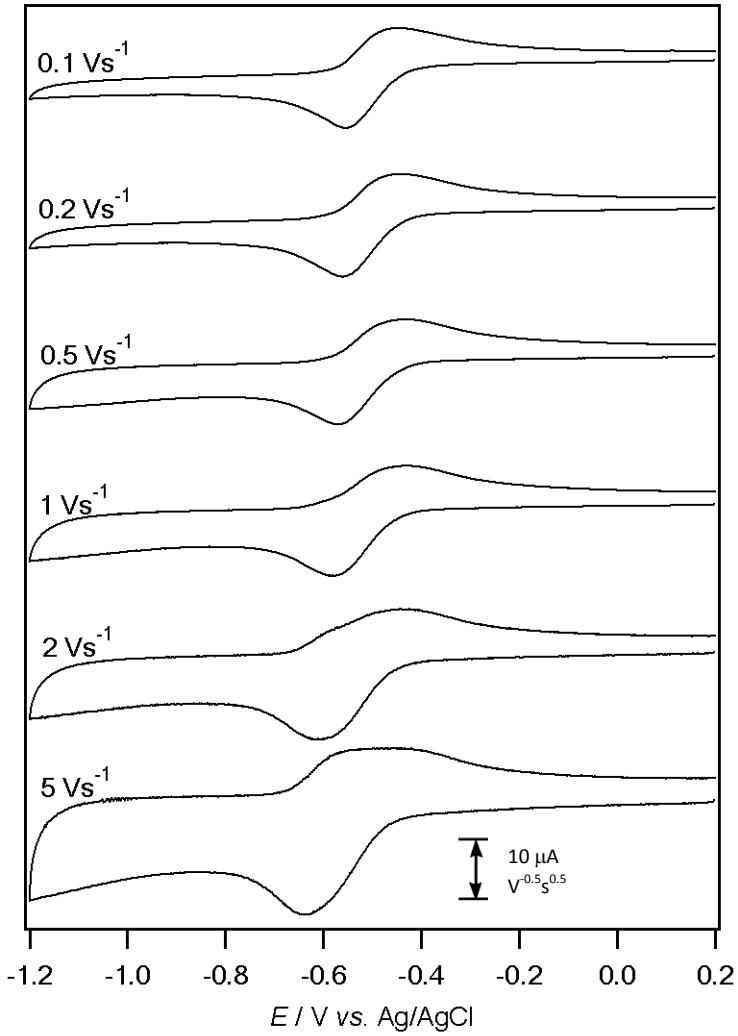

Figure A3.33. Variable scan rate cyclic voltammograms of 1 mM FAD with 0.4 M KCl in an unbuffered aqueous solution of pH 7.95, recorded at a 1 mm GC electrode at 22 (±2) ^{o}C. The current data were scaled by multiplying by $\nu^{-0.5}$.

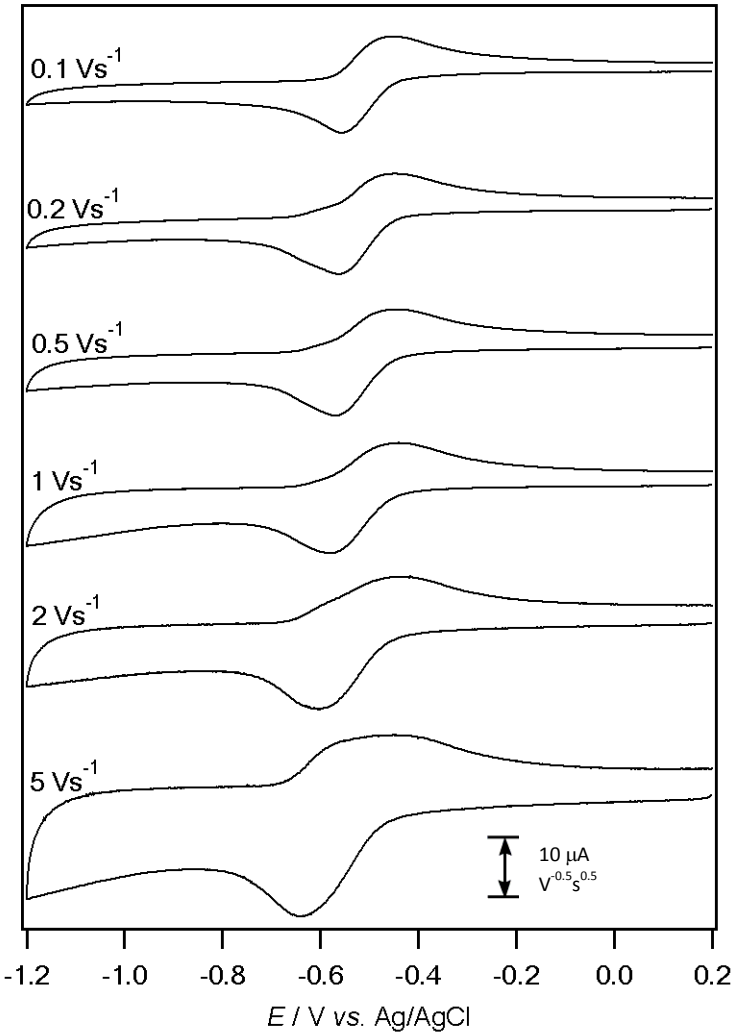

Figure A3.34. Variable scan rate cyclic voltammograms of 1 mM FAD with 0.4 M KCl in an unbuffered aqueous solution of pH 8.96, recorded at a 1 mm GC electrode at 22 (±2) ^{o}C. The current data were scaled by multiplying by $v^{-0.5}$.

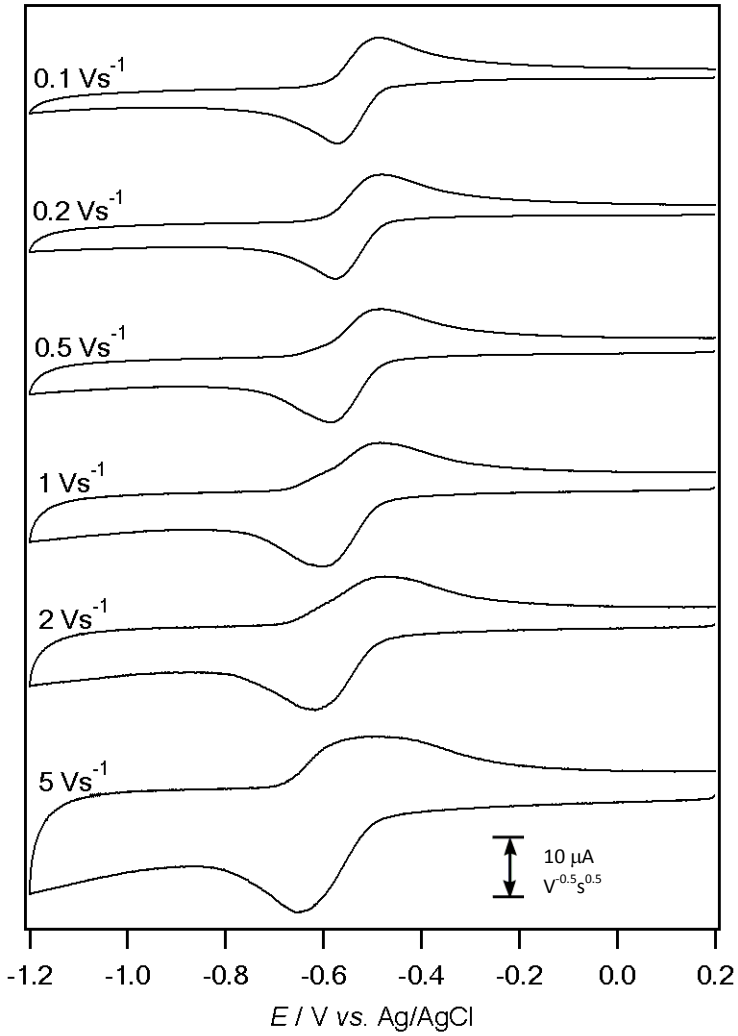

Figure A3.35. Variable scan rate cyclic voltammograms of 1 mM FAD with 0.4 M KCl in an unbuffered aqueous solution of pH 9.97, recorded at a 1 mm GC electrode at 22 (±2) ^{o}C. The current data were scaled by multiplying by $\nu^{-0.5}$.

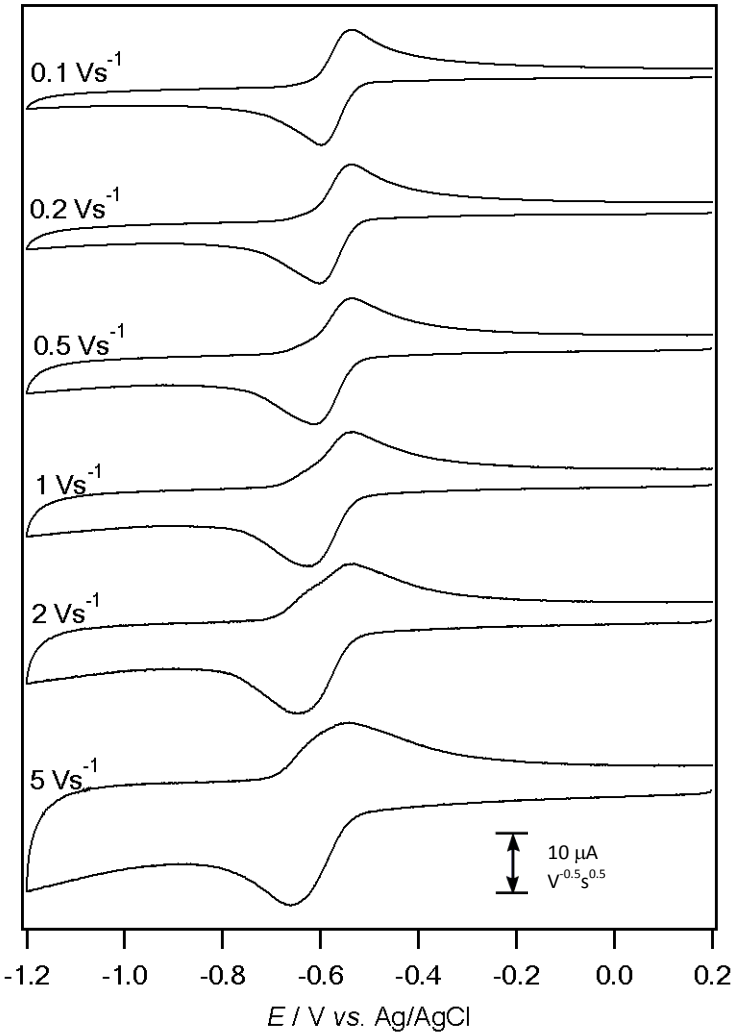

Figure A3.36. Variable scan rate cyclic voltammograms of 1 mM FAD with 0.4 M KCl in an unbuffered aqueous solution of pH 10.97, recorded at a 1 mm GC electrode at 22 (±2) ^{o}C. The current data were scaled by multiplying by $\nu^{-0.5}$.

Chapter 4

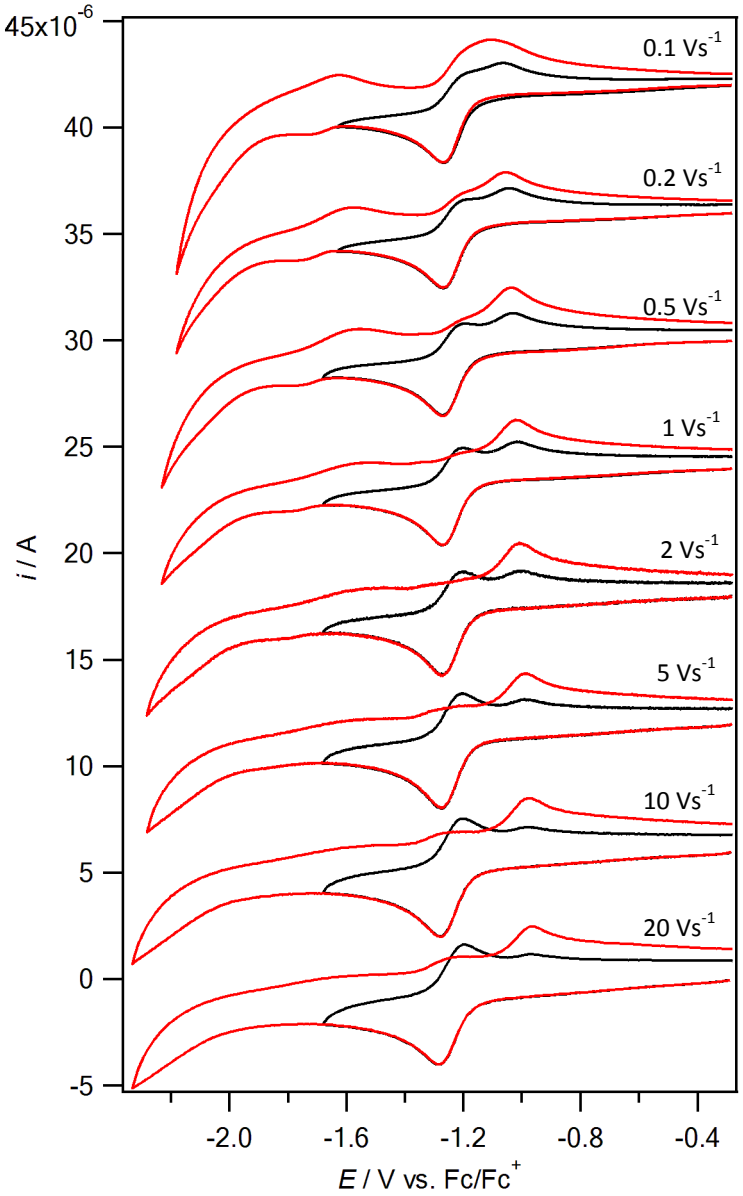

Figure A4.1. Variable scan rate cyclic voltammograms of 1 mM flavin **1** in acetonitrile with 0.2 M *n*-Bu_4NPF_6, recorded at a 1 mm Pt electrode at 22 (±2) ^oC. The current data were scaled by multiplying by $\nu^{-0.5}$.

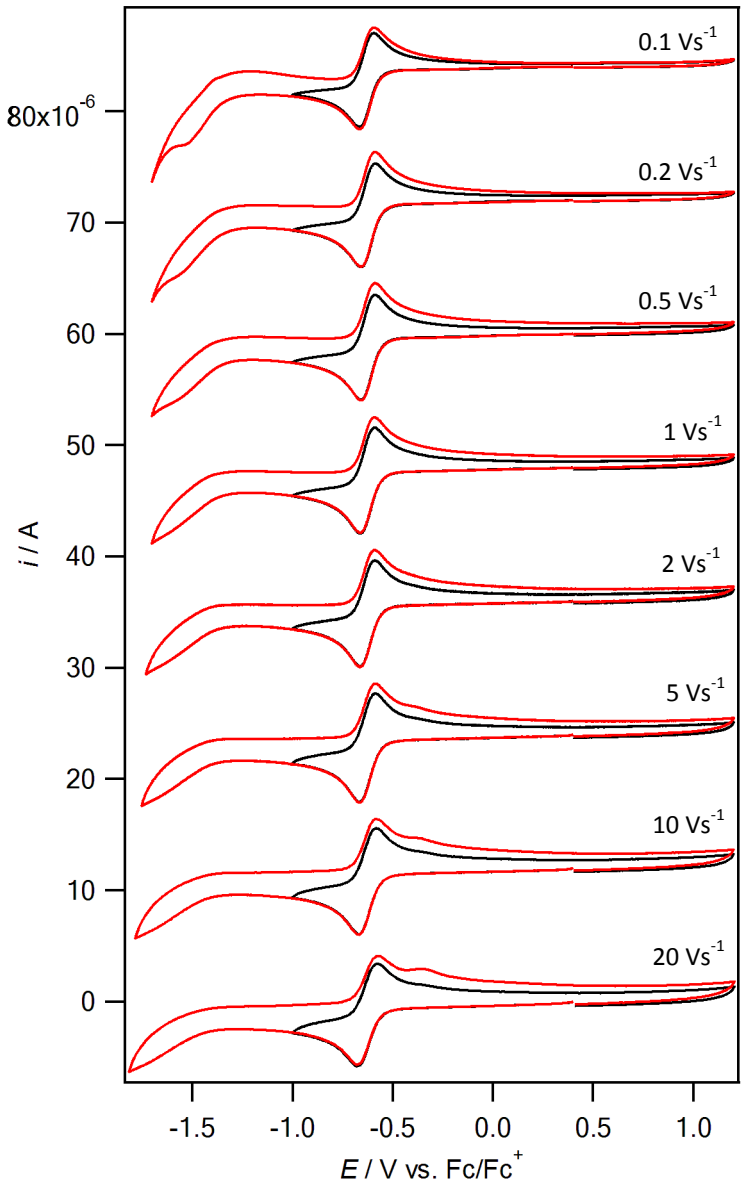

Figure A4.2. Variable scan rate cyclic voltammograms of 1 mM flavin **2** in acetonitrile with 0.2 M *n*-Bu_4NPF_6, recorded at a 1 mm Pt electrode at 22 (±2) ^{o}C. The current data were scaled by multiplying by $\nu^{-0.5}$.

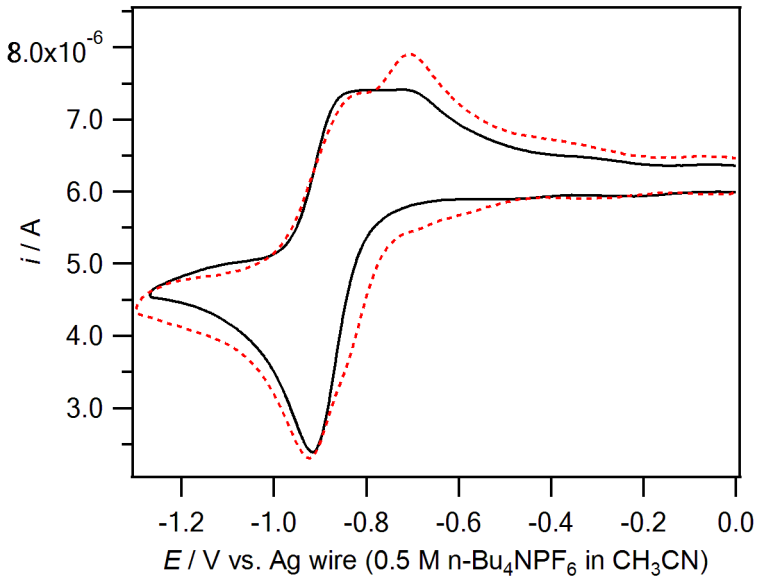

Figure A4.3. Cyclic voltammograms of 1 mM flavin **1** in DMSO with 0.2 M *n*-Bu_4NPF_6, recorded at a 1 mm Pt electrode at 22 (±2) ^{o}C, before electrolysis (black line) and after oxidation (red dashed line). The current data were scaled by multiplying by $\nu^{-0.5}$.

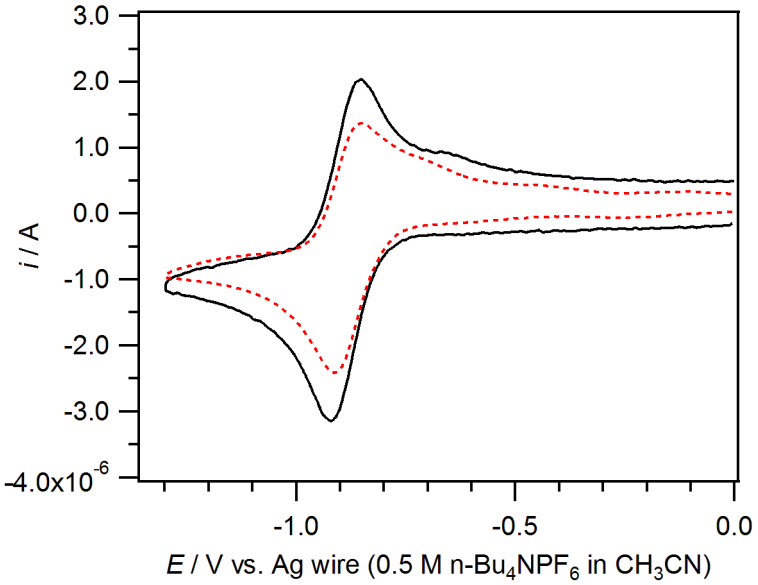

Figure A4.4. Cyclic voltammograms of 1 mM flavin **2** in DMSO with 0.2 M *n*-Bu_4NPF_6, recorded at a 1 mm Pt electrode at 22 (±2) ^{o}C, before electrolysis (black line) and after oxidation (red dashed line). The current data were scaled by multiplying by $\nu^{-0.5}$.

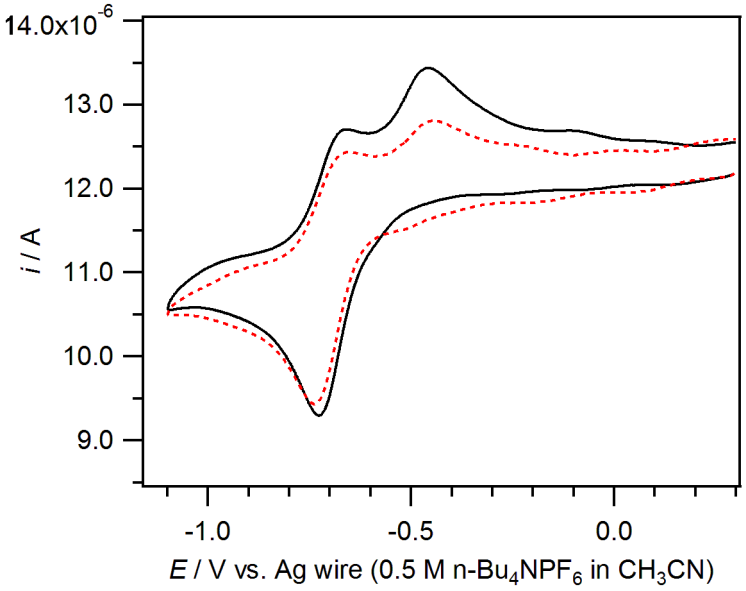

Figure A4.5. Cyclic voltammograms of 1 mM riboflavin in DMSO with 0.2 M *n*-Bu_4NPF_6, recorded at a 1 mm Pt electrode at 22 (±2) ^oC, before electrolysis (black line) and after oxidation (red dashed line). The current data were scaled by multiplying by $\nu^{0.5}$.

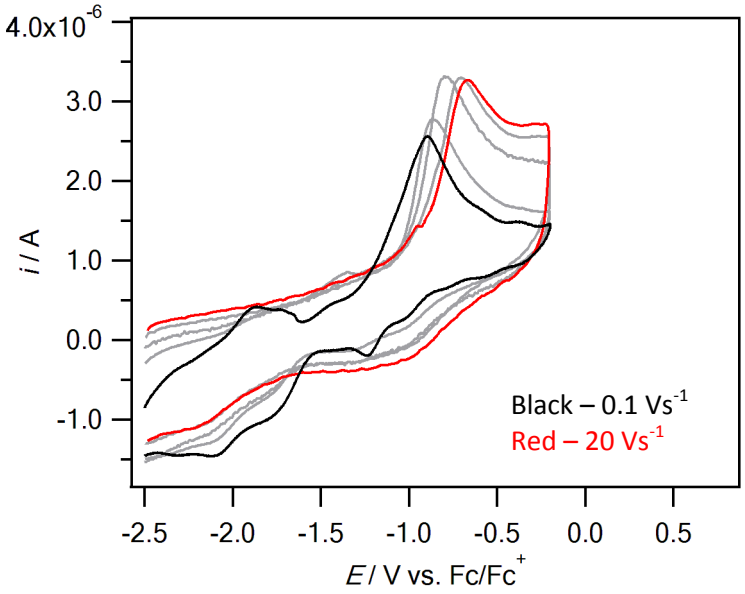

Figure A4.6. Variable scan rate cyclic voltammograms of 1 mM riboflavin in DMSO with 0.2 M *n*-Bu_4NPF_6, from 0.1 V s^{-1} (black line) to 20 V s^{-1} (red line), after 2 e^- bulk reduction, recorded at a 1 mm Pt electrode at 22 (±2) ^oC. The current data were scaled by multiplying by $\nu^{-0.5}$.